Acta Universitatis Agriculturae Sueciae

Doctoral Thesis No. 2023:7
Faculty of Forest Sciences

Chemical and physical incorporation of bio-molecules into wood materials for energy storage

Meysam Nazari

Chemical and physical incorporation of bio-molecules into wood materials for energy storage

Meysam Nazari

Faculty of Forest Sciences

Department of Forest Biomaterials and Technology/Division of Wood Science and Technology

Uppsala

SLU

SWEDISH UNIVERSITY OF AGRICULTURAL SCIENCES

DOCTORAL THESIS

Uppsala 2023

Acta Universitatis Agriculturae Sueciae
2023:7

ISSN 1652-6880
ISBN (print version) 978-91-8046-066-8
ISBN (electronic version) 978-91-8046-067-5
https://doi.org/10.54612/a.29c0tgbsfr

Swedish University of Agricultural Sciences, Department of Forest Biomaterials and Technology/Division of Wood Science and Technology, Uppsala, Sweden

Print: SLU Grafisk Service, Uppsala 2023

Chemical and physical incorporation of bio-molecules into wood materials for energy storage

Abstract

The environmental impact of fossil-based materials in the building industry and significant energy consumption in residential buildings have urged new research areas in using bio-based, renewable and sustainable materials for production of energy smart bio-based envelopes for building applications. This can be achieved by incorporation of bio-based phase change materials (BPCMs) in wood materials for energy storage in residential buildings.

In this thesis, an attempt was made to develop a new BPCM based on coconut oil (CO). The oil was converted into free fatty acids (CoFA) by alkaline saponification and mixed with oleic (OA) and linoleic (LA) acid in various proportions to obtain stable compositions with desirable working temperatures. The prepared mixtures were visually, chemically and thermally studied confirming that the combination of CoFA/LA 20:80 was the most suitable combination and used further as BPCM (x_{LA}= 0.2). The new system melts uniformly at 24.8 ºC, and freezes at two points 18 and 22 ºC, with latent heat of fusion of 100 J/g, heat capacity of around 5 J/g K, thermal conductivity of 0.2 W/m K, in liquid and 0.35 W/m K in solid phase and a good thermal stability after 700 intensive cooling/heating cycles.

BPCM (x_{LA}= 0.2) was incorporated by impregnation in solid untreated Scots pine and beech and thermally modified pine (TMP), beech (TMB) and spruce (TMS) wood. The impregnability and intensive leakage tests revealed the positive effect of thermal modification on improving permeability and decreasing leakage. A microscopy study showed that rays in both pine and beech were the main pathway for impregnation. The specific heat capacity of unmodified and thermally modified samples before impregnation were similar at around 2 J/g K, which after impregnation, increased to 4-5 J/g K. The introduction of BPCM (x_{LA}= 0.2) led to improved thermal mass and thermal conductivity of the impregnated samples. The latent heat of fusion for impregnated samples was proportional to the amount of BPCM (x_{LA}= 0.2) in the samples. Mold tests showed that BPCM (x_{LA}= 0.2) encapsulated in

studied thermally modified wood species is less susceptible to mold discoloration compared to unmodified samples.

A bio-composite consisting of wood particles impregnated with ethyl palmitate ester (EP) as BPCM and a bio-binder was studied. An optimal proportion of 25 % EP was used in the composite to minimize leakage. The composite was thermally stable to a temperature of 200 ºC. The composite thermal characteristics are similar to solid wood impregnated with BPCM. A benefit of the bio-composite was the added-value to less-valuable industrial bi-products involved in the production of energy smart bio-composite for building application, as well as possibility to produce different profiles.

Keywords: bio-based PCMs, bio-based composites, building applications, coconut oil fatty acids, energy storage, ethyl palmitate, impregnation, thermal characterization, wood materials

Author's address: Meysam Nazari, SLU, Department of Forest Biomaterials and Technology/Division of Wood Science and Technology,
P.O. Box 7008, SE-756 51 Uppsala, Sweden.
E-mail: meysam.nazari@slu.se

Kemisk och fysikalisk inkorporering av biomolekyler i trämaterial för energilagring

Abstrakt

Fossilbaserade materials miljöpåverkan på byggindustrin och betydande energiförbrukning i bostäder har drivit på utvecklingen av nya forskningsområden. Dessa forskningsområden syftar till att ta fram biobaserade, förnybara och hållbara material för framtida energismarta produkter för byggapplikationer. Detta kan uppnås genom att inkorporera biobaserade fasförändringsmaterial (BPCM) i trämaterial för energilagring i bostadshus.

I detta forskningsarbete utvecklades en ny BPCM baserad på kokosnötsolja (CO). Oljan omvandlades till fria fettsyror (CoFA) genom alkalisk förtvålning och blandades med oljesyra (OA) och linolsyra (LA) i olika proportioner för att erhålla stabila sammansättningar med önskvärda arbetstemperaturer. Blandningarna studerades visuellt, kemiskt och termiskt för att upptäcka att kombinationen av CoFA/LA 20:80, kallad BPCM (x_{LA}=0.2) var den lämpligaste kombinationen att studera vidare. Den nya BPCM smälte kongruent vid 24.8 ºC och frös vid 18 och 22 ºC, hade ett latent smältvärme på 100 J/g, värmekapacitet på 5 J/g K, värmeledningsförmåga på 0.2 W/m K i flytande och 0,35 W/m K i fast tillstånd och en god termisk stabilitet efter 700 kyl-/värmecykler.

BPCM (x_{LA}= 0.2) inkorporerades genom impregnering i massiv furu- och bokved samt termiskt modifierad furu-, bok- och granved. Impregnerings- och urlakningstester visade att termisk modifiering bidrar till att förbättra vedens permeabilitet och minska urlakningen. En mikroskopistudie visade att märgstrålar i både furu och bok var den huvudsakliga vägen för inträngning av BPCM. Den specifika värmekapaciteten för obehandlade och termiskt modifierade prover före impregnering var likartade (ungefär 2 J/g K) medan de ökade till 4-5 J/g K efter impregnering. Införandet av BPCM (x_{LA}= 0.2) ledde till förbättrad värmemassa och värmeledningsförmåga hos de impregnerade proverna. Det latenta smältvärmet för de impregnerade proverna var proportionell till mängden BPCM (x_{LA}= 0.2) i proverna.

Mögeltester visade att den termiskt modifierade veden impregnerat med BPCM (x_{LA}= 0.2) var mindre känslig för mögelpåväxt jämfört med obehandlade prover.

Ett ytterligare steg av studien var utvecklingen av en bio-komposit bestående av träpartiklar impregnerade med etylpalmitatester (EP) som BPCM och ett biobaserat bindemedel. En optimal mängd på 25 % viktprocentökning av EP i partiklarna säkerställde att kompositen inte läckte ur partiklarna. Kompositen är termiskt stabil till en temperatur på 200 ºC. De termiska egenskaperna hos kompositmaterialet liknar massivt trä impregnerat med BPCM. En fördel med bio-kompositen var mervärdet genom utnyttjande av mindre värdefulla industriella biprodukter som kan vara involverade i produktionen av energismarta bio-kompositer för byggnadstillämpning.

Nyckelord: biobaserade fasförändringsmaterial, biobaserade kompositer, byggnadsapplikationer, energilagring, etylpalmitat ester, kokosnötsoljefettsyror, impregnering, termisk karakterisering, trämaterial.

Författarens adress: Meysam Nazari, SLU, Institutionen för skogens biomaterial och teknologi/trävetenskap,
P.O. Box 7008, SE-756 51 Uppsala, Sweden.
E-mail: meysam.nazari@slu.se

Dedication

To my family…

Contents

List of publications

The present thesis is based on the following papers, which will be referred to by their Roman numerals.

I. Nazari, M., Jebrane, M. and Terziev, N., 2020. Bio-based phase change materials incorporated in lignocellulose matrix for energy storage in buildings—a review. Energies, 13(12), p.3065.

II. Nazari, M., Jebrane, M. and Terziev, N., 2021. Multicomponent bio-based fatty acids system as phase change material for low temperature energy storage. Journal of Energy Storage, 39, p.102645.

III. Nazari, M., Jebrane, M. and Terziev, N., 2022. Solid wood impregnated with a bio-based phase change material for low temperature energy storage in building application. Journal of Thermal Analysis and Calorimetry, pp.1-16.

IV. Nazari, M., Jebrane, M., Gao, J. and Terziev, N., 2022. Thermal performance and mold discoloration of thermally modified wood containing bio-based phase change material for heat storage. Energy Storage, p.e340.

V. Nazari, M., Jebrane, M. and Terziev, N., 2022. New hybrid bio-composite based on epoxidized linseed oil and wood particles hosting ethyl palmitate for energy storage in buildings. Manuscript.

The contribution of Meysam Nazari to the papers included in this thesis was as follows:

I. **Nazari**, Jebrane and Terziev designed the structure and concept of the review paper. **Nazari** prepared the first draft of the manuscript, Jebrane added parts related to encapsulation, Nano-encapsulation and graphical pictures, Terziev conducted microscopy analysis and photos and LCA part. Final draft was designed, written, edited and reviewed by **Nazari**, Jebrane and Terziev. Submitted by Jebrane.

II. **Nazari** and Jebrane designed the concept and structure of the experiments. Preparation of CoFA from CO was conducted by **Nazari** and Jebrane in the lab. FTIR tests was conducted and the results were reported by Jebrane. Gas chromatography was conducted by Ida Lager at the department of Plant Breeding, SLU. DSC tests conducted by **Nazari** and Jebrane. T-history and transient hot wire tests were done by **Nazari** and Terziev. Thermal cycling tests was conducted by **Nazari** and Jebrane. The first draft of the manuscript was written by **Nazari**, reviewed and edited by Terziev and Jebrane. Submitted by Jebrane.

III. **Nazari**, Terziev and Jebrane designed the structure and concepts of the experiments. Terziev designed the impregnation schedules. **Nazari**, Terziev and Jebrane conducted the impregnation and leaching experiments. Terziev and Jebrane conducted the microscopy part. Thermal tests including T-history, DSC and heat flow meter were conducted by **Nazari** and Terziev. The first draft was written by **Nazari** and Terziev wrote microscopy, impregnability and leaching parts of the manuscript. The final draft was provided by **Nazari** and reviewed, revised and edited by Terziev and Jebrane. Submitted by Jebrane.

IV. **Nazari**, Terziev and Jebrane designed the structure and concepts of the experiments. Terziev designed the impregnation schedules. **Nazari**, Terziev and Jebrane conducted the impregnation and leaching experiments. Gao conducted biological tests (mold tests). Thermal tests including T-history and heat flow meter were conducted by **Nazari** and Terziev. The

first draft was written by **Nazari** and Terziev wrote impregnability and leaching parts of the manuscript. Terziev and Gao wrote the biological part of the manuscript. The final draft was provided by **Nazari** and reviewed, revised and edited by Terziev, Gao and Jebrane. Submitted by Jebrane.

V. **Nazari**, Terziev and Jebrane designed the structure and concepts of the experiments. Terziev designed the impregnation schedules. **Nazari**, Terziev and Jebrane conducted the impregnation and leaching experiments. Jebrane designed and prepared the polymer based bio binder of ELO. **Nazari** and Terziev prepared the composites. T-history and moisture adsorption/desorption were conducted by **Nazari** and Terziev. TGA and DSC conducted by **Nazari** and Jebrane. The first draft of the manuscript was written by **Nazari** and reviewed, revised and edited by Terziev and Jebrane. Submitted by Jebrane.

Other publications related to the thesis work, not included in the thesis:

VI. Palanti, S., Temiz, A., Köse Demirel, G., Hekimoğlu, G., Sarı, A., Nazari, M., Jebrane, M., Schnabel, T. and Terziev, N., 2022. Bio-Based Phase Change Materials for Wooden Building Applications. Forests, 13(4), p.603.

VII. Nazari, M., Jebrane, M., Terziev, N. and Herold, N. Incorporation of organic bio-based phase change materials in wood for energy storage purposes. In: Proceeding of 15th Annual Meeting of the Northern European Network for Wood Science and Engineering (WSE), Lund, Sweden, October 9-10, 2019.

VIII. Nazari, M., Jebrane, M. and Terziev, N. Wood impregnated with multicomponent bio-based PCM for low temperature energy storage in buildings. In: Proceeding of 13rd IIR Conference on Phase-Change Materials and Slurries for Refrigeration and Air Conditioning, Vicenza, Italy, September 1-3, 2021.

Notations

Roman letters	
A	Contact surface area [m^2]
c_p	Specific heat [J/g K]
H	Enthalpy [J/g]
I	Electrical current [A]
L	Length of the hot wire, and thickness of the samples [m]
m	Mass of the materials [kg]
n	Time point [s]
Q	Heat [W]
q/a	Heat flux [W/m^2]
T	Temperature [K]
t	Time point [s]
u	Overall heat transfer coefficient [W/m^2 K]
V	Voltage [V]
Greek letters	
λ	Thermal conductivity [W/m K]
Δ	Difference
∞	Ambient
Subscripts	
f	Final
i	Initial
max	maximum
min	minimum
n	Time point
ref	Reference
$samp$	Sample

Abbreviations

BPCM	Bio-based phase change materials
CoFA	Coconut oil fatty acid
DSC	Differential scanning calorimetry
ELO	Epoxidized linseed oil
EP	Ethyl palmitate
LA	Linoleic acid
OA	Oleic acid
PCM	Phase change materials
TGA	Thermogravimetric analysis

1. Introduction

1.1 Background

Nowadays, wood materials are extensively used in construction and building applications due to the growing consciousness regarding the environmental impact of fossil-based and non-sustainable materials. Wooden materials have been used in construction for centuries due to their intrinsic properties such as origin from renewable sources, recyclability, and high ratio of strength to density. These properties make wood the best material to replace some traditionally used material in constructions [Paper I] and [1, 2]. "Wood material" is a comprehensive term of a vast number of products including sawn wood, engineered wood items, as well as many side products, e.g. wood fibers, particles, flakes, sawdust that are produced along various technological routes. Thermal properties of wood materials are characterized by moderate heat capacity, which makes them unsuitable to manage energy intermittency when used for indoor applications. Thus, extra energy is needed to compensate and regulate the temperature fluctuations inside buildings. In addition, some drawbacks such as susceptibility to bio-deterioration, moisture adsorption and dimensional instability challenge the utilization of wood for indoor applications [Papers I and IV] and [2].

Today, when energy issues are more important than ever, over 40 % of the energy generated worldwide annually is consumed in residential buildings, and needs to be managed properly, having in mind the current difficulties of energy supply and the increasing demand for energy in other sectors [Paper I] and [3-6]. *An option for efficient energy management in residential buildings is the development of engineered wood materials containing bio-based phase change materials (BPCMs) for production of energy-smart and fully bio-based materials, that improve the thermal mass*

of buildings, store excess energy in terms of latent heat and release the stored surplus when the indoor temperature decreases under the comfort limit. This green and environmentally friendly solution can also address the management of wood industry side products, to replace fossil-based construction materials and decrease the energy consumption in residential buildings. An example is the use of secondary products, e.g. sawdust, to produce bio-composites thus, adding value to less valuable industrial side products [Paper V]. Moreover, by developing sawdust composites, it is possible to design and improve some of the properties by adding additives, e.g. to minimize flammability of the bio-based phase change materials, which may not be possible when applied to solid wood.

1.2 PCMs for energy storage in buildings – state of the art

1.2.1 Importance of energy storage in buildings

The significant increase in world population to over 8 billion and rapid industrial development have led to exponential increase of energy demand. In addition, overuse of fossil-based energy resources has become one of the crucial issues related to climate changes and environmental problems [Paper I] and [3]. As already mentioned, over 40 % of the generated energy is consumed in residential buildings while contributing to ca. 30 % emitted greenhouse gases to the environment annually, thus illustrating the importance of energy saving and management in this sector [4-6]. In order to address both concerns, i.e. the growing demand for energy and climate changes, it was stated that energy storage and management approaches are as significant as developing new cleaner resources and techniques for energy generations [Paper I] and [3]. This means that the indoor temperature fluctuation needs to be controlled in order to minimize the energy intermittency inside buildings [Paper I] and [6-8]. This can be achieved by storage of excessive energy when the indoor temperature increases and release of the stored energy when the temperature decreases to minimize the temperature fluctuation and supplied energy, i.e. to use the energy more efficiently [Paper I] and [9].

1.2.2 Basics of energy storage by PCMs

Phase change materials (PCMs) are materials with an ability to respond to temperature change with changing the state of matter (phase). Within a specific temperature range, these materials experience a transition from e.g. solid to liquid phase and vice versa. During this transition, the temperature remains constant and the material stores or releases energy in terms of latent heat [8-10]. The most common used phase transition process for PCMs is solid-liquid and vice versa transition as shown in Figure 1. A PCM in solid phase absorbs energy (heat) from the ambient medium to reach its melting temperature; at the melting temperature, the material absorbs energy within an isothermal process in terms of latent heat until it is completely melted (Fig. 1, melting line). Above this temperature, the material in liquid phase absorbs more energy but in terms of sensible heat (exchange of heat during temperature change) when the temperature increases as well (Fig. 1, right part of the line). When the surrounding temperature decreases, the aforementioned process follows the opposite direction, i.e. the material releases energy to the ambient medium and transforms back to its initial phase (solid), known as solidification temperature [Paper I]. The benefit of using latent heat storage is that during an isothermal process, a reasonable amount of energy is stored and released within a narrow temperature range [8, 11].

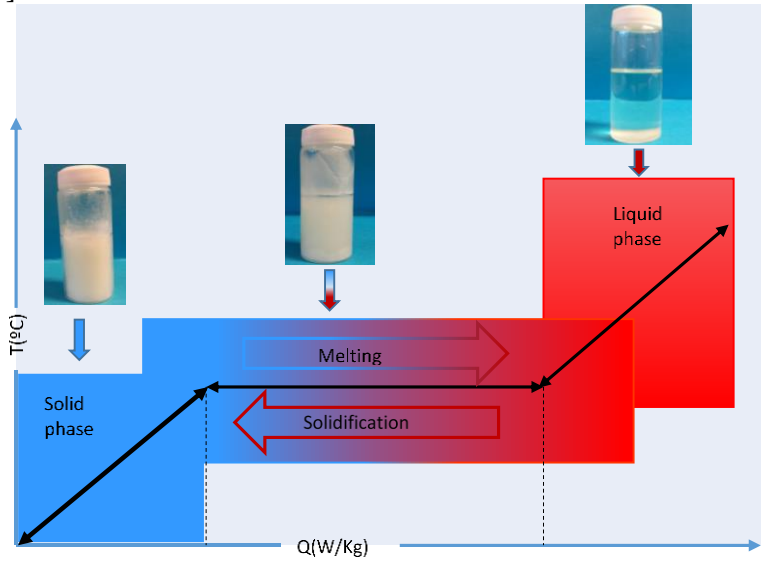

Figure 1. Heat storage mechanism of a PCM.

1.2.3 PCMs in building applications

Energy in buildings can be stored and released within a passive or active system. In the passive system, the PCM incorporated in building envelopes stores energy when the surrounding temperature meets the melting temperature of the used PCM, and releases the stored energy when the temperature decreases. In an active system, a collector stores the energy when there is less demand for energy and used later when the demand increases [7]. For building applications, the first issue that needs to be considered is the working temperature range, which is determined as *human comfort temperature*. According to the ASHRAE standard, this temperature must be in the *range 18-25 ºC* [10], i.e. the PCMs for building application should have melting and solidification temperatures in that range [Paper I].

Investigations regarding use of PCMs in the building sector are mainly focused on storing and releasing of solar energy for indoor heating. This approach is appropriate for regions with high sun radiation during the winter periods when there is an increased need for energy. However, in cold climate regions such as the Nordic countries, the approach is less suitable since the sun radiation is low during the winter. Therefore, PCMs can be used to control the indoor temperature fluctuations in residential buildings for more efficient use of energy [Paper II]. Kalnaes and Jelle [9] discussed that building constructions need to ensure a passive housing standard in cold regions. This requires significant insulation barriers to minimize heat loss through the building walls. The authors also reported that the excess energy could be stored and released when the indoor temperature decreases leading to curbing of the indoor temperature fluctuations and more efficient use of energy when the thermal mass of the indoor construction materials is boosted by use of PCMs.

A suitable PCM for building applications must possess some physical, thermal, chemical and kinetic properties. In addition, cost, availability, safety, compatibility with building's envelopes and reliability of the material need to be taken into consideration [3, 6, 9, 10, 12-15]. In terms of thermal characteristics, a suitable PCM for indoor application should have a reasonable latent heat of fusion within the human comfort temperature range [10]. In terms of physical requirements, the material must demonstrate cycling stability, low supercooling (cooling below freezing temperature without solidifying), no phase separation (creation of two or more phases from an initially homogenous phase), congruent melting (sharp melting

point), high thermal conductivity, low vapour pressure, negligible volume change and chemical stability during the phase change [Paper I].

1.2.4 Importance of using bio-based materials for building applications

Biomaterials from renewable sources will play an essential role in future technologies aiming at harmonizing the human living environment [1]. The building industry has shown an increasing interest and positive outlook of using bio-based construction materials, which guarantees future interest in bio-based products [16, 17].

Traditionally used construction materials including metals, concrete, insulation polymers and plastics lead to environmental problems, e.g. non-recyclable wastes. Approximately half of the construction materials originate from non-renewable sources. In addition, the embodied energy of building material is responsible for 10-20 % of the building's total energy consumption. In the past, some harmful materials such as asbestos, formaldehyde, and lead have been traditionally used in construction applications, which can have harmful effects on human's health. A sustainable approach to reduce the use of harmful and non-environmentally friendly construction materials can be the increased use of renewable bio-based construction materials. This can improve the indoor environment and reduce the negative impacts on climate and health [18]. Considering the above, the demand for environmentally friendly, renewable and green building materials has increased significantly over the past decade and is expected to grow continuously [19]. Green building materials used in constructions for energy management have crucial relevance to the achievement of Sustainable Development Goals (SDGs). A study [20] showed that the SDGs 7.3, 11.6 and 13.2 are essentially achievable by increased involvement of biomaterials in the building industry.

1.2.5 BPCMs for building applications

Bio-based phase change materials (BPCMs) are generally categorized as fatty acids, esters, their eutectic mixtures and some raw plant oils or animal fats. Among BPCMs, fatty acids with general formula $CH_3(CH_2)_{2n}COOH$ derived from animal and vegetable sources are considered as the most promising BPCMs. These BPCMs are categorized in six groups, i.e., caprylic, capric, lauric, myristic, palmitic, and stearic acids [13, 21- 23]. They are renewable, non-toxic, commercially available and biodegradable

[13, 23]. In addition, they possess some unique properties such as congruent melting, good chemical and thermal stability [22–24]. Because of their unique characteristics, they have been of interest in a number of studies as promising BPCMs for low to medium working temperature applications.

Yuan et al. [25] and Rozanna et al. [26] comprehensively studied the use of fatty acids and their eutectic mixtures for thermal energy storage. It can be concluded that when the working temperature is considered as the main requirement in the selection of BPCMs for passive thermal energy storage in buildings, pure fatty acids cannot meet this prerequisite. This is because there is no pure fatty acid with a melting temperature in the range of the human comfort temperature. In order to overcome this drawback, eutectic mixtures of fatty acids and their derivatives have been investigated and used for indoor applications with a working temperature in the range 18-25 ºC.

The eutectic mixtures are composed of two or more compounds. Although the mixed compounds have different melting and freezing temperatures, the eutectic mixtures melt and freeze without phase separation because the intimate mixture of crystals allows very little option of the compounds to separate [6, 9, 23]. Karaipekli and Sari [27] studied eutectic mixtures of capric, lauric, palmitic, and stearic acids. They reported that the eutectic mixtures of the acids had a working temperature in the range 18–25 °C, which makes them very promising for passive energy storage for indoor applications. Furthermore, the eutectics were incorporated in expanded vermiculate by vacuum impregnation and thermal and chemical analyses showed that the composite material was stable after 5000 cycles. Other studies focused on eutectic mixtures based on capric, lauric, myristic, palmitic, and stearic acids for building applications [28, 29]. Binary mixtures of capric-lauric, capric-myristic, capric-palmitic, capric-stearic, lauric-myristic, lauric-palmitic, and myristic-stearic acids as BPCMs for building applications were studied [28-32]. The above studies reported reasonable thermal properties and cycling stability of these mixtures for building applications.

Fatty acid esters and their eutectic mixtures are another important group of BPCMs. It was reported that some pure fatty acids suffer from certain drawbacks such as bad odor, corrosivity, and high sublimation rate. An approach to overcome the above-mentioned drawbacks is to esterify pure fatty acids to achieve thermal and physical properties in a specific range. This occurs when hydroxyl groups of fatty acids are replaced with an alkyl

group to produce fatty acid esters [10, 24]. Nikolic et al. [33] studied fatty acid esters including methyl stearate, methyl palmitate, cetyl stearate, cetyl palmitate, and their binary mixtures. The results of the binary mixtures showed a phase-transition temperature close to room temperature and it was concluded that the mixtures meet the thermal requirement for passive solar thermal storage. The thermal characterization of the eutectic mixture of these esters showed that certain incongruences appeared during heating/cooling cycling. Xu et al. [34] studied methyl palmitate (MP) and methyl stearate (MS) eutectic mixtures as BPCMs for building applications with a melting temperature of 25–40 °C and found that the BPCM showed incongruent melting for mass ratios of MP/MS of 70/30, 60/40, 50/50, and 40/60. After 360 thermal cycles, the mixtures showed reasonable thermal and chemical reliability. Butyl stearate, vinyl stearate, mixtures of ethoxylated linear alcohols [35], and methyl palmitate and methyl stearate [36] are some other esters studied as possible BPCMs. The studies reported promising thermal properties of these esters for building applications. The melting temperatures of the former group of materials was reported to be between 10 to 43 °C with a latent heat between 100 to 140 kJ/kg [35] while the latter group demonstrated a melting temperature between 23–27 °C with a latent heat of fusion of 180 kJ/kg [36]. Ethyl palmitate is another promising ester with appropriate thermal properties for indoor application [37]. It is concluded that the entire group of esters needs to be further investigated in terms of chemical stability and compatibility with other materials.

Some tropical raw fruit oils have recently been studied as possible BPCMs for low to medium working temperature applications. Palm kernel oil, Allanblackia, shea butter and coconut oil have been investigated and reported as promising BPCMs for building applications [38-41]. However, their thermal characterization results showed a multiple melting/freezing profile over the transition temperatures. In addition, some of the studied oils are susceptible to oxidation, which limits their application as PCMs in buildings [38]. Kahwaji and White [42] investigated the feasibility of using a series of edible oils including coconut oil as BPCMs. They concluded that coconut oil possesses good thermal and chemical stability after 200 melting/freezing cycles with reasonable latent heat of fusion and an appropriate phase transition temperature. However, the DSC results showed that coconut oil melts and freezes incongruently in the human comfort temperature range. The key limitations for coconut oil use as a BPCM are

significant supercooling and the transition temperatures, which are slightly outside the temperature range of interest (i.e. 20-25 ºC) that is typically required to control the temperature fluctuations in buildings. Nonetheless, if converted to free fatty acids, many plant oils can be employed as BPCMs for low temperature thermal energy storage in building applications [Paper II].

1.2.6 Wood materials hosting PCMs as building envelopes

Wood and wood-based products are the most used material of biological origin in the building and construction industry. Due to wood's renewable origin and availability, it is extensively used in construction and buildings in the European countries, Canada, USA and Australia [Paper I]. The intrinsic properties of wood and wood-based products have led these materials to replace fully or partly non-renewable buildings materials. Nowadays, more attention is paid to engineered wood elements, which demand less energy for production compared to steel and concrete. Therefore, use of timber and other wood-based materials have experienced growth during the last decade in single and multi-floor buildings, thus bringing renewability, sustainability, and climate benefits [1, 16-20, 43].

Although wood materials are extensively used in the construction industry, the thermal properties of wood are predetermined by its anatomical structure and chemical composition resulting in low to moderate density, moderate specific heat capacity and consequently, low thermal mass and ability to absorb and store thermal energy. Other limitations of wood are low thermal conductivity, dimensional instability and bio-degradability. There is a wide spectrum of treatments to improve wood's dimensional stability, decrease moisture adsorption and reduce bio-degradability. An example of a widely implemented industrial process is thermal modification, whereby the wood is heated in the range 180 ºC to 215 ºC for a defined period of time in a medium without oxygen [Papers III and IV] and [2, 44]. As a result, hemicelluloses are thermally degraded while cellulose and lignin are modified to high-molecular structures reducing the hygroscopicity and improve the dimensional stability of wood.

Low thermal mass of wood limits its energy efficiency when it is used for indoor building applications. Wood cannot store and release energy in case of temperature fluctuation and thus, extra energy should be supplied to compensate and regulate the energy balance inside buildings. This issue might be even more apparent for cold climate regions where a large amount

of the generated energy is used for heating during winter. However, if wood panels are engineered in combination with BPCMs, e.g. fatty acids or esters with appropriate working temperature, the temperature fluctuation inside buildings can be controlled leading to more efficient use of energy [2, 45]. Wood is a porous material, which makes it a promising material for use as a matrix to encapsulate BPCMs by impregnation. In addition, the progress in the design of new timber systems, e.g. konstruktionsvollholz (KVH), duo/trio laminated beams, cross-laminated timber (CLT) and laminated veneer lumber (LVL) offers new options for the integration of BPCMs. However, due to the complexity of wood structure, the process of incorporation of BPCMs is challenging and some factors such as temperature and thermo-physical properties of the BPCMs need to be considered [Papers III-V]. Wood in various forms (fibres, flour, solid wood, veneer) have been considered as a matrix to host BPCMs for building applications i.e. internal walls or in its coatings [46], flooring [2] or in the façades of the buildings [47].

Energy storage in buildings by BPCMs incorporated in wood and wood-based materials has been of interest and studies focused on eutectic mixtures of fatty acids, esters and eutectic mixtures of esters as BPCMs in solid wood, delignified solid wood, and composites of wood fibers [46-50]. Most of the above studies concentrated on using pure commercial fatty acids for making eutectic mixtures and some esters impregnated in solid wood of various species, wood fibers, particles and agricultural rests, e.g. fruit shells [51-53]. However, composites of wood/BPCMs have not yet been commercialized, which is explained by leakage of the BPCMs in long-term cycling, compatibility with the wood structure, bad odor and economic restrains.

The studies concentrated on wood/PCM composites have focused on either side wood products as containers for BPCMs or solid wood. A benefit of using side products, e.g. wood fibers, sawdust, flour, flakes, is that these materials are used predominantly to produce heat by burning, while a novel approach to production of energy-smart bio-composites for building application can add value to the vast volumes of these products [Paper V]. This approach is exemplified by studies on fatty acids or their mixtures impregnated in wood flour [48, 54] for increased latent heat storage in the composites. Paraffin was blended with poplar wood flour [55] in a bio-composite with latent heat capacity of 26.8 J/g while graphite was added to improve the thermal conductivity of the material. Other studies [56-57]

investigated composites of wood or plant fibers impregnated with PCMs for building applications, e.g. Sari et al. [56] studied incorporation of a BPCM in wood fibers. The product was thermally and chemically stable after thermal cycles within appropriate temperature range with no leakage.

Solid wood of various wood species, carbonized and delignified solid wood have also been considered as a matrix for BPCMs. Delignified wood has been studied intensively, e.g. eutectic mixture of capric-palmitic acids impregnated into delignified wood [50] at a retention of 61.2 % demonstrated no leakage, a phase transition temperature of 23.4 ºC and latent heat of 94.4 J/g with good thermal stability. Another study [49] used delignified wood as an encapsulating material for PCM claiming increased pore volume compared to the initial material. However, the approach of using delignified wood is debatable since lignin, which has the best thermal conductivity of the three structural polymers in wood, is extracted. Solid wood of alder [58] impregnated with paraffin and coated with polystyrene to avoid leakage of the PCMs was also studied. An optimum WPG of 29.9 wt% and a latent heat value of 20.62 J/g was reported. Temiz et al. [59] studied Scots pine sapwood impregnated with an eutectic mixture of capric and stearic acid. After thermal characterization of the material, it was concluded that the system wood/BPCM can be used for indoor temperature regulation and energy saving in timber buildings. Mathis et al. [2] engineered a thin upper layer of wood flooring for absorbing and storing solar energy at a temperature of 30 ºC. Oak and sugar maple wood impregnated with a commercial microencapsulated BPCM was studied and a latent heat of 7.6 J/g for the composite with 77 % improvement in thermal mass compared to the untreated wood was found.

Examples of other biomaterials as containers for BPCMs are fruit shells and BPCMs combined in energy smart composites for building applications. Series of studies of Hekimoğlu et al. [51-53] investigated the possibility of using walnut, apricot and hazelnut shells impregnated with BPCMs for producing energy smart panels. They reported that the porous structure of the ground fruit shells allows these materials to be impregnated with PCMs. It was additionally reported that the composites are chemically and thermally stable with less or no leakage after long-term cyclic testing.

1.3 Aim and objectives

The aim of the present research work was to investigate two promising BPCMs and their incorporation into wood cells in the form of *a)* solid wood, and *b)* wood particle-based composite for passive energy storage for indoor residential building applications. The specific objectives are to select, develop and optimize new fatty acid combinations and esters suitable for the target application in terms of thermal properties, sustainability, and natural occurrence. The study focused on a comprehensive thermal characterization of the new BPCMs along with their thermo-chemical stability. As stated, the study investigated the challenges of incorporation of these BPCMs into solid wood, thermally modified wood and wood particles.

Topics covered in the thesis and related to the aim of the work and the objectives of the study are presented in five articles. The first study was focused on the requirements needed for BPCMs as candidates for building applications and their problems and challenges, the second study was developing a new BPCM for the targeted application and the properties of the developed BPCMs was investigated. The third and fourth studies show the incorporation of the developed BPCM into untreated solid and thermally modified wood, and in these studies challenges, problems and improvements were comprehensively investigated. The fifth study is devoted to the challenges of production of fully bio-based composites of fibers and wood particles with a BPCM.

2. Materials, methods and characterizations

2.1 Materials

2.1.1 Solid wood and wood fibers/particles

Wood materials used in this work were solid wood samples of Scots pine (*Pinus sylvestris* L.) sapwood, beech (*Fagus sylvatica* L.), and thermally modified wood (TMW) samples (thermo-vacuum modification at 210 ºC) of Scots pine sapwood (TMP), beech (TMB) and spruce (*Picea abies* Karst. L.) (TMS) with dimensions of 9×90×90 mm along the grain and without visible defects. For fibers/particles-based composites, wood particles of Scots pine were supplied by Setra sawmill near Uppsala, Sweden. Wood fibers of spruce were provided by Stora Enso's pulp mill Kvarnsveden, Borlänge, Sweden.

2.1.2 Chemicals

Refined coconut oil (CO) and technical linoleic acid (LA) (60 %) were purchased from Sigma Aldrich. Purified oleic acid (OA) (80 %), sodium hydroxide, and sulfuric acid (95-98 %) were purchased from VWR, Merck and Sigma-Aldrich, respectively. Polyethylene glycol with an average molecular mass of 600 (PEG 600) was purchased from Sigma-Aldrich. Ethyl palmitate ester (EP) was used as commercial BPCM and purchased from Sigma-Aldrich. Epoxidized linseed oil (ELO) was purchased from Traditem GmbH, Germany.

2.2 Methods

2.2.1 Processing of BPCMs from coconut oil fatty acids

Coconut oil free fatty acids (CoFA) were prepared by a conventional alkaline saponification from CO, followed by neutralization using sulfuric acid and extracting with n-hexane. Fatty acid multicomponent mixtures were prepared by weighing and mixing of CoFA and OA or LA into glass vials, and dissolved in a minimum amount of n-hexane. After complete dissolution of the fatty acids species, the solvent was removed by evaporation under reduced pressure. After complete removal of the solvent, the mixtures were melted at 40 ºC and freezed at -20 ºC to avoid phase separation. This process of heating (40 ºC) and cooling (-20 ºC) was repeated several times to maximize homogeneity. Mixtures at various ratios of CoFA/LA and CoFA/OA were prepared and tested [Paper II].

2.2.2 Impregnation of BPCMs into solid wood

The BPCM was impregnated in untreated solid and thermally modified wood samples by a vacuum-pressure process in an autoclave. The autoclave temperature was set to 60 ºC to ensure melting of the BPCM. Before impregnation, the samples were conditioned in a climate room with 70 % relative humidity and 23 ºC for 2 weeks. Two impregnation schedules were employed to achieve medium (55 %) and high (90 %) weight percentage gains (WPGs). PEG 600 was impregnated only in Scots pine samples for leaching comparison tests. The high WPG was obtained by immersing the samples in BPCM and applying vacuum of 350 mbar for 10 min followed by 6 bar pressure for 1 h. The medium WPG was obtained when a pre-pressure of 0.75 bars for 60 min was applied instead of the initial vacuum. Wood density, impregnation parameters and the average WPG are shown in Table 1. The WPG was calculated as the difference between the initial (m_i) and final mass (m_f) of the wood sample and expressed in percent (Eq. 1) [Papers III and IV].

$$\text{WPG (\%)} = \frac{(m_f - m_i)}{m_i} \times 100 \quad (1)$$

Table 1. Wood density, impregnation parameters and average WPG.

Wood species	Density, kg/m^3	PCM	Time and vacuum depth	Pre-pressure time	Pressure time	Average WPG, %
Scots pine	506	PEG 600	-	60 min 0.75 bar	-	Medium 59.8
		PEG 600	10 min 80 %	-	60 min 6 bar	High 88.3
		BPCM	-	60 min 0.75 bar	-	Medium 56.3
		BPCM	10 min 80 %	-	60 min 6 bar	High 94.7
Beech	745	BPCM	10 min 80 %	-	60 min 6 bar	43.1
TMP	500	BPCM	-	60 min 0.75 bar	-	Medium 48
			10 min 80 %	-	60 min 6 bar	High 95
TMB	643	BPCM	10 min 80 %	-	60 min 6 bar	47
TMS	460	BPCM	10 min 80 %	-	60 min 6 bar	62

2.2.3 Elaboration of wood particle composite with EP

Ethyl palmitate ester (EP) was used as a BPCM to be integrated in a wood particle composite. Before impregnation, Scots pine particles (sawdust) were dried at 80 ºC for 24 h and sieved to pass a 2-mm screen. The autoclave temperature was set to 60 ºC to ensure melting of EP, and the sawdust particles were immersed in the ester and a vacuum of 350 mbar applied for 10 min followed by 6 bar pressure for 1 h. The impregnation schedule was designed to achieve the highest possible retention (WPG) outlined in Eq. 1. After impregnation, the particles were placed into a funnel and left in an oven at 40 ºC for 24 h to remove excessive EP on the particles surfaces. Impregnated and leached wood particles were then mixed with a determined amount of untreated fibers and subsequently blended with epoxidized linseed oil in the presence of a catalyst. The homogenized mixture was placed in a mould and pressed with a force of 12.3 kg/cm^2 at room temperature for 45 min. The pressed composite was cured in an oven at 50 ºC for 12 h. Figure 2

shows the process of wood particle composite production. The optimized proportions of materials in the composite were 25 % EP, 25 % wood (sawdust) particles, 12.5 % fibers and 37.5 % epoxidized linseed oil. Figure 3 shows the wood composite with EP [Paper V]. Control wood particle composites without EP were processed identically.

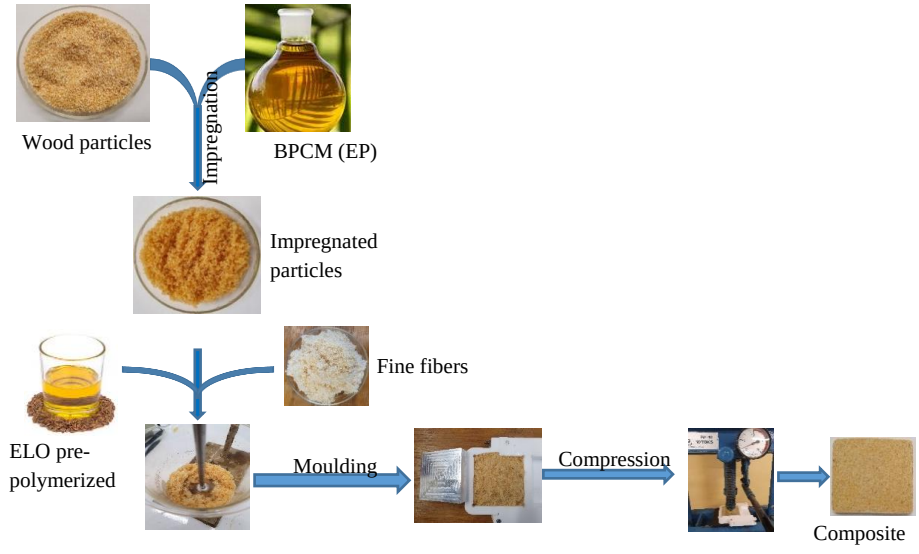

Figure 2. The process of producing wood particle composites containing EP.

Figure 3. Wood particle composites containing EP as BPCM.

2.3 Chemical, physical and thermal characterization of the new materials

2.3.1 BPCM chemical structure - FTIR spectroscopy

Fourier transform infrared (FTIR) spectroscopy was used to characterize functional groups of CO, CoFA, commercial LA and OA and the mixtures of CoFA/LA and CoFA/OA, as well as chemical stability of the mixtures after thermal cycling. A Spectrum one FTIR instrument (Perkin Elmer) equipped with an UATR Diamond accessory allowing collection of FTIR spectra without prior sample preparation was used. The spectra were measured by placing directly a film of oily sample on the surface of ATR diamond and spectra obtained baseline-corrected and normalized using the zero point at the minimum ordinate value. All FTIR spectra were collected at room temperature at a spectrum resolution of 4 cm^{-1}, with an average of 16 scans over the range from 4000 to 450 cm^{-1} [Paper II].

2.3.2 BPCM chemical composition - gas chromatography

Gas chromatography (GC) was used to determine the composition of CO, CoFA and technical OA and LA. The samples were methylated with 2 wt% H_2SO_4 in water-free methanol at 90 °C for 60 min. The fatty acid methyl esters were extracted into heptane and analyzed by GC/mass spectrometry (Agilent 6890 GC system, J&W Scientific, USA), equipped with an HP-5MS column (30 m×0.25 mm i.d., and 0.25 μm film thickness) and an Agilent 5975 mass-selective detector. Helium was used as carrier gas at a flow rate of 1 mL/min. The initial temperature of the oven was set to 60 °C for 1 min, then to 220 °C at a rate of 20 °C/min, held for 2 min, and finally to 280 °C at 10 °C/min, held for 30 min [Paper II].

2.3.3 Leaching test

After impregnation, the solid wood and thermally modified wood samples were conditioned in a cold room (10 °C) for 3 weeks. The sample weight was recorded prior to the leaching test. Each impregnated sample was placed between spruce and oak samples (imitating parquet) with identical dimensions and conditioned as the impregnated sample. The 3-layer set was pressed by a mass of 1 kg and placed in a climate chamber at 35 °C for 24 h. The cumulative leached amount of BPCM was calculated as the difference

between the mass of the sample after 8, 16 and 24 h, related to the initial mass and expressed in percent (likewise Eq. 1). For the sawdust composite with EP, the leakage test was not applicable since the temperature and duration of the processing were higher than the considered conditions for leakage test [Papers III-V].

2.3.4 Distribution of BPCM in solid wood - light microscopy

The distribution of BPCM within Scots pine and beech wood cells was studied by light microscopy. Small samples (5×5×15 mm) were cut from the inner part of the original impregnated and leached samples and semi-thin sections (20-40 µm) cut with a Leitz sliding microtome (Leitz, Wetzlar, Germany). Microscopy observations were done using a Leica DMLB light microscope (Leica, Wetzlar, Germany). No additional treatments to soften the wood before cutting were applied. Osmium tetroxide (OsO_4) and Oil Red O were used to stain the fatty acid inside the wood structure and thus detect the presence and distribution. Non-impregnated Scots pine and beech sections served as controls [Paper III].

2.3.5 Hygroscopicity of the wood particle composite

Hygroscopicity of the wood particle composites with, and without EP in a variable relative humidity was studied according to the Nordtest Project protocol [60]. The method is based on a moisture buffer value (MBV), which is the amount of moisture that a material can store and release during variations of the relative humidity (RH) of the environment [57]. Composite samples of 9×90×90 mm with, and without EP were preconditioned at 50 % RH and 23 °C for 24 h. After conditioning, the samples were weighed and placed back in the climate chamber at the same temperature and RH of 75, 95 and 33 % for 24 h. The weight of the samples was recorded at each relative humidity and after 24 h to calculate the MBV (Eq. 2) [57, 60].

$$\mathrm{MBV} = \frac{\Delta m}{A(RH\%_{max} - RH\%_{min})} \times 100 \qquad (2)$$

where MBV is the moisture buffer value, Δm is the mass variation during the adsorption/desorption phase, A is the sample surface area and RH_{max}, $RH_{\min}$ are the maximum and minimum relative humidities [Paper V].

2.3.6 Susceptibility to mold growth test

The American Wood Protection Association standard E24-06 (2015) was used to assess the susceptibility of solid wood and thermally modified wood impregnated with a BPCM to mold growth and discolouration. Three mold fungi (*Aureobasidium pullulans* (d. By.) Arnaud, *Aspergillus niger* v. Tiegh and *Penicillium brevicompactum* Dierckx) were grown on 2.5 % malt extract agar for 3 weeks. A mixed mold spore suspension was prepared and inoculated on the sterilized soil in a plastic chamber. After inoculation, the chamber was incubated in a climate room at 20 °C for 2 weeks. Afterwards, untreated, thermally modified and impregnated BPCM samples of Scots pine, spruce and beech were placed inside the chamber hanging approximately 5 cm above the soil. The climate in the chamber was maintained at 25 °C and RH higher than 95 %. After 2, 4, 6 and 8 weeks exposure, the mold growth on the sample surfaces (90 × 90 mm) was classified by visual examination according to a scale from 0 (no visible growth) to 5 (very abundant growth, 100 % coverage) [Paper IV].

2.3.7 Thermal properties of the materials

DSC

Differential scanning calorimetry (DSC) thermograms of PCMs and wood containing PCM were recorded on a DSC Mettler-Toledo DSC 3 system under a nitrogen atmosphere. For each DSC run, a sample (weight usually in the range of 14-30 mg) was hermetically sealed in a standard DSC aluminum crucible pan. For developed BPCM based on CoFA, CO, LA, OA and their mixtures as well as EP, samples were in liquid state [Papers II and V]. For solid wood composites with BPCM and composite of wood particles with EP, samples were taken from the core of the composites [Papers III and V]. For the BPCM, other fatty acids and solid wood impregnated with BPCM, the sample was first heated from room temperature to 50 ºC (above samples melting temperature) at a heating rate of 2 ºC/min and then kept at this temperature for 15 min in the DSC instrument, then cooled to -25 ºC at a cooling rate of 2 ºC/min, followed by an isothermal segment for 15 min. The second heating scans were run from -25 ºC to 50 ºC at a heating rate of 2 ºC/min followed by a 15 min isothermal segment [Paper II]. For EP and wood particle composites with EP, the DSC tests were conducted between 0 and 40 ºC at a heating rate of 2 ºC/min and cooling rate of 1 ºC/min with 5

min isothermal segment at 0 ºC and 40 ºC. This heating/cooling cycle for all tests was repeated three times to obtain acceptable reproducibility. The first cycle was discarded [Papers II, III and V], second and third cycles were found identical and thus, the results of the second cycle were reported. Prior to measurements, the DSC system was calibrated using indium and zinc.

T-history

T-history method was used to measure thermal properties including melting/freezing point, latent heat of fusion, degree of supercooling and specific heat capacity of several samples simultaneously [61, 62].

In order to measure thermal properties of EP, CO, CoFA and mixture of CoFA with LA, a T-history set-up was designed [Paper II]. Ultrapure water was used as reference. Stainless steel tubes (SS316) with internal diameter of 10 mm, 1 mm wall thickness and 150 mm length were used as containers for samples and the reference. The containers were filled to 140 mm, and 10 mm left for possible volume expansion during heating/cooling cycles. ARMAFLEX insulation material with 10 mm thickness was used to thermally insulate the tubes. With use of K-type thermocouples, the temperature changes over time for each sample and reference were recorded.

The thermocouples were placed at the centerline and in the middle of each tube. A climate chamber set at 0 ºC and an oven set at 35 ºC were used as cold ambient and hot ambient, respectively. The environment temperature inside the chamber and the oven was recorded with two separate thermocouples. Samples and reference were first preheated in the oven at 35 ºC, and then quickly transferred into the climate chamber at 0 ºC and the temperature profile recorded. Once the equilibrium temperature was reached (ca. 3 h), the sample and the reference tubes were transferred into the oven at 35 ºC and the temperature changes were recorded. Figure 4 schematically shows the T-history set-up designed for measuring thermal properties of the BPCMs.

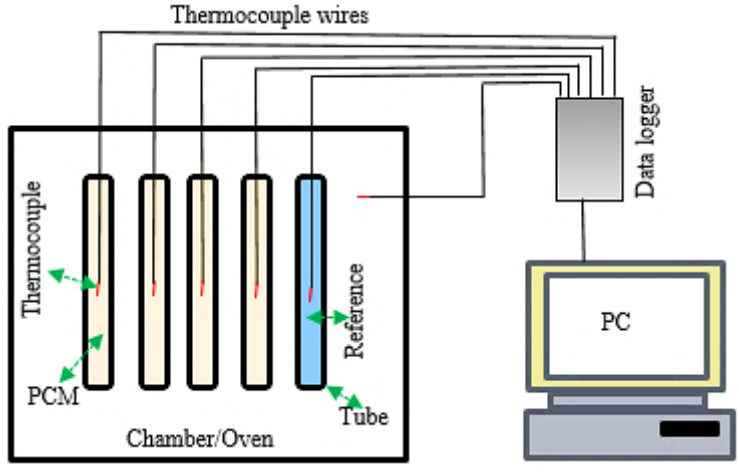

Figure 4. Schematic diagram of the set up for T-history experiments.

T-history method was also used to measure thermal properties of the untreated solid, thermally modified wood samples, BPCM-impregnated solid wood and wood particle composites with, and without EP [Papers III-V]. For this, samples and a copper (Cu) plate as reference with identical dimensions were tested simultaneously (Fig. 5). Stainless steel and aluminium plates with identical dimensions were also used to validate the results [Paper III]. The samples and reference were thermally insulated using 10 mm thickness ARMAFLEX insulation material (Fig. 6). K-type thermocouples were used to record temperature changes over time for samples and the reference. The thermocouples were placed at the centreline and in the middle of the samples. For cold and hot ambient climates, climate chamber set at 0 ºC and an oven set at 40 ºC were respectively used. The chamber and oven temperatures were recorded with two thermocouples. Samples and the reference were first preheated at 40 ºC, and then transferred into the chamber at 0 ºC and the temperature profile recorded. Once the equilibrium temperature was reached (ca. 3 h), the samples and the references were transferred back at 40 ºC and the temperature changes recorded.

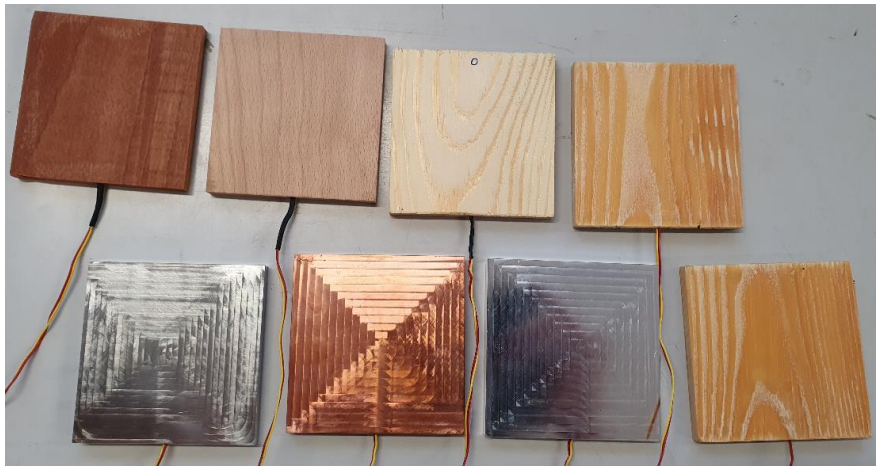

Figure 5. Samples and references without insulation.

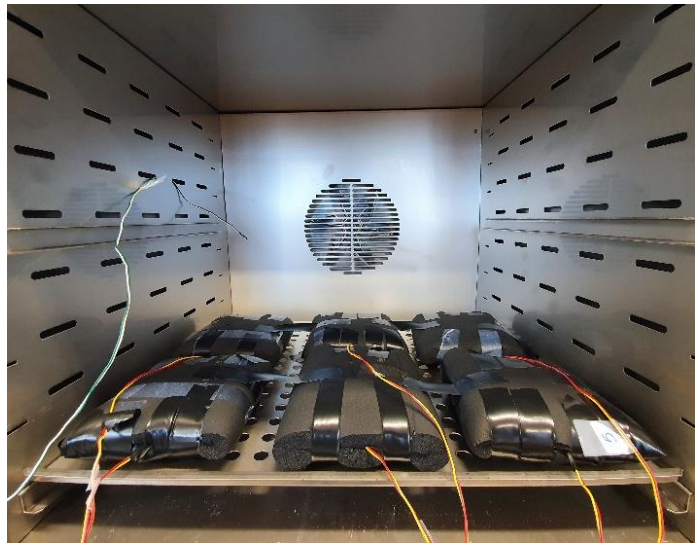

Figure 6. Insulated samples and references inside the chamber.

After the temperature profile over time for samples and the reference was recorded, the energy balance for the reference was used to calculate the overall heat transfer coefficient [Papers III-V]. Since the samples and the reference have identical dimensions and insulation, for uniform heat transfer conditions, the overall heat transfer coefficient (u) for both reference and samples were considered identical. The amount of heat transferred to/from samples in the chambers is expressed as follow:

$$Q = uA(T(t)_n - T_\infty) \quad (3)$$

where Q, u, A, $T(t)_n$ and T_∞ are respectively the transferred heat, overall heat transfer coefficient, heat transfer area, sample temperature at each time point and ambient temperature inside the oven/chamber.

The amount of heat stored/released from samples is:

$$Q = mC_p \frac{d(T_i - T(t)_n)}{dt} \quad (4)$$

where m, C_p, T_i and dt are respectively the mass of the samples, specific heat capacity, initial temperature and time interval.

The amount of transferred energy to/from the samples is stored/released in/from the samples, therefore the energy balance is:

$$Q = -uA(T(t)_n - T_\infty) = mC_p \frac{d(T(t)_n - T_i)}{dt} \quad (5)$$

By rearrangement and integration, the temperature distribution for the reference and wood samples are obtained as:

$$\int_{T_i}^{T_n} \frac{d(T(t)_n - T_\infty)}{(T(t)_n - T_\infty)} = -\int_0^{t_n} \frac{uA}{mC_p} dt \quad (6)$$

After mathematical operation:

$$\ln\left[\frac{(T(t)_n - T_\infty)}{(T_i - T_\infty)}\right] = -\frac{uA}{mC_p} t_n \quad (7)$$

As the thermo-physical properties of the reference is known, the overall heat transfer coefficient (u) is calculated using energy balance for the reference:

$$uA = -\frac{\ln\left[\frac{(T(t)_n - T_\infty)}{(T_i - T_\infty)}\right]_{ref}}{t_n} m_{ref} C_{p,ref} \quad (8)$$

uA is calculated by the energy balance for the reference according to Eq. 8, and as heat transfer area and conditions around reference and samples are identical, uA was calculated from the energy balance of the reference and used further to calculate C_p for the samples. After substitution Eq. 8 in Eq. 7, C_p of the samples is calculated as:

$$C_{p,samp} = \frac{\ln\left[\frac{(T(t)_n - T_\infty)}{(T_i - T_\infty)}\right]_{ref}}{\ln\left[\frac{(T(t)_n - T_\infty)}{(T_i - T_\infty)}\right]_{samp}} \frac{m_{ref}}{m_{samp}} C_{p,ref} \quad (9)$$

Enthalpy of the samples is obtained as:

$$\Delta H = c_{p,samp}\left(T(t)_{n,samp} - T_{samp,i}\right) \quad (10)$$

where ΔH is enthalpy change from initial point to each time point *n*.

Thermal conductivity with transient hot wire and heat flow method

Transient hot wire method was used to measure the thermal conductivity of the BPCMs, i.e. CO, CoFA, LA, OA and mixtures of CoFA with LA and OA in liquid and solid states. This method is a transient technique according to the standard methods ASTM C1113 and ISO 8894 [63]. In this method an electrically heated thin wire is immersed into an uniform and isotropic medium at a constant initial temperature, and the temperature of the wire is recorded over a short time while the wire is heating up, then with use of a particular heat conduction equation for linear heat source, the thermal conductivity is calculated [63, 64]. For this purpose, an apparatus was designed (Fig. 7), in which the wire was made of Kanthal with 150 mm length and 0.3 mm diameter. Two electrically insulated copper wires with diameter of 2 mm were used to hold the hot wire by welding its ends to the copper wires. A 0-15 volt range DC power was used to supply constant current to the wire (3.3 V, 1.31 A). Voltage and amperage were recorded using a digital multimeter. The temperature was measured with a K-type thermocouple with diameter of 1 mm and accuracy of ±0.1 ºC, which is electrically insulated and glued to the wire while the distance between the thermocouple and wire was kept 1 mm. A data logger was used to record temperature versus time with 2 sec interval. The sample was placed in a glass tube with a length of 160 mm and diameter of 20 mm, and then the hot wire set-up was embedded and fixed in the centerline of the tube. Prior to the measurements, the temperature was recorded for 6 sec to make sure there is a constant temperature inside the sample; a switch was then used to run the set-up for 30 sec. The measurements were reproduced 5 times for each sample and the average value reported. The temperature-time curve was transformed to temperature-ln(t) curve and the slope of the new curve in the linear part (R^2 = 0.99) used to calculate the thermal conductivity (Eq. 11).

$$\lambda = \frac{V.I.\Delta\ln(t)}{4\pi L.\Delta T} = \frac{V.I}{4\pi L.\left(\frac{\Delta T}{\Delta\ln(t)}\right)}. \quad (11)$$

where λ is the thermal conductivity of the sample; V and I are measured voltage and amperage; ΔT is temperature difference over a known time interval; $\Delta \ln(t)$ is the difference between two taken points on temperature-ln(t) curve; L is the length of hot wire; $\frac{\Delta \ln(t)}{\Delta T}$ is the slope of the temperature-ln(t) curve [Paper II].

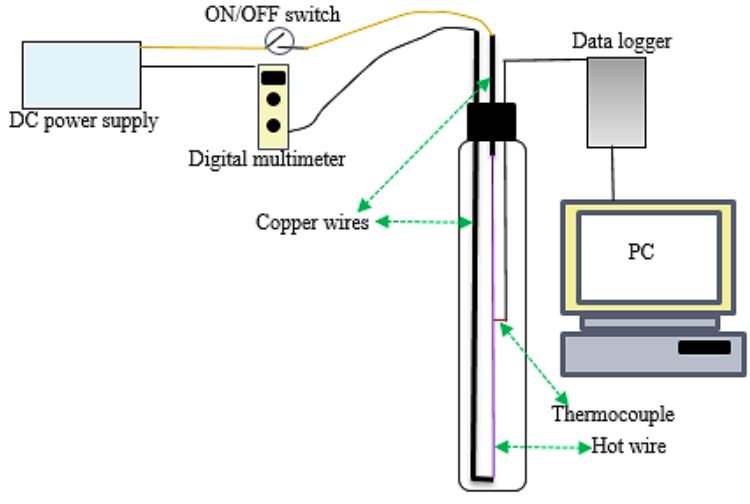

Figure 7. Schematic diagram of the transient hot wire test measurements.

Thermal conductivity of the non-impregnated and unmodified and thermally modified wood samples hosting BPCM was measured with a heat flow meter method according to the standard methods ASTM C1155-95 (2013) and ISO 9869-1:2014, shown in Figure 8 [Paper III] and [65, 66]. The aim was to measure the thermal conductivity of the samples along the thickness, therefore an insulated box was designed to minimize the heat loss from other sides of the sample. The sample's sizes in other directions were 10 times larger compared to the thickness resulting in minimizing the heat loss from the other directions. The temperature of both surfaces of each sample was recorded with K- and T-type thermocouples, and the non-contact surface of the thermocouples was insulated to minimize the effect of the environment on the measurements. A heat flux meter type FHF03 (Hukseflux, the Netherlands) measured the heat flux at the surface exposed to cold environment. Each measurement was run for 3 h to ensure a steady state process [67], and the experiment was repeated 4 times for reproducibility. After measuring the heat flux and the temperatures at both

surfaces of the samples, the thermal conductivity was calculated using Fourier's law of thermal conduction [Paper III] and [67]:

$$\lambda = \frac{q}{a}.\frac{\Delta L}{\Delta T} \quad (12)$$

where $\frac{q}{a}$ is the heat flux, ΔL is the thickness, and ΔT is temperature difference.

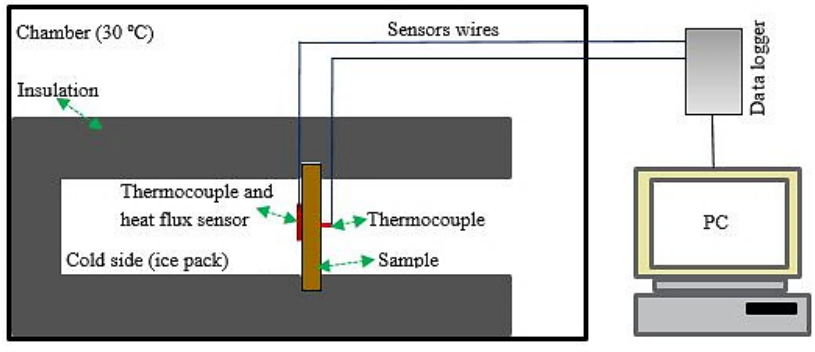

Figure 8. Schematic diagram of the designed rig for thermal conductivity.

Thermal cycling stability of the developed BPCM

An accelerated thermal cycling method was used to assess the thermal stability of the developed BPCM based on CoFA. Samples of 2 g were put in five sealed vials and another batch of samples in unsealed vials were placed in a climate chamber with a scheduled heating/cooling cycles. Seven hundred cooling/heating cycles were conducted in the climate chamber at temperature oscillating between -3 to 50 ºC, at heating and cooling rates of 2 ºC/min, with 10 min isothermal segment at -3 ºC and 50 ºC. This temperature range (-3 to 50 ºC) and isothermal segments were selected to ensure a complete solidification and melting of the BPCM during a cycle. After every 100th cycle, a vial from each composition was taken for FTIR and DSC characterization and the results compared to uncycled samples [Paper II].

Thermal stability of the wood particles-based composites hosting EP using TGA

Thermal stability of the wood particle-reinforced composite hosting EP was conducted using a TGA Mettler-Toledo TGA 2 system under nitrogen atmosphere. For each TGA run, a sample of mass usually in the range 20-30 mg was taken from each sample and placed in a standard alumina (aluminium oxide) crucible pan. The TGA tests were run between 26 ºC and 500 ºC at a

heating rate of 10 ºC/min with 5 min isothermal segment at each 26 ºC and 500 ºC [Paper V].

Thermal cycling performance of the wood particle composite containing EP

Thermal performance and cycling stability of the wood particle composites with, and without EP were studied on two identical cubes with a side length of 90 mm. Six composite plates (of each type with, and without EP) were prepared and used as internal walls of the cubes. ARMAFLEX insulation material was used to insulate the cubes. Inside each cube, 2 thermocouples were set in the middle to record the temperature behavior over time (Fig. 9). The test cubes were placed in a climate chamber with a scheduled temperature varying between 0 and 40 ºC. Initially the climate chamber temperature was set at 20 ºC for 30 min, then increased to 40 ºC with heating rate of 1 ºC/min followed by 3 h isotherm step at 40 ºC, and then the temperature decreased to 0 ºC with cooling rate of 1 ºC/min followed by 3 h isotherm step at 0 ºC. The heating/cooling process was repeated 10 times followed by 2 h rest time and another 10 cycles carried out. The temperature behavior of the cubes and the environment were monitored [Paper V].

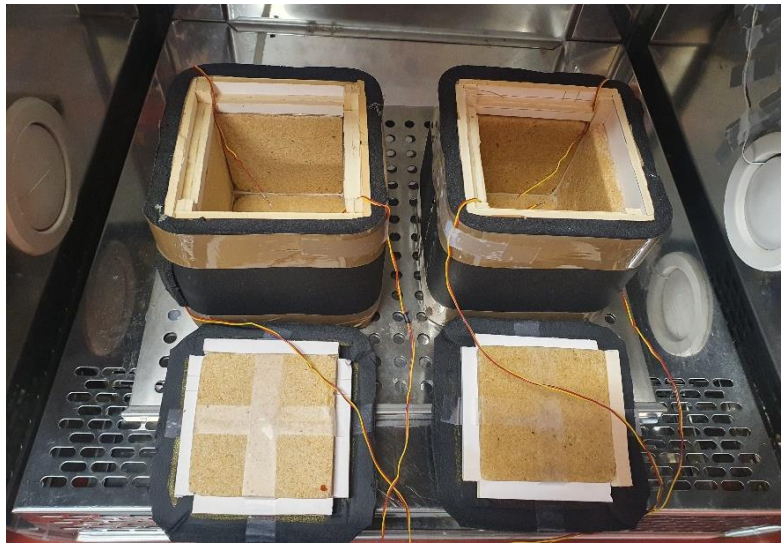

Figure 9. The designed cubes and lids for cycling test inside the climate chamber.

3. Results and discussion

3.1 Bio-based phase change materials (BPCMs)

3.1.1 Chemical characterization of synthesized BPCMs

The design of eutectic mixtures of fatty acids requires a mixture of pure fatty acids to achieve highest possible miscibility and congruency [Paper II] and [68]. However, CO and CoFA consist of various fatty acids making them unsuitable as eutectic mixtures. CoFA were derived from CO by a conventional alkaline saponification and mixed with technical OA and LA to adjust the working temperature range of the mixture with highest possible congruency. The chemical compositions of CO, CoFA, OA and LA were analyzed with GC and their respective chemical composition is shown in Table 2.

Table 2. Composition of CO, CoFA and technical OA and LA.

Fatty acids	CO	CoFA	LA	OA
Caproic (C6:0)	0.13	0	0	0
Caprylic (C8:0)	3.15	0.04	0	0
Capric (C10:0)	3.92	2.04	0	0
Lauric (C12:0)	42.96	42.14	0	0
Myristic (C14:0)	21.22	23.02	0	0
Palmitic (C16:0)	12.31	14.36	5	5
Stearic (C18:0)	4.15	4.95	2	2
Oleic (C18:1)	9.74	11.25	25	80
Linoleic (C18:2)	2.43	2.19	67	12

The prepared compositions of CoFA/LA and CoFA/OA with various proportion are shown in Table 3. Since it was not possible to use a theoretical

approach to design mixtures of CoFA/OA and CoFA/LA, a visual screening test was conducted at temperatures of 5, 15 and 22 ºC, and mixtures with melting/solidification points in the range of 18-25 ºC were selected for further thermal tests (denoted with * in Table 3) [Paper II].

Table 3. Primary prepared and selected (*) fatty acid mixtures.

formulation	Composition proportion	x_{LA}	formulation	Composition proportion	x_{OA}
LA/CoFA	70/30	0.7	**OA/CoFA**	70/30	0.7
LA/CoFA	60/40	0.6	**OA/CoFA**	60/40	0.6
LA/CoFA	50/50	0.5	**OA/CoFA**	50/50	0.5*
LA/CoFA	45/55	0.45	**OA/CoFA**	45/55	0.45*
LA/CoFA	40/60	0.4*	**OA/CoFA**	40/60	0.4*
LA/CoFA	35/64	0.35*	**OA/CoFA**	35/65	0.35*
LA/CoFA	30/70	0.3*	**OA/CoFA**	30/70	0.3
LA/CoFA	20/80	0.2*			
LA/CoFA	10/90	0.1			

CO, CoFA, LA, OA and mixtures of x_{LA} = 0.20 and x_{OA} = 0.30 were studied by FTIR and the spectra in the region of 4000-450 cm^{-1} shown in Figure 10. For CO, the main characteristic vibrations are related to absorption bands of triglycerides [69], which were observed at 2851 cm^{-1} and 2919 cm^{-1} and between 1465 cm^{-1} and 720 cm^{-1} respectively related to vibration of methyl (CH_3) and methylene (CH_2) groups. In addition, vibrations for C-O between 1173 and 1104 cm^{-1}, and carbonyl stretching vibrations at 1740 cm^{-1} were observed. The spectra results for CoFA revealed some shifts, disappearance and emergence of absorption bands due to conversion of the triglyceride ester into carboxylic acids. The main shift was observed for the carbonyl stretching vibration from 1740 to 1707 cm^{-1}, and the emergence of new absorption bands at 1412, 1284 and 934 cm^{-1} corresponding to fatty acid O-C stretching vibrations, and also disappearance of CO vibrations related to triglyceride ester (-C-O) confirmed the complete conversion of CO into CoFA. The spectra results of OA, LA and mixtures of x_{LA} = 0.20 and x_{OA} = 0.30 before thermal cycling show that the spectra for all fatty acids are similar with an exception of the band at 3008 cm^{-1} observed for OA and LA. This band is related to cis allylic (C=CH) which shows that OA and LA are unsaturated fatty acids, while it is absent for CoFA, since the fatty acid is mainly saturated [70].

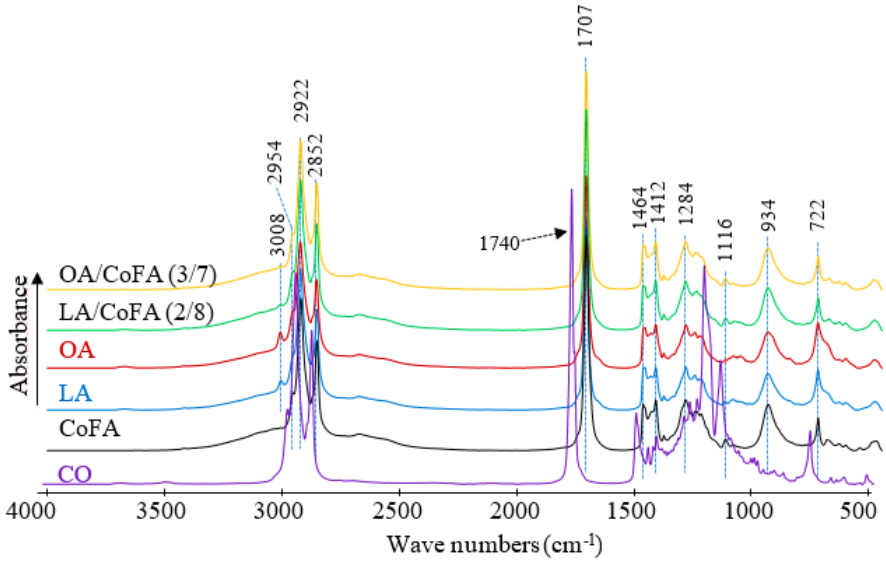

Figure 10. FTIR absorbance spectra of CO, CoFA, LA, OA and the mixtures of x_{LA}= 0.20 and x_{OA} = 0.30.

3.1.2 Thermal characterization of developed BPCMs and EP

The significance of CO conversion to CoFA in terms of thermal properties

The DSC and T-history results for CO and CoFA confirmed the importance of the conversion from raw oil to free fatty acids. As shown in Figure 11, when CO is converted to CoFA, the developed free fatty acids showed enhancement in thermal properties as PCM confirmed by higher heat flow, latent heat of fusion and working temperature. However, CoFA has a main melting peak point at 29.7 ºC and a small peak at -11 ºC due to presence of some portion of unsaturated fatty acids. During the cooling course, CoFA showed almost symmetrical overlapped exothermic peaks.

Figure 12 depicts temperature profiles for CO, CoFA and water as reference from T-history. Compared to CoFA, CO has a supercooling of approximately 2.5 ºC at 17.6 ºC, while its solidification temperature is 20 ºC. CO starts to melt at around 21 ºC and is fully melted at 26.4 ºC. CoFA solidifies at 26.4 ºC, while its melting point is 23.7 ºC, and fully melted at 28.3 ºC. Compared to CO, CoFA melts and solidifies more congruently and the temperature profile is wider than that of CO confirming its higher capacity for storing and releasing energy.

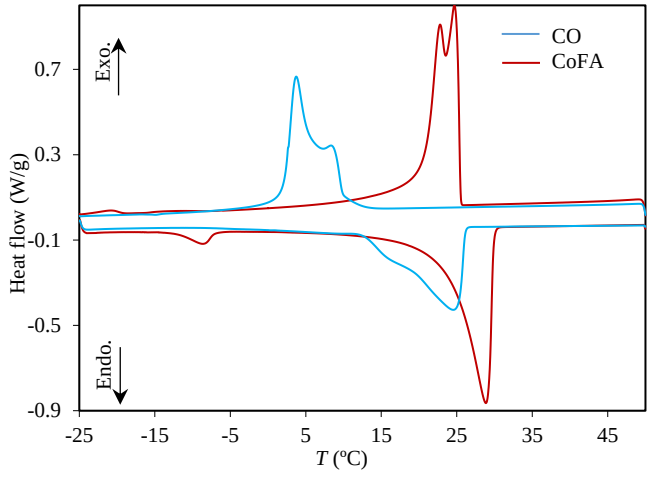

Figure 11. DSC results for CO and CoFA.

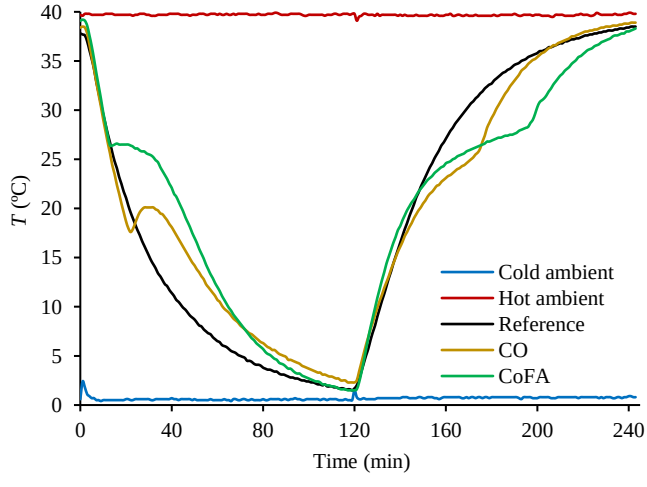

Figure 12. T-history over cooling/heating cycle for CO, CoFA and water (reference).

The DSC and T-history results for CoFA show that the material melts and freezes slightly outside the favourable working temperature range of 18-25 ºC and thus, it needs to be adjusted in order to meet the requirement for building applications.

Thermal selection criteria of the developed BPCMs

The DSC thermogram curves obtained for OA and LA and mixtures of OA/CoFA and LA/CoFA are illustrated in Figures 13-15. Figure 13 shows that commercial technical OA and LA melt and freeze congruently

confirmed by only one sharp peak for each cooling and heating process. The melting and freezing peaks for OA was respectively found at 10.8 ºC and -2 ºC, and -10.3 ºC and -14.6 ºC for LA. OA has higher heat flow and latent heat compared to LA.

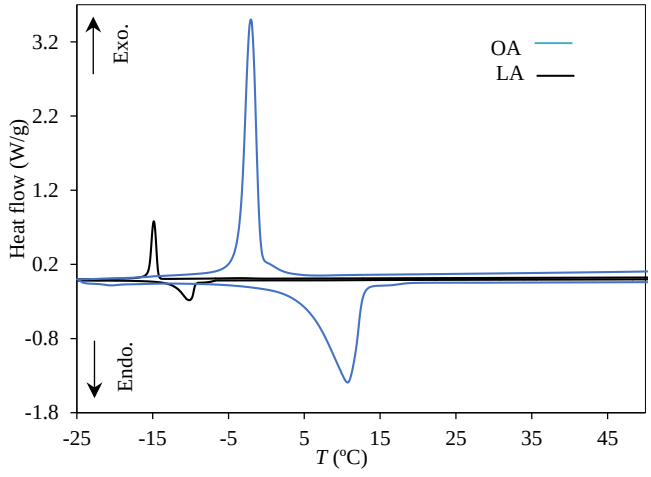

Figure 13. DSC results for OA and LA.

In order to adjust the working temperature of CoFA, it was mixed with OA and LA at different proportions. Figures 14 and 15 shows the DSC thermograms obtained for OA/CoFA (Fig. 14) and LA/CoFA (Fig. 15). It was found that the mixtures had higher phase transition temperatures, heat flow and latent heat of fusion with increased amount of CoFA. Due to the presence of two main fatty acids in each type of mixture, two peaks were observed during the heating and cooling process for all mixtures. Analysing the OA/CoFA mixtures, only the mixture of x_{OA} = 0.30 showed main peaks in the range of 18-22 ºC while the other mixtures had the main peak at temperatures outside the targeted working temperature range of 18-25 ºC. The pattern was similar for mixtures of LA/CoFA, where the mixture of x_{LA} = 0.20 showed the most favourable features.

Although OA has higher phase transition temperatures and latent heat of fusion, the DSC results confirmed that mixtures of LA/CoFA possess better working temperature range, congruency and latent heat of fusion. Among all tested mixtures, *mixture of CoFA and LA at the ratio x_{LA} = 0.20 is the best candidate as BPCM for building applications and is referred as "BPCM (x_{LA} = 0.20)" hereafter.*

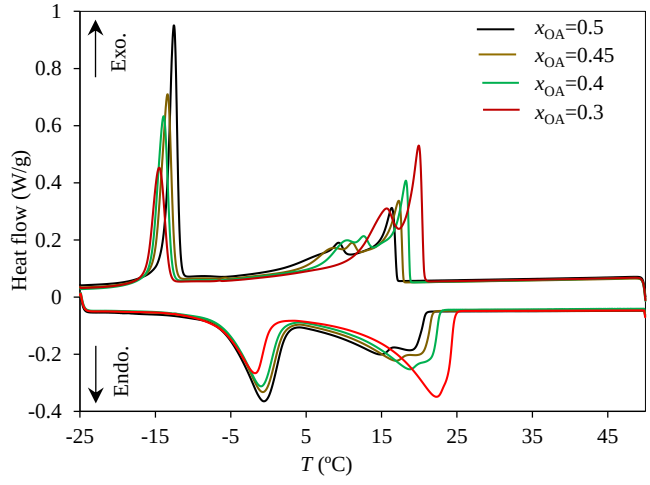

Figure 14. DSC results for mixtures of OA/CoFA.

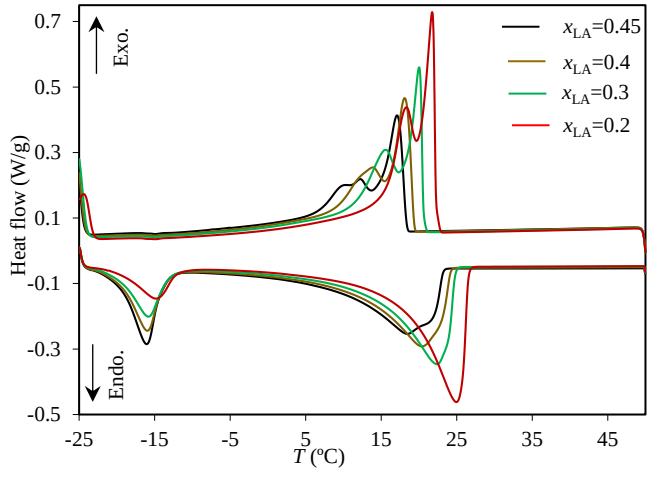

Figure 15. DSC results for mixtures of LA/CoFA.

Thermal conductivity of the mixtures was measured with transient hot wire method and the results are shown in Table 4. For each sample, five tests were run and the mean value and standard deviation were reported. Pure water was used to calibrate the set-up. It was found that the thermal conductivity of the mixtures were around 0.2 W/m K and 0.35 W/m K for liquid and solid states respectively. No relation was found between the proportion of OA, LA and CoFA in the mixtures and the thermal conductivity.

Table 4. Average thermal conductivity of materials with standard deviation in parentheses.

Samples	Mean λ (W/m K)	
	Liquid	Solid
Water	0.597 (0.016)	-
OA	0.206 (0.010)	-
LA	0.196 (0.013)	-
CO	0.200 (0.016)	-
CoFA	0.21 (0.007)	0.351 (0.015)
x_{OA} **= 0.50**	0.212 (0.004)	0.357 (0.010)
x_{OA} **= 0.45**	0.202 (0.004)	0.355 (0.011)
x_{OA} **= 0.40**	0.192 (0.009)	0.357 (0.008)
x_{OA} **= 0.30**	0.216 (0.014)	0.39 (0.007)
x_{LA} **= 0.40**	0.192 (0.005)	-
x_{LA} **= 0.35**	0.212 (0.007)	0.36 (0.03)
x_{LA} **= 0.30**	0.191 (0.001)	-
x_{LA} **= 0.20**	0.202 (0.011)	0.346 (0.012)

Thermal and chemical cycling stability of BPCM (x_{LA} = 0.20)

Thermal and chemical cycling stability of BPCM (x_{LA} = 0.20) was tested with an accelerated thermal cycling test between -3 to 50 ºC, for 700 heating/cooling cycles. After every 100 cycles, one sample of the mixture was studied with DSC and FTIR and compared with an uncycled sample. This was done for both sealed and unsealed vials. Figure 16 compares DSC results for cycled and uncycled samples. The DSC results confirmed that BPCM (x_{LA} = 0.20) is thermally stable after 700 cooling/heating cycles, where the main melting and solidification peaks experienced a slight shift (ca. 0.2 °C) to lower temperatures. No relation between number of cycles and change in phase transition temperatures was found. Small decline was also noted for the heat flow during cooling process while it remained unchanged during the heating process. The results for thermal cycling stability are in an agreement with other studies where a decrease of 6 and 10.1 % in latent heat of fusion were observed after 1500 cycles for eutectic mixtures of myristic acid/palmitic acid and myristic acid/palmitic acid/sodium stearate [71]. A decrease of 3 % in melting and solidification enthalpies after 720 thermal cycles for expanded graphite composite with palmitic acid/stearic acid eutectic mixture was also reported [72]. This shows

that BPCM (x_{LA} = 0.20) is thermally stable after cooling/melting cycling and can be used for building applications.

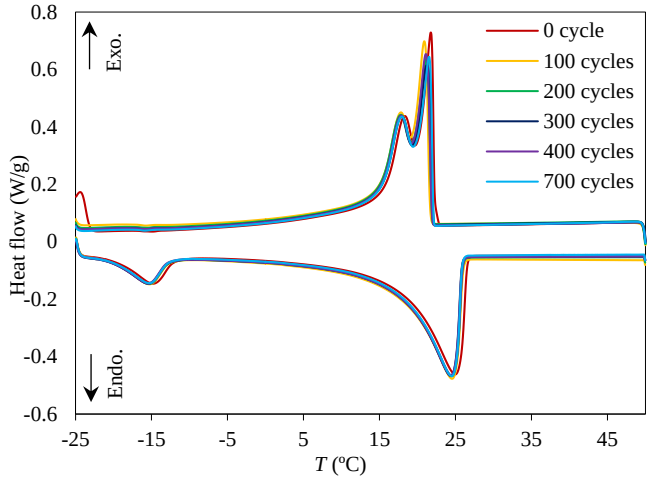

Figure 16. DSC curves of BPCM (x_{LA} = 0.20) subjected to long-term thermal cycles.

Pure polyunsaturated fatty acids, e.g. LA are susceptible to oxidation when exposed to air and temperature. The chemical stability of BPCM (x_{LA} = 0.20) in sealed and unsealed vials during a long-term cycling was studied by FTIR (Fig. 17). The vibration band at 3008 cm^{-1} is related to the unsaturated part of the mixture and a mixture cannot be considered as chemically stable if a change of this band is revealed. Apparently, the main characteristic peaks at 2954, 2922, 2852, 1707, 1464, 1412, 1284, 1116, 934 and 722 cm^{-1} remained unchanged for both sealed and unsealed vials. The peak at 3008 cm^{-1} also remained unchanged confirming that the mixture is chemically stable after thermal cycling. The physical appearance of the samples after thermal cycling did not undergo visible changes.

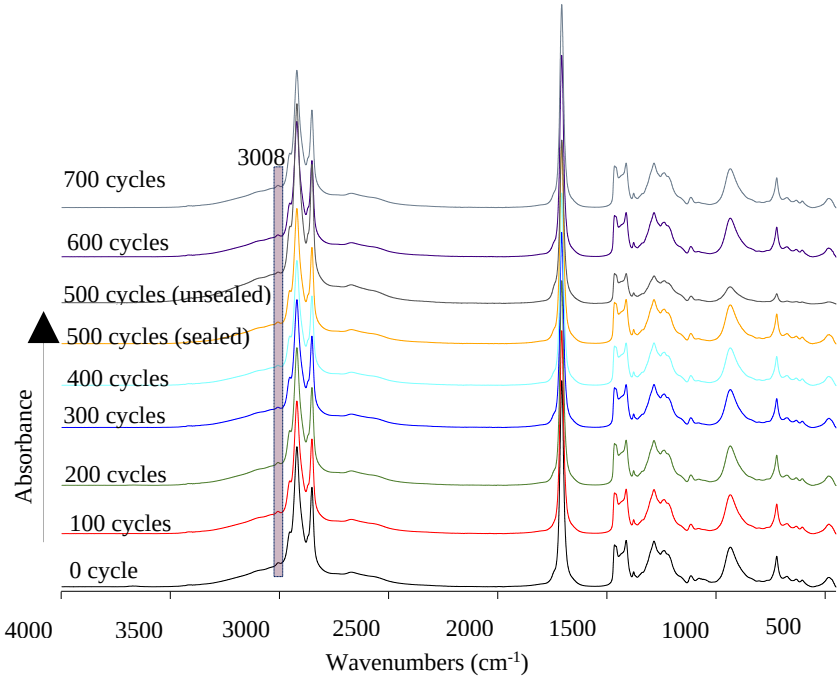

Figure 17. FTIR spectra of BPCM (x_{LA} = 0.20) before and after long-term thermal cycles.

Comparison of thermal properties of BPCM (x_{LA} = 0.20) and EP

Although BPCM (x_{LA} = 0.20) showed a chemical, thermal stability, less supercooling, no volume change and working temperature in the targeted range, in terms of enthalpy, it demonstrated moderate properties. Therefore, another less studied but promising commercial ester (EP) as BPCM for the application was comprehensively investigated. The thermal behavior of BPCM (x_{LA} = 0.20) and EP during cooling and heating courses was monitored by the T-history method and the results are depicted in Figures 18 and 19. During cooling (Fig. 18), it is observed that BPCM (x_{LA} = 0.20) starts to solidify at 23.7 ºC with some degree of supercooling at around 0.6 ºC, with a second solidification point observed at 21.7 ºC, which confirms incongruent solidification. However, both solidification points are in the targeted working range of 18-25 ºC. EP solidifies more congruently starting at 20 ºC and demonstrates supercooling at around 1.7 ºC, confirmed by complete solidification at 21.7 ºC.

During the course of heating (Fig. 19), the melting temperatures of BPCM (x_{LA} = 0.20) and EP were around 25.5 ºC and 25 ºC, and both materials melt

uniformly. EP demonstrated a wider pattern compared to BPCM (x_{LA} = 0.20) during phase transition and greater ability to keep the temperature constant for a longer time [Papers II and V].

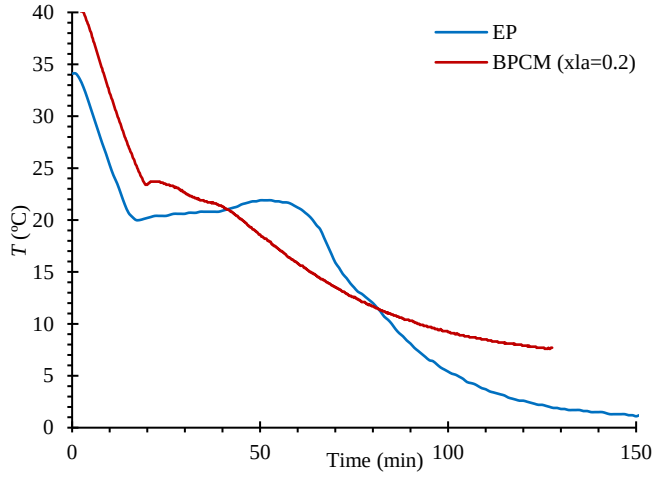

Figure 18. T-history over cooling course for BPCM (x_{LA} = 0.20) and EP.

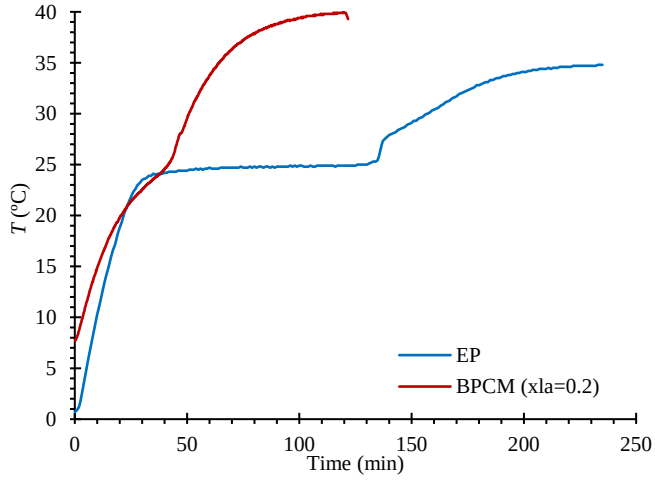

Figure 19. T-history over heating course for BPCM (x_{LA} = 0.20) and EP.

Figure 20 compares DSC thermogram results for BPCM (x_{LA} = 0.20) and EP. The results show that EP performs better as a phase change material because of its higher heat flow (enthalpy) and congruency [Papers II and V]. Nevertheless, EP shows certain changes at melting peak point due to its

polymorphic nature. The polymorphic nature of EP leads to crystallinity, which can be a problem when EP is incorporated in other materials [73, 74].

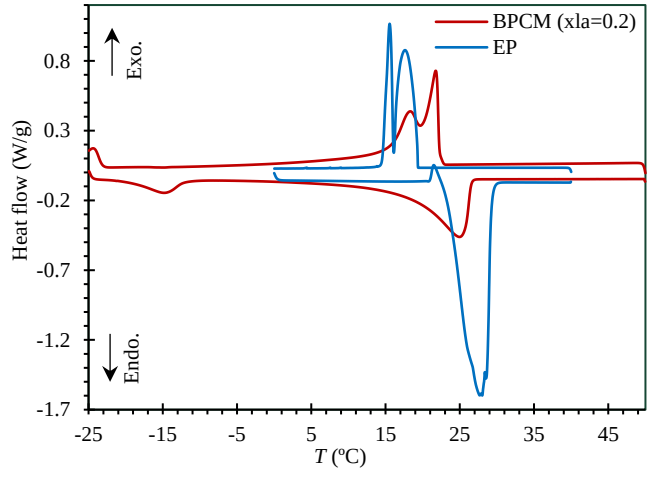

Figure 20. DSC curves of BPCM (x_{LA} = 0.20) and EP.

The calculated specific heat capacity during heating and cooling courses for BPCM (x_{LA} = 0.20) and EP are shown in Figure 21. At solid state (heating course, before melting), BPCM (x_{LA} = 0.20) has a specific heat capacity around 4.8 J/g K, which is higher than that for EP which is 3 J/g K. At liquid state (cooling course, before solidification), both materials showed an identical specific heat capacity around 3.7 J/g K. During phase transition, the parameter for EP is higher than that for BPCM (x_{LA} = 0.20).

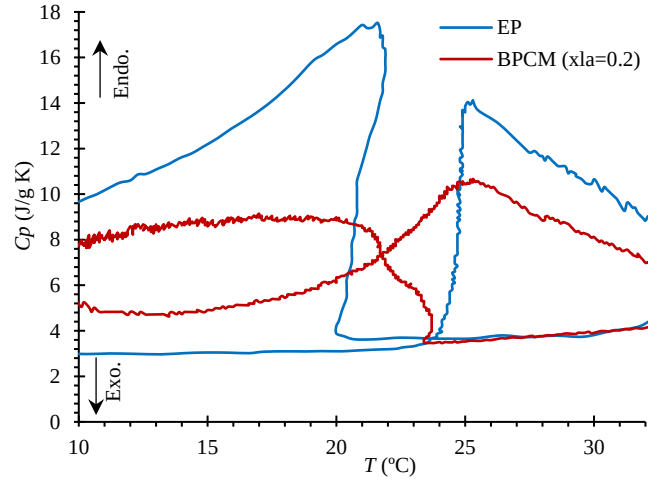

Figure 21. Melting and freezing specific heat capacity for BPCM (x_{LA} = 0.20) and EP.

The calculated enthalpy for BPCM (x_{LA} = 0.20) and EP during cooling and heating is shown in Figure 22. The samples release energy during cooling and the calculated enthalpy is negative while it turns positive during heating when the samples absorb heat. The effect of incongruency and supercooling can be observed for both materials during course of cooling. The enthalpy of EP is almost twice as higher as that of BPCM (x_{LA} = 0.20). The calculated melting and solidification enthalpies for BPCM (x_{LA} = 0.20) is respectively 104 and 78 J/g, while 200 and 160 J/g were calculated for EP.

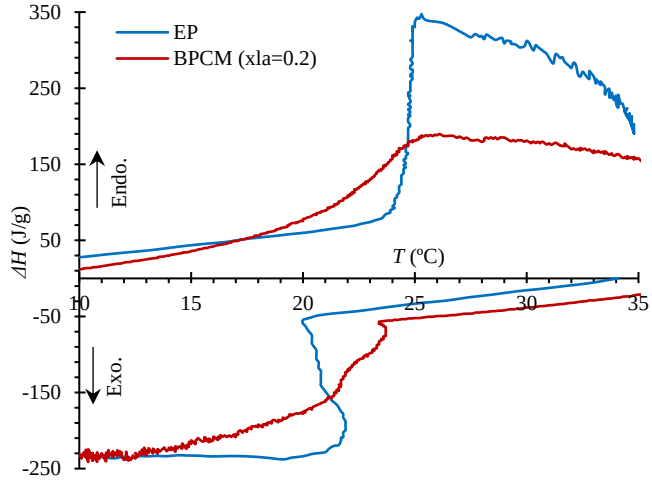

Figure 22. Melting and freezing enthalpy for BPCM (x_{LA} = 0.20) and EP.

The results showed that both materials have an appropriate working temperature range and reasonable latent heat. In terms of thermal performance, EP showed a better performance having higher enthalpy and congruent phase transition. However, a drawback of EP is its polymorphic nature leading to crystallinity [Papers II and V].

3.2 Solid Wood/BPCMs and wood particle/BPCMs

3.2.1 Incorporation of BPCMs into wood materials

Unmodified and thermally modified solid wood hosting BPCM-impregnation and leaching

The BPCM (x_{LA} = 0.20) was used for incorporation in solid and thermally modified solid wood species. The wood was impregnated and used to host and encapsulate BPCM (x_{LA} = 0.20) at WPG of 40-95 % (Table 1). It was found that Scots pine sapwood was easier to impregnate and WPGs of 56 % and 95 % were achieved while the maximum WPG for beech was 43 % due to its high density. Thermally modified pine (TMP), beech (TMB) and spruce (TMS) were impregnated, and found to be more permeable and easier to impregnate compared to unmodified samples. For thermally modified samples, a WPG of 95 % and 48 % for TMP and TMB were achieved. Spruce is a refractory wood species, but after thermal modification a WPG of 62 % was achieved confirming that thermal modification improved the impregnability of wood. The thermal modification causes thermal degradation of hemicelluloses i.e. the wood cell walls become more porous and easier for impregnation [Paper IV]. Pine was also impregnated with PEG 600 as a comparison PCM, with similar WPG as BPCM (x_{LA} = 0.20).

Although wood has large internal surface, micro- and nano cavities, e.g. cell lumen and walls, all the impregnated PCMs demonstrate leakage [Paper III]. In order to study the physical compatibility of BPCM (x_{LA} = 0.20) with solid unmodified and thermally modified samples, an intensive leaching test at 35 ºC for 24 h was conducted. The results showed that the maximum leaching of the BPCM from pine and beech wood reached 8 to 9 % respectively and 12 % for PEG. This demonstrated that the chemical structure and molecular mass of the PCM is of importance, e.g. PEG 600 is more susceptible for leaching that the BPCM (x_{LA} = 0.20). No relation between impregnation uptake and leaching was found. Thermally modified wood showed a better performance in hosting BPCM (x_{LA} = 0.20), with a maximum leakage of 5 % for TMB, 4 % for TMS and 4 and 3 % for the TMP with 95 and 48 % WPG respectively.

Wood particle-reinforced composites hosting EP elaboration

Another approach to accommodate a PCM in the wood structure is to develop a bio-composite of impregnated wood particles/fibers and a binder. Scots

pine particles, ELO and EP as BPCM were used in the study. The materials were blended and mould-pressed, followed by curing at 50 ºC for 12 h. It was observed that a part of EP on the surface of the particles leached out during the pressing step. In order to minimize the leaching of EP from the composite, various press forces and component proportions were tested. It was found that a press force of 1000 kg (12.3 kg/cm^2) and 12.5 % non-impregnated fibers in the composite were optimal to minimize leaching. Wood particles (25 %) impregnated with EP (25 % or WPG of 100 %) were used as the main part of the composite (i.e. 50 %). The non-impregnated fibers (12.5 %) in the composite played a role to absorb the exuded (or leached later) EP from the surface of the impregnated particles. Thus, the non-impregnated fibers facilitate the polymerization of ELO (37.5 %), which was the matrix binder of the composite. Since the curing/polymerization of ELO was conducted at 50 ºC for 12 h and no leaching was observed during this process, the composites were not tested for leaching at lower temperatures.

When a lower press force was applied, no EP was exuded but crystals were formed on the surface of the composite after curing. This problem was not observed when higher press forces were applied, probably because the exuded EP has been redistributed and absorbed in the non-impregnated fibers during pressing or partly leached during curing/polymerization of ELO. The problem was not reported in the literature since most of the produced composites were conducted in small scale without pressing [52, 53, 56].

3.2.2 Physical, hygroscopicity and biological performance of the composites

Distribution of the BPCM (x_{LA} = 0.20) in unmodified solid wood-microscopy

Figure 23 shows micrographs of impregnated and non-impregnated solid wood of Scots pine sapwood and beech. Non-impregnated samples were used as controls showing the anatomical elements of wood species. The reaction of the BPCM (x_{LA} = 0.20) with Oil Red O and OsO_4 was strong, and the presence of the BPCM (x_{LA} = 0.20) in the lumens of early- and latewood fibers of pine is shown in Figures 23b and c. Some fibers were full with the BPCM (x_{LA} = 0.20), while others were filled partially. The micrographs (Fig. 23b and c) furthermore confirmed that BPCM (x_{LA} = 0.20) penetrated into wood through the rays, ray fiber bordered pits and axial fiber bordered pits.

In addition, the darkish color of the cell wall when stained with OsO_4 confirmed the presence of BPCM (x_{LA} = 0.20) in the cell walls.

The penetration pathway pattern for beech solid wood was like pine, where the rays were the main pathway of the penetration of BPCM (x_{LA} = 0.20) into the cells confirmed with blackish staining of the rays in Figures 23e and f. In Figure 23e, the vessel lumens are partially filled as well as most of the fibers.

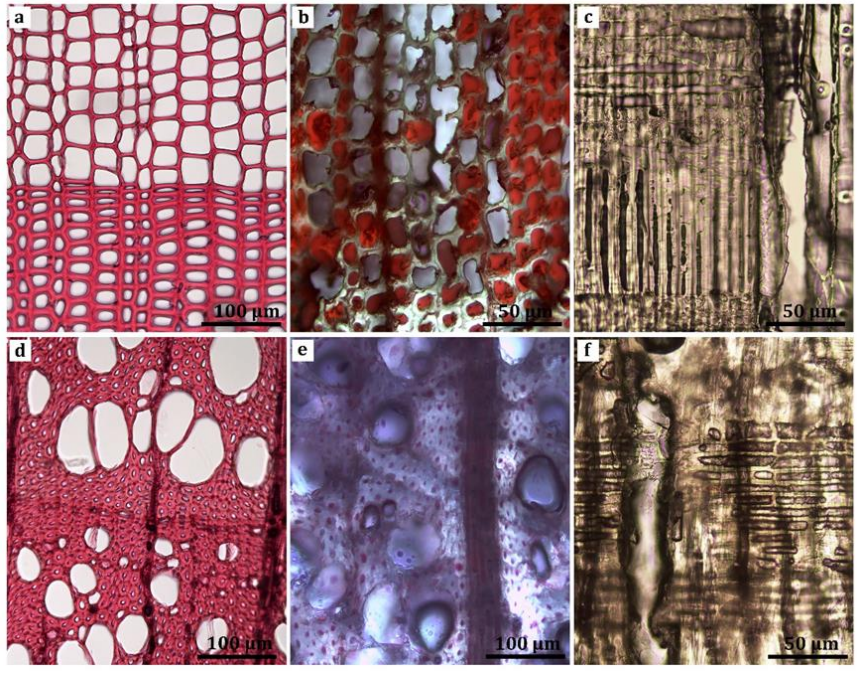

Figure 23. Safranin (Figs. 23a, d), Oil Red O (Figs. 23b, e) and osmium tetroxide (Figs. 23c, f) staining of Scots pine and beech samples impregnated with BPCM (x_{LA} = 0.20). Scots pine (a, b), transverse sections (TS) of untreated wood (a) and precipitates of BPCM (x_{LA} = 0.20) located in the cell lumens of fibers (b) and at fibers tips (c); Scots pine, radial-longitudinal section (RLS) section showing darkish staining of BPCM (x_{LA} = 0.20) present in the ray fibers and parenchyma cells and in the bordered pits and latewood cell lumens (c). The entire wood structure has reacted and has a redish/blackish colouration. Beech (d, e), TS of untreated wood (d) and precipitates of BPCM (x_{LA} = 0.20) located mainly in the fiber, rays and vessel lumens (e); Beech, TS and RLS of a broad homogeneous ray filled with BPCM (x_{LA} = 0.20) (e, f). The adjacent vessel in (f) has a thin film of BPCM (x_{LA} = 0.20) on the cell wall surface.

Susceptibility to mold discoloration of the solid wood hosting BPCM

Susceptibility of the building materials to mold growth is important since a release of mycotoxins due to mold growth can affect the health of the occupants [75]. This is even more important when BPCMs are incorporated in bio-based buildings envelopes for energy storage. The mold test was conducted to study and compare thermally modified solid wood impregnated with BPCM (x_{LA} = 0.20) with non-impregnated samples in terms of mold growth and discoloration. The results of the test in laboratory condition at optimal temperature and RH for the selected fungi are shown in Table 5.

It is observed that untreated beech wood reached rate 5 showing that the wood species is very susceptible to mold growth after only 4 weeks exposure. The pattern for pine and spruce species was found similar with rates of 4 and 3 after 8 weeks exposure. The untreated wood is very susceptible to mold growth due to the amount of available low-molecular sugars on the wood surface, e.g. glucose, fructose and sucrose [76, 77]; similar results were reported for Scots pine [78]. Although the susceptibility of spruce to mold growth varies in the literature, the present and other studies classified spruce as more resistance to mold growth compared to pine [78, 79]. The improvement of wood by thermal modification to mold growth resistance was found significant compared to unmodified solid wood. The tested thermally modified wood was not covered with mold more than 10-20 % confirming the findings of previous studies [78, 80, 81]. This is caused by the lower equilibrium moisture content of thermally modified wood compare to unmodified wood and significantly less available nutrients on the wood surface [82].

After impregnation with BPCM (x_{LA} = 0.20), all solid wood samples showed better resistance to mold growth compare to non-impregnated solid wood while the thermally modified wood impregnated with BPCM (x_{LA} = 0.20) performed best. The results showed rates of 2 and 4 for TMP and TMB samples with BPCM (x_{LA} = 0.20), while the TMS with the BPCM (x_{LA} = 0.20) was rated as 1. It is observed that the WPG had certain influence on the mold growth; the higher WPG leads to higher susceptibility to mold growth. While the BPCM (x_{LA} = 0.20) is a mixture of fatty acids that are nutrients for the mold fungi, it serves as a water-repellent formulation in wood that can postpone moisture adsorption. In addition, the growth of the most common airborne fungal genera *Cladosporium* spp., *Penicillium* spp, *Aspergillus* spp. and non-sporulating molds [83, 84] found in indoor environments can be

limited by availability of moisture. Therefore, the mold discoloration on thermally modified and thermally modified impregnated wood with BPCM (x_{LA} = 0.20) is lower compared to the non-impregnated and unmodified solid wood.

Table 5. Ratings of mold growth and discoloration on unmodified, thermally modified and thermally modified samples impregnated with BPCM (x_{LA} = 0.20) (0 – no visible growth; 1 – covering up to 10 % of surface; 2 – covering between 10 % and 30 %; 3 – covering between 30 % and 70 %; 4 – more than 70 % of surface; 5 – 100 % coverage).

Wood species and treatments	**2 weeks**	**4 weeks**	**6 weeks**	**8 weeks**
Scots pine	2	3	4	4
TMP	0	0	1	1
TMP/BPCM(x_{LA} = 0.20) 45 %	1	1	2	2
TMP/BPCM(x_{LA} = 0.20) 91 %	1	2	3	4
Spruce	2	3	3	3
TMS	0	0	0	1
TMS/BPCM(x_{LA} = 0.20) 58 %	0	1	1	1
Beech	4	5	5	5
TMB	1	1	2	2
TMB/BPCM(x_{LA} = 0.20) 43 %	2	2	3	4

Moisture adsorption/desorption ability of wood particle-reinforced composites hosting EP

The behavior of the wood particle composites with, and without EP to various humidity conditions was studied in a climate chamber at constant temperature of 23 ºC and RH of 50, 75, 95 and 33 %. After 24 h at each RH, the composites were weighed and the results shown in Figure 24. Compared to the initial weight, at 50 % RH, the composites lost mass. At RH of 95 %, 3.6 % and 5.9 % moisture was gained for the composite with and without EP showing that the presence of EP in the composite postponed/hindered the moisture adsorption. However, when the RH decreased from 95 to 33 %, the composite with EP lost 3.3 % and the composite without EP lost 6.8 % of its mass. By comparing the results of 95 and 33 % RH, the MBV, was calculated according to the Nordtest protocol [Paper V] and [57, 60]. The parameter for the composites with EP is 2.07 g/m^2 RH%, and for the composites without EP 3.2 g/m^2 RH%. The MBV showed that in both cases the value is higher than 2 g/m^2 RH%, showing the composites were in the “excellent material category”, according to Nordtest project [Paper V] and [60].

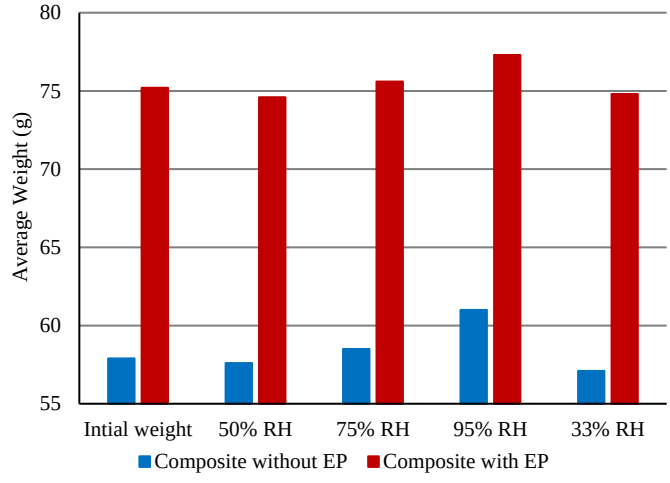

Figure 24. Moisture adsorption/desorption test for wood particle-reinforced composites at various relative humidity.

3.2.3 Thermal characteristics of the composites

Thermal conductivity of solid and thermally modified wood hosting BPCM (x_{LA} = 0.20)

Thermal conductivity of the solid and thermally modified wood was measured with a heat-flow-meter method. It was found that the thermal conductivity of untreated beech wood is higher than that of pine wood. The value of thermally modified wood was lower than that of unmodified solid wood. The conductivity along the radial direction for pine, spruce and beech was 0.11, 0.12 and 0.23 W/m K respectively, while after thermal modification the conductivity of the TMB, TMS and TMP was 0.11, 0.07 and 0.06 W/m K. The results in the study are in an agreement with the literature [85, 86]. The thermal conductivity of wood depends on the density, moisture content and wood species with a decrease after thermal modification [85, 86]. After impregnation with BPCM (x_{LA} = 0.20), it was observed that the thermal conductivity of all samples improved depending on the WPG. Since the thermal conductivity of pure BPCM (x_{LA} = 0.20) was 0.2 W/m K at liquid state and 0.35 W/m K at solid state [Paper II], i.e. higher than that of wood, the thermal conductivity of the impregnated wood was higher compared to non-impregnated wood. The conductivity of impregnated pine with 48 and 87 % WPG (after leaching) was 0.13 and 0.16

W/m K; for beech with 34 % WPG the conductivity was 0.255 W/m K. Impregnated TMP with 45 and 91 % WPG demonstrated thermal conductivity of 0.1 and 0.14 W/m K. A value of 0.12 W/m K was measured for TMS with 58 % WPG and 0.13 W/m K for TMB with 43 % WPG. The result showed an increase of the conductivity with 8.3 and 33 % for the lowest and highest WPG (after leaching), which was in agreement with previous studies. In a study [87], the thermal conductivity of carbonized pristine wood was 0.414 W/m K. When the wood was impregnated with 1-tetradecanol as PCM (with conductivity of 0.241 W/m K) a thermal conductivity of 0.515 W/m K was reported, i.e. 24 % improvement. The reported results [87] are in agreement with the results of the present study.

Thermal stability of wood particle-reinforced composite hosting EP

Thermal stability of the components forming the composite of wood particles with EP was analysed using TGA. The results depicted in Figure 25 show that ELO polymer matrix is thermally stable up to 325 ºC, at which the matrix starts to degrade and it is completely degraded at 475 ºC, concluding that the polymer matrix ensures a good thermal stability. EP demonstrates no change below 150 ºC. Above this temperature, the material lost 24 %, due likely to degradation of ester moieties when heated further to 220 ºC and completely degraded at 325 ºC. The wood particle composite with EP demonstrates three stages of degradation. The wood moisture and the organic solvent in the composite start to evaporate at temperatures below 100 ºC and up to 220 ºC when 4 % mass loss of the composite was recorded. The second step starts at 210 ºC and continues to 320 ºC, where EP is almost degraded and the composite lost 33 %. At temperatures around 325 ºC, the other components including polymer matrix, wood particles and binding fibers start to degrade and at 450 ºC only 10 % residues remain. The results show that the wood particle composite with EP is thermally stable within the expected working temperature range.

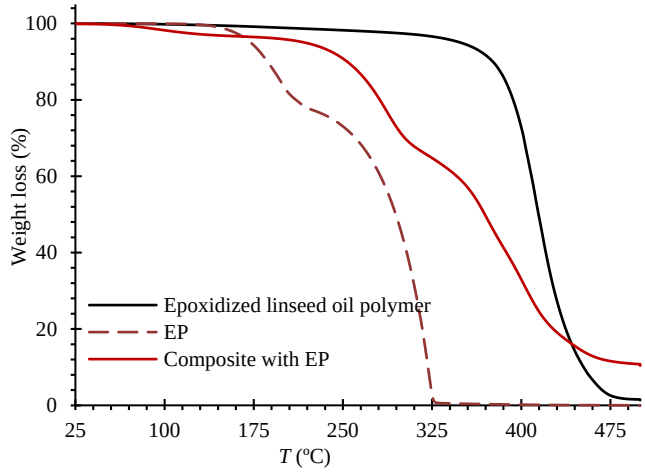

Figure 25. TGA curves for pure EP, epoxidized linseed oil polymer and the wood particle composite with EP.

Temperature behaviour of the composites over time during cooling and heating courses

Temperature behavior of solid wood, thermally modified wood impregnated with BPCM (x_{LA} = 0.20) and composite of wood particles with EP during cooling and heating is shown in Figures 26 and 27. The temperature behavior results were also compared with control materials without BPCMs and a reference (Cu plate).

When the samples were placed in the chamber at low temperature, they started to cool down (Fig. 26) until they reached a temperature at around 24 ºC, at which solid and thermally modified wood with BPCM (x_{LA} = 0.20) started to solidify with solidification completed at 22 ºC. The solidification temperature for the impregnated wood was found slightly lower than that of pure BPCM (x_{LA} = 0.20). The pattern for composites made of wood particle with EP was different from that of solid wood, observing incongruent solidification during the cooling process. The composite started to solidify at 19 ºC and was completely solidified at 12 ºC, i.e. a temperature lower than that of pure EP. The pure BPCM (x_{LA} = 0.20) and EP experienced some degree of supercooling, while this phenomenon was not observed for the composites. In addition, BPCM (x_{LA} = 0.20) underwent incongruent freezing while it was not the case for solid and thermally modified wood with BPCM (x_{LA} = 0.20). Although the pure EP solidified congruently, the wood particle composite with EP demonstrated incongruent solidification.

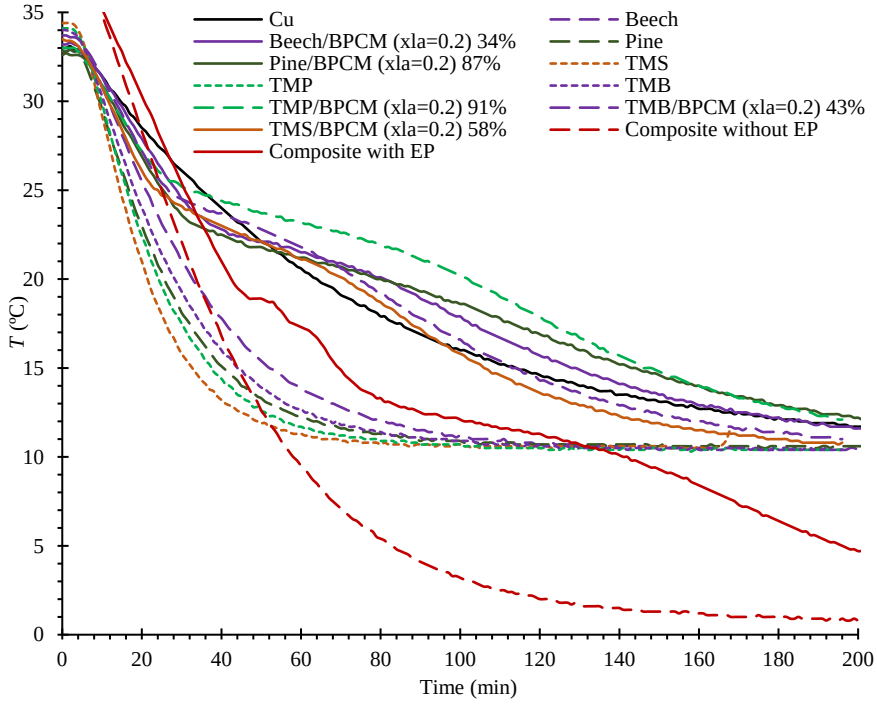

Figure 26. T-history curves over cooling cycle of solid, thermally modified wood and wood particle composite with BPCMs.

During the heating cycle (Fig. 27), pure BPCM (x_{LA} = 0.20), solid and thermally modified wood with BPCM (x_{LA} = 0.20) melt congruently and a slight temperature increase for the solid and thermally modified wood was observed when compared to pure BPCM (x_{LA} = 0.20). Unlike solid and thermally modified wood with BPCM (x_{LA} = 0.20), the wood particle composite with EP demonstrated incongruent melting confirmed by two melting points at 18 and 23 ºC, and a shift to lower temperature compared to EP was observed, which melted congruently at 24.7 ºC.

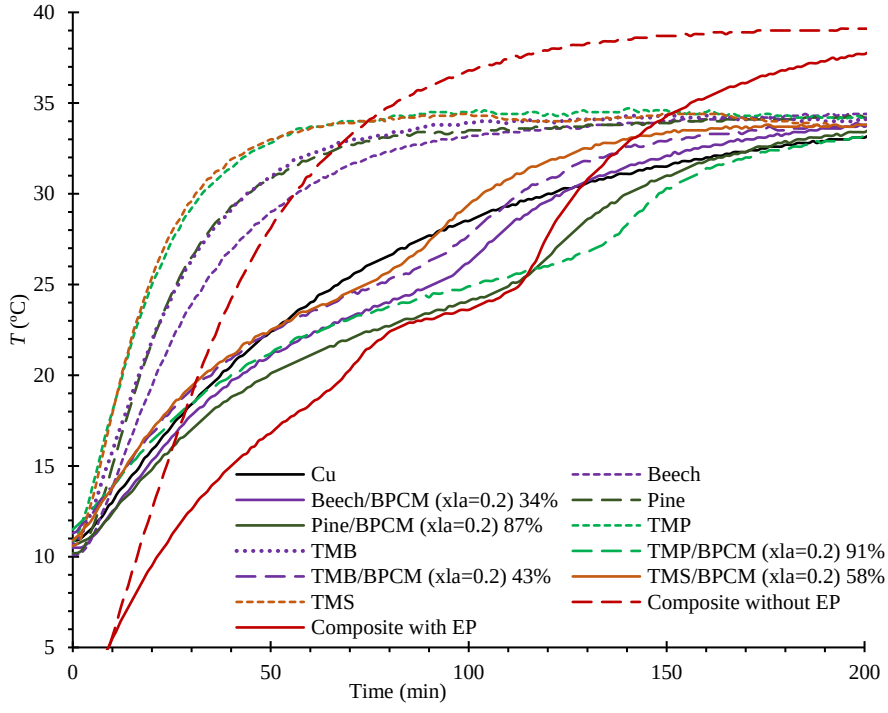

Figure 27. T-history curves over heating cycle of solid, thermally modified wood and wood particle composite with BPCMs.

The thermal behavior of the solid wood and wood composite is not related to the wood species but depends on the amount and enthalpy of the incorporated BPCM. It is observed that the wood particles composite containing 25 % EP can maintain the temperature constant almost as long as the solid wood with BPCM (x_{LA} = 0.20) but at significantly higher WPG.

The temperature profile over time shows that the control composites without BPCMs reached the equilibrium temperature faster than composites hosting BPCMs; the thermally modified wood species reached equilibrium temperature faster than the unmodified wood. This is due to the fact that the temperature profile over time is a function of thermal mass (heat capacity, mC_p) of the materials. Increase in the thermal mass leads to an increase of the ability to absorb and store energy. Materials with higher density can absorb and store more energy resulting in resistance to temperature change and postponing the process of equilibrium. Although the controls without BPCMs have similar specific heat capacity, the solid untreated wood has slightly higher density than the thermally modified wood and thus, performs

better by keeping the temperature constant for longer period. After impregnation of BPCMs in the solid wood, the specific heat capacity and density increased resulting in increased thermal mass. This allowed absorption and storage of more energy in the materials during heating and release of more energy during the cooling process. Therefore, the material demonstrates a delay in reaching the ambient temperature.

Specific heat capacity of the solid wood and wood particle-based composites

The calculated specific heat capacity of solid wood, thermally modified wood, wood particle-reinforced composite – all of the above mentioned with and without BPCMs, is shown in Figures 28 and 29. The heat capacity of wood materials is not related to density and wood species but mainly to the temperature and wood moisture content [85]. Therefore, the specific heat capacity of solid wood, thermally modified wood and wood particle-reinforced composite before incorporation of BPCMs (Fig. 28) were found similar at approximately 2 J/g K, which is in line with previous studies [85, 86]. The specific heat capacity of the wood particle-reinforced composite without EP was found slightly higher than that of solid wood, due to the other components of the composite that have an effect on the specific heat capacity. After incorporation of the BPCMs, the specific heat capacity of the solid wood and thermally modified wood showed an increase with values between 3.8 to 5 J/g K depending on the WPG. The wood particle-reinforced composite hosting EP showed a specific heat capacity of approximately 4 J/g K, i.e. an increase caused by the presence of EP, although its WPG was lower compared to solid wood (Fig. 29).

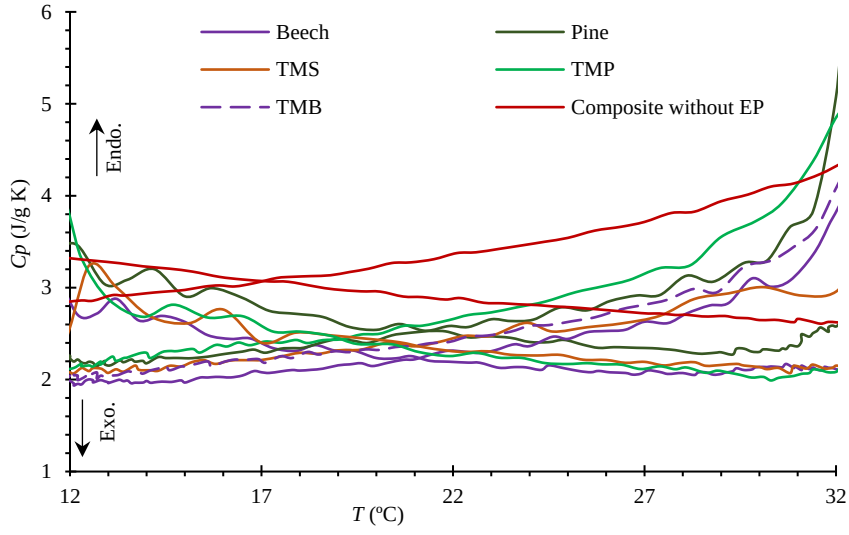

Figure 28. Specific heat capacity of solid, thermally modified wood and wood particle-reinforced composite before incorporation of BPCMs over heating/cooling courses.

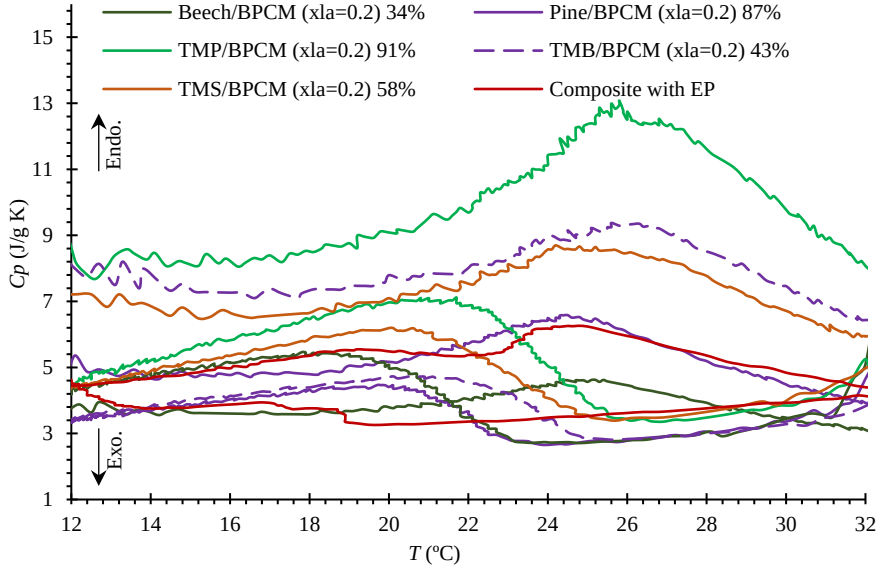

Figure 29. Melting and freezing specific heat capacity of solid, thermally modified wood and wood particle composite after incorporation of BPCMs.

Enthalpy of the elaborated materials

Figure 30 shows the calculated enthalpy for solid wood, thermally modified wood and wood particle-reinforced composites before and after incorporation of the BPCMs. The pattern of the wood and composite without BPCMs is linear where the enthalpy increases or decreases linearly with increase or decrease of the temperature, i.e. showing that the materials can absorb and release energy in terms of sensible heat.

During the phase transition, the wood and composite with BPCMs absorb and release certain amount of energy in terms of latent heat while, before and after the phase transition and likewise the materials without BPCMs, the impregnated materials handle energy in terms of sensible heat. Similar behavior for wood/BPCM is reported [2] where a dynamic heat flowmeter apparatus (DHFMA) was used. Additionally, it was found that the latent heat of fusion is proportional to the amount and enthalpy of the BPCMs incorporated into material. The latent heat of pure BPCM (x_{LA} = 0.20) and EP was reported as 100 and 200 J/g [Papers II and V], while impregnated in solid wood, the latent heat reduced to 30-44 J/g depending on the WPG. Wood particle-reinforced composite containing EP demonstrated a latent heat of 50 J/g. Despite the fact that the amount of EP is lower than the amount of BPCM (x_{LA} = 0.20) in solid wood, the enthalpy of the wood particle-reinforced composite is higher due to higher enthalpy of EP compared to BPCM (x_{LA} = 0.20). The results showed that the wood species does not affect the value of enthalpy while the type and amount of the BPCM determine the enthalpy of the material.

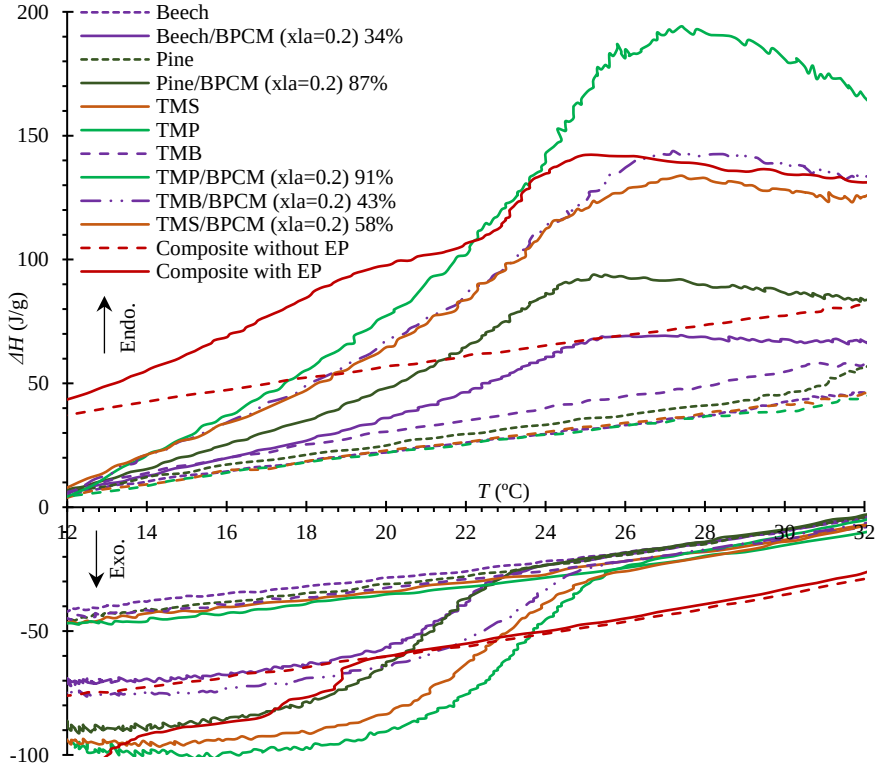

Figure 30. Melting and freezing enthalpy of solid, thermally modified wood and wood particle-reinforced composite with, and without BPCMs.

Thermal cycling performance of wood particle composites containing EP

Thermal cycling behavior of the wood particle-reinforced composites with, and without EP was studied in two identical cubes at temperatures varying between 0 and 40 ºC during a 2-week long heating/cooling process (Fig. 31). The monitored temperature over time inside the cubes demonstrates the efficiency of the wood particle-reinforced composite containing EP compared to that without EP. When the ambient temperature changes from 0 to 40 ºC, the temperature inside the cube with EP changes from 13 to 28 ºC while in the cube without EP the change is from 4 to 38 ºC. The above demonstrates that the cube with EP resists better to temperature fluctuation with storing and releasing thermal energy. The consistency of the temperature profile inside the cube with EP confirms that leakage of EP does not occur, or was insignificant.

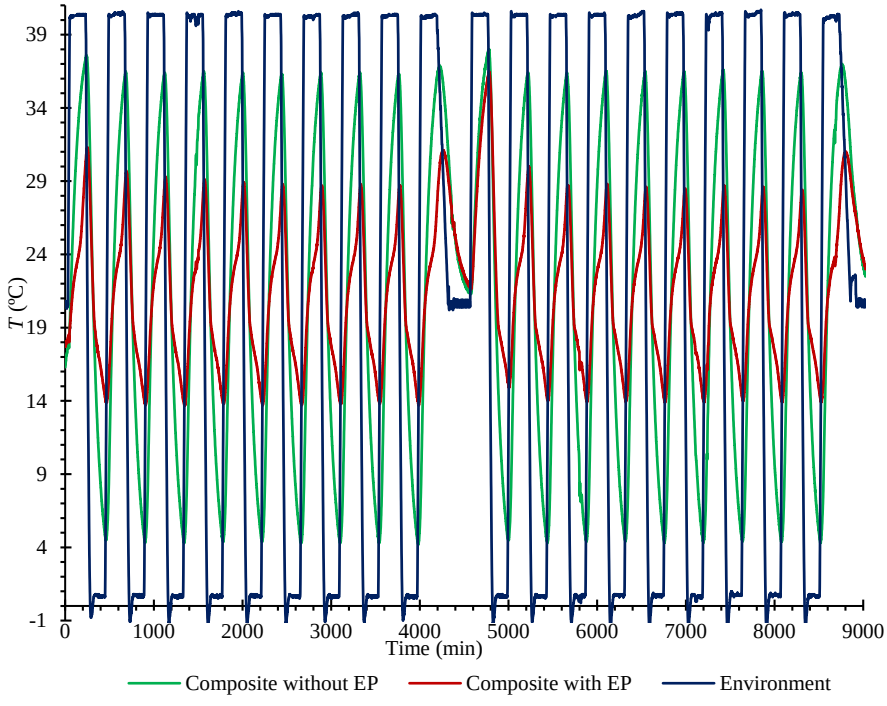

Figure 31. Thermal cycling patterns in test cubes made of wood particle composite with, and without EP.

4. Concluding remarks

This study aimed to fundamentally investigate the incorporation of BPCMs into wood-based materials producing energy-smart bio-composites for indoor use in buildings. A new BPCM was developed and compared to a commercial and lesser-used but promising BPCM. The challenges, improvements and limitations of the wood-based composites with these BPCMs were comprehensively studied.

The study showed that a passive system of BPCMs incorporated in buildings envelopes must be used to control the energy intermittency inside residential buildings for more efficient energy use in cold climate regions. The literature review revealed that the main BPCMs are fatty acids, esters and their eutectic mixtures. Although fatty acids possess desirable properties such as non-corrosivity, high latent heat of fusion, non-toxicity, reasonable thermal and chemical stability with no environmental impact, there are no pure fatty acids with indoor comfort temperature for building applications. This limitation together with the high cost of the BPCMs restricts their applications in buildings and constructions.

Considering the summarized knowledge, this study developed a new BPCM based on CO. CO was converted to CoFA and mixed with LA and OA. It was found that the multicomponent mixture of CoFA/LA at ratio 80:20 % (wt) had the best performance with 100 J/g latent heat of fusion, melting and freezing temperatures in the appropriate working range i.e. 18-25 ºC, and was thermally and chemically stable after 700 heating/cooling cycles.

The BPCM (x_{LA}= 0.2) was incorporated into solid wood of Scots pine, beech and thermally modified wood of pine, beech and spruce. The results confirmed the improvement in the thermal mass of the impregnated samples compared to non-impregnated controls. In terms of impregnability and

compatibility of the BPCM (x_{LA}= 0.2) with wood materials, it was found that thermally modified wood was easier to impregnate and retained better the BPCM in the structure compared to the unmodified solid wood. Solid and thermally modified wood had specific heat capacity of 2 J/g K, which increased to 3-5 J/g K after impregnation with the BPCM. The latent heat of fusion for impregnated unmodified and thermally modified wood was found proportional to the amount of impregnated BPCM (x_{LA}= 0.2). It was furthermore revealed that the thermal conductivity also increased by incorporation of BPCM (x_{LA}= 0.2) in wood.

Another achievement of the study was the production and characterization of a fully bio-based composite consisting of industrial bi-products (wood particles and fibers) with EP as BPCM. The study revealed certain challenges regarding the incorporation of EP and compatibility with wood material. The approach with incorporation of the ester in sawdust particles and composite of particles showed that 25 % EP in the composite would minimize the problem of leakage. Thermal stability tests of the composite confirmed stability up to 200 ºC. DSC results confirmed that some changes at the melting peak point which are probably related to crystallinity of the ester. Thermal characteristics showed that the composite had high thermal mass with ability to store and release energy in terms of latent heat of fusion at around 50 J/g, with heat capacity at around 3 J/g K. Thermal cycling analysis confirmed the effect of composite with EP compared to those without EP. It was also observed that the composite had a good thermal cycling stability.

Using sawdust as bio-based material to host BPCM making energy smart composites for building applications showed a promising opportunity to manage industrial waste and add value to a less valuable industrial bi-product. The study revealed the promising thermal properties of the new biomaterials.

5. Future work

Most studied BPCMs with properties suitable for indoor building applications have been eutectic mixture of fatty acids, esters and raw vegetable oils. The mixtures consist most often of capric acid blended with stearic, palmitic or lauric acids, in which the largest part is capric acid. Although these BPMCs showed a reliable thermal and chemical performance for the application, capric acid has a bad odor and the additional organic constituents make the eutectic mixtures expensive and restrict their use. The developed BPCM in the present work originated from coconut oil and addressed both mentioned problems, but in terms of thermal properties, it showed moderate performance. In addition, the main limitation of the studied ester is its crystallization and compatibility within bio-based matrixes. Therefore, cheaper and more reliable BPCMs from agricultural origin and industrial wastes need to be developed. Research works regarding incorporation of BPCMs in wood materials have not comprehensively investigated and handled problems with leakage and industrial scale production. There is a promising opportunity in using other wastes from the wood-working industries to produce bio-based energy smart composites with BPCMs. This requires finding additional and better bio-based binders and BPCMs. Lightweight materials with higher thermal mass using BPCMs, bio-based binders and wood materials are another opportunity for future research.

References

[1] Ramage, M.H., Burridge, H., Busse-Wicher, M., Fereday, G., Reynolds, T., Shah, D.U., Wu, G., Yu, L., Fleming, P., Densley-Tingley, D. and Allwood, J., 2017. The wood from the trees: The use of timber in construction. *Renewable and Sustainable Energy Reviews*, 68, pp.333-359.

[2] Mathis, D., Blanchet, P., Landry, V. and Lagière, P., 2018. Impregnation of wood with microencapsulated bio-based phase change materials for high thermal mass engineered wood flooring. *Applied Sciences*, 8(12), p.2696.

[3] Pasupathy, A., Velraj, R. and Seeniraj, R.V., 2008. Phase change material-based building architecture for thermal management in residential and commercial establishments. *Renewable and Sustainable Energy Reviews*, 12(1), pp.39-64.

[4] Tyagi, V.V., Kaushik, S.C., Tyagi, S.K. and Akiyama, T., 2011. Development of phase change materials based microencapsulated technology for buildings: a review. *Renewable and sustainable energy reviews*, 15(2), pp.1373-1391.

[5] Bland, A., Khzouz, M., Statheros, T. and Gkanas, E.I., 2017. PCMs for residential building applications: A short review focused on disadvantages and proposals for future development. *Buildings*, 7(3), p.78.

[6] Souayfane, F., Fardoun, F. and Biwole, P.H., 2016. Phase change materials (PCM) for cooling applications in buildings: A review. *Energy and buildings*, 129, pp.396-431.

[7] Kenisarin, M. and Mahkamov, K., 2016. Passive thermal control in residential buildings using phase change materials. *Renewable and sustainable energy reviews*, 55, pp.371-398.

[8] Kuznik, F., David, D., Johannes, K. and Roux, J.J., 2011. A review on phase change materials integrated in building walls. *Renewable and Sustainable Energy Reviews*, 15(1), pp.379-391.

[9] Kalnæs, S.E. and Jelle, B.P., 2015. Phase change materials and products for building applications: A state-of-the-art review and future research opportunities. *Energy and Buildings*, 94, pp.150-176.

[10] Sharma, R.K., Ganesan, P., Tyagi, V.V., Metselaar, H.S.C. and Sandaran, S.C., 2015. Developments in organic solid–liquid phase change materials and their applications in thermal energy storage. *Energy Conversion and Management*, 95, pp.193-228.

[11] Amaral, C., Vicente, R., Marques, P.A.A.P. and Barros-Timmons, A., 2017. Phase change materials and carbon nanostructures for thermal energy

storage: A literature review. *Renewable and Sustainable Energy Reviews*, 79, pp.1212-1228.

[12] Agyenim, F., Hewitt, N., Eames, P. and Smyth, M., 2010. A review of materials, heat transfer and phase change problem formulation for latent heat thermal energy storage systems (LHTESS). *Renewable and sustainable energy reviews*, 14(2), pp.615-628.

[13] Nazir, H., Batool, M., Osorio, F.J.B., Isaza-Ruiz, M., Xu, X., Vignarooban, K., Phelan, P. and Kannan, A.M., 2019. Recent developments in phase change materials for energy storage applications: A review. *International Journal of Heat and Mass Transfer*, 129, pp.491-523.

[14] Konuklu, Y., Ostry, M., Paksoy, H.O. and Charvat, P., 2015. Review on using microencapsulated phase change materials (PCM) in building applications. *Energy and Buildings*, 106, pp.134-155.

[15] Pielichowska, K. and Pielichowski, K., 2014. Phase change materials for thermal energy storage. *Progress in materials science*, 65, pp.67-123.

[16] Hepburn, C., Adlen, E., Beddington, J., Carter, E.A., Fuss, S., Mac Dowell, N., Minx, J.C., Smith, P. and Williams, C.K., 2019. The technological and economic prospects for CO2 utilization and removal. *Nature*, 575(7781), pp.87-97.

[17] Amiri, A., Ottelin, J., Sorvari, J. and Junnila, S., 2020. Cities as carbon sinks—classification of wooden buildings. *Environmental Research Letters*, 15(9), p.094076.

[18] Omer, M.A. and Noguchi, T., 2020. A conceptual framework for understanding the contribution of building materials in the achievement of Sustainable Development Goals (SDGs). *Sustainable Cities and Society*, 52, p.101869.

[19] Toppinen, A., Röhr, A., Pätäri, S., Lähtinen, K. and Toivonen, R., 2018. The future of wooden multistory construction in the forest bioeconomy–a Delphi study from Finland and Sweden. *Journal of forest economics*, 31, pp.3-10.

[20] Wen, B., Musa, S.N., Onn, C.C., Ramesh, S., Liang, L., Wang, W. and Ma, K., 2020. The role and contribution of green buildings on sustainable development goals. *Building and Environment*, 185, p.107091.

[21] Cabeza, L.F., Barreneche, C., Martorell, I., Miró, L., Sari-Bey, S., Fois, M., Paksoy, H.O., Sahan, N., Weber, R., Constantinescu, M. and Anghel, E.M., 2015. Unconventional experimental technologies available for phase change materials (PCM) characterization. Part 1. Thermophysical properties. *Renewable and Sustainable Energy Reviews*, 43, pp.1399-1414.

[22] Baetens, R., Jelle, B.P. and Gustavsen, A., 2010. Phase change materials for building applications: A state-of-the-art review. *Energy and buildings*, 42(9), pp.1361-1368.

[23] Sharma, A., Tyagi, V.V., Chen, C.R. and Buddhi, D., 2009. Review on thermal energy storage with phase change materials and applications. *Renewable and Sustainable energy reviews*, 13(2), pp.318-345.

[24] Sarier, N. and Onder, E., 2012. Organic phase change materials and their textile applications: an overview. *Thermochimica acta*, 540, pp.7-60.
[25] Yuan, Y., Zhang, N., Tao, W., Cao, X. and He, Y., 2014. Fatty acids as phase change materials: a review. *Renewable and Sustainable Energy Reviews*, 29, pp.482-498.
[26] Rozanna, D., Chuah, T.G., Salmiah, A., Choong, T.S. and Sa'Ari, M., 2005. Fatty acids as phase change materials (PCMs) for thermal energy storage: a review. *International journal of green energy*, 1(4), pp.495-513.
[27] Karaipekli, A. and Sarı, A., 2010. Preparation, thermal properties and thermal reliability of eutectic mixtures of fatty acids/expanded vermiculite as novel form-stable composites for energy storage. *Journal of Industrial and Engineering Chemistry*, 16(5), pp.767-773.
[28] Sharma, A., Shukla, A., Chen, C.R. and Dwivedi, S., 2013. Development of phase change materials for building applications. *Energy and Buildings*, 64, pp.403-407.
[29] Ke, H., Li, D., Zhang, H., Wang, X., Cai, Y., Huang, F. and Wei, Q., 2013. Electrospun form-stable phase change composite nanofibers consisting of capric acid-based binary fatty acid eutectics and polyethylene terephthalate. *Fibers and Polymers*, 14(1), pp.89-99.
[30] Sarı, A., 2005. Eutectic mixtures of some fatty acids for low temperature solar heating applications: Thermal properties and thermal reliability. *Applied Thermal Engineering*, 25(14-15), pp.2100-2107.
[31] Shilei, L., Neng, Z. and Guohui, F., 2006. Eutectic mixtures of capric acid and lauric acid applied in building wallboards for heat energy storage. *Energy and Buildings*, 38(6), pp.708-711.
[32] Dimaano, M.N.R. and Watanabe, T., 2002. The capric–lauric acid and pentadecane combination as phase change material for cooling applications. *Applied Thermal Engineering*, 22(4), pp.365-377.
[33] Nikolić, R., Marinović-Cincović, M., Gadžurić, S. and Zsigrai, I.J., 2003. New materials for solar thermal storage—solid/liquid transitions in fatty acid esters. *Solar energy materials and solar cells*, 79(3), pp.285-292.
[34] Xu, S., Zou, L., Ling, X., Wei, Y. and Zhang, S., 2014. Preparation and thermal reliability of methyl palmitate/methyl stearate mixture as a novel composite phase change material. *Energy and buildings*, 68, pp.372-375.
[35] Feldman, D., Shapiro, M.M. and Banu, D., 1986. Organic phase change materials for thermal energy storage. *Solar energy materials*, 13(1), pp.1-10.
[36] Feldman, D., Banu, D. and Hawes, D.W., 1995. Development and application of organic phase change mixtures in thermal storage gypsum wallboard. *Solar Energy Materials and Solar Cells*, 36(2), pp.147-157.
[37] Ke, H. and Li, Y., 2017. A series of electrospun fatty acid ester/polyacrylonitrile phase change composite nanofibers as novel form-stable phase change

materials for storage and retrieval of thermal energy. *Textile Research Journal*, 87(19), pp.2314-2322.
[38] Lawer-Yolar, G., Dawson-Andoh, B. and Atta-Obeng, E., 2019. Novel phase change materials for thermal energy storage: evaluation of tropical tree fruit oils. *Biotechnology Reports*, 24, p.e00359.
[39] Thaib, R., Amin, M. and Umar, H., 2019. Thermal properties of beef tallow/coconut oil bio PCM using t-history method for wall building applications. *European Journal of Engineering and Technology Research*, 4(11), pp.38-40.
[40] Saleel, C.A., Mujeebu, M.A. and Algarni, S., 2019. Coconut oil as phase change material to maintain thermal comfort in passenger vehicles. Journal of *Thermal Analysis and Calorimetry*, 136(2), pp.629-636.
[41] Irsyad, M., 2017, March. Heat transfer characteristics of coconut oil as phase change material to room cooling application. *In IOP Conference Series: Earth and Environmental Science* (Vol. 60, No. 1, p. 012027). IOP Publishing.
[42] Kahwaji, S. and White, M.A., 2019. Edible oils as practical phase change materials for thermal energy storage. *Applied Sciences*, 9(8), p.1627.
[43] Falk, R.H., 2009. Wood as a sustainable building material. *Forest products journal*. Vol. 59, no. 9 (Sept. 2009): pages 6-12., 59(9), pp.6-12.
[44] Esteves, B. and Pereira, H., 2009. Wood modification by heat treatment: A review. *BioResources*, 4(1), pp.370-404.
[45] Song, S., Leng, H., Xu, H., Guo, R. and Zhao, Y., 2020. Impact of urban morphology and climate on heating energy consumption of buildings in severe cold regions. *International Journal of Environmental Research and Public Health*, 17(22), p.8354.
[46] Khudhair, A.M. and Farid, M., 2021. A review on energy conservation in building applications with thermal storage by latent heat using phase change materials. *Thermal Energy Storage with Phase Change Materials*, pp.162-175.
[47] De Gracia, A., Navarro, L., Castell, A., Ruiz-Pardo, Á., Alvárez, S. and Cabeza, L.F., 2013. Experimental study of a ventilated facade with PCM during winter period. *Energy and Buildings*, 58, pp.324-332.
[48] Liang, J., Zhimeng, L., Ye, Y., Yanjun, W., Jingxin, L. and Changlin, Z., 2018. Fabrication and characterization of fatty acid/wood-flour composites as novel form-stable phase change materials for thermal energy storage. *Energy and Buildings*, 171, pp.88-99.
[49] Cheng, L. and Feng, J., 2020. Form-stable phase change materials based on delignified wood flour for thermal management of buildings. *Composites Part A: Applied Science and Manufacturing*, 129, p.105690.

[50] Ma, L., Wang, Q. and Li, L., 2019. Delignified wood/capric acid-palmitic acid mixture stable-form phase change material for thermal storage. *Solar Energy Materials and Solar Cells*, 194, pp.215-221.

[51] Hekimoğlu, G., Sarı, A., Önal, Y., Gencel, O., Tyagi, V.V. and Aslan, E., 2022. Utilization of waste apricot kernel shell derived-activated carbon as carrier framework for effective shape-stabilization and thermal conductivity enhancement of organic phase change materials used for thermal energy storage. *Powder Technology*, 401, p.117291.

[52] Hekimoğlu, G., Sarı, A., Kar, T., Keleş, S., Kaygusuz, K., Tyagi, V.V., Sharma, R.K., Al-Ahmed, A., Al-Sulaiman, F.A. and Saleh, T.A., 2021. Walnut shell derived bio-carbon/methyl palmitate as novel composite phase change material with enhanced thermal energy storage properties. *Journal of Energy Storage*, 35, p.102288.

[53] Hekimoğlu, G., Sarı, A., Kar, T., Keleş, S., Kaygusuz, K., Yıldırım, N., Tyagi, V.V., Sharma, R.K. and Saleh, T.A., 2021. Carbonized waste hazelnut wood-based shape-stable composite phase change materials for thermal management implementations. *International Journal of Energy Research*, 45(7), pp.10271-10284.

[54] Ma, L., Guo, C., Ou, R., Sun, L., Wang, Q. and Li, L., 2018. Preparation and characterization of modified porous wood flour/lauric-myristic acid eutectic mixture as a form-stable phase change material. *Energy & Fuels*, 32(4), pp.5453-5461.

[55] Guo, X., Zhang, L., Cao, J. and Peng, Y., 2018. Paraffin/wood flour/high-density polyethylene composites for thermal energy storage material in buildings: a morphology, thermal performance, and mechanical property study. *Polymer Composites*, 39(S3), pp.E1643-E1652.

[56] Sarı, A., Hekimoğlu, G. and Tyagi, V.V., 2020. Low cost and eco-friendly wood fiber-based composite phase change material: development, characterization and lab-scale thermoregulation performance for thermal energy storage. *Energy*, 195, p.116983.

[57] Sawadogo, M., Benmahiddine, F., Hamami, A.E.A., Belarbi, R., Godin, A. and Duquesne, M., 2022. Investigation of a novel bio-based phase change material hemp concrete for passive energy storage in buildings. *Applied Thermal Engineering*, 212, p.118620.

[58] Barreneche, C., Vecstaudza, J., Bajare, D. and Fernandez, A.I., 2017, October. PCM/wood composite to store thermal energy in passive building envelopes. *In IOP Conference Series: Materials Science and Engineering* (Vol. 251, No. 1, p. 012111). IOP Publishing.

[59] Temiz, A., Hekimoğlu, G., Köse Demirel, G., Sarı, A. and Mohamad Amini, M.H., 2020. Phase change material impregnated wood for passive thermal management of timber buildings. *International Journal of Energy Research*, 44(13), pp.10495-10505.

[60] Rode, C., Peuhkuri, R., Time, B., Svennberg, K., Ojanen, T. and Mukhopadhyaya, P., 2007. Moisture buffer value of building materials. *ASTM International*.

[61] Badenhorst, H. and Cabeza, L.F., 2017. Critical analysis of the T-history method: A fundamental approach. *Thermochimica Acta*, 650, pp.95-105.

[62] Solé, A., Miró, L., Barreneche, C., Martorell, I. and Cabeza, L.F., 2013. Review of the T-history method to determine thermophysical properties of phase change materials (PCM). *Renewable and Sustainable Energy Reviews*, 26, pp.425-436.

[63] Zhao, D., Qian, X., Gu, X., Jajja, S.A. and Yang, R., 2016. Measurement techniques for thermal conductivity and interfacial thermal conductance of bulk and thin film materials. *Journal of Electronic Packaging*, 138(4), p.040802.

[64] Franco, A., 2007. An apparatus for the routine measurement of thermal conductivity of materials for building application based on a transient hot-wire method. *Applied Thermal Engineering*, 27(14-15), pp.2495-2504.

[65] Meng, X., Gao, Y., Wang, Y., Yan, B., Zhang, W. and Long, E., 2015. Feasibility experiment on the simple hot box-heat flow meter method and the optimization based on simulation reproduction. *Applied Thermal Engineering*, 83, pp.48-56.

[66] Soares, N., Martins, C., Gonçalves, M., Santos, P., da Silva, L.S. and Costa, J.J., 2019. Laboratory and in-situ non-destructive methods to evaluate the thermal transmittance and behavior of walls, windows, and construction elements with innovative materials: A review. *Energy and Buildings*, 182, pp.88-110.

[67] Younsi, Z., Joulin, A., Zalewski, L., Lassue, S. and Rousse, D., 2008. Thermophysical characterization of phase change materials with heat flux sensors. *Proceedings of Eurotherm*, The Nederlands.

[68] Zhao, P., Yue, Q., He, H., Gao, B., Wang, Y. and Li, Q., 2014. Study on phase diagram of fatty acids mixtures to determine eutectic temperatures and the corresponding mixing proportions. *Applied energy*, 115, pp.483-490.

[69] Çaylı, G. and Küsefoğlu, S., 2010. A simple one-step synthesis and polymerization of plant oil triglyceride iodo isocyanates. *Journal of applied polymer science*, 116(4), pp.2433-2440.

[70] Senphan, T. and Benjakul, S., 2016. Chemical compositions and properties of virgin coconut oil extracted using protease from hepatopancreas of Pacific white shrimp. *European Journal of Lipid Science and Technology*, 118(5), pp.761-769.

[71] Fauzi, H., Metselaar, H.S., Mahlia, T.M.I. and Silakhori, M., 2014. Thermo-physical stability of fatty acid eutectic mixtures subjected to accelerated aging for thermal energy storage (TES) application. *Applied thermal engineering*, 66(1-2), pp.328-334.

[72] Zhang, N., Yuan, Y., Du, Y., Cao, X. and Yuan, Y., 2014. Preparation and properties of palmitic-stearic acid eutectic mixture/expanded graphite composite as phase change material for energy storage. *Energy*, 78, pp.950-956.

[73] Robustillo, M.D., Bessa, L.C.B.A., de Almeida Meirelles, A.J. and de Alcântara Pessôa Filho, P., 2018. Experimental data and thermodynamic modeling of solid-liquid equilibrium of binary systems containing representative compounds of biodiesel and fossil fuels: Ethyl esters and n-hexadecane. *Fuel*, 220, pp.303-317.

[74] Robustillo, M.D., Barbosa, D.F., de Almeida Meirelles, A.J. and de Alcântara Pessôa Filho, P., 2013. Solid–liquid equilibrium in ternary mixtures of ethyl laurate, ethyl palmitate and ethyl stearate. *Fluid Phase Equilibria*, 358, pp.272-281.

[75] Abbott, S.P., 2002. Mycotoxins and indoor molds. *Indoor Environment Connections*, 3(4), pp.14-24.

[76] Saranpää, P. and Höll, W., 1989. Soluble carbohydrates of Pinus sylvestris L. sapwood and heartwood. *Trees*, 3(3), pp.138-143.

[77] Terziev, N., Boutelje, J. and Larsson, K., 1997. Seasonal fluctuations of low-molecular-weight sugars, starch and nitrogen in sapwood of Pinus sylvestris L. *Scandinavian Journal of Forest Research*, 12(2), pp.216-224.

[78] Lie, S.K., Vestøl, G.I., Høibø, O. and Gobakken, L.R., 2019. Surface mould growth on wood: a comparison of laboratory screening tests and outdoor performance. *European Journal of Wood and Wood Products*, 77(6), pp.1137-1150.

[79] Blom, Å., Johansson, J. and Sivrikaya, H., 2013. Some factors influencing susceptibility to discoloring fungi and water uptake of Scots pine (Pinus sylvestris), Norway spruce (Picea abies) and Oriental spruce (Picea orientalis). *Wood Material Science & Engineering*, 8(2), pp.139-144.

[80] Frühwald, E., Li, Y. and Wadsö, L., 2008. Image analysis study of mould susceptibility of spruce and larch wood dried or heat-treated at different temperatures. *Wood Material Science and Engineering*, 3(1-2), pp.55-61.

[81] Ahmed, S.A., Sehlstedt-Persson, M. and Morén, T., 2013. Development of a new rapid method for mould testing in a climate chamber: preliminary tests. *European Journal of Wood and Wood Products*, 71(4), pp.451-461.

[82] Militz, H. and Altgen, M., 2014. Processes and properties of thermally modified wood manufactured in Europe. In *Deterioration and protection of sustainable biomaterials* (pp. 269-285). American Chemical Society.

[83] Hunter, C.A., Grant, C., Flannigan, B. and Bravery, A.F., 1988. Mould in buildings: the air spora of domestic dwellings. *International biodeterioration*, 24(2), pp.81-101.

[84] Shelton, B.G., Kirkland, K.H., Flanders, W.D. and Morris, G.K., 2002. Profiles of airborne fungi in buildings and outdoor environments in the United States. *Applied and environmental microbiology*, 68(4), pp.1743-1753.

[85] Simpson, W. and TenWolde, A., 1999. Physical properties and moisture relations of wood. *Chapter*, 3, pp.2-1.

[86] Czajkowski, Ł., Olek, W. and Weres, J., 2020. Effects of heat treatment on thermal properties of European beech wood. *European journal of wood and wood products*, 78(3), pp.425-431.

[87] Yang, H., Wang, Y., Yu, Q., Cao, G., Sun, X., Yang, R., Zhang, Q., Liu, F., Di, X., Li, J. and Wang, C., 2018. Low-cost, three-dimension, high thermal conductivity, carbonized wood-based composite phase change materials for thermal energy storage. *Energy*, 159, pp.929-936.

Popular science summary

Health and environmental issues regarding overuse of fossil and non-bio-based materials in the construction industry, and large energy consumption usage for heating residential buildings have brought new areas of research in using bio-sourced envelopes in the industry leading to “green building”. Wood is the main source of bio source materials used for centuries. Wood is a light and relatively strong material, originating from sustainable and renewable sources, making it the best solution in transformation from traditionally non-sustainable buildings to sustainable green buildings. However, due to certain drawbacks such as low thermal mass and biodegradability, wood needs to be properly engineered in order to extend its working life, tackling possible health problems related to mycotoxins from mold growth and improvement its thermal mass thus enabling it to cope with energy intermittency inside green buildings leading to using thermal energy more efficiently. A solution to improve the thermal mass of wood based materials and enable them to store excess energy and release the stored energy when it is needed is incorporation of bio-based phase change materials thus making energy smart bio-composites for building applications. The composites can store and release energy in a comfort temperature range for human body. When the temperature goes up, the composites passively absorb and store extra energy and release it when the temperature drops thus curbing temperature fluctuations inside buildings providing a more comfortable environment and using energy more efficiently. In addition, the composites’ moisture adsorption reduces and is less susceptible to mold growth and related health problems.

Populärvetenskaplig sammanfattning

Miljöfrågor kring överanvändning av fossilbaserade material i byggindustrin och kostnaden för uppvärmning i bostadshus har lett till att forskare har tagit fram nya idéer som pekar på utveckling av avancerade biomaterial för "grönt byggande". Trä bidrar avsevärt till de allra flesta biomaterial; det är ett lätt och relativt starkt material som kommer från förnybara källor och därför är det den bästa lösningen för omvandling till hållbara gröna byggnader. Några ärvda nackdelar med trä, såsom låg termisk massa och biologisk nedbrytbarhet, bidrar till utmaningar med att förbättra dess termiska massa och effektiv användning av värmeenergin i byggnader. En lösning för att förbättra den termiska massan hos träbaserade material och göra det möjligt för dem att lagra och frigöra överskottsenergin när det behövs är att införliva biobaserade fasförändringsmaterial i trämaterial och därmed utveckla energismarta bio-kompositer för byggnadsapplikationer. Bio-kompositerna kan lagra och frigöra energi i ett komforttemperaturintervall av ca. 18-21 ºC. När temperaturen ökar, absorberar och lagrar kompositerna passivt extra energi och frigör den när temperaturen sjunker, vilket dämpar temperaturfluktuationer inuti byggnader och vilket ger en mer komfortmiljö och använder energin mer effektivt. Dessutom har kompositernas en minskat fuktadsorption och de är mindre mottagliga för mögelpåväxt.

Acknowledgements

This PhD thesis is the outcome of four years PhD research on energy storage using bio-based phase change materials incorporated into bio-based building envelopes for green building applications. The research was financed by the Swedish Research Council for Sustainable Development (FORMAS), project number 2017-00686, and Smart Energy Systems Research and Innovation Program (ERA-Net E2B2) in the project "Bio-Based Phase Change Materials Integrated into Lignocellulose Matrix for Energy Store in Buildings (BIO-NRG-STORE)". The PhD study was conducted at the Department of Forest Biomaterials and Technology, Division of Wood Science and Technology, Swedish University of Agricultural Sciences (SLU), Uppsala.

I would like to express my deep gratitude to my main supervisor Dr. Mohamed Jebrane, and my special thanks and appreciation go to my main co-supervisor Prof. Nasko Terziev. I would like to thank you for your patience, guidance and help. I would like to thank my co-supervisors Prof. Geoffrey Daniel, Dr. Dinesh Fernando and Dr. Mehrdad Arshadi and my colleague Prof. Stergios Adamopoulos for learning from your experiences, knowledge and helping me to grow and broaden my perspective.

I wish to thank Malin Sandberg for administrative helps in various ways. I gratefully thank Dinesh for the kind and friendly suggestions for my life. I am very thankful to Dr. Jie Gao, for her kind helps in the lab. I would like to thank Dr. Yasser Mahmoudi Larimi, University of Manchester. Yasser opened my eyes to research and he taught me first steps in research before I started my PhD. Grateful thanks to Joran for your suggestions, supports and helps. I wish to thank Sara, Valentin, Zijia, Jakub and Agnes for being good friends and nice times. I owe my special thanks to my parents, sister and brothers for all the supports and unconditional love. Without my family, I would never be where I am now.

I

energies

MDPI

Review

Bio-Based Phase Change Materials Incorporated in Lignocellulose Matrix for Energy Storage in Buildings—A Review

Meysam Nazari, Mohamed Jebrane * and Nasko Terziev

Department of Forest Biomaterials and Technology, Swedish University of Agricultural Sciences, Vallvägen 9C, 750 07 Uppsala, Sweden; meysam.nazari@slu.se (M.N.); nasko.terziev@slu.se (N.T.)

* Correspondence: mohamed.jebrane@slu.se

Received: 27 April 2020; Accepted: 9 June 2020; Published: 13 June 2020

Abstract: Due to growing consciousness regarding the environmental impact of fossil-based and non-sustainable materials in construction and building applications, there have been an increasing interest in bio-based and degradable materials in this industry. Due to their excellent chemical and thermo-physical properties for thermal energy storage, bio-based phase change materials (BPCMs) have started to attract attention worldwide for low to medium temperature applications. The ready availability, renewability, and low carbon footprint of BPCMs make them suitable for a large spectrum of applications. Up to now, most of the BPCMs have been incorporated into inorganic matrices with only a few attempts to set the BPCMs into bio-matrices. The current paper is the first comprehensive review on BPCMs incorporation in wood and wood-based materials, as renewable and sustainable materials in buildings, to enhance the thermal mass in the environmentally-friendly buildings. In the paper, the aspects of choosing BPCMs, bio-based matrices, phase change mechanisms and their combination, interpretation of life cycle analyses, and the eventual challenges of using these materials are presented and discussed.

Keywords: bio-based PCMs; bio-based matrices; buildings and constructions; energy storage applications; wood

1. Introduction

Due to an increase in global population and technological development, the demand for energy has experienced a significant growth over recent decades. In addition, environmental problems have also been one of the biggest concerns associated with the overuse of fossil resources for generating energy. In order to cope with growing energy demands, the energy storage and management methods are as important as finding new energy sources and techniques [1]. Energy consumption in residential buildings is one of the biggest energy demanding sectors that need to be managed and controlled [2]. Recent studies [3,4] reported that more than 40% of the energy generated in the world is consumed in buildings. This represents one-third of the annual greenhouse gases emitted to the environment. Therefore, energy consumption in residential buildings needs to be managed. In this regard, there is a need to find new solutions for keeping the indoor temperature consistent and for controlling the temperature fluctuations. These new solutions should involve environmentally-friendly strategies to avoid negative impact on the environment. To meet these demands, thermal energy storage in the form of latent heat energy storage in bio-based phase change materials (BPCMs) has a role to play. Due to their unique chemical, thermal, and physical properties, BPCMs are promising materials for fulfilling the above-mentioned requirements. Using BPCMs in buildings for

thermal energy storage is a strategy to curb energy intermittency. These materials are widely used in buildings for thermal comfort, solar heating systems, thermal protection, air conditioning, etc. [4–6].

For better use of BPCMs, they need to be incorporated in the construction and buildings elements. Traditionally, phase change materials (PCMs) are incorporated into inorganic materials such as concrete and gypsum in the building elements. Recently, attention has been paid to natural, renewable, sustainable, and environmentally-friendly materials [7,8]. Wood and wood-based materials offer reliable properties, which readily meet the above-mentioned requirements. Some unique characteristics of wood and wood fibers such as renewability and sustainability, easy transformation, high mechanical strength, and proper chemical properties make them one of the best options for construction applications. Wood is widely used in constructions and buildings not only to decorate the interior spaces but also to construct frames, walls, roofs, and floors. Using bio-based materials as PCMs in combination with wood as matrices can address both managing energy consumption and environmental concerns about buildings [7–9].

PCMs incorporation into wood and wooden materials can provide production of reliable materials for utilization in constructions and buildings. Wood is a natural porous material and can be impregnated with PCMs and used in internal and external joineries to enhance thermal mass of the building, control temperature fluctuations in residential buildings, and enhances its thermal comfort [7,8,10].

There is an abundance of review papers covering various treatment and application aspects of inorganic and organic PCMs [11–24]. Most of the studies investigated PCMs incorporated in inorganic matrices. To the best knowledge of the authors, there is no comprehensive review on incorporation of BPCMs into bio-based containers for utilization in building applications. Therefore, the literature review is limited to only bio-based PCMs (BPCMs) and matrices and presents recent developments and research challenges.

2. Basics in the Phase Change Mechanism, Systems, and Analysis

In a specific range of temperature, PCMs store and release energy in terms of latent heat during the phase transition. This process occurs in three phases, i.e., solid-solid, solid-liquid, and liquid-gas [23]. In building envelopes, only a solid-liquid phase change can be considered [6,11,20,22,23]. When the material is heated up to a specific temperature, the hydrogen bonds and other attractive forces (van der Waals) in these materials become weak. The material will then absorb and store energy (heat) in an endothermic process where its phase state transients to another phase state. When the temperature drops down, the material releases the energy and, consequently, returns to its initial phase state [11,19].

2.1. Energy Conversion Mechanism

Ideally, phase transition is an isothermal process during which the temperature of the material remains almost unchanged. The isothermal process offers a reliable storage density with narrow temperature variations between storing and releasing heat [6,20,23,25]. Theoretically, the storage capacity of a latent heat system during phase transition with use of PCMs is given by the following equation [20,22,23,25].

$$Q = \int_{T_i}^{T_m} mc_p dT + ma_m \Delta h_m + \int_{T_m}^{T_f} mc_p dT \quad (1)$$

where Q, T, m, c_p, a_m, and Δh_m are storage capacity, temperature, mass of the material, specific heat capacity of the material, fraction melted, and heat of melting per unit mass, respectively. Subscribes i, m, and f, respectively, refer to initial, melting, and final states of the material. If thermo-physical properties of the material are constant, then Equation (1) is rewritten as [20,22,23,25]:

$$Q = m\left[c_p(T_m - T_i) + a_m \Delta h_m + c_p\left(T_f - T_m\right)\right] \quad (2)$$

Figure 1 shows a schematic diagram of the heat storage mechanism of PCM. The process consists of three sections. The first and the last sections are sensible heat storage while the second part presents latent heat storage. The process starts from initial temperature at a certain time and absorbs heat. Upon heating, the temperature of the material will increase and reach its melting temperature. During the melting process, the temperature remains stable and the heat will be stored in the material in the form of latent heat. By a further increase of the heat, the temperature reaches higher degrees and this extra heat is stored in the form of sensible heat. When releasing the absorbed heat, the process reverses.

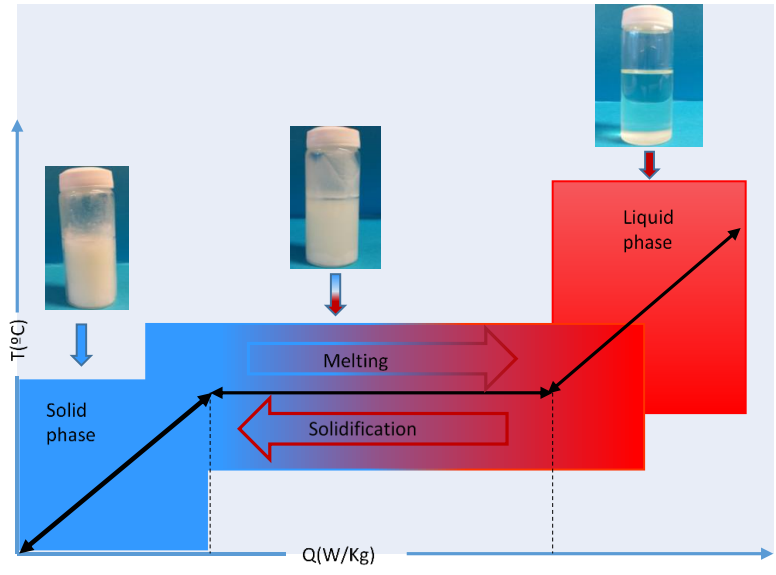

Figure 1. Heat storage mechanism in a PCM.

The governing energy equation for sensible regions (phases one and three) and latent region (phase two) when the material transfers heat by conduction is expressed by the following equations [26–29]:

For sensible storage:

$$\rho c_p \frac{\partial T}{\partial t} = k\left(\frac{\partial^2 T}{\partial x^2} + \frac{\partial^2 T}{\partial y^2} + \frac{\partial^2 T}{\partial z^2}\right) \quad (3)$$

For latent storage:

$$\rho \frac{\partial h_m}{\partial t} = k\left(\frac{\partial^2 T}{\partial x^2} + \frac{\partial^2 T}{\partial y^2} + \frac{\partial^2 T}{\partial z^2}\right) \quad (4)$$

where ρ and k are the density and thermal conductivity of the material, respectively, t is time and x, y, and z are directions. Equation (3) indicates that the temperature of the material changes (sensible storage) while, for the latent heat storage, the temperature remains constant (isothermal process) and the energy is stored by variation in enthalpy (phase change enthalpy), as described by Equation (4).

2.2. Energy Storage System Mechanism

In building applications, the process of storing and releasing energy using PCMs can be used for both passive and active systems. In the passive systems, the PCM is incorporated into the building

elements and, when the surrounded temperature reaches a melting temperature or above, the PCM will absorb the energy, and release it when the temperature falls down. In active systems, the energy is stored in PCMs in certain separate collectors during lower demands and will be released when the demands are high. This system is mainly used to store solar energy during the daytime when there is abundance of sun and release the absorbed energy during nights when there is more demand for energy [5].

2.3. Available Analytical Methods of Energy and Chemical Behavior of PCM

For thermal analysis of PCMs, differential scanning calorimetry (DSC), T-History methods, guarded hot plate, and thermo-gravimetric characterization methods have been used. DSC is the most commonly used approach to determine the PCMs' thermo-physical characteristics including melting temperature and latent heat of fusion [6,11,14]. However, this method can only be used for analyzing small and uniform test samples of PCMs [6,11]. Using the T-history method makes it possible to investigate the melting temperature, degree of super cooling, heat of fusion, specific heat, and thermal conductivity of several PCMs simultaneously [6,11,14]. Another method known as a guarded hot plate is used to analyze thermal conductivity of energy saving systems using PCMs [6,11]. Thermo-gravimetric analysis (TGA) is used to evaluate the thermal stability of PCMs [13].

Scanning electron microscopy (SEM) [15] is applied to assess the morphology of the material and particle size distribution. Fourier transform infrared spectroscopy (FTIR) and X-ray diffraction (XRD) methods are available for investigating chemical stability and compatibility of the materials [15,18].

3. Organic PCM (OPCM) for Building Applications

Studies concerning the incorporation of OPCMs in construction materials concentrated on storing and releasing solar energy for indoor heating. This pattern is suitable for regions where there is enough sun during winter times when the demands for energy is high. However, in many cold weather countries with high interest in biomaterials such as Canada and Nordic countries, there are not many sunny days during the winter periods. Therefore, using OPCMs to control indoor temperature fluctuations in residential buildings seems more interesting than storing solar energy during the daytime and releasing it during nights.

As discussed by Kalnaes and Jelle [11], in cold climates, building constructions ensure passive housing standards, which consist of using a large amount of insulation materials to reduce heating loads exchange between indoor and outdoor temperatures. The authors reported that, when the inside thermal mass of a building with incorporated PCMs increases, the exceeding energy will be stored and released when the indoor temperature drops down. This process results in temperature fluctuations control, which uses the energy more efficiently.

Various parameters should be considered when selecting a suitable PCM for building applications. This includes physical, thermal, chemical, and kinetic characteristics. In addition to these parameters, there are other aspects such as cost, availability, safety, compatibility, and reliability that need to be taken into account [1,4,11–13,15,19,22,23]. A key problem in choosing an appropriate PCM is the working temperature and latent heat of fusion. A suitable candidate PCM should fit the working temperature range and have a large latent heat of fusion.

The basic requirements for a PCM are categorized as follows.

Physical requirements: suitable phase change temperature, large latent heat of fusion, reproducible phase change or cycling stability, little super cooling, no phase separation, and good thermal conductivity.

Technical requirements: low vapor pressure, small volume change during the phase change, chemical stability of PCM, compatibility of PCM with other materials, and a safety constraint.

In terms of physical characteristics, a suitable PCM for building applications should have a phase transition temperature in the range of human comfort temperatures (i.e., around or less than 25 °C internal temperature) [1,2,5]. According to the American Society of Heating, Cooling, and Air-conditioning Engineers (ASHRAE), the room temperature for summer and winter conditions are

suggested to be in the range of 23.5–25.5 °C and 21.0–23.0 °C, respectively [22]. In these temperature ranges, a super cooling phenomenon always occurs. Therefore, considering OPCMs for this range is more rational compared to inorganics, which suffer from super cooling.

In terms of technical requirements, a material with low vapor pressure and small volume change during phase transition is preferred. Otherwise, a large container is required. A liquid-gas mechanism needs a huge container to keep the material when it changes to its gas state and it is difficult to prevent material leakage [13]. Solid-solid PCMs are not commercialized yet and need further developments. Therefore, the solid-liquid mechanism is the only possible option for construction and building applications.

OPCMs are divided into paraffins and non-paraffins [30] (Figure 2). Compared to inorganic PCMs, OPCMs have little super cooling and phase segregation and are suitable for absorption in various building materials [4,11,19–21]. Paraffins and polyethylene glycols are not bio-based but are frequently used as reference materials and, thus, are included in the review. The non-paraffin BPCMs are alcohols, fatty acids, and esters. Most of these materials are derived from raw materials such as vegetable oils and animal fat (soybean oil, coconut oil, palm oil, and beef tallow) [22,31–33]. These materials have high latent heat, no super cooling and phase separation, are less flammable, and are thermally and chemically stable for loads of cycles [22,31–33].

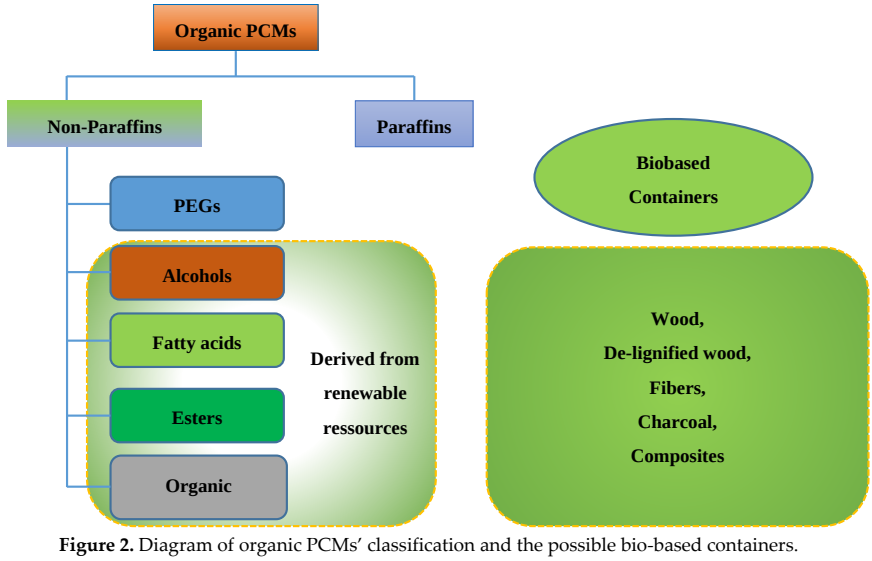

Figure 2. Diagram of organic PCMs' classification and the possible bio-based containers.

3.1. Paraffins

Paraffins (saturated hydrocarbons with C_nH_{2n+2} formula) and commercial paraffin waxes ($CH_3(CH_2)_nCH_3$) are crude oil-based products that have been extensively used to store solar energy by latent heat energy storage techniques [19,21,22,30]. Paraffins possess a high latent heat storage capacity, are non-toxic, non-reactive, non-corrosive to metals, and inexpensive. They have stable properties and good thermal and chemical reliability after loads of cycles and less likely to suffer from phase segregation and super cooling [19,22]. However, these materials have a moderate thermal energy storage density, but the most important drawback of these materials is the low thermal conductivity [19,21,22]. Paraffins can cover a wide range of temperature depending on the carbon number. The longer the average length of the hydrocarbon chain, the higher the melting temperature would be [20,21]. Paraffins with carbon chains less than 15 carbons are liquids. By increasing the number of carbon chains, the melting temperature and heat of fusion increase [21,23].

3.2. Polyethylene Glycols

Polyethylene glycol (PEG), called polyoxyethylene (POE) or polyethylene oxide, is derived from dimethyl ether chain [22]. PEGs are organic but not bio-based as they are derived from crude oil. Due to its chemical form and characteristics, PEG is soluble in water and organic solvents [22].

PEGs are provided in grades such as 400, 600, 1000, 3400, 10,000, 20,000, 35,000, 100,000, and 1,000,000 [22]. They have been widely used and investigated as potential materials for use as PCMs due to their chemical and thermal stability and due to being non-flammable, non-toxic, and non-corrosive [21,22]. These materials have large heat of fusion varying from 117 to 174 kJ/kg, high degree of crystallinity, and a melting temperature in the range of 4–70 °C depending on molecular weight [21,22]. An increase in molecular weight of a PEG leads to an increase in the heat of fusion and melting temperature [21,22].

3.3. Polyols

Polyols are divided into sugar alcohols, poly-alcohols, and glycols and are considered as medium temperature (90–200 °C) PCMs [22].

Kaizawa et al. [34] studied some materials including sugar alcohol for use as PCM finding erythritol with a large latent heat of fusion of 344 kJ/kg. A melting point of 117 °C is a promising PCM material for medium-to-high temperature applications.

Alcohols possess excellent characteristics as PCM. However, the problem with this type of BPCM is the super cooling at lower temperatures that limits their usage in the suitable range for building applications. Another problem is the volume expansion during phase transition, which requires a large matrix volume [22,35,36].

Some sugar alcohols, e.g., D-mannitol, myo-inositol, and galacitol were studied as potential PCMs. The reported results indicated that myo-inositol experienced some chemical instability. However, it was discussed that this did not affect thermal characteristics during cycles [37]. Galacitol showed poor cycling stability and D-mannitol reacted with oxygen and was not chemically stable [37].

3.4. Fatty Acids

Fatty acids with a general formula $CH_3(CH_2)_{2n}COOH$ are derived from animal and vegetable sources. Most used fatty acids are categorized in six groups, i.e., caprylic, capric, lauric, myristic, palmic, and stearic [19,20].

Fatty acids benefit from the unique and superior characteristics such as congruent melting, good chemical and thermal stabilities, non-toxic, bio-degradable, and a melting temperature range suitable for building applications if mixed together or esterified [19–21]. Fatty acids have recently attracted researcher's attention as potential BPCMs for low-to-medium energy storage applications [38,39].

Reviews by Yuan et al. [38] and Rozanna et al. [39] have focused on fatty acids and their binary mixtures as BPCMs for thermal energy storage. Yuan et al. [38] reported that the research has concentrated on saturated fatty acids but only their thermal behavior was investigated. The study concluded that it is difficult to find a pure fatty acid with a phase transition temperature in the range of a comfortable temperature. Rozzana et al. [39] focused on the application of fatty acids and their derivatives concluding that it is difficult to find any pure fatty acid suitable for passive thermal storage in buildings. However, their mixtures and esters are very promising as BPCMs for building applications.

Feldman et al. [40,41] investigated the potential use of fatty acid derivatives including butyl stearate, vinyl stearate, mixtures of ethoxylated linear alcohols [40], and methyl palmitate and methyl stearate [41] as PCMs. The former study reported melting temperatures of these materials between 10 to 43 °C with latent heat between 100 to 140 kJ/kg [40] and between 23–27 °C with latent heat of fusion of 180 kJ/kg in the latter study [41]. It was concluded that the mixtures and esters are promising for use as PCMs in building applications. Although the melting temperature of pure fatty acids is

rather high, if mixed or esterified, the thermal characteristics of the new products can fulfil the requirements of the targeted applications.

Hasan [42,43] investigated stearic and palmitic acids as BPCM in the range of 65–69 °C [42] and 57–62 °C [43]. The studies stated that both fatty acids are suitable BPCMs for thermal energy storage in domestic solar water heating systems due to their favorable phase transition temperatures for solar heating applications and large latent heat of fusion. Sari and Kaygusuz [44,45] studied thermal performance and phase change stability of stearic [44] and myristic acid [45] as BPCMs for thermal energy storage, and showed that these materials are suitable for solar water heating applications. Cedeno et al. [46] studied thermal characteristics of pure fatty acids including palmitic, stearic, and oleic acids and their binary and ternary mixtures. They defined phase transition and latent heat of fusion for these materials and revealed that oleic acid showed a solid-solid phase transition before a solid-liquid transition. Moreover, it was found that the melting temperature differed between the binary and ternary fatty acid mixtures [46].

Lin et al. [47] used a mixture of palmitic acid, polyvinyl butyral, and expanded graphite as a PCM. Thermal and chemical structures and behavior of the PCM were studied using FTIR, XRD, SEM, DSC, and TGA methods. The authors reported that the three materials integrated in a stable chemical and crystalline mixture despite physical and chemical interactions were not observed. The onset temperature of the pure palmitic acid was found at 62.9 and 60.1 °C during charging and discharging processes, respectively. However, the phase transition temperatures of the mixture was slightly lower (56–59 °C), i.e., temperatures mostly suitable for solar energy storage applications.

Sharma et al. [48] studied thermal and chemical stability and reliability of three OPCM including paraffin wax, palmitic acids, and myristic acids for 1500 melting/freezing cycles. Using DSC and FTIR, the authors reported that there were gradual changes in thermo-physical properties of the tested PCMs. However, a significant and reliable thermal and chemical stability was reported. The study also reported a decrease in melting temperature for two fatty acids after 500 thermal cycles compared to paraffin, which showed an increase in the melting temperature.

3.5. Organic-Organic Eutectics and Esters

Eutectic systems are melting compositions of two or more materials. Although these compositions have different melting and freezing temperatures, it is expected that eutectics melt and freeze without phase separation because the intimate mixture of crystals leaves little opportunity for the components to separate [4,11,20].

Fatty acid esters are an important group of BPCMs. Pure fatty acids suffer from certain drawbacks such as bad odor, corrosivity, and a high sublimation rate. In order to tackle these drawbacks and take advantage of the attractive properties of these materials, some transformations of the fatty acids are required. The most studied transformation is the esterification process to achieve desired thermal and physical properties [21]. This process consists of replacing the hydroxyl group with an alkyl group to obtain an ester [22]. The majority of BPCMs suitable for use in building passive applications are the ones involving fatty acid compositions and esters [5].

Nikolic et al. [49] studied fatty acid esters including methyl stearate, methyl palmitate, cetyl stearate, cetyl palmitate, and their binary mixtures. The mixtures showed a phase-transition temperature close to room temperature and were suitable for passive solar thermal storage. These materials were incorporated in gypsum wallboards and bricks by the impregnation technique and showed stability for a large number of thermal cycles with no changes after 18 months in service. The thermal storage capacity of the gypsum and bricks impregnated by PCM was about 10 times higher than that of ordinary materials without PCM. The thermal characterization showed some small extra peaks in addition to the main sharp peaks in the thermograms, which indicates the presence of certain incongruent melting and freezing with eutectic mixtures during the phase transition process.

Sari [50] studied eutectic mixtures of lauric acid (LA)-myristic acid (MA), lauric acid (LA)-palmitic acid (PA), and myristic acid (MA)-stearic acid (SA) as BPCMs. It was found that these mixtures have reasonable thermal properties and reliability in terms of both melting temperature and latent heat of fusion for passive solar energy storage. The melting temperature of the binary mixtures

was found to be lower than that of pure acids. Another study [51] found no deterioration in thermal properties of stearic acid esters as PCM after 1000 cycles. Four types of mannitol-fatty acids were synthesized and evaluated [52] to reveal that the phase transition temperature and latent heat of fusion of these materials vary between 42–65 °C and 145–202 J/g, respectively, which enable them as promising PCMs for active energy storage systems. The above studies concluded that the possibility of incongruent melting and freezing of the esters might be lower than that of eutectic mixtures.

For thermal energy storage for a working temperature in the range of 30–50 °C, high chain fatty acid esters of myristyl alcohol [53,54] and 1-hexadecanol [55] were proposed. These materials have interesting thermal storage potential and thermal reliability. Xu et al. [56] synthesized a fatty acid ester by making use of methyl palmitate (MP) and methyl stearate (MS) as PCMs for building applications with a melting temperature of 25–40 °C. These PCMs showed a possible incongruent melting for the mass ratio of MP/MS of 70/30, 60/40, 50/50, and 40/60. However, after 360 thermal cycles, there was still a reasonable thermal and chemical reliability. Other attempts in synthesis of eutectic PCMs focused on improvement of thermal performance. Mixtures of capric acid (CA) and lauric acid (LA) [57] for low temperature thermal energy storage were evaluated and it was found that an addition of pentadecane can enhance the thermal reliability and storage potential [58].

Mixtures of fatty acids and PEGs have been investigated and certain improvements compared to pure fatty acids or PEGs were obtained. A study reported that it is possible to obtain a homogeneous mixture of fatty acids and PEGs by mixing them in a liquid state and then freezing the mixture [22]. In this regard, various mixtures of PEG and fatty acids as PCMs to store energy in the form of latent heat were investigated [59]. The results indicated that the melting temperature range of this type of mixture and eutectic PCMs is mainly from 30 to 72 °C. The mixtures have higher latent heat of fusion when compared to that of pure fatty acids and PEGs.

Karaipekli and Sari [60] have studied mixtures of fatty acids for working temperatures in the range of 18–25 °C. Composition of capric, lauric, palmitic, and stearic acids has been incorporated in expanded vermiculate by vacuum impregnation. The melting temperature of the composite was in the range of 19–25 °C and was suitable for building applications. No phase separation was reported. The mixture was thermally and chemically stable after 5000 cycles. Sharma et al. [61] studied similar eutectics based on capric, lauric, myristic, palmitic, and stearic acids for building applications. The study reported melting temperatures of the eutectics in the range of 20–30 °C. Ke et al. [62] prepared four binary fatty acid eutectics of capric-lauric, capric-myristic, capric-palmitic, and capric-stearic acids and produced composite phase change nanofibers of the above eutectics and polyethylene terephthalate (PET). The results showed that the novel eutectic composites are suitable for building applications. Hawes et al. [63] used various OPCMs for latent heat storage in building materials and found that butyl stearate was a potential candidate. However, fire and fume generation are yet to be addressed.

3.6. Selection Criteria

Although paraffins have excellent properties as PCMs, they are derived from fossil resources. In this regard, fatty acids, fatty acid eutectics, and esters are more suitable for using in buildings and constructions. They are of plant and animal origin, i.e., of renewable and sustainable nature. Due to their unique properties and potential as PCMs, fatty acids and their homologue esters have recently attracted attention worldwide for application in buildings for lower temperature conditions. Fatty acids, fatty acid eutectic mixtures, and esters have high latent heat of fusion, good chemical stability, and remain stable after a large number of phase change cycles. However, these types of PCMs are more expensive when compared to paraffins. Some pure fatty acids, esters, and eutectics of esters with a melting temperature suitable for a building application are shown in Tables 1–4.

Table 1. Properties of two pure fatty acids suitable for the building application [23,38,39].

BPCM	Melting T (°C)	Freezing T (°C)	Latent Heat of Fusion (J/g)
Caprylic acid	16		144
Capric acid (CA)	32	25	150

Table 2. Properties of eutectic mixtures of fatty acids suitable for the building application [2,4,22,38,39].

BPCM	Proportion	Melting T (°C)	Freezing T (°C)	Latent Heat of Fusion (J/g)
CA:LA	67:33	22.8	-	154.16
CA:LA	64:36	19.62	-	149.95
CA:LA	70:30	21.09	-	124
CA:LA	45:55	21	-	143
CA:MA	74:26	22.16	21.18	154.83
CA:MA	70:30	21.79	-	123.62
CA:PA	76.5:23.5	21.85	-	173.16
CA:SA	83:17	25.39	25.2	188.15
CA:SA	70:30	23.4	-	104.9

Table 3. Properties of some fatty acid esters suitable for the building application [2,4–6,22,39,40,51].

BPCM	Melting T (°C)	Freezing T (°C)	Latent Heat of Fusion (J/g)
Butyl stearate	19–24	-	130–140
Dimethyl sabacate	21	-	120–135
Isopropyl stearate	22.12	21.99	113
Vinyl stearate	27	29	122
Propyl palmitate	19	-	186

Table 4. Properties of eutectic mixtures of fatty acid esters suitable for the building application [2,4,41,49].

BPCM	Proportion	Melting T (°C)	Freezing T (°C)	Latent Heat of Fusion (J/g)
Emerest 2325 (butyl stearate + butyl palmitate)	49:48	17–21	-	138–140
Emerest 2326 (butyl stearate + butyl palmitate)	50:48	18–22	-	140
Methyl palmitate + Methyl stearate	93:7	23	22	180
Methyl palmitate + Methyl stearate	95:5	26	23	180
Methyl palmitate + Methyl stearate	86:14	23.9	23.8	220
Methyl stearate + cetyl stearate	91:9	22.2	21.8	180
Methyl stearate + cetyl palmitate	91:9	28.2	27.9	189

Apparently, there is no ideal single pure fatty acid to fulfill all requirements for building applications. Eutectic mixture of fatty acids, fatty acid esters, and their mixtures have similar thermal characteristics, but eutectics and mixtures are more likely to suffer from a phase separation and, hence, have no congruent melting. The most important disadvantages of BPCMs are their low thermal conductivity and leakage problems.

4. BPCM Containment

4.1. Microencapsulation

Incorporation of BPCMs into building materials without encapsulation often leads to leakage. Microencapsulation is a technique where a molecule or a material in solid or liquid form is coated with another material. In this technique, a PCM is the core of a matrix to produce capsules of various shapes [2,15,21,22]. The capsules are produced in microscales in solid form and are then incorporated in another material or container, e.g., wood, for use in building elements [6,8]. The main purpose of this technique is to have better control on the PCMs in the application phase. Microencapsulated PCMs are easier to handle and less exposed to the environment in a container. The main problem with microencapsulated PCMs is the heat transfer since most of the coating materials have low thermal conductivity. Organics, inorganics, and mixtures can be used as shell materials to encapsulate the PCMs. Inorganic shell materials possess high conductivity. On the other hand, bio-based shell materials are renewable and more available.

Various techniques and methods have been employed to take advantage of the microencapsulation. Coacervation [64,65], interfacial polymerization [65–67], coatings [68], and spray drying [64] are the most used techniques. In order to cope with stresses and volume changes during the phase transition, the capsules need to possess strength and flexibility at the same time [8].

Organic materials, which are used as shells to microencapsulate BPCMs, are mainly resins, e.g., melamine-formaldehyde (MF) resin [69,70], urea-formaldehyde (UF) resin [71], poly (urea-urethane) [72], polyurea [73,74], and acrylic resin [68]. The advantage of using organic shells is that they offer structural flexibility and sufficient endurance for changing the volume during a phase transition for repeated cycles [16]. However, this type of shell material suffers from poor chemical and thermal stability [16].

4.2. Nano-encapsulation

Nano-encapsulation is another approach that has been extensively investigated due to its advantages over the other encapsulation methods, e.g., its high surface area/volume ratio that facilitates the thermal transfer and high stability [75,76]. In order to nano-encapsulate PCMs, several synthesis approaches have been developed. Liu et al. [77], Shchukina et al. [76], and Rodriguez-Cumplido [78] have summarized the most important methods for preparing nano-capsules, which include emulsion and mini-emulsion polymerizations, in-situ polymerization, interfacial polymerization, and the sol-gel technique. Most of the studies on the nano-encapsulation used n-alkanes as PCM, e.g., n-octadecane and poly (methyl methacrylate) (PMMA) as a shell. Among the investigated synthesis approaches, mini-emulsion is considered a superior technique for nano-capsulation of various materials [79]. High conductive additives such as silica [80], titania [81], alumina [82], and zinc oxide [83,84] nanoparticles have been incorporated into organic polymer shell materials to enhance the thermal conductivity and stability. Du et al. [85] included a phosphorus-based flame retardant as a crosslinking agent in the PMMA shell containing n-octadecane during the mini-emulsion polymerization process and reported an improvement in the flame-retardant properties of the nano PCMs. In addition, the incorporation of phosphorus-based flame retardant into the nano PCMs resulted in significant suppression of heat and smoke releases, and increased the residual weight and limiting oxygen index value of the composite. Recently, Yuan et al. [86] proposed a chemical reduction method to synthesize nano capsules with LA as the core and silver as the shell to increase the heat transfer performance. The obtained nano-encapsules reached 95.29 J/g thermal storage capacity with an encapsulation ratio of 67.21%. The thermal reliability of the composites was found satisfactory after 2000 cycles while the thermal conductivity of the nano-capsules was 333% more than that of the LA. Matteis et al. [87] used PEG600 as PCM encapsulated in a silica shell and compared its performance to that of a simple incorporation into a gypsum plasterboard for indoor plastered surfaces of referential residential buildings. Compared with a building without PCM, savings of 4.3% and 1.1% of heating and cooling energy were predicted.

Recently, new multifunctional, phase changing nano-capsules were investigated for thermal management and storage systems to improve the phase change performance of the existing systems. Zhou et al. [88] reported the use of n-octadecane and n-butyl stearate as binary core PCM and polyacrylate supplemented with titanium dioxide nanoparticles as hybrid shell material with a high latent heat storage performance and an encapsulated efficiency of 61.5%. The study reported that the nano-capsules possessed good thermal stability and ultraviolet absorption properties due to a combination of a compact polyacrylate–TiO_2 hybrid shell. Imran Hussain et al. [89] investigated a binary system comprising oleic acid and PEG as a core with the SiO_2/SnO_2 shell as shape-stabilized PCMs for cold thermal energy storage and reported encapsulation efficiency of 52.12% with good solidification characteristics and a lower degree of supercooling.

4.3. Shape Stabilization Using Organic Polymer Matrices

As mentioned above, encapsulation methods have a certain limitation, e.g., high preparation cost [16,90]. Moreover, the encapsulation techniques cannot enhance the thermal conductivity of PCMs [18,91]. Shape-stabilized PCM (SPCM) or form-stable composite PCM is another technique to contain the main PCMs. The advantage of the SPCM technique is that the used materials remain in their solid state even at temperatures higher than their melting points [16,92]. Umair et al. [16] reported that the micro-encapsulation technique is also a subdivision of the shape stabilization method. The shape stabilization technique can employ both organic and inorganic materials. When using organic polymer matrix as PCM's shape stabilization material, some factors need to be considered. Among these factors, chemical compatibility and thermal stability of polymers play an important role [16]. One of the prerequisites for selection of the matrix is that it should be congruent with the organic PCMs [18]. Various polymers are used as supporting material, e.g., low density polyethylene [93], styrene maleic anhydride copolymer (SMA) [94], polymethyl methacrylate [95,96], polyurethane [97], polypyrrole [98], high density polyethylene [99], polyvinyl alcohol [100–102], and a biodegradable polymer such as cellulose, chitosan, and agarose [103]. In a recent comprehensive review, Prajapati and Kandasubramanian [104] provided insights into various biopolymers utilized as capsules to overcome the leakage issues. They concluded that the low thermal conductivity resulting from using the biopolymer-framework based PCMs could be overcome by integrating hybrid nanofillers.

Among the cited matrices, polymethyl methacrylate (PMMA) has been extensively used as supporting material for preparing SPCMs. This polymer is easy to handle and process, non-toxic, has enough strength, and is cost-effective [18]. Wang and Meng [96] investigated PMMA as SPCM for capric acid (CA)-lauric acid (LA), capric acid (CA)-myristic acid (MA), capric acid (CA)-stearic acid (SA), and lauric acid (LA)-myristic acid (MA). The shape stabilization of the mixtures was performed by using a self-polymerization method. The DSC results indicated that the studied PCMs and PMMA are compatible with no chemical reaction. The phase transition temperatures of CA-LA/PMMA, CA-MA/PMMA, CA-SA/PMMA, and LA-MA/PMMA composites were 21.11, 25.16, 26.38, and 34.81 °C, i.e., suitable indoor temperatures for human comfort. The latent heat of fusion for the studied mixtures was 76.3, 96.32, 59.29, and 80.75 kJ/kg [96] and, thus, compared to PCMs without shape stabilization, the PMMA seems to reduce the latent heat of fusion of the PCMs.

Series of encapsulated palmitic acid (PA), lauric acid (LA), stearic acid (SA), and myristic acid (MA) blended with a styrene maleic anhydrate copolymer (SMA) were studied [105]. The resulting products showed good thermo-physical and chemical properties with no leakage.

Bio-based materials are also used as biodegradable supporting polymers in shape stabilization of some fatty acids and polyethylene glycols. Among these materials, gelatinized potato starch and cellulose were used as matrices in shape stabilization of PEG. The results indicated a strong intermolecular interaction between PEG and supporting materials leading to lower enthalpy value of the phase transition [106,107]. Similarly, a strong intermolecular interaction between PEG and cellulose as well as agarose and chitosan used as supporting materials were observed, while the melting temperature and latent heat of fusion experienced certain changes, but no leakage [99]. Cellulose-based composites have been investigated as potential supporting materials to shape

stabilized fatty acids. Cao et al. [108] used carboxyl methyl cellulose fibers to stabilize fatty acid eutectics by using an absorbing technique. It was reported that the PCM was absorbed into the supporting material (porous structure) and a reliable thermal stability was achieved. Another study [109] used gelatin Arabic gum to encapsulate coco fatty acid obtained from coconut oil. This process could also be considered as a shape stabilization using biodegradable supporting material. The relatively low cost and abundance of coconut oil as well as the melting temperature range (22–30 °C) makes this material an interesting PCM suitable for building applications. Moreover, studies indicated that the coco fatty acid is chemically stable and is not affected by the encapsulation process [109].

4.4. Shape Stabilization Using Inorganic Porous Materials

Porous materials have recently become attractive as supporting materials to shape stabilized OPCMs [16]. These materials have low density, a large surface area, and a wide pore size distribution, which allows them to store PCMs in the pores by capillary forces and hydrogen bonding [16,110]. The advantages of using this technique is prevention of PCM leakage and enhanced thermal conductivity of the composite. Carbon-based materials have extensively been used as supporting materials, e.g., expanded graphite (EG), graphene oxide (GO), carbon nanotube (CNT), graphite nanofibers, graphene nanoplates, and activated carbon. All of them benefit from high thermal conductivity and flexibility [16,18,111]. These materials are able to encapsulate OPCMs, but this ability depends strongly on their pore sizes and structure. In addition to fossil-based porous matrices, some porous bio-based materials such as wood and charcoal can also be used to encapsulate PCMs. One important aspect of the combination of a bio-based matrix and BPCMs is the interaction between the pore surface and PCM. If the interaction is strong, an elevated phase change temperature will be observed and vice versa. In the case when an organic bio-based material (e.g., a fatty acid) is encapsulated in a porous matrix, there is a strong interaction between pores and the PCM [18,112,113].

Sari and Karaipekli [114] studied the encapsulation of palmitic acid (PA) with expanded graphite for medium temperature utilization. Similarly, Wang et al. [115] incorporated sebacic acid into pores of expanded graphite and reported an enhanced thermal reliability and thermal conductivity compared to the pure fatty acid PCMs. Other combinations studied stearic acid/graphene oxide [116], palmitic acid/graphene nanoplates [117], and myristic acid/graphite nanoplates [118], which confirmed the improved thermal reliability and conductivity compared to pure BPCMs. Expanded graphite as supporting material not only prevents leakage of PCMs but also enhances the thermal conductivity [18].

Sheng et al. [119] used a cotton-derived carbon sponge as a bio-based organic supporting material for shape stabilization of OPCMs. The carbon sponge was produced by carbonization of cotton biomass and consisted of cotton-derived carbon fibers forming an interconnecting porous network. The obtained material was vacuum-impregnated with paraffin as PCM. The studied supporting material prevented leakage of the PCM, enhanced the thermal conductivity, and proved its properties as a shape-stabilizing matrix of PCMs for solar energy storage applications.

4.5. Incorporation of PCM in Lignocellulose Materials

Due to its renewable nature and availability, wood is extensively used in construction and buildings in the European and Nordic countries, Canada, the US, and Australia. Most of these countries need to manage energy used to heat up residential buildings especially during the winter. Wood is a porous material, which can be used as a matrix to encapsulate PCMs by the impregnation process (Figure 3). However, due to the complexity of the wood structure, the process of incorporating PCMs is challenging and some factors such as climate, building architecture, user's behavior, and thermo-physical properties of the PCMs should be considered [8].

Liang et al. [120] investigated wood-flour as an impregnatable matrix to encapsulate lauric acid (LA), myristic acid (MA), hexadecanoic acid (HA), and stearic acid (SA). It was revealed that the wood pores were filled and retained the acids by physical interaction while no leakage was observed.

However, the studied combinations/composites showed a low phase transition temperature and low latent heat of fusion compared to pure fatty acid (41 to 59 °C and 87 to 201 J/g, respectively).

Mathis et al. [8] investigated the potential use of red oak and sugar maple for impregnated floors for micro-encapsulation of BPCM (Nextek29). The PCM used in the study originated from agricultural resources, but its composition is unknown. The reported results indicated a 77% enhancement in thermal storage capacity of impregnated red oak when compared to the untreated one. For a flooring application, wood impregnated with PCM receives and stores solar energy in the working temperature range between 28 and 31 °C. The authors reported lower thermal mass for sugar maple than for red oak. Another study [7] incorporated BPCM consisting of a blend of lauric and capric acids in decorative wood-based panels (medium density fiberboards (MDF)). Initially, the PCMs were encapsulated in plastic poaches and then incorporated in grooved MDF panels. It was concluded that the wood panels filled with PCM have a suitable phase transition temperature and latent heat of fusion of 22.2 °C and 57.1 J/g, respectively. The finding is interesting since it fits well the building application of PCM for passive systems.

Yang et al. [121] studied delignified and carbonized wood samples, which were impregnated with lauric acid (LA). The composite was performed as a lightweight high porous material with a significant encapsulation ratio of more than 80% and a latent heat of 178 J/g. Li et al. [122] studied the potential use of paraffin/high density poly ethylene/wood-flour composite as a stable PCM form and as a thermal storage layer of an electric floor heating system. The resulting composite gained a proper phase change temperature for the building application of 20 to 30 °C, high latent heat of fusion, thermal conductivity, and good shape retention that positioned the composite as a promising PCM for the building application. Other studies [123,124] investigated a self-luminous wood composite for both thermal and light energy storage. In these studies, poplar wood was delignified and impregnated with tetradecanol as PCM. The obtained composite had 146 J/g latent heat of fusion and a 37 °C phase change temperature, which makes the composite suitable for building applications. Figures 3 shows incorporation of PCMs in wood for energy storage in buildings.

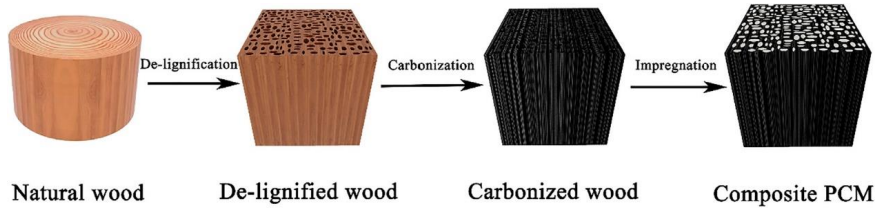

Figure 3. Schematic diagram of preparing PCM/carbonized wood composite (reprinted with permission from Reference 121).

The schematic picture of a composite material made of lignocellulose fibers impregnated with a BPCM is shown in Figure 4. Fibers can be treated to improve their hydrophobicity, fire resistance, and durability against micro-organisms. Figure 5 shows a light microscopy picture of a single fiber (mechanical pulp) impregnated with oleic acid where the fiber serves as an encapsulation cell for the BPCM. The composite can be improved further by adding a conductive polymer to encapsulate the fibers.

Ma et al. [125] investigated delignified cedar wood impregnated with capric acid-palmitic acid (PA) eutectic as a thermal energy storage system. The thermal analysis of the composite showed 94 J/g latent heat of fusion and a 23 °C phase change temperature. Furthermore, the thermal conductivity and reliability of the composite was found to be higher than that of the pure eutectic PCM.

Jamekhorshidi et al. [126] prepared a wood-polymer composite combined with micro-encapsulated PCM for application in buildings as a lightweight material. An industrial high-density polyethylene PCM (Cotene™) and pine sawdust were hot-pressed. The resulting composite showed reasonable thermal properties and a phase transition temperature with no leakage. Barreneche et al. [127] studied a coated PCM/wood composite for passive energy storage in building envelopes. The

studied composite consisted of black alder wood impregnated with RT21 and RT27 paraffins as PCMs. The impregnated wood was coated with polystyrene to enhance the structural stability of the composite. The phase transition temperatures were 20–21 °C for RT21 and 25–27 °C for RT27 paraffin. The composites are recommended for applications in the temperate region climate.

Guo et al. [128] studied incorporation of micro-encapsulated dodecanol as PCM into wood flour/high density polyethylene composite. Pre-polymer modified by polyethylene glycol was used as a matrix material to micro-encapsulate the PCM. The composite was prepared by hot-compression, and showed melting and freezing temperatures of 27.2 and 11.3 °C. In another study, Guo et al. [129] used paraffin as PCM, which was stabilized by expanded graphite and wood-flour. The use of expanded graphite considerably enhanced the thermal conductivity of the composite. The composite's melting temperature was found to be between 20 to 30 °C, which made it suitable for building applications.

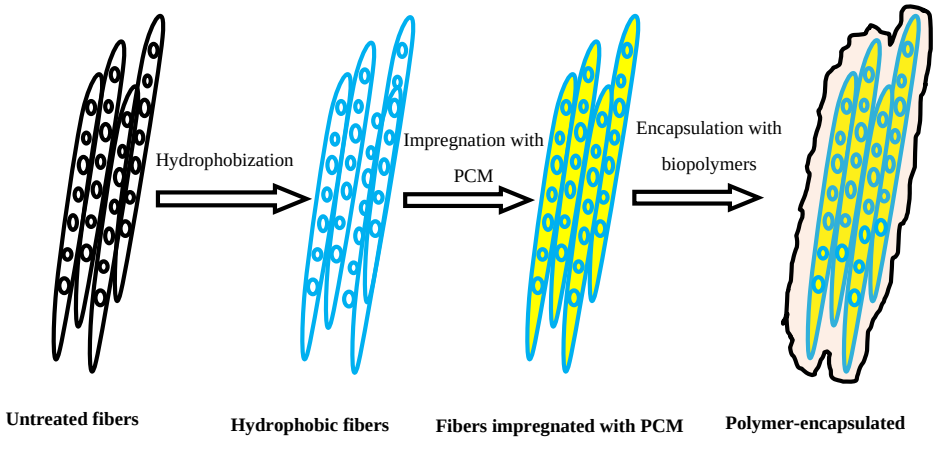

Figure 4. Schematic representation of incorporating PCMs into bio-fibers.

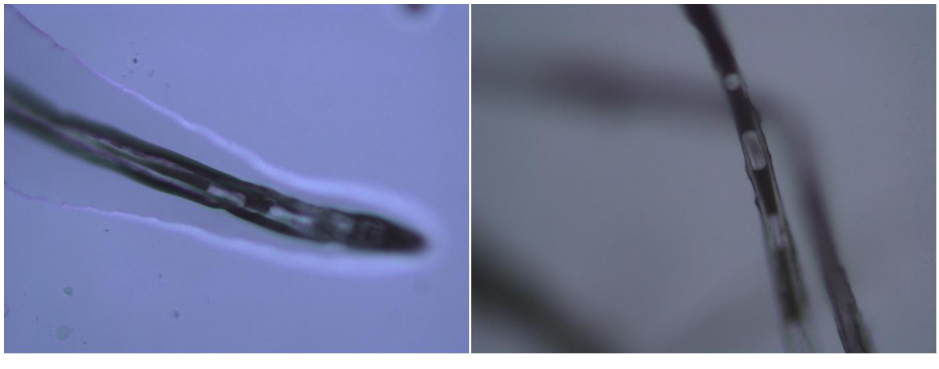

Figure 5. Microscopic images of BPCM into wood fibers.

5. Practical Challenges for Application of BPCM in Buildings

Although the BPCMs are promising for controlling the indoor temperature fluctuations in buildings, they possess a low thermal conductivity, which is approximately 0.2 W/mK. This limits their application [3,19,22]. The low thermal conductivity affects the response time to temperature

variations, which results in a slow and inefficient heat exchange rate between the PCM and the surrounding medium [3]. Some applied strategies consist of including highly conductive materials (e.g., graphite) in the matrices or in the PCM as microparticles or nanoparticles. Examples of matrices containing conductive materials include stainless steel, copper, aluminum-based matrices [130,131], porous graphite matrix [130,132,133], nanographite [134], carbon fibers [135,136], carbon nanofibers [137,138], and carbon nanotubes [138]. Sharma et al. [22] discussed that the inclusion of nanoparticles is better than microparticles and does not affect the melting point of PCM. However, due to their high-volume fraction, the addition of microparticles/nanoparticles to the matrix/PCM always results in reducing the energy density of PCM.

Parameshwaran et al. [139] investigated the effect of addition of silver nitrate nanoparticles into OPCM of polyvinyl pyrrolidone (PVP) 40,000 and found that the addition did not affect PCM's chemical behavior and characteristics. The nanoparticles improved the thermal conductivity of PCM from 0.284 to 0.765 W/mK accompanied with some changes in the melting and freezing temperatures. Wang et al. [140] used β-aluminum nitride powder as an additive to PEG to improve the thermal conductivity from 0.3847 to 0.7661 W/mK with no change in melting and freezing temperatures. Yang et al. [141] used carbonized wood poplar impregnated with tetra-decanol as PCM to prepare a high thermal conductive composite. Compared to pure tetra-decanol, the carbonized wood enhanced the conductivity of the composite by 114%. Li et al. [142] investigated the addition of 8.8% (wt) MicroMist graphite to micro-encapsulated paraffin/high density polyethylene/wood-flour composite. An enhancement in the thermal conductivity of 17.7% was observed with no negative impact on the mechanical and chemical behavior of the composite. Singh et al. [143] also found that the low thermal conductivity is a major drawback when using OPCM for low temperature applications. The authors studied carbon powder mixed with polyethylene glycol (PEG-1000) and it was inserted within aluminum and graphite fins. The thermal conductivity was increased by 40 and 33 times, respectively.

Another challenge related to energy management in building is the concept related to energy poverty. As discussed by da Cunha and de Aguiar [144], the energy consumption of the production and exploitation of buildings is related to a wide range of costs including extraction and production of the construction components from raw materials as well as building and maintenance costs during the time of exploitation. The authors introduced the concept of energy poverty related to economical limitations when less than 10% of the monthly income cannot be paid for thermal comfort in the buildings. However, Madad et al. [145] demonstrated that the use of PCM decreases the energy cost in buildings.

Apparently, the lignocellulose materials deserve research attention due to their unique characteristics as renewability, being lightweight, and porosity. As outlined in the review, the incorporated PCMs into lignocellulose lightweight envelopes, e.g., wood fibers (Figure 3), can increase the thermal inertia of these envelopes and reduce the indoor temperature fluctuations. However, the biological nature of lignocellulose materials determines their susceptibility to biodegradation by several biotic factors including bacteria, fungi, and insects. The above is valid even for the fatty acids used as PCM since they are derived from animal and vegetable sources. Flammability is also a challenge since it is often considered the most serious disadvantage of organic products in built environments. Although the BPCMs are intended for use in indoor environments, biological durability as well as fire resistance are important challenges that need to be addressed if plant fibers, wood, or wood-based composites are used as matrices for PCMs in building applications. Since very limited attempts [121,123–125] have been made to incorporate BPCMs into wood-based products, there are no studies investigating the long-term biological durability and fire resistance of the combinations of BPCMs and lignocellulose materials as matrices.

Most of the PCMs are susceptible to leakage when integrated into building envelopes, which seriously limits their application. Although suitable for encapsulation of BPCMs, the lignocellulose in any form can hardly prevent the leakage during exploitation [104]. Studies indicated that the leakage of PCM during the transition phase could be avoided by embedding them into suitable supporting materials. It is probable that an additional coating of the impregnated lignocellulose

matrices will be necessary to eliminate the leakage. It is further discussed by Frigione et al. [146] that leakage and incompatibility of PCM can negatively affect the mechanical and durability properties of the construction components. Mathis et al. [147] studied the use of a BPCM in wood-based panels for energy storage in a cold climate. Plastic bags with a commercial BPCM (Puretemp®23, unspecified composition) with a melting temperature of 23 °C were inserted in wood-based panels, i.e., a lignocellulose container. The authors concluded that the combination of a wood-based container and BPCM improved the energy efficiency and performance of the entire wooden construction in a cold climate, which resulted in energy savings during the winter and improved thermal comfort during the summer.

The comprehensive interest of all renewable materials to address the climate changes and cover the increasing demand for clean energy has led to enhanced research and developments of BPCM materials. The outstanding ability of the BPCMs to maintain internal temperatures and ensure a large energy storage density within a relatively narrow temperature range is expected to result in an accelerated demand of these materials. Consequently, a decrease in the availability and increase of the cost of the BPCM is predicted.

6. Life Cycle Assessments

Life cycle assessments (LCAs) have been applied for buildings or building systems [148–151] to demonstrate the environmental impact and the suitability of the materials. However, LCA of PCMs, which are considered as a material or included in a building, are restricted to a small number of studies. A review [152] has summarized nine publications on LCAs of PCMs for building applications. These studies focused on paraffin (organic PCM but originating from fossil sources), salt hydrates, and esters of stearic acid [153,154] incorporated in alveolar bricks and concrete [155,156], rammed earth matrix [157,158], tiles [159], and ventilated double skin facades [160]. It is concluded that the esters (i.e., BPCMs) have lower impact on the environment in the production stage when compared to the salt hydrates. Inclusion of salt hydrates and esters resulted in 9% and 10.5% impact reduction compared to the crude oil-based paraffin [154].

The system boundaries that have been employed in LCA studies of PCMs in buildings have been frequently selected for manufacturing and disposal stages [154,155] with an addition of the operation stage [159] or plant cultivation, manufacture, and transport stages [161]. A study which compares raw, waste palm oils and paraffin [161] demonstrated that palm oil production generated the most negative impact on the resources, ecosystem, and human health (15.5, 170, and 103.9 mPt), which is significantly higher than the values of paraffin (37.6, 4.2, and 9.2 mPt). The above is explained by the high CO_2 emissions as well as land and water consumption needed for the plant cultivation. On the other hand, when the polluter that pays a principle is applied, the waste palm oil showed the lowest impact of the three studied PCMs. Thus, the environmental advantages of BPCMs are not self-evident and their selection for building applications should be done in consideration of LCA.

LCA of PCMs is often combined with life cycle cost assessment [162]. Two BPCMs [163], i.e., dodecanoic acid produced from palm oil and ethyl hexadecanoate generated from algae and used in a solar heating application, were assessed in terms of embodied energy and CO_2 emissions. Dodecanoic acid showed ca. three years payback time for both energy and carbon emissions and proved to be viable as BPCM. On the other hand, the high embodied energy of ethyl hexadecanoate showed a payback time of more than 30 years for use in domestic thermal buffering applications. Another study [164] employed life cycle cost analysis to demonstrate that the payback time of an unspecified BPCM varied from 7.5 to 14.5 years when applied with and without insulation in a test dwelling.

The results of the LCAs for a product can differ in dependence on the employed tools. A study [165] compared the suitability of streamlined LCA (SLCA) based on Bilan Produit tool and a full LCA to reveal their robustness when a wood-based panel with an incorporated BPCM (mixture of 64% capric acid and 36% lauric acid) was studied. The BPCM had the highest impact regarding the non-renewable energy and resource consumption impact categories. Middle density and high density fibreboards of the panel were contributed to acidification, eutrophication, and aquatic eco-toxicity.

It can be concluded that a limited number of PCMs, particularly those of bio-origin, have been subjected to a life cycle and cost assessment. The results vary because various PCMs and material characteristics, system boundaries, and LCA tools have been employed. Nevertheless, LCA is a valuable tool for selecting BPCMs with low environmental impact for building applications.

7. Conclusions

This review focuses on the incorporation of BPCMs in lignocellulose materials for thermal energy storage in building applications. Due to to their sustainability and renewability, the combination of BPCMs and wood-based matrices will result in fully bio-based materials for energy management. The review presents and discusses various aspects of some promising BPCMs, energy characteristics, and wood-based materials as matrices. Summarizing the findings in the reviewed articles, the following conclusions can be drawn.

1. Among the investigated OPCMs, fatty acids, their derivatives, and their eutectic mixtures are the most promising bio-based materials that can be used as PCMs. They have been extensively investigated for solar energy applications but have not been explored for controlling indoor temperature fluctuations.
2. BPCMs benefit from some properties such as non-corrosivity, high latent heat of fusion, suitable melting temperature, non-toxicity, reasonable thermal and chemical stability, and lack of any environmental impact.
3. In cold temperate regions (e.g., Canada, North-European countries) with few sunny days in the winter, using PCMs for controlling the indoor temperature intermittency is rather interesting than for storing solar energy. However, only a few pure fatty acids have phase change temperatures in the range of human comfort (i.e., 18–25 °C). A further functionalization of the fatty acids is a prerequisite for the application in a building sector.
4. Most of the PCMs are incorporated in wallboard and ceiling board gypsum while only a few studies investigated the possibility of incorporating BPCMs into wood and wood-based materials. Using wood as a matrix appears as a significant improvement of the thermal mass of a "green" building.
5. Encapsulation and shape stabilization are the most used approaches for incorporating PCMs. Recently, special attention has been paid to shape stabilization using porous materials and fibers. This method is cheaper and have no side effect compared to encapsulation that reduces thermal performance of the PCM.
6. The main limiting factor of using BPCMs is their low thermal conductivity, which can be improved by inclusion of metallic, carbon-based nanoparticles as well as by using carbon and a graphite-based scaffold for encapsulation.
7. Wood and wood-based materials, e.g., delignified wood and carbonized wood, wood-flour, and wood fibers are interesting biomaterials for cost-effective and shape-stabilized BPCMs. Utilization of these materials will result in lightweight construction materials and enhancement in the thermal mass of buildings.
8. Use of BPCM can introduce a negative impact on the environment and, thus, LCA appears as a compulsory tool for selecting BPCM with a low impact for building applications.

Author Contributions: The manuscript was written through equal contributions of all authors who have given approval to the final version of the manuscript.

Funding: The Swedish Research Council for Environment, Agricultural Sciences and Spatial Planning (FORMAS) grant number 2017-00686, funded this research.

Conflicts of Interest: The authors declare no conflict of interest.

References

1. Pasupathy, A.; Velraj, R.; Seeniraj, R. Phase change material-based building architecture for thermal management in residential and commercial establishments. *Renew. Sustain. Energy Rev.* **2008**, *12*, 39–64, doi:10.1016/j.rser.2006.05.010.
2. Tyagi, V.; Kaushik, S.; Tyagi, S.; Akiyama, T. Development of phase change materials based microencapsulated technology for buildings: A review. *Renew. Sustain. Energy Rev.* **2011**, *15*, 1373–1391, doi:10.1016/j.rser.2010.10.006.
3. Bland, A.; Khzouz, M.; Statheros, T.; Gkanas, E.I. PCMs for Residential Building Applications: A Short Review Focused on Disadvantages and Proposals for Future Development. *Buildings* **2017**, *7*, 78, doi:10.3390/buildings7030078.
4. Souayfane, F.; Fardoun, F.; Biwole, P.H. Phase change materials (PCM) for cooling applications in buildings: A review. *Energy Build.* **2016**, *129*, 396–431, doi:10.1016/j.enbuild.2016.04.006.
5. Kenisarin, M.M.; Mahkamov, K. Passive thermal control in residential buildings using phase change materials. *Renew. Sustain. Energy Rev.* **2016**, *55*, 371–398, doi:10.1016/j.rser.2015.10.128.
6. Kuznik, F.; David, D.; Johannes, K.; Roux, J.-J. A review on phase change materials integrated in building walls. *Renew. Sustain. Energy Rev.* **2011**, *15*, 379–391, doi:10.1016/j.rser.2010.08.019.
7. Mathis, D.; Blanchet, P.; Landry, V.; Lagiere, P. Thermal characterization of bio-based phase changing materials in decorative wood-based panels for thermal energy storage. *Green Energy Environ.* **2019**, *4*, 56–65, doi:10.1016/j.gee.2018.05.004.
8. Mathis, D.; Blanchet, P.; Landry, V.; Lagière, P. Impregnation of Wood with Microencapsulated Bio-Based Phase Change Materials for High Thermal Mass Engineered Wood Flooring. *Appl. Sci.* **2018**, *8*, 2696, doi:10.3390/app8122696.
9. Asdrubali, F.; Ferracuti, B.; Lombardi, L.; Guattari, C.; Evangelisti, L.; Grazieschi, G. A review of structural, thermo-physical, acoustical, and environmental properties of wooden materials for building applications. *Build. Environ.* **2017**, *114*, 307–332, doi:10.1016/j.buildenv.2016.12.033.
10. Chen, F.; Kessel, A. and Wolcott, M.; 2012. A novel energy saving wood product with phase change materials. *In Proceedings of the 55th International Convention of Society of Wood Science and Technology*, Beijing, China, August, 27–31, 2012
11. Kalnæs, S.E.; Jelle, B. Phase change materials and products for building applications: A state-of-the-art review and future research opportunities. *Energy Build.* **2015**, *94*, 150–176, doi:10.1016/j.enbuild.2015.02.023.
12. Agyenim, F.; Hewitt, N.J.; Eames, P.; Smyth, M. A review of materials, heat transfer and phase change problem formulation for latent heat thermal energy storage systems (LHTESS). *Renew. Sustain. Energy Rev.* **2010**, *14*, 615–628, doi:10.1016/j.rser.2009.10.015.
13. Nazir, H.; Batool, M.; Osorio, F.J.B.; Isaza-Ruiz, M.; Xu, X.; Vignarooban, K.; Phelan, P.; Inamuddin; Kannan, A.N.M. Recent developments in phase change materials for energy storage applications: A review. *Int. J. Heat Mass Transf.* **2019**, *129*, 491–523, doi:10.1016/j.ijheatmasstransfer.2018.09.126.
14. Cabeza, L.F.; Barreneche, C.; Martorell, I.; Miró, L.; Sari-Bey, S.; Fois, M.; Paksoy, H.; Sahan, N.; Weber, R.R.; Constantinescu, M.; et al. Unconventional experimental technologies available for phase change materials (PCM) characterization. Part 1. Thermophysical properties. *Renew. Sustain. Energy Rev.* **2015**, *43*, 1399–1414, doi:10.1016/j.rser.2014.07.191.
15. Konuklu, Y.; Ostry, M.; Paksoy, H.; Charvát, P. Review on using microencapsulated phase change materials (PCM) in building applications. *Energy Build.* **2015**, *106*, 134–155, doi:10.1016/j.enbuild.2015.07.019.
16. Umair, M.M.; Zhang, Y.; Iqbal, K.; Zhang, S.; Tang, B. Novel strategies and supporting materials applied to shape-stabilize organic phase change materials for thermal energy storage—A review. *Appl. Energy* **2019**, *235*, 846–873, doi:10.1016/j.apenergy.2018.11.017.
17. Wei, G.; Wang, G.; Xu, C.; Ju, X.; Ju, X.; Du, X.; Yang, Y. Selection principles and thermophysical properties of high temperature phase change materials for thermal energy storage: A review. *Renew. Sustain. Energy Rev.* **2018**, *81*, 1771–1786, doi:10.1016/j.rser.2017.05.271.
18. Khadiran, T.; Hussein, M.Z.; Zainal, Z.; Rusli, R. Encapsulation techniques for organic phase change materials as thermal energy storage medium: A review. *Sol. Energy Mater. Sol. Cells* **2015**, *143*, 78–98, doi:10.1016/j.solmat.2015.06.039.
19. Baetens, R.; Jelle, B.; Gustavsen, A. Phase change materials for building applications: A state-of-the-art review. *Energy Build.* **2010**, *42*, 1361–1368, doi:10.1016/j.enbuild.2010.03.026.
20. Sharma, A.; Tyagi, V.; Chen, C.; Buddhi, D. Review on thermal energy storage with phase change materials and applications. *Renew. Sustain. Energy Rev.* **2009**, *13*, 318–345, doi:10.1016/j.rser.2007.10.005.
21. Sarier, N.; Onder, E. Organic phase change materials and their textile applications: An overview. *Thermochim. Acta* **2012**, *540*, 7–60, doi:10.1016/j.tca.2012.04.013.

22. Sharma, R.; Ganesan, P.B.; Tyagi, V.; Metselaar, H.S.C.; Sandaran, S. Developments in organic solid–liquid phase change materials and their applications in thermal energy storage. *Energy Convers. Manag.* **2015**, *95*, 193–228, doi:10.1016/j.enconman.2015.01.084.
23. Pielichowska, K.; Pielichowski, K. Phase change materials for thermal energy storage. *Prog. Mater. Sci.* **2014**, *65*, 67–123, doi:10.1016/j.pmatsci.2014.03.005.
24. Rathod, M.K.; Banerjee, J. Thermal stability of phase change materials used in latent heat energy storage systems: A review. *Renew. Sustain. Energy Rev.* **2013**, *18*, 246–258, doi:10.1016/j.rser.2012.10.022.
25. Amaral, C.; Vicente, R.; Marques, P.A.; Barros-Timmons, A. Phase change materials and carbon nanostructures for thermal energy storage: A literature review. *Renew. Sustain. Energy Rev.* **2017**, *79*, 1212–1228, doi:10.1016/j.rser.2017.05.093.
26. Turkyilmazoglu, M. Stefan problems for moving phase change materials and multiple solutions. *Int. J. Therm. Sci.* **2018**, *126*, 67–73, doi:10.1016/j.ijthermalsci.2017.12.019.
27. Kośny, J.; Kossecka, E.; Brzeziński, A.; Tleoubaev, A.; Yarbrough, D. Dynamic thermal performance analysis of fiber insulations containing bio-based phase change materials (PCMs). *Energy Build.* **2012**, *52*, 122–131, doi:10.1016/j.enbuild.2012.05.021.
28. Ye, R.; Lin, W.; Fang, X. Zhang, Z.; A numerical study of building integrated with CaCl2· 6H2O/expanded graphite composite phase change material. *App. Therm. Eng.*, 126, 480–488.
29. Ogoh, W Groulx, D. October. Stefan's problem: Validation of a one–dimensional solid–liquid phase change heat transfer process. *In Procceedings of the Excerpt from the Proceedings of the COMSOL Conference*, Boston.
30. Gulfam, R.; Zhang, P.; Meng, Z. Advanced thermal systems driven by paraffin-based phase change materials—A review. *Appl. Energy* **2019**, *238*, 582–611, doi:10.1016/j.apenergy.2019.01.114.
31. Jeong, S.-G.; Chung, O.; Yu, S.; Kim, S.; Kim, S. Improvement of the thermal properties of Bio-based PCM using exfoliated graphite nanoplatelets. *Sol. Energy Mater. Sol. Cells* **2013**, *117*, 87–92, doi:10.1016/j.solmat.2013.05.038.
32. Yu, S.; Jeong, S.-G.; Chung, O.; Kim, S. Bio-based PCM/carbon nanomaterials composites with enhanced thermal conductivity. *Sol. Energy Mater. Sol. Cells* **2014**, *120*, 549–554, doi:10.1016/j.solmat.2013.09.037.
33. Jeong, S.-G.; Lee, J.-H.; Seo, J.; Kim, S. Thermal performance evaluation of Bio-based shape stabilized PCM with boron nitride for energy saving. *Int. J. Heat Mass Transf.* **2014**, *71*, 245–250, doi:10.1016/j.ijheatmasstransfer.2013.12.017.
34. Kaizawa, A.; Maruoka, N.; Kawai, A.; Kamano, H.; Jozuka, T.; Senda, T.; Akiyama, T. Thermophysical and heat transfer properties of phase change material candidate for waste heat transportation system. *Heat Mass Transf.* **2007**, *44*, 763–769, doi:10.1007/s00231-007-0311-2.
35. Jiang, Y.; Hussain, H.; Kressler, J. Poly(vinyl alcohol) Cryogel Formation Using Biocompatible Ice Nucleating Agents. *Macromol. Mater. Eng.* **2014**, *300*, 181–190, doi:10.1002/mame.201400229.
36. Elefsiniotis, A.; Becker, T.; Schmid, U. Thermoelectric Energy Harvesting Using Phase Change Materials (PCMs) in High Temperature Environments in Aircraft. *J. Electron. Mater.* **2013**, *43*, 1809–1814, doi:10.1007/s11664-013-2880-9.
37. Solé, A.; Neumann, H.; Niedermaier, S.; Martorell, I.; Schossig, P.; Cabeza, L.F. Stability of sugar alcohols as PCM for thermal energy storage. *Sol. Energy Mater. Sol. Cells* **2014**, *126*, 125–134, doi:10.1016/j.solmat.2014.03.020.
38. Yuan, Y.; Zhang, N.; Tao, W.; Cao, X.; He, Y. Fatty acids as phase change materials: A review. *Renew. Sustain. Energy Rev.* **2014**, *29*, 482–498, doi:10.1016/j.rser.2013.08.107.
39. Rozanna, D.; Chuah, T.G.; Salmiah, A.; Choong, T.S.Y.; Sa'Ari, M. Fatty Acids as Phase Change Materials (PCMs) for Thermal Energy Storage: A Review. *Int. J. Green Energy* **2005**, *1*, 495–513, doi:10.1081/ge-200038722.
40. Feldman, D.; Shapiro, M.; Banu, D. Organic phase change materials for thermal energy storage. *Sol. Energy Mater.* **1986**, *13*, 1–10, doi:10.1016/0165-163390023-7.
41. Feldman, D.; Banu, D.; Hawes, D. Development and application of organic phase change mixtures in thermal storage gypsum wallboard. *Sol. Energy Mater. Sol. Cells* **1995**, *36*, 147–157, doi:10.1016/0927-024800168-r.
42. Hasan, A. Thermal energy storage system with stearic acid as phase change material. *Energy Convers. Manag.* **1994**, *35*, 843–856, doi:10.1016/0196-890490034-5.
43. Hasan, A. Phase change material energy storage system employing palmitic acid. *Sol. Energy* **1994**, *52*, 143–154, doi:10.1016/0038-092x(94)90064-7.
44. Sarı, A.; Sarı, A.; Kaygusuz, K. Thermal energy storage system using stearic acid as a phase change material. *Sol. Energy* **2001**, *71*, 365–376, doi:10.1016/s0038-092x(01)00075-5.
45. Sarı, A.; Kaygusuz, K. Thermal performance of myristic acid as a phase change material for energy storage application. *Renew. Energy* **2001**, *24*, 303–317, doi:10.1016/s0960-148100167-1.

46. Cedeño, F.O.; Prieto, M.M.; Espina, A.; GarcíaJ.R. Measurements of temperature and melting heat of some pure fatty acids and their binary and ternary mixtures by differential scanning calorimetry. *Thermochim. Acta* **2001**, *369*, 39–50, doi:10.1016/s0040-603100752-8.
47. Lin, Y.; Zhu, C.; Alva, G.; Fang, G. Palmitic acid/polyvinyl butyral/expanded graphite composites as form-stable phase change materials for solar thermal energy storage. *Appl. Energy* **2018**, *228*, 1801–1809, doi:10.1016/j.apenergy.2018.07.068.
48. Sharma, R.K.; Ganesan, P.B.; Tyagi, V.V. Long-term thermal and chemical reliability study of different organic phase change materials for thermal energy storage applications. *J. Therm. Anal. Calorim.* **2016**, *124*, 1357–1366, doi:10.1007/s10973-016-5281-5.
49. Nikolic, R.; Marinović-Cincović, M.; Gadzuric, S.; Zsigrai, I. New materials for solar thermal storage—Solid/liquid transitions in fatty acid esters. *Sol. Energy Mater. Sol. Cells* **2003**, *79*, 285–292, doi:10.1016/s0927-024800412-9.
50. Sarı, A. Eutectic mixtures of some fatty acids for low temperature solar heating applications: Thermal properties and thermal reliability. *Appl. Therm. Eng.* **2005**, *25*, 2100–2107, doi:10.1016/j.applthermaleng.2005.01.010.
51. Sarı, A.; Biçer, A.; Karaipekli, A. Synthesis, characterization, thermal properties of a series of stearic acid esters as novel solid–liquid phase change materials. *Mater. Lett.* **2009**, *63*, 1213–1216, doi:10.1016/j.matlet.2009.02.045.
52. Sarı, A.; Sarı, A. Thermal energy storage properties of mannitol–fatty acid esters as novel organic solid–liquid phase change materials. *Energy Convers. Manag.* **2012**, *64*, 68–78, doi:10.1016/j.enconman.2012.07.003.
53. Aydın, A.A.; Okutan, H. High-chain fatty acid esters of myristyl alcohol with odd carbon number: Novel organic phase change materials for thermal energy storage—2. *Sol. Energy Mater. Sol. Cells* **2011**, *95*, 2417–2423, doi:10.1016/j.solmat.2011.04.018.
54. Aydın, A.A. Diesters of high-chain dicarboxylic acids with 1-tetradecanol as novel organic phase change materials for thermal energy storage. *Sol. Energy Mater. Sol. Cells* **2012**, *104*, 102–108, doi:10.1016/j.solmat.2012.04.030.
55. Aydın, A.A.; Aydın, A. High–chain fatty acid esters of 1–hexadecanol for low temperature thermal energy storage with phase change materials. *Solar Energy Materials and Solar Cells*, 1996, 93–100.
56. Xu, S.; Zou, L.; Ling, X.; Wei, Y.; Zhang, S. Preparation and thermal reliability of methyl palmitate/methyl stearate mixture as a novel composite phase change material. *Energy Build.* **2014**, *68*, 372–375, doi:10.1016/j.enbuild.2013.09.038.
57. Shilei, L.; Neng, Z.; Guohui, F. Eutectic mixtures of capric acid and lauric acid applied in building wallboards for heat energy storage. *Energy Build.* **2006**, *38*, 708–711, doi:10.1016/j.enbuild.2005.10.006.
58. Dimaano, M.N.R.; Watanabe, T. The capric–lauric acid and pentadecane combination as phase change material for cooling applications. *Appl. Therm. Eng.* **2002**, *22*, 365–377, doi:10.1016/s1359-431100095-3.
59. Pielichowski, K.; Flejtuch, K.; Pielichowska, K. Differential Scanning Calorimetry Study of Blends of Poly(ethylene glycol) with Selected Fatty Acids. *Macromol. Mater. Eng.* **2003**, *288*, 259–264, doi:10.1002/mame.200390022.
60. Karaipekli, A.; Sarı, A. Preparation, thermal properties and thermal reliability of eutectic mixtures of fatty acids/expanded vermiculite as novel form-stable composites for energy storage. *J. Ind. Eng. Chem.* **2010**, *16*, 767–773, doi:10.1016/j.jiec.2010.07.003.
61. Sharma, A.; Shukla, A.; Chen, C.; Dwivedi, S. Development of phase change materials for building applications. *Energy Build.* **2013**, *64*, 403–407, doi:10.1016/j.enbuild.2013.05.029.
62. Ke, H.; Li, D.; Zhang, H.; Wang, X.; Cai, Y.; Huang, F.; Wei, Q. Electrospun form-stable phase change composite nanofibers consisting of capric acid-based binary fatty acid eutectics and polyethylene terephthalate. *Fibers Polym.* **2013**, *14*, 89–99, doi:10.1007/s12221-013-0089-4.
63. Hawes, D.; Feldman, D.; Banu, D. Latent heat storage in building materials. *Energy Build.* **1993**, *20*, 77–86, doi:10.1016/0378-778890040-2.
64. Hawlader, M.; Uddin, M.; Khin, M.M. Microencapsulated PCM thermal-energy storage system. *Appl. Energy* **2003**, *74*, 195–202, doi:10.1016/s0306-261900146-0.
65. Saih, D.; Vroman, I.; Giraud, S.; Bourbigot, S. Microencapsulation of ammonium phosphate with a polyurethane shell part I: Coacervation technique. *React. Funct. Polym.* **2005**, *64*, 127–138, doi:10.1016/j.reactfunctpolym.2005.05.004.
66. Liang, C.; Lingling, X.; Hongbo, S.; Zhibin, Z. Microencapsulation of butyl stearate as a phase change material by interfacial polycondensation in a polyurea system. *Energy Convers. Manag.* **2009**, *50*, 723–729, doi:10.1016/j.enconman.2008.09.044.

67. Cho, J.-S.; Kwon, A.; Cho, C.G. Microencapsulation of octadecane as a phase-change material by interfacial polymerization in an emulsion system. *Colloid Polym. Sci.* **2002**, *280*, 260–266, doi:10.1007/s00396-001-0603-x.
68. Kaygusuz, K.; Alkan, C.; Sarı, A.; Uzun, O. Encapsulated Fatty Acids in an Acrylic Resin as Shape-stabilized Phase Change Materials for Latent Heat Thermal Energy Storage. *Energy Sources, Part. A: Recover. Util. Environ. Eff.* **2008**, *30*, 1050–1059, doi:10.1080/15567030701258212.
69. Su, J.-F.; Wang, L.-X.; Ren, L. Preparation and characterization of double-MF shell microPCMs used in building materials. *J. Appl. Polym. Sci.* **2005**, *97*, 1755–1762, doi:10.1002/app.21205.
70. Chen, Z.; Wang, J.; Yu, F.; Zhang, Z.; Gao, X. Preparation and properties of graphene oxide-modified poly(melamine-formaldehyde) microcapsules containing phase change material n-dodecanol for thermal energy storage. *J. Mater. Chem. A* **2015**, *3*, 11624–11630, doi:10.1039/C5TA01852H.
71. Su, J.; Wang, L.; Ren, L. Fabrication and thermal properties of microPCMs: Used melamine-formaldehyde resin as shell material. *J. Appl. Polym. Sci.* **2006**, *101*, 1522–1528, doi:10.1002/app.23151.
72. Yoo, Y.; Martinez, C.; Youngblood, J.P. Synthesis and Characterization of Microencapsulated Phase Change Materials with Poly(urea−urethane) Shells Containing Cellulose Nanocrystals. *ACS Appl. Mater. Interfaces* **2017**, *9*, 31763–31776, doi:10.1021/acsami.7b06970.
73. Park, S.; Lee, Y.; Kim, Y.S.; Lee, H.M.; Kim, J.H.; Cheong, I.W.; Koh, W.-G. Magnetic nanoparticle-embedded PCM nanocapsules based on paraffin core and polyurea shell. *Colloids Surf. A Physicochem. Eng. Asp.* **2014**, *450*, 46–51, doi:10.1016/j.colsurfa.2014.03.005.
74. Zhang, H.; Wang, X. Synthesis and properties of microencapsulated n-octadecane with polyurea shells containing different soft segments for heat energy storage and thermal regulation. *Sol. Energy Mater. Sol. Cells* **2009**, *93*, 1366–1376, doi:10.1016/j.solmat.2009.02.021.
75. Sukhorukov, G.; Fery, A.; Möhwald, H. Intelligent micro- and nanocapsules. *Prog. Polym. Sci.* **2005**, *30*, 885–897, doi:10.1016/j.progpolymsci.2005.06.008.
76. Shchukina, E.; Graham, M.; Zheng, Z.; Shchukin, D. Nanoencapsulation of phase change materials for advanced thermal energy storage systems. *Chem. Soc. Rev.* **2018**, *47*, 4156–4175, doi:10.1039/c8cs00099a.
77. Liu, C.; Rao, Z.; Zhao, J.; Huo, Y.; Li, Y. Review on nanoencapsulted phase change materials: Preparation, Characterization and Heat transfer enhancement. *Na. En. 13*, 814–826.
78. Rodríguez-Cumplido, F.; Gelves, E.P.; Chejne-Jana, F. Recent developments in the synthesis of microencapsulated and nanoencapsulated phase change materials. *J. Energy Storage* **2019**, *24*, 100821, doi:10.1016/j.est.2019.100821.
79. Fuensanta, M.; Paiphansiri, U.; Romero-Sánchez, M.D.; Guillem, C.; Buendia, A.M.L.; Landfester, K. Thermal properties of a novel nanoencapsulated phase change material for thermal energy storage. *Thermochim. Acta* **2013**, *565*, 95–101, doi:10.1016/j.tca.2013.04.028.
80. Fang, G.; Chen, Z.; Li, H. Synthesis and properties of microencapsulated paraffin composites with SiO2 shell as thermal energy storage materials. *Chem. Eng. J.* **2010**, *163*, 154–159, doi:10.1016/j.cej.2010.07.054.
81. Cao, L.; Tang, F.; Fang, G. Preparation and characteristics of microencapsulated palmitic acid with TiO2 shell as shape-stabilized thermal energy storage materials. *Sol. Energy Mater. Sol. Cells* **2014**, *123*, 183–188, doi:10.1016/j.solmat.2014.01.023.
82. Pan, L.; Tao, Q.; Zhang, S.; Wang, S.; Zhang, J.; Wang, S.; Wang, Z.; Zhang, Z. Preparation, characterization and thermal properties of micro-encapsulated phase change materials. *Sol. Energy Mater. Sol. Cells* **2012**, *98*, 66–70, doi:10.1016/j.solmat.2011.09.020.
83. Li, F.; Wang, X.; Wu, D. Fabrication of multifunctional microcapsules containing n -eicosane core and zinc oxide shell for low-temperature energy storage, photocatalysis, and antibiosis. *Energy Convers. Manag.* **2015**, *106*, 873–885, doi:10.1016/j.enconman.2015.10.026.
84. Teng, T.-P.; Yu, C.-C. Characteristics of phase-change materials containing oxide nano-additives for thermal storage. *Nanoscale Res. Lett.* **2012**, *7*, 611, doi:10.1186/1556-276X-7-611.
85. Du, X.; Wang, S.; Du, Z.; Cheng, X.; Wang, H. Preparation and characterization of flame–retardant nanoencapsulated phase change materials with poly(methyl methacrylate) shells for thermal energy storage. *J. Mat. Chem. A.* , 6, pp. 17519–17529.
86. Yuan, H.; Bai, H.; Zhang, J.; Zhang, Z. Synthesis of Nanoencapsulated Phase Change Materials with Ag Shell for Thermal Energy Storage. *In Proceedings of the 11th International Conference on Porous Metals and Metallic Foams* (MetFoam 2019) Dearborn, MI, USA Springer Science and Business Media LLC, 2020; pp. 687–694.
87. De Matteis, V.; Cannavale, A.; Martellotta, F.; Rinaldi, R.; Calcagnile, P.; Ferrari, F.; Ayr, U.; Fiorito, F. Nano-encapsulation of phase change materials: From design to thermal performance, simulations and toxicological assessment. *Energy Build.* **2019**, *188–189*, 1–11, doi:10.1016/j.enbuild.2019.02.004.

88. Zhou, J.; Zhao, J.; Cui, Y.; Cheng, W. Synthesis of bifunctional nanoencapsulated phase change materials with nano-TiO_2 modified polyacrylate shell for thermal energy storage and ultraviolet absorption. *Polym. Int.* **2019**, *69*, 140–148, doi:10.1002/pi.5924.
89. Imran Hussain, S.; Ameelia Roseline, A.; Kalaiselvam, S. Bifunctional nanoencapsulated eutectic phase change materials core with SiO_2/SnO_2 nanosphere shell for thermal and electrical energy storage. *Mat. Design*, *154*, 291–301.
90. Zhang, Y.; Xiu, J.; Tang, B.; Lu, R.; Zhang, S.-F. Novel semi-interpenetrating network structural phase change composites with high phase change enthalpy. *AIChE J.* **2017**, *64*, 688–696, doi:10.1002/aic.15956.
91. Regin, A.F.; Solanki, S.; Saini, J. Heat transfer characteristics of thermal energy storage system using PCM capsules: A review. *Renew. Sustain. Energy Rev.* **2008**, *12*, 2438–2458, doi:10.1016/j.rser.2007.06.009.
92. Wang, C.; Feng, L.; Li, W.; Zheng, J.; Tian, W.; Li, X. Shape-stabilized phase change materials based on polyethylene glycol/porous carbon composite: The influence of the pore structure of the carbon materials. *Sol. Energy Mater. Sol. Cells* **2012**, *105*, 21–26, doi:10.1016/j.solmat.2012.05.031.
93. Krupa, I.; Miková, G.; Luyt, A.S. Phase change materials based on low-density polyethylene/paraffin wax blends. *Eur. Polym. J.* **2007**, *43*, 4695–4705, doi:10.1016/j.eurpolymj.2007.08.022.
94. SánchezL.; Lacasa, E.; Carmona, M.; Rodríguez, J.; SánchezP.; Silva, M.L.S.; Rodríguez, J. Applying an Experimental Design to Improve the Characteristics of Microcapsules Containing Phase Change Materials for Fabric Uses. *Ind. Eng. Chem. Res.* **2008**, *47*, 9783–9790, doi:10.1021/ie801107e.
95. Alkan, C.; Sarı, A. Fatty acid/poly(methyl methacrylate) (PMMA) blends as form-stable phase change materials for latent heat thermal energy storage. *Sol. Energy* **2008**, *82*, 118–124, doi:10.1016/j.solener.2007.07.001.
96. Wang, L.; Meng, D. Fatty acid eutectic/polymethyl methacrylate composite as form-stable phase change material for thermal energy storage. *Appl. Energy* **2010**, *87*, 2660–2665, doi:10.1016/j.apenergy.2010.01.010.
97. Wang, X.; Yu, X.; Tian, C.; Wang, J. Preparation and characterization of form-stable paraffin/polyurethane composites as phase change materials for thermal energy storage. *Energy Convers. Manag.* **2014**, *77*, 13–21, doi:10.1016/j.enconman.2013.09.015.
98. Silakhori, M.; Metselaar, H.S.C.; Mahlia, T.M.I.; Fauzi, H.; Baradaran, S.; Naghavi, M.S. Palmitic acid/polypyrrole composites as form-stable phase change materials for thermal energy storage. *Energy Convers. Manag.* **2014**, *80*, 491–497, doi:10.1016/j.enconman.2014.01.023.
99. Cai, Y.; Wei, Q.; Huang, F.; Lin, S.; Chen, F.; Gao, W. Thermal stability, latent heat and flame retardant properties of the thermal energy storage phase change materials based on paraffin/high density polyethylene composites. *Renew. Energy* **2009**, *34*, 2117–2123, doi:10.1016/j.renene.2009.01.017.
100. Li, Z.; He, W.; Xu, J.; Jiang, M. Preparation and characterization of in situ grafted/crosslinked polyethylene glycol/polyvinyl alcohol composite thermal regulating fiber. *Sol. Energy Mater. Sol. Cells* **2015**, *140*, 193–201, doi:10.1016/j.solmat.2015.04.014.
101. Sari, A; Kaygusuz, K. Poly (vinyl alcohol)/fatty acid blends for thermal energy storage. *Ene. Sour., 29*, 873–883.
102. Sari, A.; Akcay, M.; Soylak, M. Polymer–stearic acid blends as form–stable phase change material for thermal energy storage. *En. Sour., 27*, 1535–1546.
103. Şentürk, S.B.; Kahraman, D.; Alkan, C.; Gokce, I. Biodegradable PEG/cellulose, PEG/agarose and PEG/chitosan blends as shape stabilized phase change materials for latent heat energy storage. *Carbohydr. Polym.* **2011**, *84*, 141–144, doi:10.1016/j.carbpol.2010.11.015.
104. Prajapati, D.G.; Kandasubramanian, B. Biodegradable Polymeric Solid Framework-Based Organic Phase-Change Materials for Thermal Energy Storage. *Ind. Eng. Chem. Res.* **2019**, *58*, 10652–10677, doi:10.1021/acs.iecr.9b01693.
105. Sarı, A.; Alkan, C.; Karaipekli, A.; Önal, A. Preparation, characterization and thermal properties of styrene maleic anhydride copolymer (SMA)/fatty acid composites as form stable phase change materials. *En. Conv. Manag., 49*, 373–380.
106. Pielichowska, K.; Pielichowski, K. Biodegradable PEO/cellulose-based solid-solid phase change materials. *Polym. Adv. Technol.* **2010**, *22*, 1633–1641, doi:10.1002/pat.1651.
107. Pielichowska, K.; Pielichowski, K. Novel biodegradable form stable phase change materials: Blends of poly(ethylene oxide) and gelatinized potato starch. *J. Appl. Polym. Sci.* **2010**, *116*, 1725–1731, doi:10.1002/app.31615.
108. Cao, L.; Tang, Y.; Fang, G. Preparation and properties of shape-stabilized phase change materials based on fatty acid eutectics and cellulose composites for thermal energy storage. *Energy* **2015**, *80*, 98–103, doi:10.1016/j.energy.2014.11.046.
109. Özonur, Y.; Mazman, M.; Paksoy, H.; Evliya, H. Microencapsulation of coco fatty acid mixture for thermal energy storage with phase change material. *Int. J. Energy Res.* **2006**, *30*, 741–749, doi:10.1002/er.1177.

110. Lv, P.; Liu, C.; Rao, Z. Review on clay mineral-based form-stable phase change materials: Preparation, characterization and applications. *Renew. Sustain. Energy Rev.* **2017**, *68*, 707–726, doi:10.1016/j.rser.2016.10.014.
111. Liu, S.; Han, L.; Xie, S.; Jia, Y.; Sun, J.; Jing, Y.; Zhang, Q. A novel medium-temperature form-stable phase change material based on dicarboxylic acid eutectic mixture/expanded graphite composites. *Sol. Energy* **2017**, *143*, 22–30, doi:10.1016/j.solener.2016.12.027.
112. Radhakrishnan, R.; Gubbins, K.E. Free energy studies of freezing in slit pores: An order–parameter approach using Monte Carlo simulation. *Mol. Phy., 96*, 1249–1267.
113. Radhakrishnan, R.; Gubbins, K.E.; Watanabe, A.; Kaneko, K. Freezing of simple fluids in microporous activated carbon fibers: Comparison of simulation and experiment. *J. Chem. Phys.* **1999**, *111*, 9058–9067, doi:10.1063/1.480261.
114. Sarı, A.; Karaipekli, A. Preparation, thermal properties and thermal reliability of palmitic acid/expanded graphite composite as form-stable PCM for thermal energy storage. *Sol. Energy Mater. Sol. Cells* **2009**, *93*, 571–576, doi:10.1016/j.solmat.2008.11.057.
115. Wang, S.; Qin, P.; Fang, X.; Zhang, Z.; Wang, S.; Liu, X. A novel sebacic acid/expanded graphite composite phase change material for solar thermal medium-temperature applications. *Sol. Energy* **2014**, *99*, 283–290, doi:10.1016/j.solener.2013.11.018.
116. Li, B.; Liu, T.; Hu, L.; Wang, Y.; Nie, S. Facile preparation and adjustable thermal property of stearic acid–graphene oxide composite as shape-stabilized phase change material. *Chem. Eng. J.* **2013**, *215*, 819–826, doi:10.1016/j.cej.2012.11.077.
117. Mehrali, M.; Latibari, S.T.; Mehrali, M.; Mahlia, T.M.I.; Metselaar, H.S.C.; Sanjani, M.S.N.; Sadeghinezhad, E.; Akhiani, A.R. Preparation and characterization of palmitic acid/graphene nanoplatelets composite with remarkable thermal conductivity as a novel shape-stabilized phase change material. *Appl. Therm. Eng.* **2013**, *61*, 633–640, doi:10.1016/j.applthermaleng.2013.08.035.
118. Ince, Şeyma; Seki, Y.; Ezan, M.A.; Turgut, A.; Erek, A. Thermal properties of myristic acid/graphite nanoplates composite phase change materials. *Renew. Energy* **2015**, *75*, 243–248, doi:10.1016/j.renene.2014.09.053.
119. Sheng, N.; Nomura, T.; Zhu, C.; Habazaki, H.; Akiyama, T. Cotton-derived carbon sponge as support for form-stabilized composite phase change materials with enhanced thermal conductivity. *Sol. Energy Mater. Sol. Cells* **2019**, *192*, 8–15, doi:10.1016/j.solmat.2018.12.018.
120. Liang, J.; Zhimeng, L.; Ye, Y.; Yanjun, W.; Jingxin, L.; Changlin, Z. Fabrication and characterization of fatty acid/wood-flour composites as novel form-stable phase change materials for thermal energy storage. *Energy Build.* **2018**, *171*, 88–99, doi:10.1016/j.enbuild.2018.04.044.
121. Yang, Z.; Deng, Y.; Li, J. Preparation of porous carbonized woods impregnated with lauric acid as shape-stable composite phase change materials. *Appl. Therm. Eng.* **2019**, *150*, 967–976, doi:10.1016/j.applthermaleng.2019.01.063.
122. Li, J.; Xue, P.; He, H.; Ding, W.; Han, J. Preparation and application effects of a novel form-stable phase change material as the thermal storage layer of an electric floor heating system. *Energy Build.* **2009**, *41*, 871–880, doi:10.1016/j.enbuild.2009.03.009.
123. Yang, H.; Chao, W.; Wang, S.; Yu, Q.; Cao, G.; Yang, T.; Liu, F.; Di, X.; Li, J.; Wang, C.; et al. Self-luminous wood composite for both thermal and light energy storage. *Energy Storage Mater.* **2019**, *18*, 15–22, doi:10.1016/j.ensm.2019.02.005.
124. Yang, H.; Wang, Y.; Yu, Q.; Cao, G.; Yang, R.; Ke, J.; Di, X.; Liu, F.; Zhang, W.; Wang, C. Composite phase change materials with good reversible thermochromic ability in delignified wood substrate for thermal energy storage. *Appl. Energy* **2018**, *212*, 455–464, doi:10.1016/j.apenergy.2017.12.006.
125. Ma, L.; Wang, Q.; Li, L. Delignified wood/capric acid-palmitic acid mixture stable-form phase change material for thermal storage. *Sol. Energy Mater. Sol. Cells* **2019**, *194*, 215–221, doi:10.1016/j.solmat.2019.02.026.
126. Jamekhorshid, A.; Sadrameli, S.; Barzin, R.; Farid, M. Composite of wood-plastic and micro-encapsulated phase change material (MEPCM) used for thermal energy storage. *Appl. Therm. Eng.* **2017**, *112*, 82–88, doi:10.1016/j.applthermaleng.2016.10.037.
127. Barreneche, C.; Vecstaudza, J.; Bajare, D.; Fernandez, A. PCM/wood composite to store thermal energy in passive building envelopes. *IOP Conf. Ser. Mater. Sci. Eng.* **2017**, *251*, 12111, doi:10.1088/1757-899x/251/1/012111.
128. Guo, X.; Cao, J.; Peng, Y.; Liu, R. Incorporation of microencapsulated dodecanol into wood flour/high-density polyethylene composite as a phase change material for thermal energy storage. *Mater. Des.* **2016**, *89*, 1325–1334, doi:10.1016/j.matdes.2015.10.068.

129. Guo, X.; Zhang, S.; Cao, J. An energy-efficient composite by using expanded graphite stabilized paraffin as phase change material. *Compos. Part A Appl. Sci. Manuf.* **2018**, *107*, 83–93, doi:10.1016/j.compositesa.2017.12.032.
130. Cabeza, L.F.; Mehling, H.; Hiebler, S.; Ziegler, F. Heat transfer enhancement in water when used as PCM in thermal energy storage. *Appl. Therm. Eng.* **2002**, *22*, 1141–1151, doi:10.1016/s1359-431100035-2.
131. A Khateeb, S.; Farid, M.; Selman, J.; Al-Hallaj, S. Design and simulation of a lithium-ion battery with a phase change material thermal management system for an electric scooter. *J. Power Sources* **2004**, *128*, 292–307, doi:10.1016/j.jpowsour.2003.09.070.
132. Py, X.; Olives, R.; Mauran, S. Paraffin/porous-graphite-matrix composite as a high and constant power thermal storage material. *Int. J. Heat Mass Transf.* **2001**, *44*, 2727–2737, doi:10.1016/s0017-931000309-4.
133. Sedeh, M.M.; Khodadadi, J. Thermal conductivity improvement of phase change materials/graphite foam composites. *Carbon* **2013**, *60*, 117–128, doi:10.1016/j.carbon.2013.04.004.
134. Li, M. A nano-graphite/paraffin phase change material with high thermal conductivity. *Appl. Energy* **2013**, *106*, 25–30, doi:10.1016/j.apenergy.2013.01.031.
135. Fukai, J.; Hamada, Y.; Morozumi, Y.; Miyatake, O. Effect of carbon-fiber brushes on conductive heat transfer in phase change materials. *Int. J. Heat Mass Transf.* **2002**, *45*, 4781–4792, doi:10.1016/s0017-931000179-5.
136. Fukai, J.; Kanou, M.; Kodama, Y.; Miyatake, O. Thermal conductivity enhancement of energy storage media using carbon fibers. *Energy Convers. Manag.* **2000**, *41*, 1543–1556, doi:10.1016/s0196-890400166-1.
137. Cui, Y.; Liu, C.; Hu, S.; Yu, X. The experimental exploration of carbon nanofiber and carbon nanotube additives on thermal behavior of phase change materials. *Sol. Energy Mater. Sol. Cells* **2011**, *95*, 1208–1212, doi:10.1016/j.solmat.2011.01.021.
138. Fan, L.-W.; Fang, X.; Wang, X.; Zeng, Y.; Xiao, Y.-Q.; Yu, Z.-T.; Xu, X.; Hu, Y.-C.; Cen, K. Effects of various carbon nanofillers on the thermal conductivity and energy storage properties of paraffin-based nanocomposite phase change materials. *Appl. Energy* **2013**, *110*, 163–172, doi:10.1016/j.apenergy.2013.04.043.
139. Parameshwaran, R.; Jayavel, R.; Kalaiselvam, S. Study on thermal properties of organic ester phase-change material embedded with silver nanoparticles. *J. Therm. Anal. Calorim.* **2013**, *114*, 845–858, doi:10.1007/s10973-013-3064-9.
140. Wang, W.; Yang, X.; Fang, Y.; Ding, J.; Yan, J. Enhanced thermal conductivity and thermal performance of form-stable composite phase change materials by using β-Aluminum nitride. *Appl. Energy* **2009**, *86*, 1196–1200, doi:10.1016/j.apenergy.2008.10.020.
141. Yang, H.; Wang, Y.; Yu, Q.; Cao, G.; Sun, X.; Yang, R.; Zhang, Q.; Liu, F.; Di, X.; Li, J.; et al. Low-cost, three-dimension, high thermal conductivity, carbonized wood-based composite phase change materials for thermal energy storage. *Energy* **2018**, *159*, 929–936, doi:10.1016/j.energy.2018.06.207.
142. Li, J.; Xue, P.; Ding, W.; Han, J.; Sun, G. Micro-encapsulated paraffin/high-density polyethylene/wood flour composite as form-stable phase change material for thermal energy storage. *Sol. Energy Mater. Sol. Cells* **2009**, *93*, 1761–1767, doi:10.1016/j.solmat.2009.06.007.
143. Singh, R.; Sadeghi, S.; Shabani, B. Thermal Conductivity Enhancement of Phase Change Materials for Low-Temperature Thermal Energy Storage Applications. *Energies* **2018**, *12*, 75, doi:10.3390/en12010075.
144. Cunha, S.; De Aguiar, J.L.B. Phase change materials and energy efficiency of buildings: A review of knowledge. *J. Energy Storage* **2020**, *27*, 101083, doi:10.1016/j.est.2019.101083.
145. Madad, A.; Mouhib, T.; Mouhsen, A. Phase Change Materials for Building Applications: A Thorough Review and New Perspectives. *Buildings* **2018**, *8*, 63, doi:10.3390/buildings8050063.
146. Frigione, M.; Lettieri, M.; Sarcinella, A. Phase Change Materials for Energy Efficiency in Buildings and Their Use in Mortars. *Materials* **2019**, *12*, 1260, doi:10.3390/ma12081260.
147. Mathis, D.; Blanchet, P.; Lagière, P.; Landry, V. Performance of Wood-Based Panels Integrated with a Bio-Based Phase Change Material: A Full-Scale Experiment in a Cold Climate with Timber-Frame Huts. *Energies* **2018**, *11*, 3093, doi:10.3390/en11113093.
148. Bribian, I.Z.; Uson, J.A.A.; Scarpellini, S. Life cycle assessment in buildings: State-of-the-art and simplified LCA methodology as a complement for building certification. *Build. Environ.* **2009**, *44*, 2510–2520, doi:10.1016/j.buildenv.2009.05.001.
149. Zabalza B.; Valero, C.A.; Aranda, U.A. Life cycle assessment of building materials Comparative analysis of energy and environmental impacts and evaluation of the eco–efficiency improvement potential. *Build. Env.*, *46*, 1133–1140.
150. Chau, C.K.; Leung, T.; Ng, W. A review on Life Cycle Assessment, Life Cycle Energy Assessment and Life Cycle Carbon Emissions Assessment on buildings. *Appl. Energy* **2015**, *143*, 395–413, doi:10.1016/j.apenergy.2015.01.023.

151. Kovacic, I.; Zoller, V. Building life cycle optimization tools for early design phases. *Energy* **2015**, *92*, 409–419, doi:10.1016/j.energy.2015.03.027.
152. Kylili, A.; Fokaides, P.A. Life Cycle Assessment (LCA) of Phase Change Materials (PCMs) for building applications: A review. *J. Build. Eng.* **2016**, *6*, 133–143, doi:10.1016/j.jobe.2016.02.008.
153. De Gracia, A.; Rincón, L.; Castell, A.; Jimenez, M.; Boer, D.; Medrano, M.; Cabeza, L.F. Life Cycle Assessment of the inclusion of phase change materials (PCM) in experimental buildings. *Energy Build.* **2010**, *42*, 1517–1523, doi:10.1016/j.enbuild.2010.03.022.
154. Menoufi, K.; Castell, A.; Farid, M.; Boer, D.; Cabeza, L.F. Life Cycle Assessment of experimental cubicles including PCM manufactured from natural resources (esters): A theoretical study. *Renew. Energy* **2013**, *51*, 398–403, doi:10.1016/j.renene.2012.10.010.
155. Menoufi, K.; Castell, A.; Navarro, L.; Pérez, G.; Boer, D.; Cabeza, L.F. Evaluation of the environmental impact of experimental cubicles using Life Cycle Assessment: A highlight on the manufacturing phase. *Appl. Energy* **2012**, *92*, 534–544, doi:10.1016/j.apenergy.2011.11.020.
156. Castell, A.; Menoufi, K.; De Gracia, A.; Rincón, L.; Boer, D.; Cabeza, L.F. Life Cycle Assessment of alveolar brick construction system incorporating phase change materials (PCMs). *Appl. Energy* **2013**, *101*, 600–608, doi:10.1016/j.apenergy.2012.06.066.
157. Serrano, S.; Barreneche, C.; Rincón, L.; Boer, D.; Cabeza, L.F. Stabilized rammed earth incorporating PCM: Optimization and improvement of thermal properties and Life Cycle Assessment. *Energy Procedia* **2012**, *30*, 461–470, doi:10.1016/j.egypro.2012.11.055.
158. Serrano, S.; Barreneche, C.; Rincón, L.; Boer, D.; Cabeza, L.F. Optimization of three new compositions of stabilized rammed earth incorporating PCM: Thermal properties characterization and LCA. *Constr. Build. Mater.* **2013**, *47*, 872–878, doi:10.1016/j.conbuildmat.2013.05.018.
159. Uson, J.A.A.; Ferreira, G.A.F.; López-Sabirón, A.M.; Toledo, M.D.M.; Bribian, I.Z. Phase change material applications in buildings: An environmental assessment for some Spanish climate severities. *Sci. Total. Environ.* **2013**, *444*, 16–25, doi:10.1016/j.scitotenv.2012.11.012.
160. De Gracia, A.; Navarro, L.; Castell, A.; Boer, D.; Cabeza, L.F. Life cycle assessment of a ventilated facade with PCM in its air chamber. *Sol. Energy* **2014**, *104*, 115–123, doi:10.1016/j.solener.2013.07.023.
161. Fabiani, C.; Pisello, A.L.; Barbanera, M.; Cabeza, L.F. Palm oil-based bio-PCM for energy efficient building applications: Multipurpose thermal investigation and life cycle assessment. *J. Energy Storage* **2020**, *28*, 101129, doi:10.1016/j.est.2019.101129.
162. Konstantinidou, C.A.; Lang, W.; Papadopoulos, A.M.; Santamouris, M. Life cycle and life cycle cost implications of integrated phase change materials in office buildings. *Int. J. Energy Res.* **2018**, *43*, 150–166, doi:10.1002/er.4238.
163. Noël, J.A.; Allred, P.M.; White, M.A. Life cycle assessment of two biologically produced phase change materials and their related products. *Int. J. Life Cycle Assess.* **2014**, *20*, 367–376, doi:10.1007/s11367-014-0831-1.
164. Panayiotou, G.; Kalogirou, S.; Tassou, S.A. Evaluation of the application of Phase Change Materials (PCM) on the envelope of a typical dwelling in the Mediterranean region. *Renew. Energy* **2016**, *97*, 24–32, doi:10.1016/j.renene.2016.05.043.
165. Heidari, M.D.; Mathis, D.; Blanchet, P.; Amor, B. Streamlined Life Cycle Assessment of an Innovative Bio-Based Material in Construction: A Case Study of a Phase Change Material Panel. *Forests* **2019**, *10*, 160, doi:10.3390/f10020160.

II

Journal of Energy Storage 39 (2021) 102645

Contents lists available at ScienceDirect

Journal of Energy Storage

journal homepage: www.elsevier.com/locate/est

Multicomponent bio-based fatty acids system as phase change material for low temperature energy storage

Meysam Nazari, Mohamed Jebrane *, Nasko Terziev

Department of Forest Biomaterials and Technology, Swedish University of Agricultural Sciences, Vallvägen 9C, 750 07 Uppsala, Sweden

ARTICLE INFO

Keywords:
Bio-based PCMs
Coconut oil fatty acids
Energy storage in buildings
Multicomponent mixtures

ABSTRACT

In this study, new multicomponent mixtures of fatty acids for low temperature thermal energy storage applications have been developed. The new mixtures were based on coconut oil fatty acids (CoFA) and commercial grades of oleic (OA) and linoleic acid (LA). Refined coconut oil (CO) was first converted into free fatty acids by alkaline saponification. The prepared CoFA were then mixed with OA or LA at various compositions to prepare stable bio-based phase change materials (BPCMs). The thermal behavior including melting/solidification temperatures, specific heat and enthalpy of the developed mixtures were investigated by means of differential scanning calorimetry (DSC) and T-history. Transient hot wire method was used to measure thermal conductivity of the PCMs. The chemical stability and thermal reliability of the mixtures were assessed stepwise from 100 to 700 melt/freeze cycles by attenuated total reflectance-Fourier transform infrared spectroscopy (ATR-FTIR) and DSC. Based on DSC and T-history results, the phase transition of the developed PCMs were in line with the range of human comfort temperatures i.e. 18-25 °C, with no incongruent melting and less than 0.6 °C super cooling, whereas specific heat and enthalpy of the new mixtures were in the range of 1-5 J/g K, and 40-100 J/g. The FTIR and DSC results indicated that the PCMs mixtures are chemically and thermally stable. The thermal conductivity of the mixtures were in average 0.2 W/m K, in liquid phase and 0.35 W/m K, in solid phase. Out of the different developed combinations, the mixture of LA/CoFA (20/80) showed distinguished performance and can be considered as potential BPCM for low temperature thermal energy storage applications.

1. Introduction

Increasing world populations and technologies development lead to increase in demand for energy. Moreover, environmental concerns regarding climate change have increased over the last decades. In order to address the growth in energy demands and considering environmental concerns, methods to store and manage energy are as important as searching for new energy resources [1]. Among the sectors that consume considerable energy, residential building uses over 40% of the total globally generated energy, contributing to 30% of the emitted greenhouse gases [2-4]. Managing energy consumption in building sector by maintaining the indoor temperature constant and minimizing the temperature fluctuations inside the buildings are considered as a potential solution to govern the energy consumption [5,6]. In this context, energy storage in form of latent heat thermal energy using phase change materials (PCMs) is an attractive solution due to high-energy storage density with small difference between storing and releasing functions. Several categories of materials have been investigated as PCMs, including organic compounds (fatty acids, PEG and Paraffins) and inorganic systems (salt and salt hydrates) [6-10]. These materials are widely used in building sector to control the indoor temperature fluctuations by integrating them into buildings elements [1, 6,11,12]. Most of these strategies involving incorporation of organic phase change materials (OPCMs) into construction materials mainly focused on storing and releasing solar energy for indoors heating. This pattern is suitable for regions where there is enough sun during winter periods when the demands for energy is high. However, in cold-weather countries such as Canada and Nordic countries, the sunny days during the winter periods are limited. Thus, using PCMs to control indoor temperature fluctuations in residential buildings seems more interesting than storing solar energy during daytimes and releasing it during nights in these countries.

Among the investigated OPCMs, fatty acids are considered as the most promising materials because they are renewable, non-toxic, commercially available at low cost, and biodegradable [13,14]. Furthermore, fatty acids benefit from the unique and superior characteristics such as congruent melting, chemical and thermal stability

* Corresponding author.
E-mail address: mohamed.jebrane@slu.se (M. Jebrane).

https://doi.org/10.1016/j.est.2021.102645
Received 30 November 2020; Received in revised form 23 April 2021; Accepted 27 April 2021
Available online 13 May 2021

Nomenclature

A	Contact surface area [m^2]
Bi	Biot number
c_p	Specific heat [J/g K]
D	Diameter [m]
H	Enthalpy [J/g]
h	Heat transfer coefficient [W/m^2 K]
I	Electrical current [A]
λ	Thermal conductivity [W/m K]
L	Length of the wire [m]
$LMTD$	Logarithmic mean temperature difference [K]
m	Mass of the materials [kg]
n	Time point [s]
P	Independent variables
Q	Heat [W]
R	Dependent variables
r	Radius [m]
T	Temperature [K]
t	Time [s]
U	Uncertainty
u	Overall heat transfer coefficient [W/m^2 K]
V	Voltage [V]

Greek symbol

δ	Characteristics length [m]
Δ	Difference
∞	Ambient

Subscripts

f	Final
in	Inner side
ins	Insulation
o	Initial
out	Outer side
pcm	Sample
r	Reference
tube	Tube container
tot	Total
∞	Ambient

Abbreviatio

BPCM	Bio-based phase change materials
CO	Coconut oil
CoFA	Coconut oil fatty acid
DSC	Differential scanning calorimetry
FTIR	Fourier-transform infrared spectroscopy
LA	Linoleic acid
OA	Oleic acid
OPCM	Organic phase change materials
PCM	Phase change materials

[15-17] and, thus constitute potential Bio-based PCMs (BPCMs) for low to medium temperature energy storage applications [13,14]. According to the American Society of Heating, Cooling and Air-conditioning Engineers (ASHRAE), the room temperature for summer and winter conditions are suggested to be in the range of 23.5-25.5°C and 21.0-23.0°C respectively [7]. However, most of the pure fatty acids have phase transition temperatures outside the standard temperature range [13,14], and thus cannot be used directly. By mixing two or several fatty acid together, stable mixtures with phase transition temperatures suitable for low thermal energy storage applications can be obtained. Several studies have been conducted on fatty acid mixtures to find stable mixtures as BPCMs [18-25]. Recently, capric and lauric acids were studied when incorporated into wallboards for low temperature thermal energy storage for heating and cooling applications [21]. The thermal stability of the eutectic mixture was stable after 360 cycles and can serve for latent heat storage in building applications. Another study reported that the addition of alkanes (e.g. pentadecane) to capric-lauric mixtures could enhance the thermal reliability and storage potential for cooling applications [22]. Ma et al. [20] studied the eutectic mixture of capric-palmitic acids impregnated into delignified wood and reported a retention of 61.2% without leakage, and the composite displayed a phase transition temperature of 23.4 °C and latent heat of 94.4 J/g with good thermal stability. Mathis et al. [18] investigated the performance of capric-lauric mixtures and two other commercial BPCMs packed in plastic pouches integrated into fiberboards panels. The studied BPCMs were thermally stable after thermal cycling and showed a phase transition temperature and latent heat storage appropriate for building applications. Karaipekli and Sari [23] studied mixtures of fatty acids including compositions of capric, lauric, palmitic and stearic acids, incorporated in expanded vermiculite for working temperatures in the range of 18-25 °C. The mixtures were thermally and chemically stable after 5000 cycles with melting temperatures in the range of 19.09-25.64 °C and latent heats ranging from 61.03 to 72.02 J/g, i.e. suitable for building. Similar mixtures comprising capric, lauric, myristic, palmitic and stearic acids were investigated by Sharma et al. [24]; and melting temperatures in the range 20-30°C and latent heat ranging from 100 to 160 J/g were recorded. Ke et al. [25] reported similar results for the above-mentioned binary fatty acid mixtures incorporated in polyethylene terephthalate (PET), while when tertiary compositions were prepared, different behaviors were observed [26]. Most of these combinations are promising but they suffer from phase separation in solid phase due to the immiscibility of the two fatty acid species [27,28].

Some tropical fruit oils and their derivatives have been recently investigated as a promising bio resourced PCMs. In this context, several studies reported the potential of palm kernel oil, Allanblackia, shea butter and coconut oil as promising phase change materials for building applications [29-32]. Most of these plant oils are polymorphic with a multiple melting/freezing profile over the transition temperatures. Moreover, some of the studied oils are susceptible to oxidation hence limiting their application as PCMs in buildings [29]. Kahwaji and White [33] investigated the feasibility of using a series of edible oils including coconut oil as PCM. They concluded that coconut oil showed a good thermal and chemical stability after 200 melting/freezing cycles with reliable latent heat of fusion and phase transition temperature. However, the DSC results showed that coconut oil melts and freezes quit incongruently at the desired temperature range. The key limitation for coconut oil is the large supercooling in addition to the transition temperatures, which are slightly outside the temperatures of interest (i.e. 20-25 °C) that is typically required to control temperature fluctuations in buildings. Nonetheless, if converted to free fatty acids, these bio-oils can be used as PCM for low thermal energy storage in building applications.

To overcome the limitation of coconut oil as PCM to control energy intermittency inside residential buildings hence using energy more efficiently, new mixtures with a phase transition temperature in the range of human comfort temperatures were prepared. These new mixtures were based on coconut oil fatty acids, technical oleic and linoleic acids.

2. Experimental

2.1. Materials

Refined coconut oil (CO) and technical linoleic acid (LA) (60%) were purchased from Acros. Purified oleic acid (80%), sodium hydroxide, and sulfuric acid (95-98%) were purchased from VWR, Merck and sigma-Aldrich, respectively. All other solvents were ACS-grade and used without further purification. Coconut oil free fatty acids (CoFA) were prepared by a conventional alkaline saponification followed by neutralization using sulfuric acid and extracted with n-hexane.

Fatty acid mixtures were prepared by weighing and mixing of CoFA and OA or LA into a glass vial, and dissolved in a minimum amount of n-hexane. After complete dissolution of the fatty acids species, the solvent was removed by evaporation under reduced pressure. After complete removal of solvent, the mixtures were melted at 40 °C and freezed at -20 °C to avoid phase separation. This process of heating (40 °C) and cooling (-20 °C) was repeated several times to maximize homogeneity.

2.2. Methods

2.2.1. Fourier Transform Infrared spectroscopy (FTIR-ATR)

Characteristic functional groups of CO and CoFA as well as those of the commercial fatty acids and the mixtures were examined by a Spectrum one FTIR instrument (Perkin Elmer) equipped with an UATR Diamond accessory allowing collection of FTIR spectra without prior sample preparation. The spectra were measured by placing directly a film of oily sample on the surface of ATR diamond and spectra obtained baseline-corrected and normalized using the zero point at the minimum ordinate value. All FTIR spectra were collected at room temperature at a spectrum resolution of 4 cm^{-1}, with an average of 16 scans over the range from 4000 to 450 cm^{-1}.

2.2.2. Gas chromatography (GC-MS) of CoFA

CoFA samples were methylated with 2wt % H_2SO_4 in water-free methanol at 90°C for 60 min. The fatty acid methyl esters were extracted into heptane and analyzed by gas chromatography/mass spectrometry (Agilent 9000 gas chromatograph system, Intuvo, USA), equipped with an HP-5MS column (30 m × 0.25 mm i.d., and 0.25 μm film thickness) and an Agilent 5975 mass-selective detector. Helium was used as carrier gas at a flow rate of 1 mL/min. The initial temperature of the oven was set at 60°C for 1 min, then to 220°C at a rate of 20°C/min, held for 2 min, and finally to 280°C at 10°C/min, held for 30 min. The compositions of technical OA, LA and CoFA are reported in Table 1.

2.2.3. Differential Scanning Calorimetry (DSC)

Differential scanning calorimetry (DSC) thermograms were recorded on a DSC Mettler-Toledo DSC 3 system under a nitrogen atmosphere. For each DSC run, a sample of weight usually in the range 14-20 mg was hermetically sealed in a standard DSC aluminum crucible pan. The sample was first heated from room temperature to 50 °C (above samples melting temperature) at a heating rate of 2 °C/min and then kept at this temperature for 15 min in the DSC instrument, then cooled to -25 °C, followed by an isothermal segment for 15 min. The second heating scans were run from -25 °C to 50 °C at a heating rate of 2 °C/min followed by a 15 min isothermal segment [27]. This heating-cooling cycle was repeated three times to obtain an acceptable reproducibility [28]. The first cycle was discarded as recommended by Gallart-Sirvent et al. [34], second and third cycles were found identical and thus, the results of the second cycle were reported herein. Prior to measurements, the DSC system was calibrated using indium and zinc.

Table 1
Compositions of technical OA, LA and CoFA.

Fatty acids	CO	CoFA	Technical LA	Technical OA
Caproic (C6:0)	0.13	0.0	0	0
Caprylic (C8:0)	3.15	0.04	0	0
Capric (C10:0)	3.92	2.04	0	0
Lauric (C12:0)	42.96	42.14	0	0
Myristic (C14:0)	21.22	23.02	0	0
Palmitic (C16:0)	12.31	14.36	5	5
Stearic (C18:0)	4.15	4.95	2	2
Oleic (C18:1)	9.74	11.25	25	80
Linoleic (C18:2)	2.43	2.19	67	12

2.2.4. Thermal conductivity of PCMs by transient hot wire method

Thermal conductivity of the fatty acid mixtures was measured according to the standard methods ASTM C1113 and ISO 8894 with some modifications. This technique known as transient hot wire method is used to measure the thermal conductivity of liquids and solids [35]. This implies a particular heat conduction equation that is valid for a linear heat source in a homogenous and isotropic medium at uniform initial temperature [36,37]. The method considers one dimensional radial heat flow inside a homogenous and isotropic test medium. An electrically heated wire is inserted into a sample initially at uniform and constant temperature, and the temperature of the heat source is recorded with respect to time during a brief heating period [35-38]. A schematic illustration of the in-house made apparatus to measure the thermal conductivity of the PCMs is shown in the Fig. 1. The used hot wire was made of Kanthal with 150 mm length and 0.3 mm diameter. Two electrically insulated copper wires with diameter of 2 mm were used to hold the hot wire by welding its ends to the copper wires. A 0-15 volt range D. C power supply was used to supply constant current to the wire (3.3 V, 1.31 A). Voltage and amperage were recorded using a digital multimeter. The temperature was measured with a K-type thermocouple with diameter of 1 mm and accuracy of ±0.1 °C, which is electrically insulated and glued to the wire while the distance between the thermocouple and wire was kept 1 mm. A data logger was used to record temperature versus time with two seconds interval. The sample was placed in a glass tube with a length of 160 mm and a diameter of 20 mm, and then the hot wire set-up was embedded and fixed in the centerline of the tube. Prior to the measurements, the temperature was recorded for 6 sec to make sure there is a constant temperature inside the sample; a switch was then used to run the set-up for 30 sec. The measurements were reproduced five times for each sample and the average results are reported. The temperature-time curve was then transformed to temperature-ln(t) curve and the slope of the new curve in the linear part ($R^2 = 0.99$) is used to calculate the thermal conductivity Eq. (1).

$$\lambda = \frac{V.I.\Delta\ln(t)}{4\pi L.\Delta T} = \frac{V.I}{4\pi L.\left(\frac{\Delta T}{\Delta\ln(t)}\right)}. \quad (1)$$

where λ is the thermal conductivity of the sample; V and I are measured voltage and amperage; ΔT is temperature difference over a known time interval; $\Delta\ln(t)$ is the difference between two taken points on temperature-ln(t) curve; L is the length of hot wire; $\frac{\Delta\ln(t)}{\Delta T}$ is the slope of the temperature-ln(t) curve.

2.2.5. T-history, specific heat capacity and enthalpy

T-history method is used to measure melting/freezing point, latent heat of fusion, degree of super cooling and specific heat capacity of several samples simultaneously [39-44]. The T-history set up used in this study was based on [39,43] with some modification and is shown schematically in Fig. 2 (left). Four PCM samples and ultrapure water as reference were tested simultaneously. Stainless steel tubes (SS316) with internal diameter of 10 mm, 1 mm wall thickness and 150 mm length were used as containers for PCM samples and reference material (Fig. 2 (right)). The containers were filled with PCMs up to 140 mm, while 10 mm was left for possible volume expansion during heating/cooling cycles. The containers are thermally insulated using 10 mm thickness ARMAFLEX insulation material [39,41-43]. K-type thermocouples were

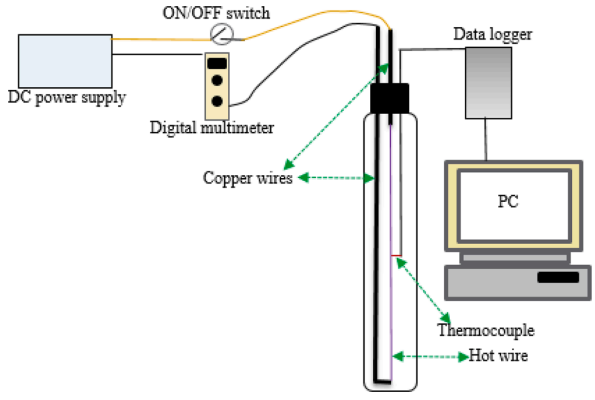

Fig. 1. Schematic diagram of the transient hot wire test set.

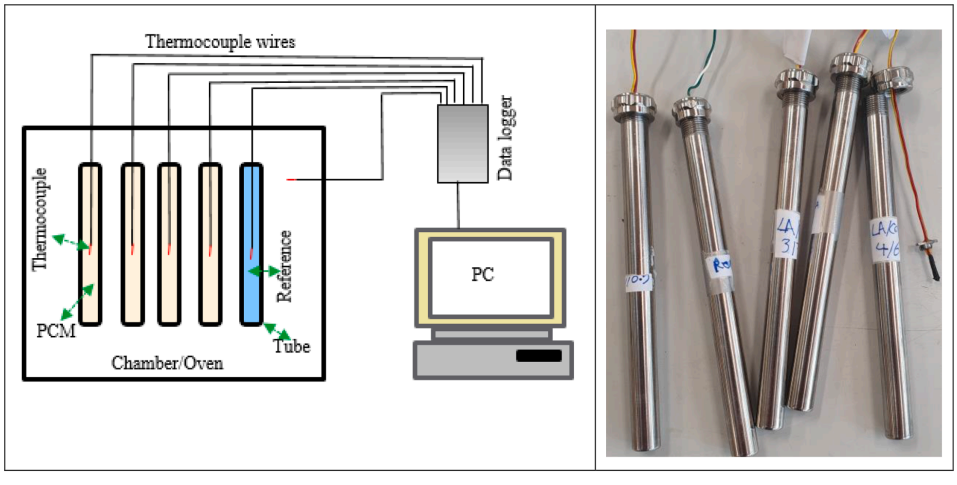

Fig. 2. PCM containers used for T-history experiments (right), and schematic diagram of the set up (left).

used to record temperature changes over time for each sample and reference. The thermocouples were placed at the centerline and in the middle of each container. For cold and hot ambient, two separate chambers were employed, a climate chamber was used as cold ambient fixed at 6 °C, and an oven was used as hot ambient fixed at 40 °C (Fig. 3), the ambient chamber/oven temperatures were recorded with two separate thermocouples. Samples and reference were first preheated in the oven at 40 °C, and then quickly transferred into the climate chamber at 6 °C and the temperature profile was recorded. Once the equilibrium temperature was reached (ca. 2 h), the samples and the reference tubes were transferred into the oven at 40 °C and the temperature changes were recorded. The process (cooling/heating) was repeated twice to verify the reproducibility of the results.

T-history is based on lumped capacitance method, requiring a negligible temperature gradient inside samples during heating/cooling process. This is possible by maintaining a low Biot (Bi) number, expressed in Eq. (2). A low Bi number is reached when the external heat resistance is maintained as high as possible compared to internal heat resistance inside the tube (samples). By using thermal insulation to increase the outer thermal resistance, a Bi number less than 0.1 can be achieved [39]. The thermal resistance of all the heat transfer components contributing to heat transport to/from the material inside the containers are illustrated in Fig. 4. The outer thermal resistance contributes to the outer overall heat transfer coefficient (u), while the internal thermal resistance defined in green color (see Fig. 4) is related to materials inside the tubes. Both the tube and the insulation were considered as outer resistance components. Thus, the outer overall heat transfer coefficient could be described by Eq. 3.

$$\mathrm{Bi} = \frac{u.r}{2.\lambda} \tag{2}$$

where u, r and λ are respectively overall heat transfer coefficient, radius of the container and thermal conductivity of the material.

$$\frac{1}{uA_{tube,in}} = \frac{1}{hA_{ins,out}} + \frac{\ln\left(D_{ins,out}/D_{ins,in}\right)}{2\pi L.\lambda_{ins}} + \frac{\ln\left(D_{tube,out}/D_{tube,in}\right)}{2\pi L.\lambda_{tube}}. \tag{3}$$

where A and D are heat transfer area and tube diameter. Subscribes *tube*

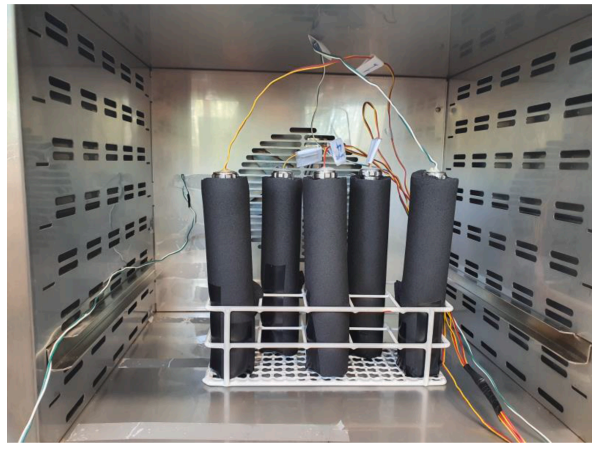

Fig. 3. Samples inside the climate chamber.

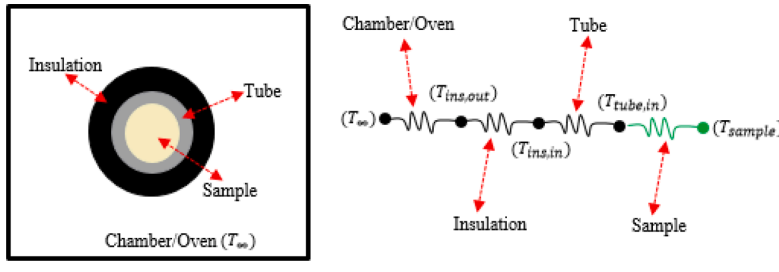

Fig. 4. Cross section schematic diagram of the set-up, with related thermal resistance diagram.

and *ins* refer to the tube container and insulation respectively. h is the convective heat transfer coefficient inside chamber and around samples (insulation body). Subscribes *in* and *out* refers respectively to the inner and outer sides. Internal thermal resistance of main sample is $\delta/\lambda_{pcm}.A_{tube,in}$; δ is characteristics length ($r/2$). The Bi number will be internal thermal resistance per external thermal resistance (Eq. 3), thus the Eq. (2) is obtained.

Energy balance for the reference was considered to obtain overall heat transfer coefficient. The overall heat transfer coefficient (u) for the reference and PCMs are identical since the tubes, thermal insulation and heat transfer condition around them are similar, and according to Eq. (3) these parameters contribute to overall heat transfer coefficient (u). In this study, only the temperature inside the reference and PCMs were recorded and the tubes and the thermal insulation were considered as external thermal resistance, i.e. the energy balance is accepted only for the materials inside the containers. The materials receive/release energy and their temperature changes. As the thermo-physical properties of the reference is known, the amount of energy which is absorbed/released by reference is calculated by Eq. (4) [39,41].

$$Q_{tot} = m.c_p.\left(T_{r,f} - T_{r,o}\right)/\Delta t, \tag{4}$$

where Q_{tot} is the total energy received/released over half a cycle (cooling or heating); m and c_p are respectively the mass and the specific heat capacity of the reference; $T_{r,f}$ and $T_{r,o}$ are final and initial temperatures of the reference; and Δt is the time interval. Since the reference does not undergo phase transition in the considered temperature range, it is possible to consider logarithmic mean temperature difference (LMTD) to obtain the overall heat transfer coefficient (u) as follow:

$$Q_{tot} = uA_{tube,in}.LMTD \tag{5}$$

where LTMD is defined in Eq. (6):

$$LMTD = \frac{\left(T_{r,f} - T_\infty\right) - \left(T_{r,o} - T_\infty\right)}{\ln\left(\frac{\left(T_{r,f} - T_\infty\right)}{\left(T_{r,o} - T_\infty\right)}\right)} \tag{6}$$

where T_∞ is the chamber/oven temperature; Q_{tot} is obtained by Eq. (4). The other temperatures are known, the thermal conductivity determined by transient hot wire, the parameter u is calculated by Eq. (5), and thus, Bi number is calculated.

Specific heat capacity (c_p) of the samples was calculated with the following set of energy balance for reference and PCMs. Eqs. (4) and (5) are equivalent and instead of LMTD it is possible to use the difference between the samples temperature and ambient temperature at each time point. However, by Eq. (5) we obtain overall heat coefficient for the whole half cycle and not at each time point [39,41].

$$m_r.c_{p,r}.\frac{\left(T_r^n - T_{r,o}\right)}{\Delta t} = uA_{tube,in}.\left(T_r^n - T_\infty\right) \tag{7}$$

$$m_{pcm}.c_{p,pcm}.\frac{\left(T^{n}_{pcm}-T_{pcm,o}\right)}{\Delta t}=uA_{tube,in}.\left(T^{n}_{pcm}-T_{\infty}\right) \quad (8)$$

$uA_{tube,in}$ is obtained from Eq. (7) and then substituted in Eq. (8) and by rearrangement, specific heat capacity is obtained as follow:

$$c_{p,pcm}=\frac{m_r.c_{p,r}.\left(T^{n}_{r}-T_{r,o}\right)}{m_{pcm}\left(T^{n}_{pcm}-T_{pcm,o}\right)}.\frac{\left(T^{n}_{pcm}-T_{\infty}\right)}{\left(T^{n}_{r}-T_{\infty}\right)} \quad (9)$$

Enthalpy of the samples is obtained as [39,41]:

$$\Delta H=c_{p,pcm}\left(T^{n}_{pcm}-T_{pcm,o}\right) \quad (10)$$

where ΔH is enthalpy change from initial point to each time point *n*.

3. Results and discussions

3.1. Visual assessment and selection

In order to design eutectic mixtures with high possible miscibility with the highest possible congruency, theoretical models such as Schröeder-Van Laar approach were employed [45]. However, in this study, the starting material (CoFA) consist of several fatty acids at various proportions (Table 1), thus using theoretical models to predict the eutectic temperatures and the corresponding compositions is not applicable. Therefore, a screening test was conducted to find miscible and stable mixtures, which have phase transition temperature that fits building application. In this regard, the mixtures of LA/CoFA and OA/CoFA (Table 2) were subjected to a visual screening test by exposing the mixtures to temperatures of 5, 15 and 22 °C (Fig. 5) to estimate the phase transition temperatures. The compositions with desirable phase transitions, marked with asterisk (*), were then selected and subjected to further thermal characterization.

Fig. 5 shows phase transition behavior of the mixtures at 5, 15 and 22 °C for LA/CoFA and OA/CoFA mixtures. The screening tests showed that the phase transition temperature of the mixtures increases with increasing the CoFA content. At 5 °C, LA/CoFA compositions with x_{LA}= 0.70 and 0.60, and OA/CoFA compositions x_{OA} = 0.70 are at mushy state, i.e. these compositions have an approximate phase transition around this temperature. LA/CoFA compositions with x_{LA}= 0.50 and 0.45, and OA/CoFA compositions with x_{OA} = 0.60 are at mushy state at 15 °C, while LA/CoFA compositions with x_{LA}= 0.40, 0.35, 0.30 and 0.20 and those of OA/CoFA with x_{OA} = 0.50; 0.45; 0.40 and 0.30 show phase transition at around 22 °C.

3.2. FTIR characterization of CO, CoFA and mixtures

FTIR spectra of refined CO and CoFA at mid region (4000-450 cm^{-1}) is shown in Fig. 6. CO spectrum showed a typical characteristic of absorption bands for triglycerides [46]. The main characteristic vibrations were the stretching vibration of methyl (CH_3) and methylene (CH_2) groups respectively at 2851cm^{-1} and 2919 cm^{-1}, as well as the bending vibrations at 1465 cm^{-1} and 720 cm^{-1}; the C-O stretching vibrations between 1173 and 1104 cm^{-1} and the carbonyl stretching vibrations at 1740 cm^{-1} ($\nu_{C=O}$). Compared to CO, the spectrum recorded for CoFA showed a shift of some absorptions bands, emergence of new and disappearance of others as a result of conversion of the triglyceride ester into carboxylic acid. The prominent shift was observed for the carbonyl stretching vibration at 1707 cm^{-1}, the new absorption bands were observed at 1412, 1284 and 934 cm^{-1} which corresponds to fatty acid O-C stretching vibrations. In addition, the CO vibrations related to triglyceride ester (-C-O) were not found in the CoFA spectrum, thus confirming the complete conversion of CO into CoFA.

Table 2
Primary prepared and selected (*) fatty acid mixtures.

Composition			Composition		
formulation	proportion	x_{LA}	formulation	proportion	x_{OA}
LA/CoFA	70/30	0.7	OA/CoFA	70/30	0.7
LA/CoFA	60/40	0.6	OA/CoFA	60/40	0.6
LA/CoFA	50/50	0.5	OA/CoFA	50/50	0.5*
LA/CoFA	45/55	0.45	OA/CoFA	45/55	0.45*
LA/CoFA	40/60	0.4*	OA/CoFA	40/60	0.4*
LA/CoFA	35/64	0.35*	OA/CoFA	35/65	0.35*
LA/CoFA	30/70	0.3*	OA/CoFA	30/70	0.3
LA/CoFA	20/80	0.2*			
LA/CoFA	10/90	0.1			

To prepare a PCM with transient temperatures in the range of human comfort, the obtained CoFA was mixed with OA and LA at various compositions. The chemical stability of the new PCMs was studied by the ATR-FTIR spectroscopy. Fig. 7 shows the spectra of CoFA, OA, LA, and the mixtures x_{LA} = 0.20 and x_{OA} = 0.30 before thermal cycling. The spectra were similar and displayed the typical vibration bands of fatty acids with the exception of the band at 3008 cm^{-1}, attributed to the cis allylic (C=CH) not observed in the CoFA spectrum, as CoFA consist mostly of saturated fatty acids [47] while OA and LA contains unsaturated fatty acids. This vibration (at 3008 cm^{-1}) could be further used to monitor any chemical changes in the mixture (e.g. rancidification) after thermal cycling.

3.3. Thermal analysis by DSC

Fig. 8 shows the thermal characteristics of CO at various cooling/heating rates. The obtained DSC results showed that CO's transition temperatures are strongly dependent on the cooling/heating scanning rates. The higher cooling/heating rate leads to higher heat flow. During the course of heating, onset and offset temperatures depend on the heating rate, while the peak point remains almost unchanged in all cases. The main variations in temperature could be observed during cooling process, where higher scanning rate leads to lower onset, offset and peak temperatures. Tan and Che Man [48] observed similar behavior when thermal characteristics of CO was studied at a series of heating rates ranging from 1 to 20 °C/min. These results emphasize the importance of T-history method that uses bigger sample size, when the thermal characteristics of the small-scale material depend strongly on the cooling/heating scanning rates. For the studied fatty acids, the cooling/heating rate of 2 °C/min was employed as per recommend in ref. [27].

Fig. 9 shows the DSC curves obtained for CO and CoFA (Fig. 9a), OA and LA (Fig. 9b), OA/CoFA (Fig. 9c) and LA/CoFA (Fig. 9d). In both heating and cooling thermograms of CO (Fig 9a), two overlapping peaks were observed; a small shoulder peak embedded in a principal endothermic/exothermic peak as a result of the difference in the proportion of saturated and unsaturated triacylglycerol (TAG) and fatty acids (FA) [49]. Conversion of CO into free fatty acids (CoFA) resulted in enhancement in its thermal capability as PCM, demonstrated by the higher heat flow, latent heat of fusion (see Table 3), melting and freezing temperatures compared to crude CO. In the heating profile of CoFA (Fig. 9a), a main endothermic peak was observed at 29.7 °C ascribed to the melting point of saturated fatty acids, while the small endothermic peak observed at -11 °C was associated with the melting point of unsaturated fatty acids fraction. The CoFA cooling curve showed almost symmetrical overlapped exothermic peaks attributed to crystallization of the saturated fatty acids and a small peak at -20 °C corresponding to the crystallization of the unsaturated fatty acids proportion.

Compared to CoFA, OA and LA melt and freeze congruently (Fig. 9b), displaying only one broad endothermic peak and one sharp exothermic peak. The melting and freezing points of OA were at 10.8 °C and -2 °C, which is in line with the temperatures range reported in literatures [27, 28]. The small-observed deviation between the present study and the literature data [27,28] in melting and freezing points for OA was mainly

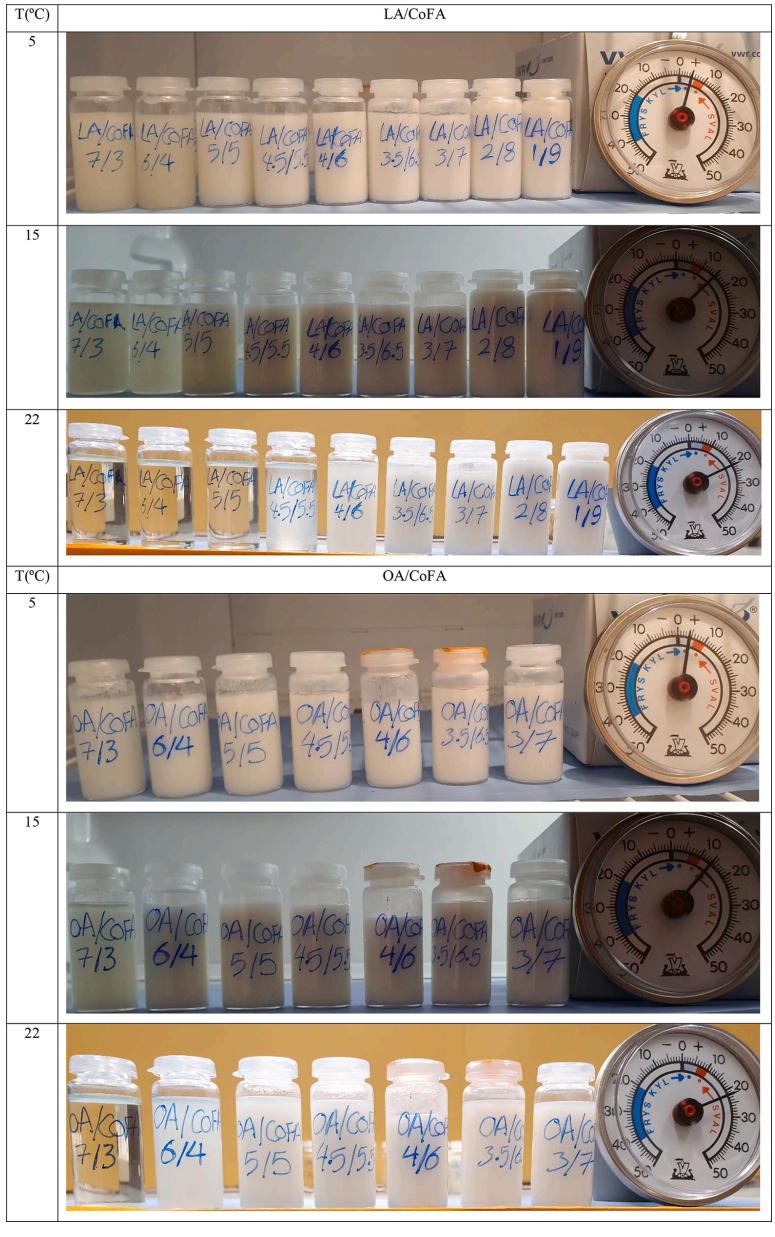

Fig. 5. Primary prepared LA/CoFA and OA/CoFA with different compositions.

attributed to the purity of OA. Indeed, the current study used a technical OA (80%), while Inoue et al. [27,28] employed a pure OA grade. For LA the melting and freezing points were at -10.3 °C and -14.6 °C, which is in agreement with data reported in ref. [50]. OA showed higher phase transition heat flow and latent heat (Table 3) and temperature compared to LA [50].

When OA or LA were mixed with CoFA (Figs. 9c-d), the mixtures showed a tendency of increased phase transition temperatures, heat flow and latent heat of fusion (Table 3) when the amount of CoFA increases in the mixtures. All the mixtures showed two endothermic peak during the

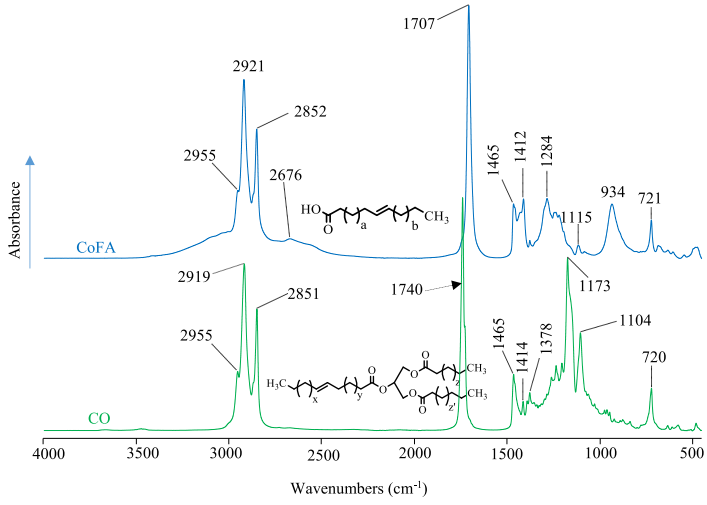

Fig. 6. FTIR absorbance spectra of coconut oil (CO) and coconut oil fatty acids (CoFA).

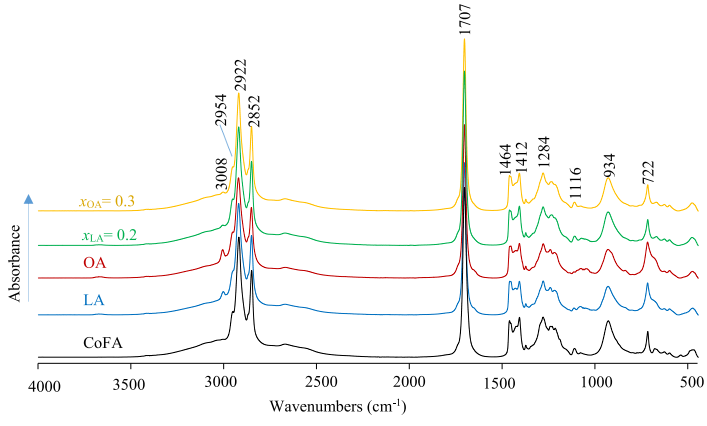

Fig. 7. FTIR absorbance spectra of CoFA, LA, OA, the mixture with x_{LA}= 0.20 and the mixture with x_{OA} = 0.30.

melting process and two exothermic peak in the solidification process, attributed respectively to the melting and freezing points of the fatty acid species in the mixtures. However, the melting and solidification points of the mixtures were higher than the melting and freezing points of the technical fatty acids. In DSC heating thermograms obtained for OA/CoFA mixtures, except the composition x_{OA} = 0.30, all the other mixtures showed a small shoulder embedded in the major endothermic peak at temperatures of 18-22 °C and another sharp endothermic peak at lower temperatures at around -1 °C. The cooling curves also displayed one sharp exothermic peak at temperatures between -13 °C and -15 °C, and a shoulder embedded in major exothermic peak at higher temperatures in the range of 10-22 °C; in all cases the intensity of the peaks change with the decrease of the OA content in the mixtures. Item for the mixtures involving LA, two major endothermic and two exothermic peaks were observed. The exothermic peak at higher temperatures (22 °C) consist of two overlapping peaks in which the intensity of the minor peak decrease as the LA content in the mixture increases, while at lower temperatures (-25 °C) only one sharp exothermic peak was observed. Similar behavior was noticed during heating process. Considering the DSC curves of CoFA (Fig. 9a) and those of the CoFA mixtures (Figs. 9c-d) together, it could be concluded that the observed incongruent freezing behavior was a result of the small incongruency observed for CoFA during freezing process. Although the DSC results of commercial OA showed higher phase transition temperature, heat flow and latent heat of fusion compared to LA, mixtures prepared with LA/CoFA showed higher phase transition heat flow and latent heat of fusion (Table 3). The calorimetric information proved that the mixtures with LA were better in terms of latent heat of fusion and melt congruently compared to those containing OA. Comparable studies [27] involving mixtures of Lauric acid, which is the main fatty acid comprising up to 50% of the refined CO [47], and high purity OA, showed a melting point of mixtures close to that of pure OA and the mixture process leaded to decrease in the

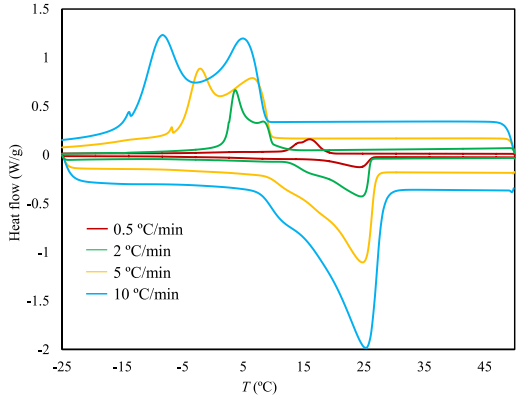

Fig. 8. DSC thermograms of CO at cooling/heating rates varying from 0.5 to 10 °C/min.

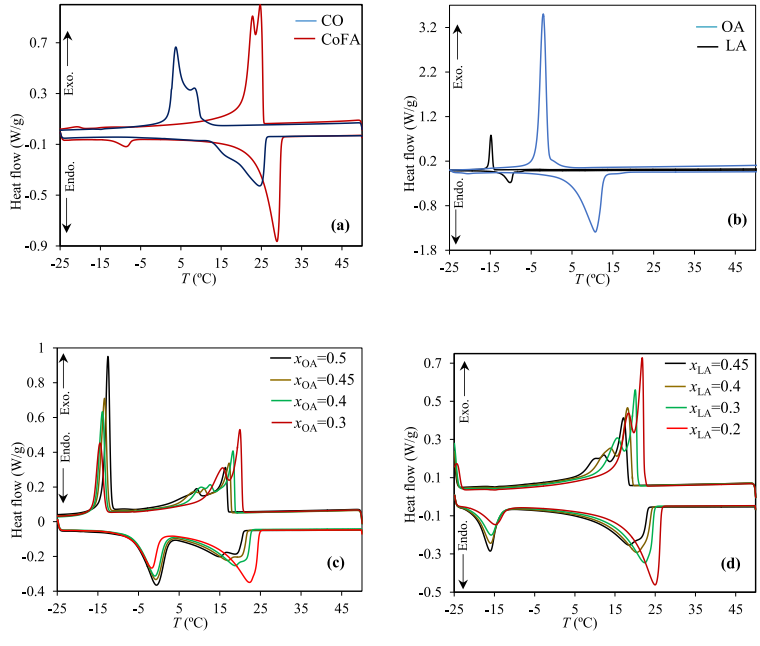

Fig. 9. DSC thermograms obtained for: (a) CO and CoFA, (b) OA and LA, (c) CoFA/OA and (d) CoFA/LA.

melting point of OA as seen in the present study.

In DSC study, temperatures at onset, peak points and end temperatures were reported. The materials start to melt and freeze at T_{onset} (melting/freezing temperatures) and at this temperature; the materials are in mushy state. In order to reach the highest possible absorbing/realizing energy in the considered range, the materials should meet their melting/freezing peak point at the favorable range, and thus peak point was reported through the study. The phase transition temperatures and the enthalpy of fusion are reported in Table 3.

From Table 3 and Fig. 8, CoFA starts to melt at 23.9 °C, a temperature in the target range; however, its melting peak point occurs at 28.5 °C, little outside the suitable temperature range. Thus, it is important to adjust the phase transition behavior of CoFA by mixing it with other fatty acids. In this study, commercial OA and LA were selected and mixed with CoFA to adjust the phase transition temperature of the mixtures. Furthermore, both commercial fatty acids have lower phase transition temperatures and when mixed with the main material, if any incongruency is supposed to happen, it will occur at temperatures far below the target working temperature range.

Table 3
Phase transition temperatures of the PCMs with DSC.

PCMs	Freezing process			Melting process			ΔH_{fusion} (J/g)
	T_{onset}(°C)	T_{peak}(°C)	T_{endset}(°C)	T_{onset}(°C)	T_{peak}(°C)	T_{endset}(°C)	
OA	-0.7	-2	-3.4	4.5	10.8	12.73	93
LA	-14.2	-14.6	-15.5	-12.5	-10.3	-9.3	85.5
CO	6.7	4; 8	2.2	14.5	24.4	26.1	100
CoFA	25.6	23; 25.6	21.1	23.9	28.5	29.8	122.7
$x_{OA} = 0.50$	16.6	16.5	5	7	18.9	20.8	34
$x_{OA} = 0.45$	18	17.5	5	8.7	17	25.6	41
$x_{OA} = 0.40$	18.9	18.4	5	10.5	18.8	22.7	49
$x_{OA} = 0.30$	20.6	15; 20.2	8.8	14.4	22.2	24.7	63
$x_{LA} = 0.40$	18.4	17.3	14.4	8.8	18.4	23.2	63
$x_{LA} = 0.35$	19.4	13.8; 18.3	7.3	11.3	20.3	24.2	70.4
$x_{LA} = 0.30$	20.7	15.7; 20.2	10.2	13.8	22.3	24.8	77.3
$x_{LA} = 0.20$	22.4	22; 18.5	14.7	17.5	24.8	26.5	94

3.4. Thermal conductivity measurement with transient hot wire

Fig. 10 exemplifies the temperature-ln(t) profiles obtained from transient hot wire experiments measured in both solid and liquid states for $x_{LA} = 0.20$ and ultrapure water. Before each measurement, the experiment set up was calibrated using pure water, which showed a mean value of 0.597 W/m K, and is in an agreement with the reference value of 0.6 W/m K [51]. The segment (10 sec) of the graph where there is a linear trend, with higher R^2 >0.99, was selected to calculate the thermal conductivity using the Eq. (1). The results are reported in Table 4 where the values are means of five measurements.

The thermal conductivity values of the tested mixtures were around 0.2 W/m K for samples at liquid state and around 0.35 W/m K, at solid state. The thermal conductivities of mixtures at liquid state were comparable to those of individual fatty acids and no relationship was found between the mass fraction of OA or LA in the mixtures and the thermal conductivity. The reproducibility of the experiments was acceptable as demonstrated by the low standard deviation values. The experimental uncertainty due to measurement instrument including thermocouple, caliper and multimeter was determined and found to be 1.92%. The details of the calculations are given in the experimental uncertainty analysis section.

3.5. Thermal analysis with T-history

T-history method requires a negligible temperature gradient inside the samples to fulfil the lumped capacitance assumption, which achieved when Bi number is small (Bi<0.1) [39]. As the thermal conductivity was determined to be around 0.2 W/m K, and the overall heat transfer coefficient of 5.13 W/m^2 K, was calculated Eqs. 4-(6), the Bi number was found to be 0.06 (Eq. (2)), i.e. satisfying the considered assumption.

Fig. 11 shows T-history profiles for CO, CoFA and water as reference. The figure shows that CO undergoes a large supercooling (around 2.5 °C), while this is negligible for CoFA. CO cools down to 17.6 °C, the temperature at which supercooling occurs, then the temperature goes up to 20 °C, which is the solidification temperature. During heating process,

Table 4
Average thermal conductivity of materials with standard deviation in parentheses.

Samples	Mean λ (W/m K)	
	Liquid	Solid
Water	0.597 (0.016)	-
OA	0.206 (0.010)	-
LA	0.196 (0.013)	-
CO	0.200 (0.016)	-
CoFA	0.21 (0.007)	0.351 (0.015)
$x_{OA} = 0.50$	0.212 (0.004)	0.357 (0.010)
$x_{OA} = 0.45$	0.202 (0.004)	0.355 (0.011)
$x_{OA} = 0.40$	0.192 (0.009)	0.357 (0.008)
$x_{OA} = 0.30$	0.216 (0.014)	0.39 (0.007)
$x_{LA} = 0.40$	0.192 (0.005)	-
$x_{LA} = 0.35$	0.212 (0.007)	0.36 (0.03)
$x_{LA} = 0.30$	0.191 (0.001)	-
$x_{LA} = 0.20$	0.202 (0.011)	0.346 (0.012)

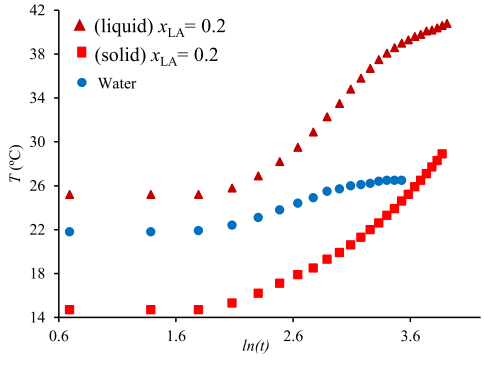

Fig. 10. Temperature-ln(t) profiles of tested sample $x_{LA} = 0.20$, in a solid and liquid states and water.

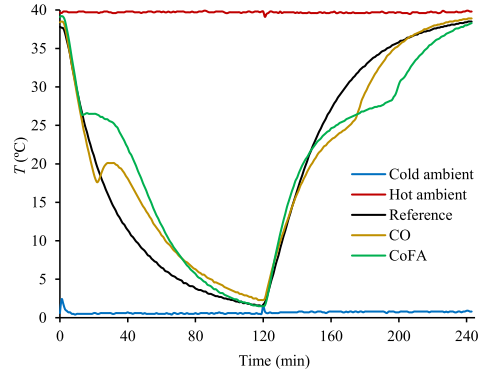

Fig. 11. T-history over cooling/heating cycle for CO, CoFA and water (reference).

CO starts to melt at temperature around 21 °C, and is fully melted at 26.4 °C. The solidifying temperature for CoFA is 26.4 °C, and it starts to melt at 23.7 °C fully melted at 28.3 °C. For both cooling and heating process, during phase transition, the profile for CoFA is wider than that of CO indicating that CoFA can store and release more energy compared to CO.

Fig. 12 shows the T-history profile for LA/CoFA (Fig. 12a) and OA/CoFA (Fig. 12b) mixtures over two heating/cooling cycles. Ultrapure water was used as reference, and the measured ambient temperatures were constant throughout the experiments with ± 0.8 °C maximum deviation. Once placed in the climate chamber at 6 °C, the test samples and reference temperatures decrease gradually from the starting temperature at 40 °C and continues to decease with the time until it reaches the chamber's ambient temperature (6 °C). During the course of cooling cycles, a phase change transition was observed for all the mixtures between the temperature ranges from 21.3 to 17.6 °C for OA/CoFA and from 23.1 to 19.6 °C for LA/CoFA mixtures. When the cooling process continued, some mixtures experienced a second solidification point around 18 and 12.5 °C for OA/CoFA and between 19 and 14.5 °C for LA/CoFA mixtures. Small subcooling effect, less than 0.6 °C, was observed in all cases. During heating cycles, only one phase transition was noticed for each mixture, which means the mixtures melt congruently. The melting temperature ranges were found around 19.6 to 23.1 °C for OA/CoFA and between 20.7 and 25.5 °C for LA/CoFA mixtures. A deviation of all the formulations curves from the reference curve was noticed when the temperature profiles approaches the cold (6 °C) or hot ambient temperature (40 °C) probably due to differences in thermal conductivity.

Enlargement of the heating/cooling curves in the phase transition regions (Fig. 13), showed that above phase transition, mixtures tend to deviate and increment forehead than others, indicating a greater heat capacity of some mixtures than the others. These increments were found to increase with the increase of CoFA content in the mixtures. Furthermore, compositions with high CoFA content experienced higher phase transition temperature than those with low CoFA content (Fig. 13).

Fig. 14 shows the specific heat capacity and the enthalpy for OA/CoFA and LA/CoFA mixtures calculated using Eqs. (9) and (10) during cooling and heating processes. The calculated heat capacity OA/CoFA (Fig. 14a) is in the range of 0.5-3.5 J/g K, and for LA/CoFA (Fig. 14b) is in the range of 0.9-5.5 J/g K (during phase transition). For both mixture types, the heat capacity tends to increase when the portion of CoFA increases in the compositions. During cooling process, due to incongruent freezing and small degree of subcooling, there is certain inevitable difficulties in interpreting the C_p. However, as it is seen from the figures, super cooling effect was small, and it has no significant effect on the measured C_p. Fig.s 14c and 14d respectively show enthalpy for OA/CoFA and LA/CoFA mixtures for cooling and heating process during the

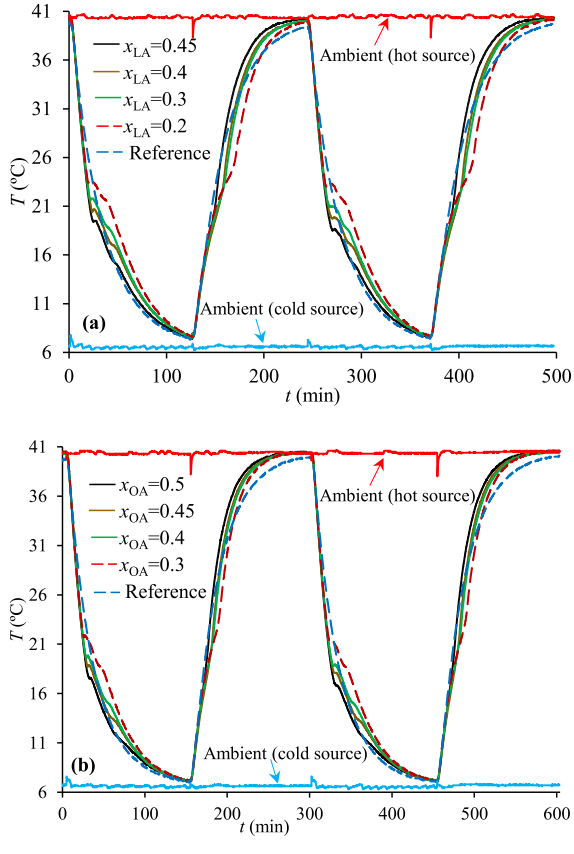

Fig. 12. T-history over two heating/cooling cycles for (a) LA/CoFA and (b) OA/CoFA mixtures.

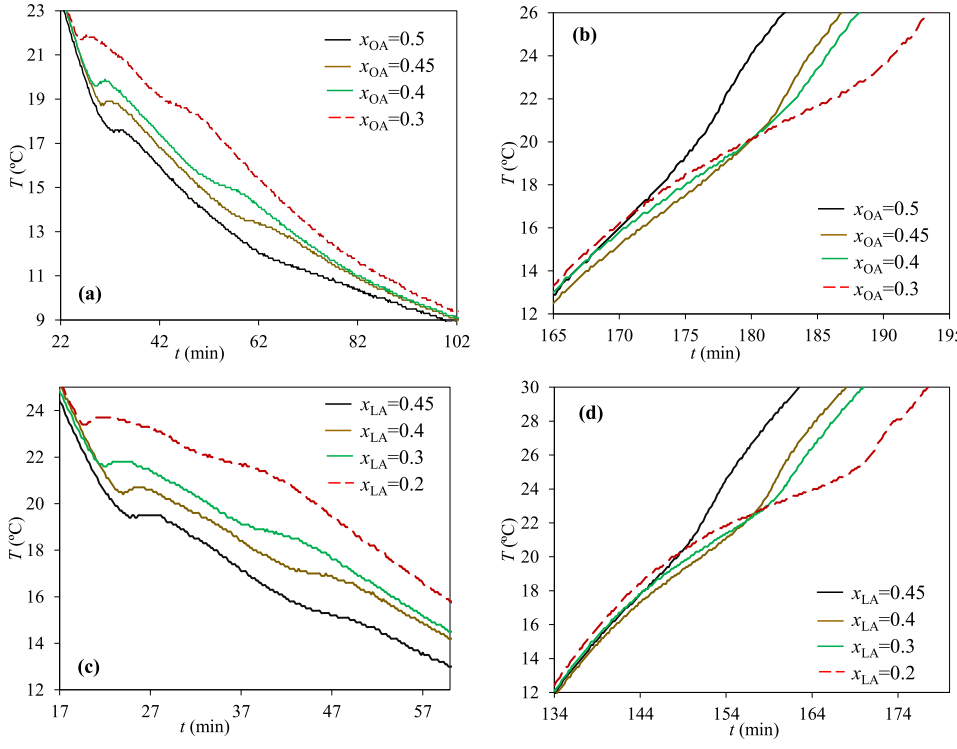

Fig. 13. T-history curves enlargements in the transition regions during cooling (a,c) and heating process (b,d) for OA/CoFA and LA/CoFA mixtures.

first cycle calculated by Eq. (10). The values of cooling process are negative, i.e. the samples released energy while the values are positive during heating since the samples absorb energy. The effect of inevitable incongruent phase transition during cooling process is observed likewise C_p and even an effect of super cooling can be seen. Phase transition temperatures, melting/freezing C_p and enthalpy are tabulated in Table 5.

Due to incongruent freezing during cooling process, two different transition temperatures were observed, as a consequence, part of energy is released in the form of sensible energy, thus explaining the difference between the values for cooling and heating for C_p and enthalpy (Table 5). From the result, $x_{LA} = 0.20$ can be selected as the most promising material, since it absorbs and releases more energy compared to other materials in the studied temperature range. Moreover, its heat capacity is considerably higher than of the other mixtures. Within the OA/CoFA group, the mixture with composition with $x_{OA} = 0.30$ shows best properties. However, LA/CoFA mixtures show better performance.

3.6. Comparison between DSC and T-history

DSC and T-history methods were used to compare the thermophysical properties of the OA/CoFA and LA/CoFA mixtures. Compared to DSC experiments, which require very small amounts of sample with rapid response times, T-history uses larger amount of samples comparable to the real applications of the PCMs [44]. Moreover, DSC results are dependent on the cooling/heating rates, in particular during cooling process, thus T-history method gives more reliable results. T-history results indicated that all the tested combinations displayed a super cooling phenomenon, which was not evident from the DSC results (Figs. 9a-d). A comparison of the phase transition temperatures and enthalpies calculated from DSC and from T-history is summarized in Table 6. The results indicated that for samples having less or no incongruent melting, the determined melting peak points from the both methods were comparable. However, due to the incongruent freezing and super cooling observed during cooling process, the determined results from the two methods were slightly different but still in a reasonable agreement. Table 6 also shows the calculated enthalpy for fatty acid mixtures obtained by T-history and DSC methods. The results support the conclusion that compositions with congruent phase transitions, both methods provide comparable results; however, the difference in calculated enthalpies between the methods is greater for compositions undergoing super cooling and incongruency during cooling process.

Small difference in sub-cooling effect has been observed between DSC and bulk sample T-history method. Calculation of enthalpy gives more insight of PCM thermal energy storage and and discharge capacity and design of the storage system. However, for the comparison of PCM properties and considering the operating temperature for maximum energy storage and discharge, evaluation of PCM enthalpy is essential. DSC and T-history study's outcome indicates that $x_{LA} = 0.20$ has the largest enthalpy and heat capacity and an operating temperature in the range of 18-25°C, which makes it a promising candidate for using as BPCM for building applications.

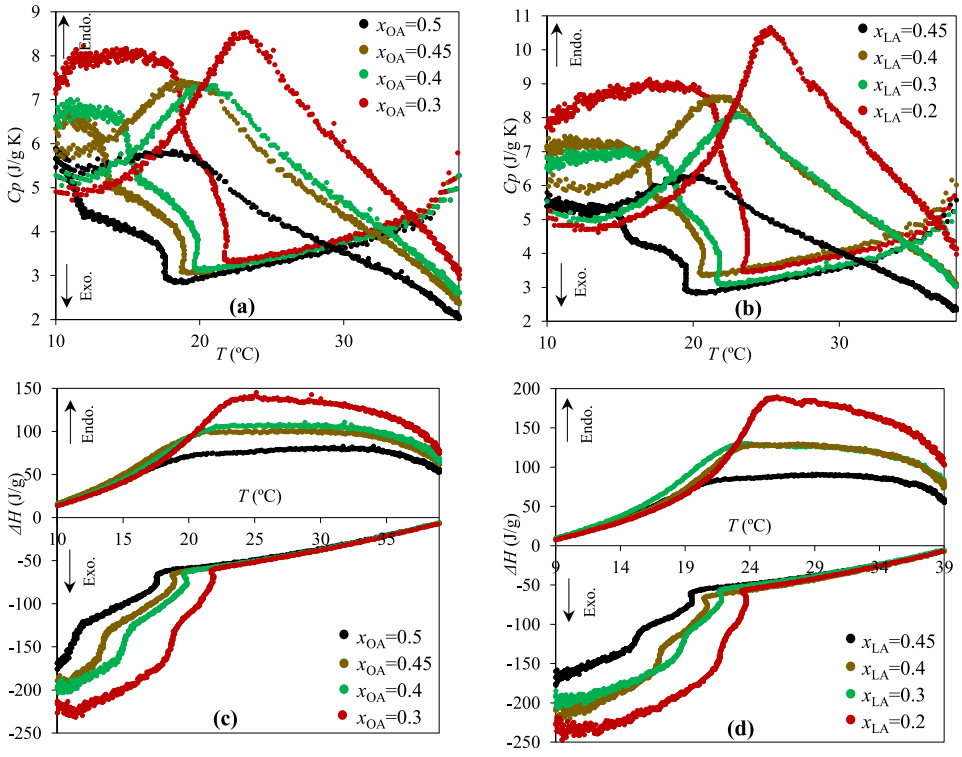

Fig. 14. Melting and freezing specific heat capacity for (a) OA/CoFA and (b) LA/CoFA mixtures, and enthalpy for (c) OA/CoFA and (d) LA/CoFA.

Table 5
Thermal properties of the samples obtained by T-history.

Samples	T (°C)		C_p (J/g K)		ΔH (J/g)	
	Freezing	Melting	Freezing	Melting	Freezing	Melting
x_{OA} = 0.50	11.9; 17.4	19.6	0.7; 1.4	0.5	16; 44	38
x_{OA} = 0.45	13.2; 18.8	20.7	0.8; 1.6	1.63	17; 37	49
x_{OA} = 0.40	15; 19.7	21	0.8; 1.6	1.95	16; 42	53
x_{OA} = 0.30	18.6; 21.7	23.1	1.6; 2	3.5	21; 43	76
x_{LA} = 0.40	15.3; 19.5	20.7	0.8; 1.2	0.9	16; 29	51
x_{LA} = 0.35	17; 20.6	22.5	1; 1.6	2.7	23; 37	67
x_{LA} = 0.30	18.8; 21.8	23.1	1.3; 1.6	3	20; 40	73
x_{LA} = 0.20	21.7; 23.7	25.5	2.3; 2.8	5.5	24; 54	104

3.7. Accelerated thermal cycling

Samples were subjected to an accelerated thermal cycling to access the thermal stability of BPCMs. Accelerated cooling/heating cycles in most cases are carried out from 100 to 1000 cycles [52-57]. In this work an accelerated thermal cycling test with 700 cooling/heating cycles was performed in a climate chamber oscillating between -3 to 50 °C, at heating and cooling rates of 2 °C/min, with 10 min isothermal segment at -3 °C and 50 °C. The temperature range (-3 to 50 °C) and isothermal segments were selected to ensure a complete solidification and melting of the PCM during a cycle. For each composition, five vials with 2 g PCM each were prepared, sealed and placed in a climate chamber for thermal cycling. After each 100th cycle, a vial from each composition was taken for chemical (FTIR) and thermal (DSC) characterization. By prompting clarity, only the results of the composition $x_{LA} = 0.20$ were reported. The obtained DSC curves of $x_{LA} = 0.20$ subjected to 100, 200, 300, 400 and 700 thermal cycles are shown in Fig. 15. After 100 heating /cooling cycles, the DSC curves of the studied PCMs showed identical exothermic and endothermic peaks as before cycling process in terms of shape; however a slow shift (ca. 0.2°C) to lower temperatures were observed during both melting and solidification processes. No relationship was observed between the number of thermal cycles and the changes in phase transition temperatures. Thermal cycling resulted also in a small reduction in solidification heat flow, while the melting heat flow remained almost unchanged. These changes in phase transition temperatures and heat flows were below 1% even after 700 heating/cooling cycles, indicating that the material has very good thermal cycling stability. The changes in phase transition temperatures (melting/solidification) as well as the heat flows losses after thermal cycling is common phenomenon when mixtures of fatty acid were studied [58,59]. Fauzi et al. [58] reported that the changes of melting point of myristic acid/palmitic acid and myristic acid/palmitic acid/sodium stearate eutectic mixtures were irregular but of acceptable magnitude, and a

Table 6
Phase transition temperature and enthalpy comparison between T-history and DSC.

Samples	Freezing point T (°C)		Melting point T (°C)		Freezing enthalpy (J/g)		Melting enthalpy (J/g)	
	T-history	DSC	T-history	DSC	T-history	DSC	T-history	DSC
$x_{OA} = 0.50$	11.9; 17.4	9.8; 16.5	19.6	15.5; 18.9	16; 44	48.8	38	34
$x_{OA} = 0.45$	13.2; 18.8	11.3; 17.5	20.7	17; 20.4	17; 37	55.1	49	41
$x_{OA} = 0.40$	15; 19.7	13.3; 18.4	21	18.8	16; 42	53.2	53	49
$x_{OA} = 0.30$	18.6; 21.7	15; 20.2	23.1	22.2	21; 43	70.1	76	63
$x_{LA} = 0.40$	15.3; 19.5	13; 17.3	20.7	18.4	16; 29	68.5	51	63
$x_{LA} = 0.35$	17; 20.6	13.8; 18.3	22.5	20.3	23; 37	75.7	67	70.4
$x_{LA} = 0.30$	18.8; 21.8	15.7; 20.2	23.1	22.3	20; 40	80.7	73	77.3
$x_{LA} = 0.20$	21.7; 23.7	18.5; 22	25.5	24.8	24; 54	92.8	104	93

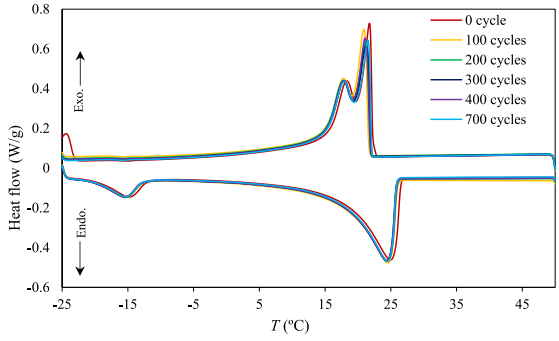

Fig. 15. DSC curves of $x_{LA} = 0.20$ subjected to long-term thermal cycles.

decrease between 6 and 10.1% in latent heat of fusion were observed after 1500 cycles. A study on thermal stability of a composite made of palmitic acid/stearic acid eutectic mixture as PCM and expanded graphite was performed by Zhang et al. [59] reported a loss below 3% in melting and solidification enthalpies after 720 thermal cycles. Thus, the observed changes in thermal properties such as melting temperatures and latent heat of fusion of LA/CoFA mixture are in agreement with the literature and constitute reliable BPCM for thermal energy storage in building applications.

Changes in phase transition temperatures and enthalpy lost of PCMs after thermal cycling are caused by the degradation of PCM components, and/or presence of impurities in the fatty acids used in preparation of

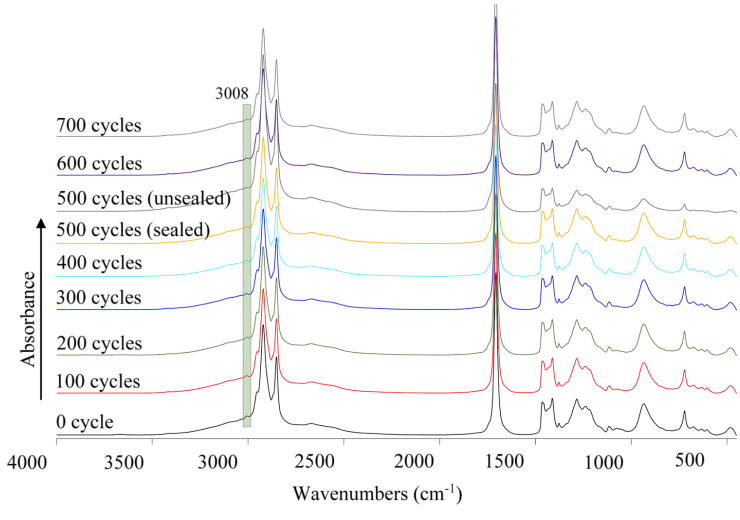

Fig. 16. FTIR spectra of $x_{LA} = 0.20$ before and after long-term thermal cycles.

the mixtures [58-63]. In this study, the physical appearance of the studied mixtures after 700 cycles remained unchanged. To prove the chemical stability of the mixtures, sealed and unsealed samples were analyzed by FTIR before and after thermal cycling and the obtained spectra are shown in Fig. 16 (only the spectra of the mixture $x_{LA} = 0.20$ were reported). The samples subjected to thermal cycling showed the same characteristic absorption peaks as the uncycled sample, namely vibrations at 2954, 2922, 2852, 1707, 1464, 1412, 1284, 1116, 934 and 722 cm^{-1}. All the absorption peaks remained at the same frequency band and have the same intensities, and there is no appearance or disappearance of peaks, indicating that the chemical structure of the mixture was not altered during the thermal cycling. This result was corroborated by the physical appearance of samples, which did not change after thermal cycles. Thus, the observed shifts in phase transition temperatures and loss in enthalpy, after heating/cooling cycles, was not caused by the chemical structure degradation but rather by the presence of impurities in the commercial LA and synthesized CoFA. Similar results were reported in the literature when fatty acid binary and tertiary mixtures were subjected to long-term thermal cycles [58,60,63,64].

Pure LA is a polyunsaturated fatty acid; it is susceptible to oxidation when exposed to air, humidity and temperature. In order to assess the chemical stability of the LA and LA/CoFA mixtures during thermal cycling, unsealed samples of LA and $x_{LA} = 0.20$ were subjected to thermal cycling process likewise sealed samples. DSC and FTIR results after 500 cycles showed no differences between sealed and unsealed samples. The unchanged vibration at 3008 cm^{-1} (Fig. 16), confirms the thermal and chemical stability of the mixture.

4. Experimental uncertainty analysis

Experimental uncertainty associated with the thermal conductivity measurements by transient hot wire, specific heat capacity and enthalpy by T-history are introduced by the combination of the experimental errors, the calculations error and the accuracy of the measurement tools. In the current study, the overall errors were related to thermocouples, multimeter used to measure electrical voltage and current, balance to measure weight of the samples, and the caliper to measure the lengths. The uncertainty of the thermocouple is ± 0.1 °C, that of multimeter is ± 0.01 V, and that of balance and caliper are respectively 0.0000002 kg, and 0.00002 m. The uncertainty analysis was calculated using Kline and McClintock method [65]. The uncertainty is calculated by using Eq. (11).

$$U_R = \left[\sum_{i=1}^{n}\left(\frac{\partial R}{\partial P_i}U_{P_i}\right)^2\right]^{\frac{1}{2}}, 1 \le i \le n \quad (11)$$

where R and P_i are dependent and independent variables respectively. U_R and U_{P_i} are the uncertainties for the dependent and the independent variables respectively. The non-dimensional form of Eq. (11) is $\left(\left(\frac{U_R}{R}\right) \times 100\right)$ which is in percentage [65-67]. The independent measured variables used to calculate the experimental uncertainties were summarized in Table 7.

Table 7
Measured variables, experimental uncertainties and specifications of the used equipment.

Measured variable	Nomenclature	Nomenclature of uncertainty	Nominal value	Absolut uncertainty
Voltage	V	U_V	3.3 V	0.01 V
Amperage	A	U_I	1.31 A	0.01 A
Mean ΔT in hot wire	T	U_T	6 °C	0.1 °C
Length of hot wire	L	U_L	0.15 m	0.00002 m
Maximum $(T_r^n - T_{r,i})$ in T-history	T	U_T	33 °C	0.1 °C
Maximum $(T_{pcm}^n - T_{pcm,i})$ in T-history	T	U_T	33 °C	0.1 °C
Maximum $(T_{pcm}^n - T_\infty)$ in T-history	T	U_T	33 °C	0.1 °C
Maximum $(T_r^n - T_\infty)$ in T-history	T	U_T	33 °C	0.1 °C
Average mass of samples	m	U_m	0.009 kg	0.0000002 kg
Average mass of reference	m	U_m	0.01 kg	0.0000002 kg

4.1. Thermal conductivity uncertainty calculation

Based on Eqs. (1) and (11), it is possible to calculate the uncertainties of thermal conductivity using the following Eq. (12):

$$U_\lambda = \left[\left(\frac{\partial\lambda}{\partial V}U_V\right)^2 + \left(\frac{\partial\lambda}{\partial I}U_I\right)^2 + \left(\frac{\partial\lambda}{\partial\Delta T}U_T\right)^2 + \left(\frac{\partial\lambda}{\partial L}U_L\right)^2\right]^{1/2}, \quad (12)$$

where, U_V, U_I, U_L and U_T are respectively the uncertainty for multimeter, caliper and thermometer (Table 7). The uncertainty related to time was assumed to be zero. By applying some mathematical calculations, the Eq. (12), evolve into;

For Δln(t), the value of 0.54 was considered and the mean nominal value of 0.2 W/m K, was considered to normalize the uncertainty of the thermal conductivity. By using Table 7 values in Eq. (13), and after

$$U_\lambda = \left[\left(\frac{I.\Delta\ln(t)}{4\pi L.\Delta T}U_V\right)^2 + \left(\frac{V.\Delta\ln(t)}{4\pi L.\Delta T}U_I\right)^2 + \left(\frac{V.I.\Delta\ln(t)}{4\pi L}.\frac{1}{\Delta T^2}U_T\right)^2 + \left(\frac{V.I.\Delta\ln(t)}{4\pi.\Delta T}.\frac{1}{L^2}U_L\right)^2\right]^{1/2} \quad (13)$$

normalization $\left(\left(\frac{U_R}{R}\right) \times 100\right)$, the uncertainty associated with the measuring instruments used to determine thermal conductivity was found to be 1.92%.

4.2. Enthalpy and C_p uncertainty calculation

Similar approach used for thermal conductivity uncertainty was adopted to calculate the specific heat capacity and enthalpy uncertainties. For this, uncertainty of the heat capacity for reference (water) was assumed to be zero and the nominal value was 4.189 J/g K. Considering Eqs. (9) and (10) together with Eq. (11), the uncertainty for C_p and ΔH are expressed respectively as follow:

$$U_{c_p} = \left[\left(\frac{\partial c_p}{\partial m_r}U_m\right)^2 + \left(\frac{\partial c_p}{\partial m_{pcm}}U_m\right)^2 + \left(\frac{\partial c_p}{\partial\left(T_r^n - T_{r,i}\right)}U_T\right)^2 + \left(\frac{\partial c_p}{\partial\left(T_{pcm}^n - T_{pcm,i}\right)}U_T\right)^2 + \left(\frac{\partial c_p}{\partial\left(T_{pcm}^n - T_\infty\right)}U_T\right)^2 + \left(\frac{\partial c_p}{\partial\left(T_r^n - T_\infty\right)}U_T\right)^2\right]^{1/2}, \quad (14)$$

$$U_{\Delta H} = \left[\left(\frac{\partial \Delta H}{\partial c_{p,pcm}}U_{c_p}\right)^2 + \left(\frac{\partial \Delta H}{\partial\left(T_{pcm}^n - T_{pcm,i}\right)}U_T\right)^2\right]^{1/2} \quad (15)$$

After mathematical operation, the following Eqs. (16) and (17) are obtained:

$$U_{c_p} = \left[\left(\frac{c_{p,r}.\left(T_r^n - T_{r,i}\right)}{m_{pcm}\left(T_{pcm}^n - T_{pcm,i}\right)}.\frac{\left(T_{pcm}^n - T_\infty\right)}{\left(T_r^n - T_\infty\right)}U_m\right)^2 + \left(\frac{m_r.c_{p,r}.\left(T_r^n - T_{r,i}\right)}{\left(m_{pcm}\right)^2\left(T_{pcm}^n - T_{pcm,i}\right)}.\frac{\left(T_{pcm}^n - T_\infty\right)}{\left(T_r^n - T_\infty\right)}U_m\right)^2 + \left(\frac{m_r.c_{p,r}}{m_{pcm}\left(T_{pcm}^n - T_{pcm,i}\right)}.\frac{\left(T_{pcm}^n - T_\infty\right)}{\left(T_r^n - T_\infty\right)}U_T\right)^2 + \left(\frac{m_r.c_{p,r}.\left(T_r^n - T_{r,i}\right)}{m_{pcm}\left(T_{pcm}^n - T_{pcm,i}\right)^2}.\frac{\left(T_{pcm}^n - T_\infty\right)}{\left(T_r^n - T_\infty\right)}U_T\right)^2 + \left(\frac{m_r.c_{p,r}.\left(T_r^n - T_{r,i}\right)}{m_{pcm}\left(T_{pcm}^n - T_{pcm,i}\right)}.\frac{1}{\left(T_r^n - T_\infty\right)}U_T\right)^2 + \left(\frac{m_r.c_{p,r}.\left(T_r^n - T_{r,i}\right)}{m_{pcm}\left(T_{pcm}^n - T_{pcm,i}\right)}.\frac{\left(T_{pcm}^n - T_\infty\right)}{\left(T_r^n - T_\infty\right)^2}U_T\right)^2\right]^{1/2}, \quad (16)$$

$$U_{\Delta H} = \left[\left(\left(T_{pcm}^n - T_{pcm,i}\right)U_{c_p}\right)^2 + \left(c_{p,pcm}U_T\right)^2\right]^{1/2} \quad (17)$$

By replacing the variables in Eq. (16) with the values in Table 7, the heat capacity uncertainty (U_{c_p}) was found to be 0.02821 J/g K, which is needed later to calculate uncertainty of enthalpy. This value was subsequently normalized ($\left(\frac{U_R}{R}\right) \times 100$) using the mean nominal value of 2 J/g K. The uncertainty associated with the measuring instrument used to calculate heat capacity was found to be 1.4%. The normalized enthalpy uncertainty was then deducted using the calculated U_{c_p}, values in Table 7 and Eq. (17), and the mean nominal value of 60 J/g, and found to be 1.73%.

5. Conclusions

The main conclusions of the study are listed below:

- DSC results showed that the conversion of CO into CoFA resulted in significant improvements in thermal capability and latent heat of fusion, in addition to a more congruent phase transition temperatures.
- Comparison of OA and LA, DSC results revealed that OA has a higher latent heat of fusion than LA. However, when mixed with CoFA, the mixtures LA/CoFA have a better performance in terms of congruency, phase transition temperatures and latent heat of fusion than OA/CoFA mixtures.
- Thermal conductivity measurement with transient hot wire method showed that the thermal conductivities of the studied combinations were 0.2 and 0.35 W/m K, in liquid and solid states, respectively.
- T-history method was used to measure enthalpy, phase transition temperatures and heat capacity of the mixtures, and the results were compared with those obtained using DSC. Both DSC and T-history results confirmed that the mixture LA/CoFA with the composition $x_{LA} = 0.20$ has the highest heat capacity and enthalpy.
- The thermal performance stability of the studied mixtures after accelerated thermal cycling showed that the mixtures were thermally stable and less than 1% change in phase transition temperature and enthalpy were noticed after 700 cycles. Furthermore, FTIR analysis showed that the mixtures were chemically stable after thermal cycling. Therefore, these new fatty acid mixtures could be a potential BPCM for energy storage in building applications.

Author statement

All persons who meet authorship criteria are listed as authors, and all authors certify that they have participated sufficiently in the work to take public responsibility for the content, including participation in the concept, design, analysis, writing, or revision of the manuscript. Furthermore, each author certifies that this material or similar material has not been and will not be submitted to or published in any other journal before its appearance in the journal of energy storage.

Declaration of Competing Interest

We confirm that there is a financial support for this work by FORMAS, project number 2017-00686. We confirm that the manuscript has been read and approved by all named authors and that there are no other persons who satisfied the criteria for authorship but are not listed. All the authors have approved the order of authors listed in the manuscript. We further confirm that we have given due consideration to the protection of intellectual property associated with this work and that there are no impediments to publication, including the timing of publication,

with respect to intellectual property. In so doing we confirm that we have followed the regulations of our institutions concerning intellectual property. We understand that the Corresponding Author (Assoc. Prof. M. Jebrane) is the sole contact for the Editorial process. He is responsible for communicating with the other authors about progress, submissions of revisions and final approval of proofs of the paper.

Acknowledgments

The authors would like to thank Moritz Sanne from University for Sustainable Development Eberswalde for his support with DSC screening tests. We also acknowledge Ida Lager (Department of Plant Breeding, Swedish University of Agricultural Sciences, Alnarp, Sweden) for her support with GC-MS analyses. The authors also acknowledge the financial support by FORMAS, project number 2017-00686.

References

[1] A. Pasupathy, R. Velraj, R.V. Seeniraj, Phase change material-based building architecture for thermal management in residential and commercial establishments, Renewable Sustainable Energy Rev. 12 (2008) 39–64.
[2] V.V. Tyagi, S.C. Kaushik, S.K. Tyagi, T. Akiyama, Development of phase change materials based microencapsulated technology for buildings: A review, Renewable Sustainable Energy Rev. 15 (2011) 1373–1391.
[3] A. Bland, M. Khzouz, T. Statheros, E.I. Gkanas, PCMs for residential building applications: a short review focused on disadvantages and proposals for future development, Buildings 7 (2017) 78, https://doi.org/10.3390/buildings7030078.
[4] F. Souayfane, F. Fardoun, P.H. Biwole, Phase change materials (PCM) for cooling applications in buildings: a review, Energy Build. 129 (2016) 396–431.
[5] S.E. Kalnæs, B.P. Jelle, Phase change materials and products for building applications: a state-of-the-art review and future research opportunities, Energy Build. 94 (2015) 150–176.
[6] M. Nazari, M. Jebrane, N. Terziev, Bio-based phase change materials incorporated in lignocellulose matrix for energy storage in buildings—a review, Energies 13 (2020) 3065, https://doi.org/10.3390/en13123065.
[7] R.K. Sharma, P. Ganesan, V.V. Tyagi, H.S.C. Metselaar, S.C. Sandaran, Developments in organic solid–liquid phase change materials and their applications in thermal energy storage, Energy Convers. Manage. 95 (2015) 193–228.
[8] M. Kenisarin, K. Mahkamov, Passive thermal control in residential buildings using phase change materials, Renewable Sustainable Energy Rev. 55 (2016) 371–398.
[9] Y. Zhao, X. Min, Z. Huang, Y. Liu, X. Wu, M. Fang, Honeycomb-like structured biological porous carbon encapsulatingPEG: a shape-stable phase change material with enhanced thermal conductivity for thermal energy storage, Energy Build. 158 (2018) 1049–1062.
[10] X. Min, M. Fang, Z. Huang, Y. Liu, Y. Huang, R. Wen, T. Qian, X. Wu, Enhanced thermal properties of novel shape-stabilized PEG composite phase change materials with radial mesoporous silica sphere for thermal energy storage, Sci. Rep. 5 (1) (2015) 1–11.
[11] H. Nazir, M. Batool, F.J.B. Osorio, M.I. Ruiz, X. Xu, K. Vignarooban, P. Phelan, A.M. Kannan Inamuddin, Recent developments in phase change materials for energy storage applications: a review, Int. J. Heat Mass Transfer 129 (2019) 491–523.
[12] F. Kuznik, D. David, K. Johannes, J.J. Roux, A review on phase change materials integrated in building walls, Renewable Sustainable Energy Rev. 15 (2011) 379–391.
[13] Y. Yuan, N. Zhang, W. Tao, X. Cao, Y. He, Fatty acids as phase change materials: a review, Renewable Sustainable Energy Rev. 29 (2014) 482–498.
[14] D. Rozanna, T.G. Chuah, A. Salmiah, T.S.Y. Choong, M. Saari, Fatty acids as phase change materials (pcms) for thermal energy storage: a review, Int. J. Green Energy 1 (4) (2005) 495–513.
[15] N. Sarier, E. Onder, Organic phase change materials and their textile applications: an overview, Thermochim. Acta 540 (2012) 7–60.
[16] R. Baetens, B.P. Jelle, A. Gustavsen, Phase change materials for building applications: a state-of-the-art review, Energy Build. 42 (2010) 1361–1368.
[17] A. Sharma, V.V. Tyagi, C.R. Chen, D. Buddhi, Review on thermal energy storage with phase change materials and applications, Renewable Sustainable Energy Rev. 13 (2009) 318–345.
[18] D. Mathis, P. Blanchet, V. Landry, P. Lagiere, Thermal characterization of bio-based phase changing materials in decorative wood-based panels for thermal energy storage, Green Energy Environ. 4 (2019) 56–65.
[19] D. Mathis, P. Blanchet, V. Landry, P. Lagiere, Impregnation ofWood with Microencapsulated Bio-Based Phase Change Materials for High Thermal Mass Engineered Wood Flooring, Appl. Sci. 8 (12) (2018) 2696, https://doi.org/10.3390/app8122696.
[20] L. Ma, Q. Wang, L. Li, Delignified wood/capric acid-palmitic acid mixture stable-form phase change material for thermal storage, Sol. Energy Mater. Sol. Cells 194 (2019) 215–221.
[21] L. Shilei, Z. Neng, F. Guohui, Eutectic mixtures of capric acid and lauric acid applied in building wallboards for heat energy storage, Energy Build. 38 (2006) 708–711.
[22] M.N.R. Dimaano, T. Watanabe, The capric–lauric acid and pentadecane combination as phase change material for cooling applications, Appl. Therm. Eng. 22 (2002) 365–377.
[23] A. Karaipekli, A. Sari, Preparation, thermal properties and thermal reliability of eutectic mixtures of fatty acids/expanded vermiculite as novel form-stable composites for energy storage, J. Ind. Eng. Chem. 16 (2010) 767–773.
[24] A. Sharma, A. Shukla, C.R. Chen, S. Dwivedi, Development of phase change materials for building applications, Energy Build. 64 (2013) 403–407.
[25] H. Ke, D. Li, H. Zhang, X. Wang, Y. Cai, F. Huang, Q. Wei, Electrospun form-stable phase change composite nanofibers consisting of capric acid-based binary fatty acid eutectics and polyethylene terephthalate, Fibers Polym. 14 (1) (2013) 89–99.
[26] K. Kant, A. Shukla, A. Sharma, Ternary mixture of fatty acids as phase change materials for thermal energy storage applications, Energy Reports 2 (2016) 274–279.
[27] T. Inoue, Y. Hisatsugu, R. Ishikawa, M. Suzuki, Solid–liquid phase behavior of binary fatty acid mixtures: 2. Mixtures of oleic acid with lauric acid, myristic acid, and palmitic acid, Chem. Phys. Lipids 127 (2) (2004) 161–173.
[28] T. Inoue, Y. Hisatsugu, R. Yamamoto, M. Suzuki, Solid–liquid phase behavior of binary fatty acid mixtures: 1. oleic acid/stearic acid and oleic acid/behenic acid mixtures, Chem. Phys. Lipids 127 (2) (2004) 143–152.
[29] G. Lawer-Yolar, B. Dawson-Andoh, E. Atta-Obeng, Novel phase change materials for thermal energy storage: evaluation of tropical tree fruit oils, Biotechnol. Rep. 24 (2019) e00359.
[30] R. Thaib, M. Amin, H. Umar, Thermal properties of beef tallow/coconut oil bio PCM using T-history method for wall building applications, Eur. J. Eng. Res. Sci. 4 (11) (2019) 38–40.
[31] C. Ahamed Saleel, M. Abdul Mujeebu, Salem Algarni, Coconut oil as phase change material to maintain thermal comfort in passenger vehicles, J. Therm. Anal. Calorim. 136 (2019) 629–636.
[32] M. Irsyad, Heat transfer characteristics of coconut oil as phase change material to room cooling application, in: IOP Conference Series: Earth and Environmental Science 60, IOP Publishing, 2017, 012027.
[33] S. Kahwaji, M.A. White, Edible oils as practical phase change materials for thermal energy storage, Appl. Sci. 9 (8) (2019) 1627.
[34] P. Gallart-Sirvent, M. Martín, G. Villorbina, M. Balcells, A. Solé, C. Barrenche, L. F. Cabeza, R. Canela-Garayoa, Fatty acid eutectic mixtures and derivatives from non-edible animal fat as phase change materials, RSC Adv. 7 (39) (2017) 24133–24139.
[35] D. Zhao, X. Qian, X. Gu, S.A. Jajja, R. Yang, Measurement techniques for thermal conductivity and interfacial thermal conductance of bulk and thin film materials, J. Electron. Packag. 138 (4) (2016), 040802.
[36] F. Frusteri, V. Leonardi, S. Vasta, G. Restuccia, Thermal conductivity measurement of a PCM based storage system containing carbon fibers, Appl. Therm. Eng. 25 (2005) 1623–1633.
[37] A. Sarı, A. Karaipekli, Thermal conductivity and latent heat thermal energy storage characteristics of paraffin/expanded graphite composite as phase change material, Appl. Therm. Eng. 27 (2007) 1271–1277.
[38] A. Franco, An apparatus for the routine measurement of thermal conductivity of materials for building application based on a transient hot-wire method, Appl. Therm. Eng. 27 (2007) 2495–2504.
[39] J.N.W. Chiu, V. Martin, Submerged finned heat exchanger latent heat storage design and its experimental verification, Appl. Energy 93 (2012) 507–516.
[40] H. Badenhorst, L.F. Cabeza, Critical analysis of the T-history method: a fundamental approach, Thermochim. Acta 650 (2017) 95–105.
[41] P. Tan, M. Brütting, S. Vidi, H.P. Ebert, P. Johansson, A.S. Kalagasidis, Characterizing phase change materials using the T-History method: on the factors influencing the accuracy and precision of the enthalpy-temperature curve, Thermochim. Acta 666 (2018) 212–228.
[42] S.N. Gunasekara, R. Pan, J.N.W. Chiu, V. Martin, Polyols as phase change materials for surplus thermal energy storage, Appl. Energy 162 (2016) 1439–1452.
[43] S.N. Gunasekara, J.N.W. Chiu, V. Martin, P. Hedström, The experimental phase diagram study of the binary polyols system erythritol-xylitol, Sol. Energy Mater. Sol. Cells 174 (2018) 248–262.
[44] A. Solé, L. Miró, C. Barreneche, I. Martorell, L.F. Cabeza, Review of the T-history method to determine thermophysical properties of phase change materials (PCM), Renewable Sustainable Energy Rev. 26 (2013) 425–436.
[45] P. Zhao, Q. Yue, H. He, B. Gao, Y. Wang, Q. Li, Study on phase diagram of fatty acids mixtures to determine eutectic temperatures and the corresponding mixing proportions, Appl. Energy 115 (2014) 483–490.
[46] G. Çaylı, S. Küsefoğlu, A simple one-step synthesis and polymerization of plant oil triglyceride iodo isocyanates, Appl. Polymer 116 (4) (2010) 2433–2440.
[47] T. Senphan, S. Benjakul, Chemical compositions and properties of virgin coconut oil extracted using protease from hepatopancreas of Pacific white shrimp, Eur. J. Lipid Sci. Technol. 118 (2016) 761–769.
[48] C.P. Tan, Y.B. Che Man, Differential scanning calorimetric analysis of palm oil, palm oil based products and coconut oil: effects of scanning rate variation, Food Chem. 76 (1) (2002) 89–102.
[49] T.S.T. Mansor, Y.B. Che Man, M. Shuhaimi, Employment of Differential Scanning Calorimetry in Detecting Lard Adulteration in Virgin Coconut Oil, J. Am. Oil Chem. Soc. 89 (2012) 485–496.
[50] S. Ueno, A. Miyazaki, J. Yano, Y. Furukawa, M. Suzuki, K. Sato, Polymorphism of linoleic acid (*cis*-9, *cis*-12-Octadecadienoic acid) and a-linolenic acid (*cis*-9, *cis*-12, *cis*-15-Octadecatrienoic acid), Chem. Phys. Lipids 107 (2000) 169–178.
[51] V. Wylen, G. John, R.E. Sonntag, C. Borgnakke, Fundamentals of classical thermodynamics, Wiley, New York, 1976.

[52] R.K. Sharma, P. Ganesan, V.V. Tyagi, Long-term thermal and chemical reliability study of different organic phase change materials for thermal energy storage applications, J. Therm. Anal. Calorim. 124 (3) (2016) 1357–1366.
[53] A. Sari, Thermal energy storage properties of mannitol–fatty acid esters as novel organic solid–liquid phase change materials, Energy Convers. Manage. 64 (2012) 68–78.
[54] S. Xu, L. Zou, X. Ling, Y. Wei, S. Zhang, Preparation and thermal reliability of methyl palmitate/methyl stearate mixture as a novel composite phase change material, Energy Build. 68 (2014) 372–375.
[55] S. Liu, L. Han, S. Xie, Y. Jia, J. Sun, Y. Jing, Q. Zhang, A novel medium-temperature form-stable phase change material based on dicarboxylic acid eutectic mixture/expanded graphite composites, Sol. Energy 143 (2017) 22–30.
[56] N. Sheng, T. Nomura, C. Zhu, H. Habazaki, T. Akiyama, Cotton-derived carbon sponge as support for form-stabilized composite phase change materials with enhanced thermal conductivity, Sol. Energy Mater. Sol. Cells 192 (2019) 8–15.
[57] Z. Yang, Y. Deng, J. Li, Preparation of porous carbonized woods impregnated with lauric acid as shape-stable composite phase change materials, Appl. Therm. Eng. 150 (2019) 967–976.
[58] H. Fauzi, H.S.C. Metselaar, T.M.I. Mahlia, M. Silakhori, Thermo-physical stability of fatty acid eutectic mixtures subjected to accelerated aging for thermal energy storage (TES) application, Appl. Therm. Eng. 66 (2014) 328–334.
[59] N. Zhang, Y. Yuan, Y. Du, X. Cao, Y. Yuan, Preparation and properties of palmitic-stearic acid eutectic mixture/expanded graphite composite as phase change material for energy storage, Energy 78 (2014) 950–956.
[60] A. Sari, Eutectic mixtures of some fatty acids for latent heat storage: thermal properties and thermal reliability with respect to thermal cycling, Energy Convers. Manage. 47 (2006) 1207–1221.
[61] T. Matsui, M. Yoshida, H. Yamasaki, Y. Hatate, Thermal properties of multicomponent fatty acids as solid–liquid phase change materials for cooling applications, Chem. Eng. Commun. 194 (1) (2007) 129–139.
[62] A. Karaipekli, A. Sari, K. Kaygusuz, Thermal Properties and Long-term Reliability of Capric Acid/Lauric Acid and Capric Acid/Myristic Acid Mixtures for Thermal Energy Storage, Energy Sources, Part A 30 (13) (2008) 1248–1258.
[63] H. Fauzi, H.S.C. Metselaar, T.M.I. Mahlia, M. Silakhori, H. Chyuan Ong, Thermal characteristic reliability of fatty acid binary mixtures as phasechange materials (PCMs) for thermal energy storage applications, Appl. Therm. Eng. 80 (2015) 127–131.
[64] S. Himran, A. Suwono, G.A. Mansoori, Characterization of Alkanes and Paraffin Waxes for Application as Phase Change Energy Storage Medium, Energy Sources 16 (1) (1994) 117–128.
[65] S.J. Kline, F. McClintock, Describing uncertainties in single-sample experiment, Mech. Eng. 75 (1953) 3–8.
[66] R.J. Moffat, Describing the uncertainties in experimental results, Exp. Therm. Fluid Sci. 1 (1) (1988) 3–17.
[67] H.W. Coleman, W.G. Steele, Experimentation, Validation, and Uncertainty Analysis for Engineers, 3rd ed., John Wiley and Sons Inc., Hoboken, New Jersey, 2009.

III

Journal of Thermal Analysis and Calorimetry (2022) 147:10677–10692
https://doi.org/10.1007/s10973-022-11285-9

Solid wood impregnated with a bio-based phase change material for low temperature energy storage in building application

Meysam Nazari[1] · Mohamed Jebrane[1] · Nasko Terziev[1]

Received: 24 August 2021 / Accepted: 17 February 2022 / Published online: 16 March 2022

Abstract
Wood impregnated with a multicomponent mixture of fatty acids as a bio-based phase change material (BPCM) to improve its thermal characteristics was studied. The studied wood/BPCM composites can be used as internal elements in buildings for energy storage. Scots pine and beech sapwood were impregnated with a multicomponent mixture of linoleic acid and coconut oil fatty acids at a ratio of 20:80. Leakage test was conducted and revealed that the maximum leakage for pine and beech were 9 and 8%, respectively. Light microscopy was employed to demonstrate the distribution of the BPCM in the wood structure. Rays in both pine and beech wood served as pathways for impregnation of the BPCM to partly fill the tracheid lumens (pine) and vessels (beech). Thermal characterization of the studied samples employed T-history and DSC methods, concluding that the impregnated wood had significant thermal mass, ability to store excessive energy in terms of latent heat and keep the temperature constant for long time. The specific heat capacity of the impregnated samples was 4–5 J g^{-1} K^{-1} i.e., higher than that of the untreated control samples of ca. 2 J g^{-1} K^{-1}. The thermal conductivity of the samples before and after the impregnation was measured using heat flow meter method and the results showed that the untreated beech wood had higher thermal conductivity compared to pine and the parameter improved when the cell lumens were filled with the BPCM. Scots pine wood with to 80% mass percentage gain (MPG) after impregnation demonstrated an increment in thermal conductivity of 33% while Scots pine and beech with 43 and 38% MPG demonstrated an increase of the conductivity with 8 and 11%, respectively.

Keywords Beech · Bio-based PCMs · Building applications · Energy storage · Impregnation · Leaching · PCM distribution · Scots pine · Thermal characterization

Abbreviations

BPCM	Bio-based phase change materials
CoFA	Coconut oil fatty acid
DSC	Differential scanning calorimetry
LA	Linoleic acid
PCM	Phase change materials

List of symbols

A	Heat transfer area [m^2]
C_p	Specific heat [J g^{-1} K^{-1}]
L	Thickness of the samples [m]
m	Mass of the samples [kg]
P	Independent variables
Q	Heat [W]
q/a	Heat flux [W m^{-2}]
R	Dependent variables
T	Temperature [°C]
t	Time [s]
U	Uncertainty
u	Overall heat transfer coefficient [W m^{-2} K^{-1}]

Greek symbol

λ	Thermal conductivity [W m^{-1} K^{-1}]
Δ	Difference
∞	Ambient

Subscripts

f	Final
i	Initial
n	Time point
ref	Reference
samp	Sample

✉ Mohamed Jebrane
mohamed.jebrane@slu.se

[1] Department of Forest Biomaterials and Technology, Swedish University of Agricultural Sciences, Vallvägen 9C, 750 07 Uppsala, Sweden

Introduction

Development of bio-materials from renewable sources is essential for future technologies to harmonize the human living environment [1]. The building industry has an overall positive outlook and guarantees future interest in bio-based products, with high percent of using timber in single and multi-floor buildings during the last decade [2, 3].

Traditionally used construction materials including metals, concrete, insulation polymers and plastics impose environmental problems, e.g. non-recyclable wastes. Globally, around half of the construction materials origins from non-renewable resources. Moreover, the embodied energy of building material is responsible for 10–20% of the building's total energy consumption. In addition, some materials (asbestos, formaldehyde, and lead) can have a harmful effect on the human's health. A sustainable solution can be the increased utilisation of renewable bio resource construction materials for a better indoor environment and reduction of the negative impacts on climate and health [4]. Considering the above, the demand for environmentally friendly, renewable and green building materials has increased significantly over the past few years and it is expected to grow continuously[5]. Green building materials used in constructions to energy management have a crucial relevance to achievement of sustainable development goals (SDGs). A study [6] showed that SDGs 7.3, 11.6 and 13.2 are essentially achievable by increased building with bio-materials. In order to address the mentioned problems related to non-renewable construction materials, more attention lays on engineered wood elements as bio-based, renewable, sustainable and recyclable material to replace currently used traditional materials in modern single and multistory building constructions [5]. Manufacturing of wooden-based construction materials demands less energy compared to steel and concrete and the wastes are recycable [7].

Low thermal mass of wood limits its energy efficiency when it is used for internal applications. The wood material cannot store and release extra energy in case of temperature fluctuation and thus, extra energy should be supplied to compensate and regulate the energy balance inside buildings. This issue might be even more apparent for cold climate regions where a large amount of the generated energy is expended for heating during winter. However, if wooden panels are engineered in a combination with bio-based phase change materials, e.g. fatty acids or esters with appropriate working temperature, the temperature fluctuation inside buildings can be controlled. Stored latent heat can be released when the temperature drops down under the comfort temperature and the energy is applied more efficiently [8–10]. The progress in the design of new timber systems, e.g. konstruktionsvollholz (KVH), duo/trio laminated beams, cross-laminated timber (CLT) and laminated veneer lumber (LVL) offers new options for the integration of bio-based phase change materials (BPCM) to increase the efficiency and reduce the energy demand of the buildings.

Wood in various forms (fibers, flour, solid wood, veneer) is a cheap bio-container for encapsulation of PCMs, widely used as a building material and thus, can naturally be integrated with BPCMs [9]. BPCMs can be incorporated in the internal walls or in its coatings [11], flooring [10] or in the façades of the buildings [12]. As energy savings become an inevitable part of modern buildings, synergy between BPCM and wood comprises various options, e.g. wood flour [13, 14], and surface treatment of solid wood and wood composites [15–17] to host the BPCMs.

The majority of studies concentrated on wood/PCM composites where the wood can be in a form of flour, solid or delignified wood. Examples are fatty acids or their mixtures were impregnated in wood flour [18, 19] for increased latent heat storage in the composites. Paraffin was blended with poplar wood flour [20] in a bio-composite with latent heat capacity of 26.8 J g^{-1} while graphite was added to improve the thermal conductivity of the material.

Recently, delignified wood has been studied intensively, e.g. an eutectic mixture of capric-palmitic acids impregnated into delignified wood [21] at a retention of 61.2% demonstrated no leakage, a phase transition temperature of 23.4 °C and latent heat of 94.4 J g^{-1} with good thermal stability. Another study [22] used delignified wood as an encapsulating material for impregnation of PCM claiming increased pore volume compared to the initial material. However, the approach of using delignified wood is debatable since lignin, having best thermal conductivity of the three structural polymers in wood, has been extracted.

Solid wood of alder [23] impregnated with paraffin and coated with polystyrene to avoid the leakage of the PCMs. An optimum mass percentage gain of 29.9 mass% and a latent heat value of 20.62 J g^{-1} was reported. Temiz et al. [24] studied Scots pine sapwood impregnated with an eutectic mixture of capric acid (CA) and stearic acid (SA). After thermal characterization of the material, it was concluded that the system wood/CA-SA can be used for indoor temperature regulation and energy saving in timber buildings. Solid wood as a BPCM carrier is particularly suitable for flooring. Because of the floor heating systems construction, the engineered wood floor can undergo many heating/cooling phases and thus, ensure significant gain of latent heat. In a study, Mathis et al. [10] engineered the thin upper layer of wood flooring for absorbing and storing solar energy at a temperature of 30 °C. Oak and sugar maple wood impregnated with a commercial microencapsulated BPCM (Nextek29) was studied and a latent heat of 7.6 J g^{-1} for the composite

with 77% improvement in thermal mass compared to the untreated wood was found.

The research ideas above still have to cope with the inherited disadvantages of wood namely, moderate heat capacity and low thermal mass and thus, low ability to absorb and store thermal energy, low thermal conductivity, dimensional instability and bio-degradability.

The approach of using wood/BPCM composites for passive energy storage within the comfort temperature range should address certain questions including comprehensive studies regarding the impregnability, leaching of the BPCM, and comprehensive thermal analyses of the composite including temperature behavior, thermal mass, heat capacity, thermal conductivity and enthalpy. The material characterisation must be carried out in a comparison with untreated wood and/or other building materials. Wood impregnability and leaching of the BPCM have often been neglected and there is a scarcity of information about the impregnation of BPCMs in the wood cell wall and lumen. According to the current knowledge, the above questions have rarely been studied comprehensively to show deeper interaction between BPCM and the wood matrix. A drawback of previous studies is the use of small size samples for DSC, which cannot give deep understanding and insight of the thermal behavior of the entire composite.

The present study focuses on solid wood of two widely used wood species for building in Europe namely, Scots pine (softwood) and beech (hardwood). A special emphasis has been set on the impregnability of the wood and a study on leaching was conducted to analyze the problem when a recently developed BPCM [25] has been selected and employed. The aim of the study was to reveal the thermal characteristics of the solid wood using DSC, T-history and heat flow meter method to investigate the feasibility of the two wood species for encapsulation of the BPCM for building purposes.

Experimental

Materials

A previously developed BPCM composed of coconut oil fatty acids (CoFA) and linoleic acid (LA) mixed in a ratio of 80:20 [25] was used through the study. Polyethylene glycol with an average molecular mass of 600 (PEG 600) was purchased from Sigma-Aldrich and was used as a reference PCM in the leaching test. Wood samples of Scots pine (*Pinus sylvestris* L.) sapwood and beech (*Fagus sylvatica* L.) with dimensions of $9 \times 90 \times 90$ mm along the grain and without visible defects were used throughout the study.

Methods

Incorporation of PCMs into wood and leaching test

The BPCM was impregnated in the wood samples by a vacuum-pressure process in an autoclave. Target retentions expressed by the mass percentage gain (MPG) of the sample were set to 55 and 90%, i.e. low and high. The autoclave temperature was set to 60 °C to ensure melting of the BPCM. PEG 600 was impregnated only in Scots pine samples. The wood samples were conditioned in a climate chamber to 12% moisture content prior to the impregnation. The high MPG was achieved by immersing the samples in BPCM and applying a vacuum of 350 mbar for 10 min followed by 6 bar pressure for 1 h. The low MPG was achieved when a pre-pressure of 0.75 bars for 60 min was applied instead of vacuum step. Wood density, impregnation parameters and the average MPG are shown in Table 1.

The MPG was calculated as the difference between the initial (m_i) and final mass (m_f) of the wood sample and expressed in percent (Eq. 1).

Table 1 Wood density, impregnation parameters and average MPG. Standard deviations in parentheses, 5 samples per treatment

Wood species	Density, kg m^{-3}	PCM	Time and vacuum depth	Pre-pressure time	Pressure time	Average MPG, %
Scots pine	506/88	PEG 600	–	60 min 0.75 bar	–	Low 59.8/1.9
		PEG 600	10 min 80%	–	60 min 6 bar	High 88.3/2.5
		BPCM	–	60 min 0.75 bar	–	Low 56.3/3.7
		BPCM	10 min 80%	–	60 min 6 bar	High 94.7/5.7
Beech	745/53	BPCM	10 min 80%	–	60 min 6 bar	43.1/4.4

$$\text{MPG}\ (\%) = \frac{\left(m_f - m_i\right)}{m_i} \times 100 \quad (1)$$

After the impregnation, the samples were conditioned in a cold room (10 °C) for 3 weeks and the mass was recorded prior to the leaching tests. To assess the leaching rate, each impregnated sample was placed between spruce and oak samples. Both spruce and oak samples had identical dimensions as the treated sample and were conditioned at room climate prior to the test. The 3-layer set was pressed by a mass of 1 kg and placed in a climate chamber at 35 °C for 24 h. The cumulative leached amount of BPCM was calculated as a difference between the mass of the sample after 8, 16 and 24 h and related to the initial mass and expressed in percent (likewise Eq. 1).

Light microscopy

Impregnated and leached samples were cut to sub-samples; only those located in the inner part of the samples were taken for microscopy observations. The sub-samples had dimensions of 5 × 5 × 15 mm and semi-thin Sections (20–40 µm) were cut by a Leitz sliding microtome (Leitz, Wetzlar, Germany) and examined using Leica DMLB light microscope (Leica, Wetzlar, Germany). No additional treatments to soften the wood before cutting were applied.

Osmium tetroxide (OsO_4) was used as a specific/chemical marker known to react strongly with ethylene bonds of unsaturated triglycerides being reduced to osmium black (OsO_2). Apart from its common use as a post-fixative for electron microscopy, it reacts strongly with the ethylene bonds of a number of fatty acids including the cis-linoleic acid and cis-linolenic acids [26] used here in the present BPCM preparation.

To visualize the BPCM in the wood structure, observations were made on sections from the inner regions of the samples treated with 1% w/v of OsO_4 for 1 h at room temperature. Some wood sections were stained with Oil Red O that reacts and stains also the available fatty acids. The untreated Scots pine and beech sections were stained with safranin.

Differential scanning calorimetry (DSC)

Differential scanning calorimetry (DSC) curves of the PCM and PCM impregnated into wood were recorded on a DSC Mettler-Toledo DSC 3 system under a nitrogen atmosphere. For each DSC run, a sample of mass usually in the range 14–20 mg was taken from the core of each sample and hermetically sealed in a standard DSC aluminum crucible pan. The DSC tests were conducted between − 25 and 50 °C at a heating rate of 2 °C min^{-1} with 15 min isothermal segment at each − 25 and 50 °C. This heating–cooling cycle was repeated three times to obtain an acceptable reproducibility. Prior to measurements, the DSC system was calibrated using indium and zinc.

Thermal conductivity of PCMs by heat flow meter method

Thermal conductivity of the wood/BPCM composite was measured according to the standard methods ASTM C1155-95 (2013) and ISO 9869-1:2014, known as heat flow meter method with some modifications [27, 28]. A schematic illustration of the experimental set-up used to measure the thermal conductivity is shown in Fig. 1. Since the purpose is to measure thermal conductivity along the thickness of samples, an insulated box was designed to minimize the heat loss from other sample's sides. Moreover, the samples are ten times bigger in other directions than thickness, which guarantees low heat loss from other directions. Two thermocouples of K- and T-type were used to measure the temperature at the both surfaces of the sample. To avoid the effect of the surrounding environment on the measurements, the non-contact surface of the thermocouples were insulated. A heat flux meter type FHF03 supplied from Hukseflux, the Netherlands was used to measure the heat flux at the surface exposed to cold environment. Each measurement was run for

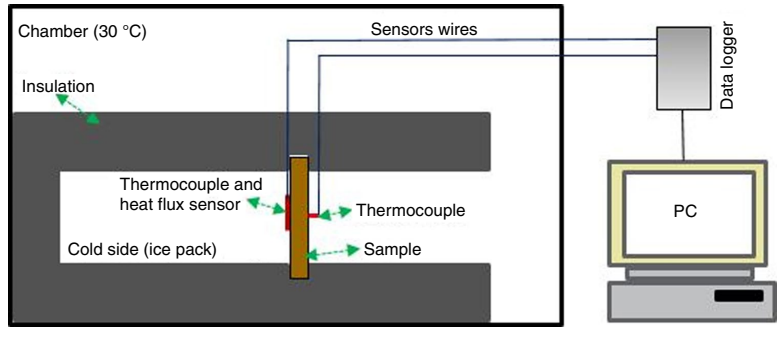

Fig. 1 Schematic diagram of the designed rig for thermal conductivity measurements

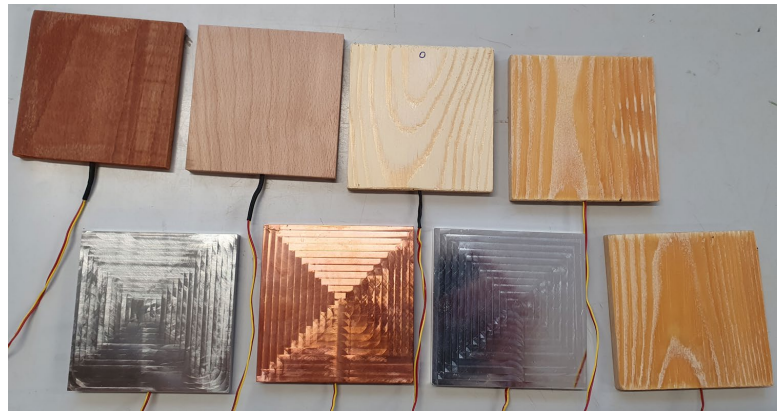

Fig. 2 Samples and references without insulation

Table 2 Thermal and physical properties of references

	Copper (SS 5011-04)	Aluminium (SS 4212)	Stainless steel (SS 2343)
Mass/g	657.6	200.3	581.9
Dimension/mm	9×90×90	9×90×90	9×90×90
Thermal conductivity/W m^{-1} K^{-1}	395	167–216	72–79
Specific heat capacity/J g^{-1} K^{-1}	0.385	0.89	0.45–0.46

3 h to ensure a steady state process [29] and the experiment was repeated 4 times for reproducibility. After measuring the heat flux and the temperatures at both surfaces of the samples, the thermal conductivity was calculated by applying Fourier's law of thermal conduction [29]:

$$\lambda = \frac{q}{a} \times \frac{\Delta L}{\Delta T}, \tag{2}$$

where $\frac{q}{a}$ is the heat flux, ΔL is the thickness, and ΔT is temperature difference.

T-history, specific heat capacity and enthalpy

T-history method was used to measure thermal properties of several samples simultaneously [30, 31] including melting/freezing point, latent heat of fusion, degree of super cooling and specific heat capacity. Untreated control wood samples, samples impregnated with BPCM (wood/BPCM composites), and metal plates (copper, aluminum and stainless steel) with identical dimensions were tested simultaneously (Fig. 2). The copper plate was used as main reference to obtain overall heat transfer coefficient (u). This parameter was then used to calculate the thermal properties of aluminum and stainless steel, which were then compared with the known data of these materials (Table 2) to verify and validate our approach. The samples and references were

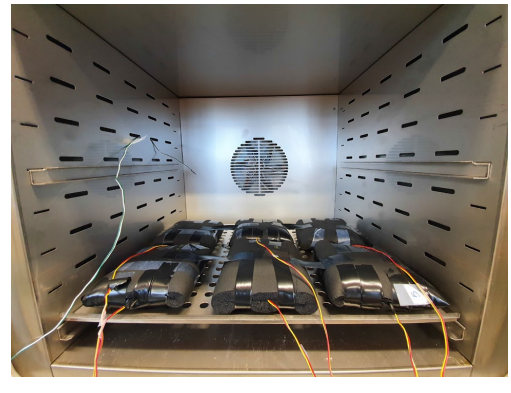

Fig. 3 Insulated samples and references inside the chamber

thermally insulated using 10 mm thickness ARMAFLEX insulation material (Fig. 3). K-type thermocouples were used to record temperature changes over time for samples and references. The thermocouples were placed at the centerline and in the middle of the samples. For cold and hot ambient climates, two chambers were employed, the former used for cold ambient climate fixed at 10 °C, while the latter chamber was used for hot ambient climate set at 35 °C. The

chamber's temperatures were recorded with two separate thermocouples. Figures 2 and 3 show the photographs of the samples and references with and without insulation. Thermal and physical properties of the references are summarized in Table 2. Samples and references were first preheated at 35 °C, and then quickly transferred into the chamber at 10 °C and the temperature profile was recorded. Once the equilibrium temperature was reached (ca. 3 h), the samples and the references were transferred back at 35 °C and the temperature changes were recorded.

Energy balance for the reference was employed to obtain the overall heat transfer coefficient. Since the wooden samples and the metal reference have identical dimensions and insulation for uniform heat transfer conditions, the overall heat transfer coefficient (u) for both reference and wood samples were considered identical. The amount of heat transferred to/from samples in the chamber is expressed as follow:

$$Q = uA\left(T(t)_{\mathrm{n}} - T_{\infty}\right), \tag{3}$$

where Q, u, A, $T(t)_{\mathrm{n}}$ and T_{∞} are, respectively, the transferred heat, overall heat transfer coefficient, heat transfer area, sample temperature at each time point and ambient temperature inside oven/chamber.

The amount of heat stored/released from samples is:

$$Q = mC_{\mathrm{p}}\frac{\mathrm{d}\left(T_{\mathrm{i}} - T(t)_{\mathrm{n}}\right)}{dt}, \tag{4}$$

where m, C_{p}, T_{i} and dt are, respectively, the mass of the samples, specific heat capacity, initial temperature and time interval.

The amount of transferred energy to/from the samples is stored/released in/from the samples, then the energy balance is:

$$Q = -uA\left(T(t)_{\mathrm{n}} - T_{\infty}\right) = mC_{\mathrm{p}}\frac{\mathrm{d}\left(T(t)_{\mathrm{n}} - T_{\mathrm{i}}\right)}{dt} \tag{5}$$

By rearrangement and integration, the temperature distribution for the reference and wood samples are obtained as:

$$\int_{T_{\mathrm{i}}}^{T_{\mathrm{n}}} \frac{d\left(T(t)_{\mathrm{n}} - T_{\infty}\right)}{\left(T(t)_{\mathrm{n}} - T_{\infty}\right)} = -\int_{0}^{t_{\mathrm{n}}} \frac{uA}{mC_{\mathrm{p}}}dt \tag{6}$$

After mathematical operation:

$$\ln\left[\frac{\left(T(t)_{\mathrm{n}} - T_{\infty}\right)}{\left(T_{\mathrm{i}} - T_{\infty}\right)}\right] = -\frac{uA}{mC_{\mathrm{p}}}t_{\mathrm{n}} \tag{7}$$

As the thermo-physical properties of the reference is known, the overall heat transfer coefficient (u) is calculated using energy balance for the reference:

$$uA = -\frac{\ln\left[\frac{\left(T(t)_{\mathrm{n}} - T_{\infty}\right)}{\left(T_{\mathrm{i}} - T_{\infty}\right)}\right]_{\mathrm{ref}}}{t_{\mathrm{n}}} m_{\mathrm{ref}}C_{\mathrm{p,ref}} \tag{8}$$

uA is calculated by the energy balance for the reference according to Eq. 8, and as heat transfer area and conditions around reference and wood samples are identical, uA was calculated from the energy balance of the reference and used further to calculate C_{p} for the wood samples. After substitution Eq. 8 in Eq. 7, C_{p} of the samples is calculated as:

$$C_{\mathrm{p,samp}} = \frac{\ln\left[\frac{\left(T(t)_{\mathrm{n}} - T_{\infty}\right)}{\left(T_{\mathrm{i}} - T_{\infty}\right)}\right]_{\mathrm{ref}}}{\ln\left[\frac{\left(T(t)_{\mathrm{n}} - T_{\infty}\right)}{\left(T_{\mathrm{i}} - T_{\infty}\right)}\right]_{\mathrm{samp}}} \frac{m_{\mathrm{ref}}}{m_{\mathrm{samp}}} C_{\mathrm{p,ref}} \tag{9}$$

Enthalpy of the samples is obtained as [25]:

$$\Delta H = c_{\mathrm{p,samp}}\left(T(t)_{\mathrm{n,\ samp}} - T_{\mathrm{samp,i}}\right), \tag{10}$$

where ΔH is enthalpy change from initial point to each time point n.

Results and discussion

Impregnation, leaching and PCM distribution

Under the studied conditions, MPG of up to 95% were achieved for pine, while a maximum of 43% MPG was possible for beech (Table 1). This is due mainly to the density and the anatomical features of beech. After impregnation and conditioning, the samples were leached at 35 °C and the cumulative rates of leached BPCM after 8, 16 and 24 h are plotted in Fig. 4.

Porous materials with low density, large internal surface area and various dimensions of cell lumens and cell wall cavities are suitable for storage of BPCMs. Nevertheless, most of the PCMs are susceptible to leakage [32] and thus, any lignocellulose material as a form of encapsulation can hardly prevent the leakage during exploitation [33]. Contrary, composite materials with additives, e.g. wood flour [34], wood-polymer composites [35] or copolymers [36] demonstrated no leaching. The above findings can be questioned since the leaching has been monitored after short time of 15–30 min. Compared to the mentioned encapsulation forms, the incorporated BPCM into solid wood in this study displayed low leaching rates under tested conditions. Due to the chemical structure and the molecular mass of PEG 600, this material leaches more than BPCM (*ca.* 7–8% PEG 600 vs. 2–4% PBCM). Regardless the initial retention, PEG 600 leaches gradually until it reaches *ca.* 12% after 24 h. The BPCM showed better stability in the wood and only a total of *ca.* 8 to 9% were leached for the low and

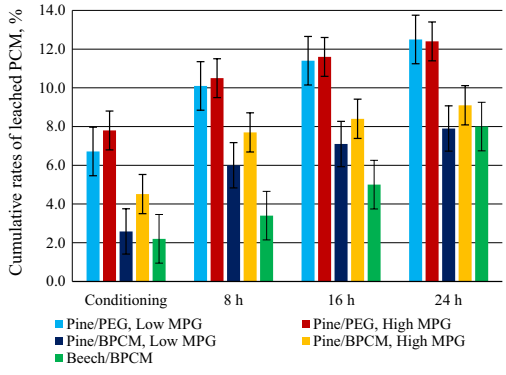

Fig. 4 Leaching rates of PEG 600 and BPCM from Scots pine and beech samples after 24 h at 35 °C. The real values of the target retentions of 50 and 90% are shown in Table 1

high MPGs. It should be mentioned that the effect of moisture is not considered in the results above. Particularly, in the stage of conditioning, some moisture will be adsorbed in the wood and thus, the actual value of leaching should be somewhat higher. The beech samples showed a similar leaching behavior as pine reaching 8% leachate after 24 h. Apparently, leaching is a serious hinder in the application of BPCMs since a significant part of the material can be lost. The demonstrated values are only after short period but the trend shows that the process will continue further and higher values will be reached before the BPCM achieves the point of equilibrium with the ambient conditions.

The impregnated samples were studied by light microscopy (Fig. 5) to reveal the penetration and distribution of the BPCM within the wood structure. All images were derived by light microscopy observations on sections from the inner regions of the impregnated samples. Outer regions showed similar but more intense reactions. Dry sectioning of samples was conducted to prevent any diffusion of the BPCM using pretreatment with polar/unpolar liquids and to reduce possible smearing during the sectioning process. As the wood has a high hardness and the sections were quite thick, it was possible to focus on cell layers beneath the section surface thereby confirming the specific presence of the BPCM in the wood structure. OsO_4 as a staining agent is known to react with compounds in both vapor and liquid phases, thus it is not known which phase were responsible for the strong reactions recorded. A multi-illustration of the BPCM distribution in the wood structure of Scots pine and beech is shown in Fig. 5.

Safranin-stained untreated control sections of Scots pine and beech showed the structure without the BPCM, i.e. empty anatomical elements. Strong reactions of both OsO_4 and Oil Red O with the BPCM were observed in the lumens of early- and latewood tracheids (Fig. 5b, c) and in the tips of axial tracheids (Fig. 5c) of Scots pine samples where the fatty acid mixture was found as precipitate. Some tracheids were completely filled while in some other the BPCM was found distributed on the internal cell wall. Light microscopy and staining observations confirmed the pathway for penetration of the BPCM into the wood was via the rays with a strong purple-black staining of the contents of the ray tracheids and parenchyma cells (Fig. 5b, c); ray tracheid bordered pits and axial tracheid bordered pits recognized (Fig. 5c). The staining reaction within the tracheid lumens and rays cells was very strong (i.e. reflecting the amount of BPCM present) but even the reaction with secondary cell wall layers was distinct in the transverse sections colored with Oil Red O (Fig. 5b) where a yellowing of the middle lamella and S2 walls was noted. The RLS sections stained with OsO4 (Fig. 5c), a darkish staining was achieved confirming the presence of some amount of BPCM in the cell walls.

The pathway for penetration of the BPCM into the beech wood was via the rays with a strong blackish staining of the contents (Fig. 5e, f). The vessel lumens are only partly filled with the BPCM (Fig. 5e) because part of the material has been leached. The majority of beech fibers were found filled with the BPCM while the BPCM in the vessels was found distributed on the cell wall surface (Fig. 5e, f).

The above observations and the staining reactions of the cell walls are suggestive that in addition to penetration of the wall that a thin film is produced along the exposed surfaces of the cell walls. Unlike most polar oxidizing agents, OsO_4 is able to penetrate both hydrophobic (i.e. high surface tension) and hydrophilic (low surface tension) lipids thus within the 1 h period the treated wood cell walls would had allowed penetration.

Thermal conductivity measurement with heat flow meter

Figure 6 shows the result of the heat flow meter method. It depicts the temperatures at both sample's surfaces and the measured heat flux. The monitored parameter profiles reached their steady state after almost 1 h, while the tests was conducted for approximately 3 h [29, 37], and the result at the steady part was used to calculate the thermal conductivity of the samples using Eq. 2. The experimental uncertainty due to measurement instrument including thermocouple, heat flux sensor and caliper on results calculated from Eq. 2 was determined and found to be 3.34%. The details of the calculations are given in the experimental uncertainty analysis section.

The measured thermal conductivities of wood and wood/BPCM composites are plotted in Fig. 7. The thermal conductivity of pine and beech were 0.12 and 0.23 W m^{-1} K^{-1},

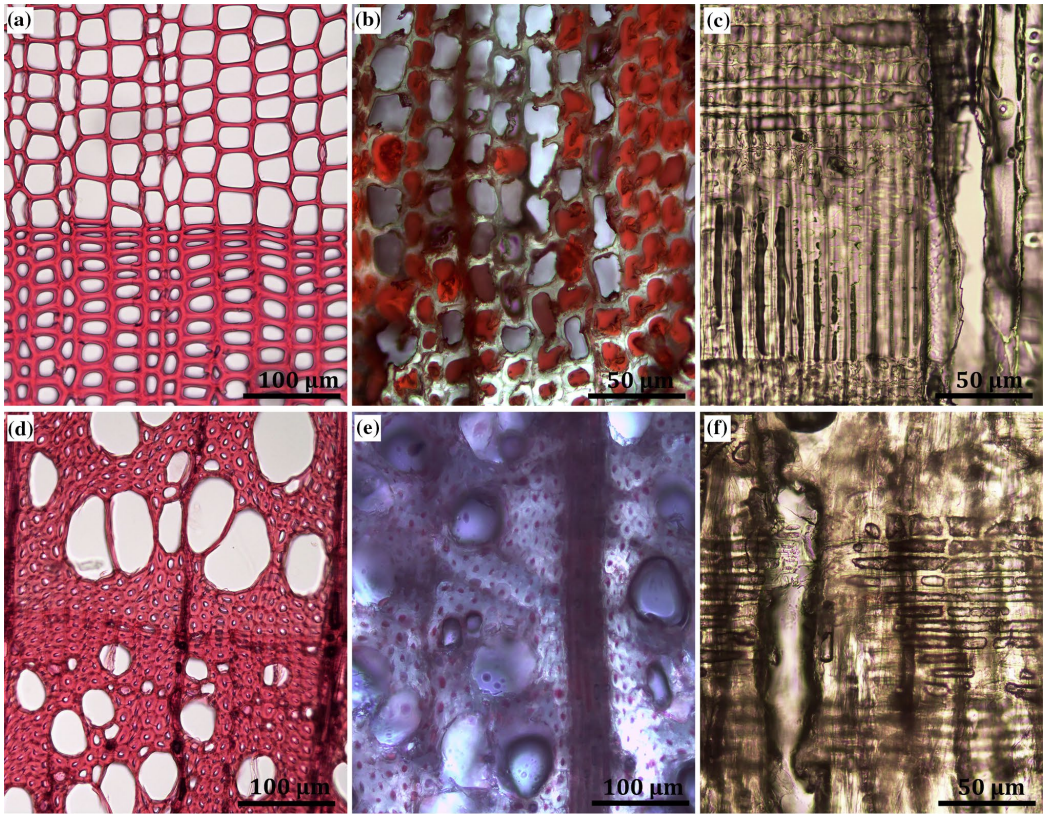

Fig. 5 Safranin (**a**, **d**), Oil Red O (**b**, **e**) and osmium tetroxide (**c**, **f**) staining of Scots pine and beech samples impregnated with BPCM. Scots pine (**a**, **b**), transverse sections (TS) of untreated wood (**a**) and precipitates of BPCM located in the cell lumens of tracheids (**b**) and at tracheid tips (**c**); Scots pine, radial-longitudinal section (RLS) section showing darkish staining of the BPCM present in the ray tracheids and parenchyma cells and in the bordered pits and latewood cell lumens (**c**). The entire wood structure has reacted and has a redish/blackish colouration. Beech (**d**, **e**), TS of untreated wood (**d**) and precipitates of BPCM located mainly in the fiber, rays and vessel lumens (**e**); Beech, TS and RLS of a broad homogeneous ray filled with BPCM (**e**, **f**). The adjacent vessel in (**f**) has a thin film of the BPCM on the cell wall surface

respectively, which were in line with the reported values in the literature [38, 39]. Previous studies [38] discussed that thermal conductivity of wood materials varies with density, moisture content and wood species. The thermal conductivity of pine was reported to be in the range 0.1–0.14 W m^{-1} K^{-1}, depending on the species. Czajkowski et al. [39] studied thermal conductivity of beech and reported a value of 0.24 W m^{-1} K^{-1} along the radial direction, while other study [38] reported a value of 0.19 W m^{-1} K^{-1}. These studies corroborate the funding of the present study.

The thermal conductivity of the BPCM was ca. 0.2 W m^{-1} K^{-1} at liquid state and ca. 0.35 W m^{-1} K^{-1} at solid state [25], i.e. higher than that of wood. The impregnated BPCM into wood is expected to improve the thermal conductivity of the composites. During thermal conductivity measurements, the temperature at the cold surface was 21–22 °C, while at the warm surface it was in the range 24–27 °C, indicating that the temperature of the composites was probably in the range 23–25 °C. This suggest that the BPCM inside the composites was at its mushy state during the tests. The thermal conductivity of BPCM at mushy state is slightly higher than liquid state; however, the exact value is unknown. The measured thermal conductivity of pine/BPCM composites with 43 and 78% MPGs were 0.13 and 0.16 W m^{-1} K^{-1}, respectively, which shows improvement of 8.3 and 33%, respectively. Beech/BPCM with 38% MPG, demonstrated a value of 0.255 W m^{-1} K^{-1}, showing 11% improvement.

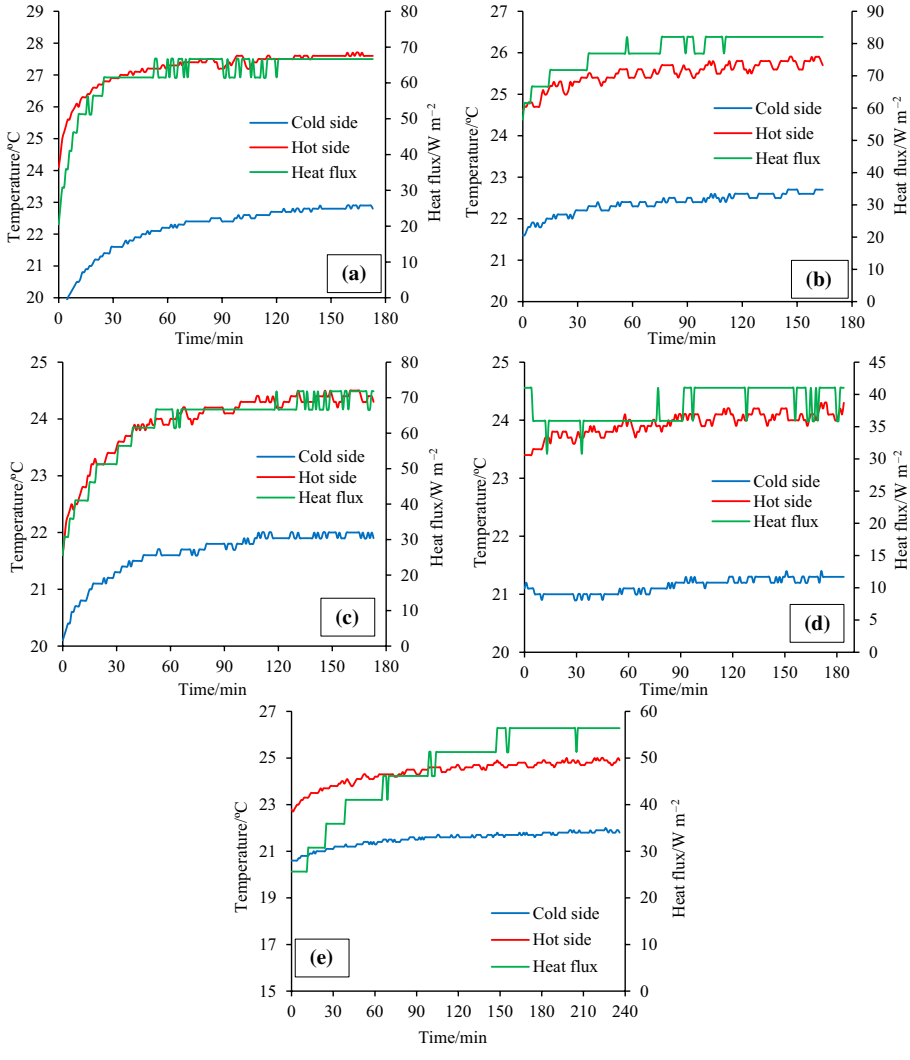

Fig. 6 Measured temperatures at both sides and heat flux for thermal conductivity. **a** Pine, **b** Beech, **c** Beech/BPCM 38%, **d** Pine/BPCM 43%, **e** Pine/BPCM 78%

The observed differences between impregnated pine and beech at comparable PCM retentions could be explained by the density and anatomical features of the wood species. The results showed also that the thermal conductivity increases with increasing of the MPG of BPCM. Yang et al. [40] studied the thermal properties of wood/PCM composite using carbonized pristine wood and 1-tetradecanol as PCM. The thermal conductivity value of the PCM at 25 °C was 0.241 W m^{-1} K^{-1}, for the carbonized wood at the same temperature and at radial direction, it was 0.414 W m^{-1} K^{-1}, while after full cell impregnation (maximum MPG), the thermal conductivity of the composite reached 0.515 W m^{-1} K^{-1}, thus showing 24% improvement. The study, likewise the present study showed that higher MPG leads to increase of the thermal conductivity.

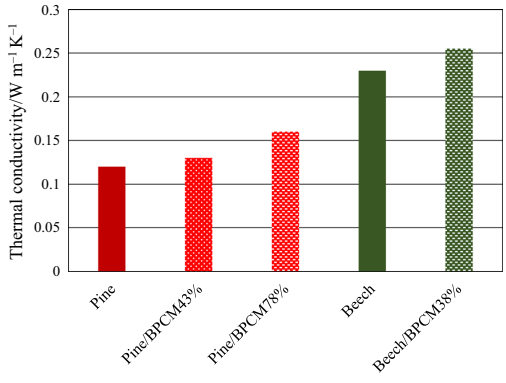

Fig. 7 Calculated thermal conductivity of the samples

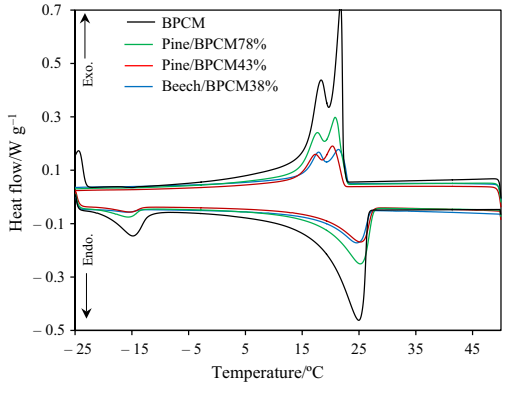

Fig. 8 DSC curves obtained for BPCM and for the wood/BPCM composites

Thermal analysis by DSC and T-history

Figure 8 shows the DSC curves obtained for BPCM (*80/20 ratio*) [25], and wood/BPCM composites. The patterns of heat flow for BPCM and Wood/BPCM composite were similar but with a slight shift in onset and endset temperatures. The heat flow and enthalpy measured for the wood/BPCM were lower than that of the pure BPCM, as the proportions of BPCM in the composite were ca. 43 and 78% for pine and 38% for beech, and the wood itself does not have latent heat. In addition, the most prominent peak of the pure BPCM decreased after incorporation in wood and two small peaks at lower temperatures, which are probably related to crystalline points of the BPCM were probably shifted to lower temperatures after impregnation into wood. The measured latent heat of fusion for BPCM was 94 J g^{-1} [25], but it was reduced to 30 and 43 J g^{-1} after incorporation into pine with 43 and 78% MPG and to 27 J g^{-1} for beech/BPCM with 38% MPG. Similar trend was reported [21, 40] when PCM was incorporated into wood. Yang et al. [40] studied carbonized wood fully impregnated with 1-tetradecanol as PCM, and reported a lower latent heat of fusion compared to pure PCM as a results of the reduction in latent heat per mass. By comparing carbonized and non-carbonized wood as supporting material, it was proven that the latent heat of the PCM/wood composite depends mainly on the content of PCM incorporated in the composite. Additional study [41] with delignified wood as substrate and a PCM retention of 65% reported lower latent heat of fusion than that of pure PCM. Ma et al. [21] used delignified and undelignified cedar wood as substrates impregnated with eutectic mixture of capric/palmitic acids at a retentions of 61.2 and 46.8%, respectively. A reduction in latent heat of fusion after incorporation into wood and a proportional relationship between the latent heat of fusion and the amount of impregnated PCM was reported. Additionally, a small temperature shift in onset and endset was reported.

Figure 9 shows the T-history profile for the samples and references during the cooling (9a) and heating process (9b). The copper plate (Cu) was used as the main reference and aluminum (Al) and stainless steel (SS) plates were used in order to validate the experimental results. The measured ambient temperatures were constant throughout the experiments with ± 0.8 °C maximum deviation. Once placed in the climate chamber at 10 °C, the samples and the references' temperatures decrease gradually from the starting temperature at 35 °C and continues to decease with the time until it reaches the chamber's ambient temperature (10 °C). During the course of cooling cycles, a phase change transition was observed for all the wood/BPCM composites at temperature around 22.3 °C which is lower than that of pure BPCM, which is around 24 °C. In addition, during cooling process the pure BPCM experienced a small degree of supercooling and solidifies incongruently, once impregnated into wood, no incongruence and supercooling were observed. During heating course, the pure BPCM and wood/BPCM composites melt congruently, and unlike the cooling course, the composites experiences a slight increase in phase transition temperature during heating cycle.

During the cooling and heating processes (Fig. 9), untreated pine and beech samples reached the equilibrium faster than the impregnated samples. For metal plates, Al reached the equilibrium quickly compared to Cu and SS due to the thermal mass (heat capacity, mC_p) of the samples. The temperature profile of the materials in transient conduction condition (Eq. 7) is a function of thermal mass of the materials (mC_p). Increment in (mC_p) leads to absorption and storage more energy by the material during heating and release more energy during cooling process, resulting in delay for

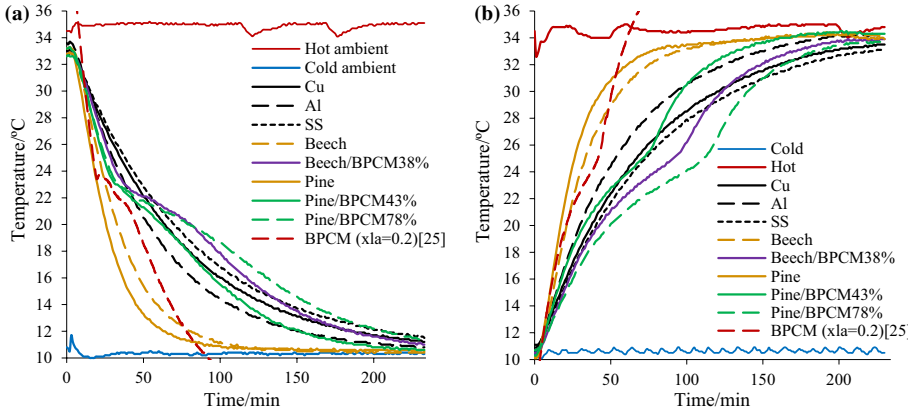

Fig. 9 T-history curves over cooling/heating cycle for **a** cooling and **b** heating

reaching the ambient temperature. Although pine and beech have comparable specific heat capacity, pine has less thermal mass than beech due to difference in density and thus, pine wood reached the ambient temperature faster. Despite high specific heat capacity of Al, its thermal mass was lower than that of Cu and SS, due to lower density.

Impregnation of BPCM into wood samples resulted in increase in thermal mass of the composite. Pine/BPCM at 43% MPG showed a thermal mass comparable to Al, and during the phase transition it performs as Cu and SS. For Beech/BPCM at 38% MPG, the thermal mass was found higher than pine composite with comparable retentions due to the higher thermal mass of beech. Beech/BPCM composite had even higher thermal mass than Cu and SS during the phase transition. Pine/BPCM at 78% MPG had highest mC_p and thus, able to absorb/release more energy.

Figure 10 shows the specific heat capacity for the tested samples calculated using Eq. 9 during cooling and heating processes. In this study, Cu was used as reference to calculate the overall heat transfer of the samples (Eq. 8), and then this parameter was used to calculate the specific heat capacity of other samples. Al and SS plates with known thermal characteristics were used to validate and approve the results. The measurements indicated that the specific heat capacity of Al and SS were 0.9 and 0.46 J g^{-1} K^{-1}, respectively, and were in line with the known properties of these materials (Table 2). As mentioned above, the heat capacity of wood is mainly temperature and moisture content dependent, while density and wood species has negligible effect

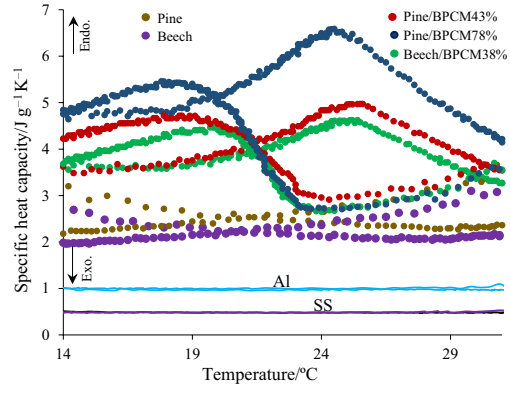

Fig. 10 Melting and freezing specific heat capacity for wood, composite samples, Al and SS

[38]. The measured heat capacity of wood at room temperature and moisture content of 12% was reported to be around 1.5–2 J g^{-1} K^{-1} [38]. In this study, the measured heat capacity of the untreated pine and beech samples were found to be ca. 2 J g^{-1} K^{-1}, similar to the reported results in the literature [38]. The results revealed that the incorporation of PCM into wood resulted in considerable improvement in specific heat capacity of the composite; the specific heat capacity increases proportionally to the content of the BPCM. The calculated heat capacity of beech/BPCM (38% MPG), pine/

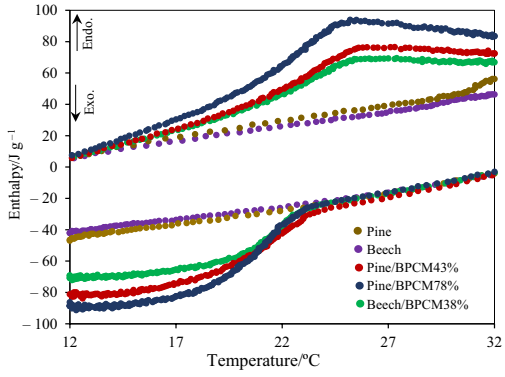

Fig. 11 Melting and freezing enthalpy for the samples

BPCM (43% MPG) and pine/BPCM (78% MPG) was ca. 3.8, 4.3 and 5 J g^{-1} K^{-1}, respectively.

Figure 11 shows the measured enthalpy for wood species and wood/BPCM composites during cooling and heating process. Untreated wood has no latent heat of fusion and the energy is stored as sensible heat during the heating, illustrated by a linear increase of enthalpy with temperature. Similar pattern was reported [10] where a dynamic heat flowmeter apparatus (DHFMA) was used to analyze heat storage capacity of wooden samples and it was found that during cooling, the untreated wood released the absorbed energy in a form of sensible heat identically to heating. The values obtained during cooling were negative indicating dissipation of energy to the ambient environment, while during heating the values were positive i.e., wood absorbed energy.

The wood/BPCM composites absorb and store heat in the form of latent heat during phase transition and in the form of sensible heat outside the transition region. The latent heat of pure BPCM is around 100 J g^{-1} [25], and it reduces to ca. 44 J g^{-1} for pine/BPCM composite of 78% MPG, and 30 J g^{-1} at 43% MPG, while this value for beech/BPCM at 38% MPG was ca. 30 J g^{-1}. The enthalpy values during cooling and heating process were found to be similar. The enthalpy of wood/PCM composite depends on the enthalpy of the PCM, whereby PCMs with higher enthalpy results in composite with additional enthalpy.

Thermal properties of tested samples with DSC, T-history and heat flow meter are tabulated in Table 3. Except some differences observed during the cooling, the results from DSC and T-history are in good agreement. T-history method used large samples that cooled down naturally in the chamber and thus, the results are more reliable [25] compared to the DSC where a limited amount of the sample was analyzed and the cooling rate affected the results.

Experimental uncertainty analysis

Experimental uncertainty associated with the thermal conductivity measurements by heat flow meter, specific heat capacity and enthalpy by T-history are introduced by the combination of the experimental errors, the calculations error and the accuracy of the measurement tools. In the current study, the overall errors were related to heat flux sensors, thermocouples, balance to measure mass of the samples, and the caliper to measure the dimensions of the samples. The uncertainty of the thermocouple is ± 0.1 °C, heat flux meter ± 0.001 W m^{-2}, balance and caliper are, respectively, 0.0000002 kg, and 0.00002 m. The uncertainty analysis was calculated using Kline and McClintock method [42]. The uncertainty was calculated using the Eq. (11).

$$U_{\mathrm{R}} = \left[\sum_{\mathrm{i}=1}^{\mathrm{n}} \left(\frac{\partial R}{\partial P_{\mathrm{i}}} \times U_{\mathrm{P_i}}\right)^2\right]^{\frac{1}{2}}, \; 1 \leq \mathrm{i} \leq n, \tag{11}$$

where R and P_{i} are dependent and independent variables, respectively. U_{R} and $U_{\mathrm{P_i}}$ are the uncertainties for the dependent and the independent variables, respectively. The non-dimensional form of Eq. (11) is $((\frac{U_{\mathrm{R}}}{R}) \times 100)$ which is in percentage [42–45]. The independent measured variables used to calculate the experimental uncertainties are summarized in Table 4.

Table 3 Thermal properties of the treated and untreated wood samples. DSC results within parentheses

Thermal properties	BPCM	Untreated woods		Impregnated samples		
		Pine	Beech	Pine/BPCM78%	Pine/BPCM43%	Beech/BPCM38%
Melting point (DSC) °C	25.5 (24.8)	–	–	25.1 (26.1)	25.4 (26.3)	25.7 (24.9)
Solidifying point (DSC) °C	21.7; 23.7 (18.5; 22)	–	–	22.7 (21.2; 16.53)	22.7 (18.9; 16)	22.5 (22.2; 17.4)
Melting enthalpy (DSC) J g^{-1}	104 (93)	–	–	44 (42.4)	32 (30.2)	30 (27)
solidifying enthalpy (DSC) J g^{-1}	24; 54 (92.8)	–	–	42 (40.4)	30 (29.1)	30 (26)
Specific heat capacity J g^{-1} K^{-1}	2; 5	2–3	2–3	2.7–4.8	3–4	2.9–3.9
Thermal conductivity W m^{-1} K^{-1}	0.2	0.12	0.23	0.16	0.13	0.255

Table 4 Measured variables, experimental uncertainties and specifications of the used equipment

Measured variable	Nomenclature	Nomenclature of uncertainty	Nominal value	Absolut uncertainty
Heat flux (mean value)	q/a	$U_{\frac{q}{a}}$	64 W m^{-2}	0.001 W m^{-2}
Mean ΔT in heat flow meter	T	U_{T}	3 °C	0.1 °C
Thickness of the samples	L	U_{L}	0.009 m	0.00002 m
Maximum $\left(T_{\mathrm{i}}-T_{\infty}\right)_{\mathrm{samp}}$ in T-history	T	U_{T}	23 °C	0.1 °C
Maximum $\left(T_{\mathrm{i}}-T_{\infty}\right)_{\mathrm{ref}}$ in T-history	T	U_{T}	23 °C	0.1 °C
Maximum $\left(T(t)_{\mathrm{n}}-T_{\infty}\right)_{\mathrm{samp}}$ in T-history	T	U_{T}	25 °C	0.1 °C
Maximum $\left(T(t)_{\mathrm{n}}-T_{\infty}\right)_{\mathrm{ref}}$ in T-history	T	U_{T}	25 °C	0.1 °C
Average mass of samples	m	U_{m}	0.05 kg	0.0000002 kg
Mass of reference	m	U_{m}	0.66 kg	0.0000002 kg

Thermal conductivity uncertainty calculation

Based on Eqs. 2 and 11, it is possible to calculate the uncertainties of thermal conductivity using the following Eq. 12:

$$U_{\lambda}=\left[\left(\frac{\partial\lambda}{\partial\frac{q}{a}}\times U_{\frac{q}{a}}\right)^{2}+\left(\frac{\partial\lambda}{\partial\Delta L}\times U_{\mathrm{L}}\right)^{2}+\left(\frac{\partial\lambda}{\partial\Delta T}\times U_{\mathrm{T}}\right)^{2}\right]^{1/2} \tag{12}$$

where, $U_{\frac{q}{A}}$, U_{L} and U_{T} are, respectively, the uncertainty for heat flux meter, caliper and thermocouple (Table 4). By applying some mathematical calculations, the Eq. 12, evolves into;

$$U_{\lambda}=\left[\left(\frac{\Delta\mathrm{L}}{\Delta T}\times U_{\frac{q}{a}}\right)^{2}+\left(\frac{q}{a\times\Delta T}\times U_{\mathrm{L}}\right)^{2}+\left(\frac{q\times\Delta\mathrm{L}}{a}\times\frac{1}{\Delta T^{2}}\times U_{\mathrm{T}}\right)^{2}\right]^{1/2} \tag{13}$$

$$\frac{U_{\lambda}}{\lambda}=\left[\left(\frac{U_{\frac{q}{a}}}{\frac{q}{a}}\right)^{2}+\left(\frac{U_{\mathrm{L}}}{\Delta L}\right)^{2}+\left(\frac{U_{\mathrm{T}}}{\Delta T}\right)^{2}\right]^{1/2} \tag{14}$$

By substituting the nominal and uncertainty values from Table 4, in Eq. 14, the normalized $\left(\left(\frac{U_{\mathrm{R}}}{R}\right)\times 100\right)$ uncertainty associated with the measuring instruments used to determine thermal conductivity was found to be 3.34%.

Enthalpy and C_p uncertainty calculation

Similar approach used for the calculation of the uncertainty associated with thermal conductivity was adopted to calculate the specific heat capacity and enthalpy uncertainties. For this, uncertainty of the heat capacity for reference (Cu) was assumed to be 0 and the nominal value was 0.385 J g^{-1} K^{-1}. Considering Eqs. 9 and 10 together with Eq. 11, the uncertainty for C_p and ΔH are expressed, respectively, as follow:

$$U_{c_{\mathrm{p}}}=\left[\left(\frac{\partial c_{\mathrm{p}}}{\partial m_{\mathrm{ref}}}\times U_{\mathrm{m}}\right)^{2}+\left(\frac{\partial c_{\mathrm{p}}}{\partial m_{\mathrm{samp}}}\times U_{\mathrm{m}}\right)^{2}+\left(\frac{\partial c_{\mathrm{p}}}{\partial\left(T(t)_{\mathrm{n}}-T_{\infty}\right)_{\mathrm{ref}}}\times U_{\mathrm{T}}\right)^{2}+\left(\frac{\partial c_{\mathrm{p}}}{\partial\left(T(t)_{\mathrm{n}}-T_{\infty}\right)_{\mathrm{samp}}}\times U_{\mathrm{T}}\right)^{2}+\left(\frac{\partial c_{\mathrm{p}}}{\partial\left(T_{\mathrm{i}}-T_{\infty}\right)_{\mathrm{ref}}}\times U_{\mathrm{T}}\right)^{2}+\left(\frac{\partial c_{\mathrm{p}}}{\partial\left(T_{\mathrm{i}}-T_{\infty}\right)_{\mathrm{samp}}}\times U_{\mathrm{T}}\right)^{2}\right]^{1/2} \tag{15}$$

$$U_{\Delta\mathrm{H}}=\left[\left(\frac{\partial\Delta H}{\partial c_{\mathrm{p,samp}}}\times U_{c_{\mathrm{p}}}\right)^{2}+\left(\frac{\partial\Delta H}{\partial\left(T(t)_{\mathrm{n,samp}}-T_{\mathrm{i}}\right)}\times U_{\mathrm{T}}\right)^{2}\right]^{1/2} \tag{16}$$

After mathematical operation, the following Eqs. 17 and 18 are obtained:

$$U_{c_p}=\left[\left(\frac{\ln\left[\frac{(T(t)_n-T_\infty)}{(T_i-T_\infty)}\right]_{ref}}{\ln\left[\frac{(T(t)_n-T_\infty)}{(T_i-T_\infty)}\right]_{samp}}\times\frac{1}{m_{samp}}\times C_{p,ref}\times U_m\right)^2+\left(\frac{\ln\left[\frac{(T(t)_n-T_\infty)}{(T_i-T_\infty)}\right]_{ref}}{\ln\left[\frac{(T(t)_n-T_\infty)}{(T_i-T_\infty)}\right]_{samp}}\times\frac{m_{ref}}{(m_{samp})^2}\times C_{p,ref}\times U_m\right)^2+\left(\frac{\frac{1}{(T(t)_n-T_\infty)_{ref}}}{\ln\left[\frac{(T(t)_n-T_\infty)}{(T_i-T_\infty)}\right]_{samp}}\times\frac{m_{ref}}{m_{samp}}\times C_{p,ref}\times U_T\right)^2+\left(\frac{\ln\left[\frac{(T(t)_n-T_\infty)}{(T_i-T_\infty)}\right]_{ref}}{\left(\ln\left[\frac{(T(t)_n-T_\infty)}{(T_i-T_\infty)}\right]_{samp}\right)^2}\times\frac{(-1)}{(T(t)_n-T_\infty)_{samp}}\times\frac{m_{ref}}{m_{samp}}\times C_{p,ref}\times U_T\right)^2+\left(\frac{\frac{-1}{(T_i-T_\infty)_{ref}}}{\ln\left[\frac{(T(t)_n-T_\infty)}{(T_i-T_\infty)}\right]_{samp}}\times\frac{m_{ref}}{m_{samp}}\times C_{p,ref}\times U_T\right)^2+\left(\frac{\ln\left[\frac{(T(t)_n-T_\infty)}{(T_i-T_\infty)}\right]_{ref}}{\left(\ln\left[\frac{(T(t)_n-T_\infty)}{(T_i-T_\infty)}\right]_{samp}\right)^2}\times\frac{1}{(T_i-T_\infty)_{samp}}\times\frac{m_{ref}}{m_{samp}}\times C_{p,ref}\times U_T\right)^2\right]^{1/2}\quad(17)$$

$$U_{\Delta H}=\left[\left(\left(T(t)_{n,samp}-T_i\right)\times U_{c_p}\right)^2+\left(c_{p,samp}\times U_T\right)^2\right]^{1/2}\quad(18)$$

The uncertainties for specific heat capacity and enthalpy in non-dimensional form are as:

$$\frac{U_{c_p}}{c_p}=\left[\left(\frac{U_m}{m_{ref}}\right)^2+\left(\frac{U_m}{m_{samp}}\right)^2+\left(\frac{U_T}{(T(t)_n-T_\infty)_{ref}\times\ln\left[\frac{(T(t)_n-T_\infty)}{(T_i-T_\infty)}\right]_{ref}}\right)^2+\left(\frac{-U_T}{(T(t)_n-T_\infty)_{samp}\times\ln\left[\frac{(T(t)_n-T_\infty)}{(T_i-T_\infty)}\right]_{samp}}\right)^2+\left(\frac{-U_T}{(T_i-T(t)_n)_{ref}\times\ln\left[\frac{(T(t)_n-T_\infty)}{(T_i-T_\infty)}\right]_{ref}}\right)^2+\left(\frac{U_T}{(T_i-T_\infty)_{samp}\times\ln\left[\frac{(T(t)_n-T_\infty)}{(T_i-T_\infty)}\right]_{samp}}\right)^2\right]^{1/2}\quad(19)$$

$$\frac{U_{\Delta H}}{\Delta H}=\left[\left(\frac{U_{c_p}}{c_p}\right)^2+\left(\frac{U_T}{(T(t)_{n,samp}-T_i)}\right)^2\right]^{1/2}\quad(20)$$

By replacing the variables in Eq. 17 with the values in Table 4, the heat cavity uncertainty (U_{c_p}) was found to be 0.48 J g^{-1} K^{-1}, which is needed later to calculate uncertainty of enthalpy. The normalized uncertainty ($\left(\frac{U_R}{R}\right)\times 100$) (Eq. 19) associated with the measuring instrument used to calculate heat capacity was found to be 9.6%. The normalized enthalpy uncertainty was then deducted using the calculated U_{c_p}., values in Table 4 and Eq. 20, found to be 9.7%.

Conclusions

Scots pine sapwood and beech wood impregnated with BPCM proved to be composites with enhanced thermal mass with a potential for building applications. The important findings of the study are summarized as follow:

- Wood is a suitable material for "encapsulation" of PCM since it is easy to impregnate at controllable MPG by a combination of vacuum and pressure. Leaching of BPCM is a problem that could not be solved in the present study. Leaching test showed that pine and beech samples leached 8–9% of the impregnated BPCM after 24 h at 35 °C. However, the tested BPCM leached significantly less than PEG 600.
- Rays which are radial anatomical elements in both pine and beech wood served as pathways for impregnation of the BPCM. Part of the tracheid lumens (pine) and vessels (beech) were filled with BPCM which was also found as a precipitate on the cell wall. There is an indication that part of the BPCM can be impregnated in the wood cell wall.
- Thermal conductivity measurement with heat flowmeter method showed that the thermal conductivity of beech is twice as high as that of pine due to its high density. The results showed that, the thermal conductivity of the composites improved after impregnation depending on the MPG of the BPCM.
- DSC results showed that the latent heat of the composites depends on the latent heat of BPCM, by increasing the impregnation retention the latent heat of the composite increases. The phase transition temperatures slightly differed from those of BPCM.
- The thermal mass and heat capacity of the wood/BPCM composites was increased compared with the untreated wood. The untreated wood store/release energy as a sensible heat, while after impregnation the composites can store/release energy in forms of sensible heat before and after phase transition and as a latent heat during the phase transition.

Acknowledgements The study has been carried out within the framework of Smart Energy Systems Research and Innovation Program (ERA-Net E2B2) in the project "Bio-Based Phase Change Materials Integrated into Lignocellulose Matrix for Energy Store in Buildings (BIO-NRG-STORE)". The authors thank also the financial support by

the Swedish Research Council for Sustainable Development (FORMAS), project number 2017-00686.

Funding Open access funding provided by Swedish University of Agricultural Sciences.

References

1. Ramage MH, Burridge H, Busse-Wicher M, Fereday G, Reynolds T, Shah DU, Wu G, Yu L, Fleming P, Densley-Tingley D, Allwood J. The wood from the trees: the use of timber in construction. Renew Sustain Energy Rev. 2017;68:333–59.
2. Hepburn C, Adlen E, Beddington J, Carter EA, Fuss S, Mac Dowell N, Minx JC, Smith P, Williams CK. The technological and economic prospects for CO 2 utilization and removal. Nature. 2019;575(7781):87–97.
3. Amiri A, Ottelin J, Sorvari J, Junnila S. Cities as carbon sinks—classification of wooden buildings. Environ Res Lett. 2020;15(9):094076.
4. Omer MA, Noguchi T. A conceptual framework for understanding the contribution of building materials in the achievement of sustainable development goals (SDGs). Sustain Cities Soc. 2020;52:101869.
5. Toppinen A, Röhr A, Pätäri S, Lähtinen K, Toivonen R. The future of wooden multistory construction in the forest bioeconomy–a Delphi study from Finland and Sweden. J For Econ. 2018;31:3–10.
6. Wen B, Musa SN, Onn CC, Ramesh S, Liang L, Wang W, Ma K. The role and contribution of green buildings on sustainable development goals. Build Environ. 2020;185:107091.
7. Falk RH. Wood as a sustainable building material. For Prod J. 2009;59(9):6–12.
8. Song S, Leng H, Xu H, Guo R, Zhao Y. Impact of urban morphology and climate on heating energy consumption of buildings in severe cold regions. Int J Environ Res Public Health. 2020;17(22):8354.
9. Nazari M, Jebrane M, Terziev N. Bio-based phase change materials incorporated in lignocellulose matrix for energy storage in buildings—a review. Energies. 2020;13(12):3065.
10. Mathis D, Blanchet P, Landry V, Lagière P. Impregnation of wood with microencapsulated bio-based phase change materials for high thermal mass engineered wood flooring. Appl Sci. 2020;8(12):2696.
11. Khudhair AM, Farid MM. A review on energy conservation in building applications with thermal storage by latent heat using phase change materials. Energy Convers Manage. 2004;45:263–75.
12. De Gracia A, Navarro L, Castell A, Ruiz-Pardo A, Alvárez S, Cabeza LF. Experimental study of a ventilated facade with PCM during winter period. Energy Build. 2013;58:324–32.
13. Chen F, Kessel A, Wolcott M. A novel energy saving wood product with PCM. In: Proceedings of 55th International Convention of Society of Wood Science & Technology, Bejing, China. 2012
14. Li J, Xue P, Ding W, Han J, Guolin S. Micro-encapsulated paraffin/high-density polyethylene/wood flour composite as form-stable phase change material for thermal energy storage. Sol Energy Mater Sol Cells. 2009;93:1761–7.
15. Hu L, Lyu S, Fu F, Huang J, Wang S. Preparation and properties of multifunctional thermochromic energy-storage wood materials. J Mat Sci. 2016;51:2716–26.
16. Hui B, Li Y, Huang Q, Li G, Li J, Cai L, Yu H. Fabrication of smart coatings based on wood substrates with photoresponsive behavior and hydrophobic performance. Mater Des. 2015;84:277–84.
17. Zerriaa A, Ganaoui MEL, Gerardin C, Tazibt A, Gabsi S. Physical incorporation of particles in a porous media: a path to a smart wood. Eur Phys J Appl Phys. 2016. https://doi.org/10.1051/epjap/2015150458.
18. Jiang L, Liu Z, Yuan Y, Wang Y, Lei J, Zhou C. Fabrication and characterization of fatty acid/wood-flour composites as novel form-stable phase change materials for thermal energy storage. Energy Build. 2018;171:88–99.
19. Ma L, Guo C, Ou R, Sun L, Wang Q, Li L. Preparation and characterization of modified porous wood flour/lauric-myristic acid eutectic mixture as a form-stable phase change material. Energy Fuels. 2018;32:5453–61.
20. Guo X, Zhang L, Cao J, Peng Y. Paraffin/wood flour/high-density polyethylene composites for thermal energy storage material in buildings: a morphology, thermal performance, and mechanical property study. Polym Compos. 2018;39:E1643–52.
21. Ma L, Wang Q, Li L. Delignified wood/capric acid-palmitic acid mixture stable-form phase change material for thermal storage. Sol Energy Mater Sol Cells. 2019;194:215–21.
22. Cheng L, Feng J. Form-stable phase change materials based on delignified wood flour for thermal management of buildings. Compos A. 2020;129:105690.
23. Barreneche C, Vecstaudza J, Bajare D, Fernandez AI. PCM/wood composite to store thermal energy in passive building envelopes. IMST IOP Conf Ser Mater Sci Eng. 2017;251:012111.
24. Temiz A, Hekimoglu G, Demirel GK, Sarı A, Amini MHM. Phase change material impregnated wood for passive thermal management of timber buildings. Int J Energy Res. 2020;44(13):10495–505. https://doi.org/10.1002/er.5679.
25. Nazari M, Jebrane M, Terziev N. Multicomponent bio-based fatty acids system as phase change material for low temperature energy storage. J Energy Storage. 2021;39:102645.
26. Adams CWM, Abdulla YH, Bayliss OB. Osmium tetroxide as a histochemical and histological reagent. Histochemie. 1967;9:68–77.
27. Meng X, Gao Y, Wang Y, Yan B, Zhang W, Long E. Feasibility experiment on the simple hot box-heat flow meter method and the optimization based on simulation reproduction. Appl Therm Eng. 2015;83:48–56.
28. Soares N, Martins C, Gonçalves M, Santos P, da Silva LS, Costa JJ. Laboratory and in-situ non-destructive methods to evaluate the thermal transmittance and behavior of walls, windows, and construction elements with innovative materials: a review. Energy Build. 2019;182:88–110.
29. Younsi Z, Joulin A, Zalewski L, Lassue S, Rousse D. Thermophysical characterization of phase change materials with heatflux sensors. In: Proceedings of Eurotherm, 5th European Thermal-Sciences Conference, Eindhoven, The Netherlands. 2008. ISBN 978-90-386-1274-4.

30. Badenhorst H, Cabeza LF. Critical analysis of the T-history method: a fundamental approach. Thermochim Acta. 2017;650:95–105.
31. Solé A, Miró L, Barreneche C, Martorell I, Cabeza LF. Review of the T-history method to determine thermophysical properties of phase change materials (PCM). Renew Sust Energ Rev. 2013;26:425–36.
32. Nazir H, Batool M, Osorio FJB, Ruiz MI, Xu X, Vignarooban K, Phelan P, Kannan AM. Recent developments in phase change materials for energy storage applications: a review. Int J Heat Mass Transf. 2019;129:491–523.
33. Prajapati DG, Kandasubramanian B. Biodegradable polymeric solid framework-based organic phase-change materials for thermal energy storage. Ind Eng Chem Res. 2019;58:10652–77.
34. Liang J, Zhimeng L, Ye Y, Yanjun W, Jingxin L, Changlin Z. Fabrication and characterization of fatty acid/wood-four composites as novel form-stable phase change materials for thermal energy storage. Energy Build. 2018;171:88–99.
35. Jamekhorshid A, Sadrameli SM, Barzin R, Farid MM. Composite of wood-plastic and micro-encapsulated phase change material (MEPCM) used for thermal energy storage. Appl Therm Eng. 2017;112:82–8.
36. Sari A, Alkan C, Karaipekli A, Onal A. Preparation, characterization and thermal properties of styrene maleic anhydride copolymer (SMA)/fatty acid composites as form stable phase change materials. Energy Convers Manage. 2008;49:373–80.
37. Joulin A, Younsi Z, Zalewski L, Lassue S, Rousse DR, Cavrot JP. Experimental and numerical investigation of a phase change material: thermal-energy storage and release. Appl Energy. 2011;88:2454–62.
38. Simpson W, TenWolde A. Physical properties and moisture relations of wood. In: Wood handbook: wood as an engineering material. General technical report FPL-GTR-113. Madison: USDA Forest Service, Forest Products Laboratory; 1999. p. 3.1-3.24.
39. Czajkowski L, Olek W, Weres J. Effects of heat treatment on thermal properties of European beech wood. Eur J Wood Wood Prod. 2020;78:425–31.
40. Yang H, Wang Y, Yu Q, Cao G, Sun X, Yang R, Zhang Q, Liu F, Di X, Li J, Wang C, Li G. Low-cost, three-dimension, high thermal conductivity, carbonized wood-based composite phase change materials for thermal energy storage. Energy. 2018;159:929–36.
41. Yang H, Wang Y, Yu Q, Cao G, Yang R, Ke J, Di X, Liu F, Zhang W, Wang C. Composite phase change materials with good reversible thermochromic ability in delignified wood substrate for thermal energy storage. Appl Energy. 2018;212:455–64.
42. Kline SJ, McClintock F. Describing uncertainties in single-sample experiment. Mech Eng. 1953;75:3–8.
43. Nazari M, Vahid DJ, Saray RK, Mahmoudi Y. Experimental investigation of heat transfer and second law analysis in a pebble bed channel with internal heat generation. Int J Heat Mass Transf. 2017;114:688–702.
44. Moffat RJ. Describing the uncertainties in experimental results. Exp Therm Fluid Sci. 1988;1(1):3–17.
45. Coleman HW, Steele WG. Experimentation, validation, and uncertainty analysis for engineers. 3rd ed. Hoboken: Wiley; 2009.

IV

Received: 1 February 2022 | Revised: 13 March 2022 | Accepted: 30 March 2022

DOI: 10.1002/est2.340

RESEARCH ARTICLE

ENERGY STORAGE WILEY

Thermal performance and mold discoloration of thermally modified wood containing bio-based phase change material for heat storage

Meysam Nazari | **Mohamed Jebrane** | **Jie Gao** | **Nasko Terziev**

Department of Forest Biomaterials and Technology, Swedish University of Agricultural Sciences, Uppsala, Sweden

Correspondence
Mohamed Jebrane, Department of Forest Biomaterials and Technology, Swedish University of Agricultural Sciences, Vallvägen 9C, 750 07 Uppsala, Sweden.
Email: mohamed.jebrane@slu.se

Funding information
Swedish Research Council for Sustainable Development (FORMAS)

Abstract

The work presents the results of thermal performance and mold discoloration of thermally modified wood-based composites incorporating multicomponent fatty acids as a bio-based phase change materials (BPCM). Thermally modified Scots pine (TMP), beech (TMB), and spruce (TMS) sapwood were impregnated with a multicomponent mixture of linoleic acid and coconut oil fatty acids at a ratio of 20:80. Samples with different BPCM uptakes were analyzed in the temperature range typical for building indoor conditions. Leakage tests were conducted and revealed that the maximum leakage for all the samples is 3% to 5%. T-history and heat flowmeter methods were used to evaluate the thermal characteristic of the composites. The incorporation of BPCM into thermally modified woods (TMWs) resulted in significant thermal mass improvements, expressed by the ability of the composites to store excessive energy in terms of latent heat and keep the temperature constant for long time. The specific heat capacity of the TMWs was around 2 J/g K, which increased to 4 to 8 J/g K after impregnation with BPCM, depending on the impregnation uptake. Results showed also that TMB has higher thermal conductivity than TMP and TMS, while incorporating of BPCM into these materials resulted in even improved thermal conductivity. Results showed that the thermal conductivity of TMP increased after incorporation of BPCM from 0.06 W/m K to 0.1 and 0.14 W/m K for TMP/BPCM with 48% and 95% uptake respectively. Mold tests showed that BPCM encapsulated in TMWs is less susceptible to mold discoloration compared to untreated wood.

KEYWORDS

bio-based PCMs, energy storage, mold discoloration, thermal properties, thermally modified wood

Abbreviations: BPCM, Bio-based phase change material; CoFA, Coconut oil fatty acid; LA, Linoleic acid; PCM, Phase change material; TMB, Thermally modified beech; TMP, Thermally modified pine; TMS, Thermally modified spruce; TMW, Thermally modified wood; WPG, Weight percentage gain.

1 | INTRODUCTION

Bio-based materials from renewable sources become an inevitable part of the future technologies for human living environment, in particular in building and construction applications. Therefore, use of timber and other wood-based materials has experienced growth during the last decade in single and multi-floor buildings, due to the high ratio of strength to density, thus bringing renewability, sustainability, and climate benefits.[1-5]

Due to its chemical composition and anatomical structure, wood is sensitive to moisture and a nutrient for the microorganisms.[6] In addition, wood's moderate specific heat capacity and low density predetermine its low thermal mass, which limits its ability to respond to the temperature fluctuation and energy intermittency in buildings.[7] Furthermore, many commercially used wood species (eg, spruce) posses low permeability making it difficult for applications where an impregnation is needed.

A common industrial approach to improve the dimensional stability and durability of wood is thermal modification, whereby the wood is heated up in the range of 180°C to 215°C for a defined period of time in a medium without oxygen.[8] As a result, hemicelluloses are thermally degraded while cellulose and lignin are modified to high-molecular structures to reduce the hygroscopicity and improve the dimensional stability of wood.

The thermal mass of wood can be improved by incorporation of phase change materials (PCMs) into its porous structure. Wood in various forms (fibers, flour, solid wood, veneer) is a cheap bio-container that can naturally be integrated with based phase change materials (BPCMs)[9] and used as a building material with heat storage function. The composite material of wood and BPCMs can be incorporated in the internal walls,[10] flooring[7] or in the façades of the buildings.[11] A series of recently published studies investigated the importance of BPCMs, mainly fatty acids and their eutectic mixtures, for different applications in construction and building sectors and reported a promising thermal and chemical properties with appropriate working temperature, latent heat, and chemical stability.[12-14]

Wood impregnated with PCMs can be used in internal and external joineries to enhance the thermal mass of the building, control temperature fluctuations, and improve the thermal comfort in residential buildings.[9] As energy savings become an inevitable part of modern building, synergy between BPCM and wood comprises various options, for example, wood flour,[15,16] wood fibers,[17] and surface treatment of solid wood and wood composites[18-20] to host the BPCMs. Wood-BPCM composites working at temperatures of 18°C to 25°C can absorb extra heat and release it when the temperature decreases under a given comfort value to ensure more efficiently use of heat energy.

Studies regarding wood/PCM composites are concentrating on wood flour, solid or delignified wood. Examples are fatty acids or their mixtures impregnated in wood flour[21,22] or paraffin blended with poplar wood flour and graphite[23] to achieve latent heat capacity of 26.8 J/g. Recently, delignified wood has been studied intensively, for example, an eutectic mixture of capric-palmitic acids impregnated into delignified wood[24] with a retention of 61.2% demonstrated no leakage, a phase transition temperature of 23.4°C and latent heat of 94.4 J/g with good thermal stability. Another study[25] used delignified wood as an encapsulating material for impregnation of PCM claiming increased pore volume compared to the initial material. However, the approach of using delignified wood is debatable since lignin, having best thermal conductivity of the three structural polymers in wood, has been extracted.

Solid wood of alder[26] with 29.9 wt% retention of paraffin and coated with polystyrene to prevent leakage of the PCMs showed a latent heat value of 20.62 J/g. Temiz et al.[27] studied Scots pine sapwood impregnated with a eutectic mixture of capric acid (CA) and stearic acid (SA). After thermal characterization of the material, it was concluded that the system wood/CA-SA can be used for indoor temperature regulation and energy saving in timber constructions. Solid wood as a container for BPCM is particularly suitable for flooring. Placed directly above the source of heat, the engineered wood-BPCM floor can undergo many heating/cooling phases and thus, ensures significant gain of latent heat. In a study, Mathis et al.[7] engineered a thin upper layer of wood flooring for absorbing and storing solar energy at a temperature of 30°C. Oak and sugar maple wood impregnated with a commercial microencapsulated BPCM (Nextek29) demonstrated a latent heat of 7.6 J/g for the composite with 77% improvement in thermal mass compared to the untreated wood.

The above research ideas still have to cope with the inherited disadvantages of wood namely, moderate heat capacity and low thermal mass and thus, low ability to absorb and store thermal energy, low thermal conductivity, dimensional instability and bio-degradability. The above features of wood are of importance when BPCM are impregnated in the wood structure for heat storage in buildings. An example is the gap in the knowledge about mold growth on the wood and wood composites containing organic PCM with no findings in the literatures. Eventual mold growth and release of mycotoxins can affect the human health[28] which proves the need and importance of material testing.

Although widely used for external claddings of buildings, thermally modified wood has not been studied with regard to its ability to encapsulate BPCMs for heat storage. The present study focuses on thermally modified solid wood of Scots pine, spruce (softwoods) and beech (hardwood) as a container for BPCMs. A special emphasis has been set on the impregnability and leachability of the thermally modified woods (TMWs) and susceptibility to mold discoloration. The aim of the study is to reveal the thermal characteristics of the thermally treated wood-BPCM composite by using T-history and heat flow meter method and to investigate the feasibility of the TMW for encapsulation of the BPCM for building applications.

2 | EXPERIMENTAL

2.1 | Materials

A BPCM composed of coconut oil fatty acids (CoFA) and linoleic acid (LA) mixed in a ratio of 80:20[29] was used through the study. TMW samples (thermo-vacuum modification at 210°C) of Scots pine (*Pinus sylvestris* L.) (TMP) sapwood, beech (*Fagus sylvatica* L.) (TMB) and spruce (*Picea abies* Karst.) (TMS) with dimensions of $9 \times 90 \times 90$ mm along the grain and without visible defects were used throughout the study.

2.2 | Methods

2.2.1 | Incorporation of BPCM into TMWs and leaching test

The thermally modified samples were impregnated in an autoclave at temperature of 60°C to ensure melting and penetration of the BPCM in a vacuum-pressure process. Before the impregnation, the samples were conditioned for 2 weeks at 23°C and 70% relative humidity. Two impregnation schedules were employed; high weight percentage gain (WPG) was achieved by immersing the samples in BPCM and applying a vacuum of 350 mbar for 10 min followed by 6 bar pressure for 1 h. Low WPG was achieved when a pre-pressure of 0.75 bars for 60 min was applied instead of vacuum step. Wood density, impregnation parameters and the average WPG are shown in Table 1.

The WPG was calculated as the difference between the initial (m_i) and final weight (m_f) of the wood sample and expressed in percent (Equation 1).[26]

$$\mathrm{WPG}\,(\%) = \frac{(m_f - m_i)}{m_i} \times 100 \tag{1}$$

After the impregnation, the samples were conditioned in a cold room (10°C) for 3 weeks and the weight was recorded prior to the leaching tests. To assess the leaching rate of the BPCM, each impregnated sample was placed between two other untreated spruce and oak samples with identical dimensions. The 3-layer set was pressed by a mass of 1 kg and placed in a climate chamber at 35°C for 24 h. The cumulative leached amount of BPCM was calculated as a difference between the weight of the sample after 8, 16, and 24 h and related to the initial weight and expressed in percent (likewise Equation 1).

2.2.2 | Thermal conductivity of TMWs/BPMC composites by heat flow meter method

The thermal conductivity of the samples was measured according to standards ASTM C1155-95 (2013) and ISO 9869-1:2014, known as heat flow meter method with some modifications.[30,31] The set-up is schematically depicted in Figure 1. An insulated box was used to minimize the heat loss from the samples' sides. In addition,

TABLE 1 Wood density, impregnation parameters, and average weight percentage gain (WPG)

Wood species	Density, kg/m^3	Duration and vacuum depth	Duration, pre-pressure	Pressure	Average WPG, %
TMP	500 (88)	-	60 min 0.75 bar	-	48 (low)
		10 min 80%	-	60 min 6 bar	95 (high)
TMB	643 (53)	10 min 80%	-	60 min 6 bar	47
TMS	460 (57)	10 min 80%	-	60 min 6 bar	62

Note: Number of tested samples per treatment were 4, SD in parenthesis.

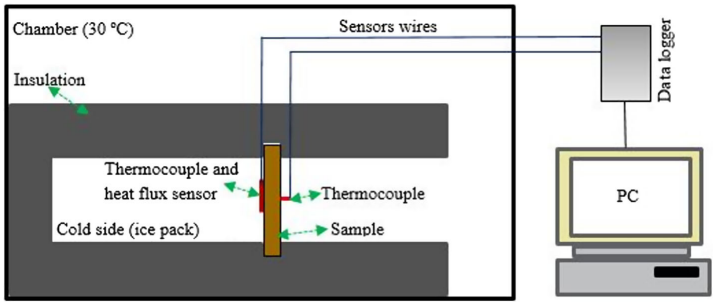

FIGURE 1 Schematic diagram of the designed rig for thermal conductivity

the samples were 10 times larger (90 mm) than the thickness (9 mm) to guarantee a low heat loss from other directions. Two thermocouples of K- and T-type were used to measure the temperature at the both surfaces of the sample. To avoid the effect of the surrounding environment on the measurements, the noncontact surface of the thermocouples were insulated. A heat flux meter type FHF03 supplied from Hukseflux, the Netherlands was used at the surface exposed to cold environment. Each measurement was run for 3 h to ensure a steady state process[32] and the experiment was repeated four times for reproducibility. After measuring the heat flux and the temperatures at both surfaces of the samples, the thermal conductivity was calculated by applying Fourier's law of thermal conduction[32]:

$$\lambda = \frac{q}{a} \cdot \frac{\Delta L}{\Delta T} \tag{2}$$

where $\frac{q}{a}$ is the heat flux, ΔL is the thickness, and ΔT is temperature difference.

2.2.3 | T-history, specific heat capacity, and enthalpy

T-history method was used to measure thermal properties of several samples simultaneously[33-35] including melting/freezing point, latent heat of fusion, degree of super cooling and specific heat capacity. Unimpregnated TMWs sample, TMW impregnated with BPCM (TMWs/BPCM composite), and a copper (Cu) plate as reference with identical dimensions were tested simultaneously. The copper plate was used as main reference to obtain overall heat transfer coefficient (u). This parameter was then used to calculate the thermal properties of the other samples. The samples and reference were thermally insulated using 10 mm thickness ARMAFLEX insulation material. K-type thermocouples were used to record temperature changes over time for samples and references. The thermocouples were placed at the centerline and in the middle of the samples. For cold and hot ambient climate, two chambers were employed, the former used for cold ambient climate fixed at 10°C, while the latter chamber was used for hot ambient climate set at 35°C. The chamber's temperatures were recorded with two separate thermocouples. Thermal and physical properties of the reference is summarized in Table 2. Samples and reference were first preheated at 35°C, and then quickly transferred into the chamber at 10°C and the temperature profile was recorded. Once the equilibrium temperature was reached (ca. 3 h), the samples and the references were transferred back at 35°C and the temperature changes were recorded.

TABLE 2 Thermal and physical properties of references

	Copper (SS 5011-04)
Weight (g)	657.6
Dimension (mm)	9 × 90 × 90
Thermal conductivity (W/m K)	395
Specific heat capacity (J/g K)	0.385

Energy balance for the reference was employed to obtain the overall heat transfer coefficient. Since the wooden samples and the metal reference have identical dimensions and insulation for uniform heat transfer conditions, the overall heat transfer coefficient (u) for both reference and wood samples were considered identical. The amount of heat transferred to/from samples in the chamber is expressed as follow[33]:

$$Q = uA\left(T(t)_n - \mathrm{T}_\infty\right) \tag{3}$$

where Q, u, A, $T(t)_n$, and T_∞ are respectively the transferred heat, overall heat transfer coefficient, heat transfer area, sample temperature at each time point and ambient temperature inside oven/chamber.

The amount of heat stored/released from samples is:

$$Q = mC_p \frac{d\left(T_i - T(t)_n\right)}{dt} \tag{4}$$

where m, C_p, T_i, and dt are respectively the mass of the samples, specific heat capacity, initial temperature, and time interval.

The amount of transferred energy to/from the samples is stored/released in/from the samples, then the energy balance is:

$$Q = -uA\left(T(t)_n - T_\infty\right) = mC_p \frac{d\left(T(t)_n - T_i\right)}{dt} \tag{5}$$

By rearrangement and integration, the temperature distribution for the reference and wood samples are obtained as:

$$\int_{T_i}^{T_n} \frac{d\left(T(t)_n - T_\infty\right)}{\left(T(t)_n - T_\infty\right)} = -\int_0^{t_n} \frac{uA}{mC_p} dt \tag{6}$$

After mathematical operation:

$$\ln\left[\frac{\left(T(t)_n - T_\infty\right)}{\left(T_i - T_\infty\right)}\right] = -\frac{uA}{mC_p} t_n \tag{7}$$

As the thermo-physical properties of the reference is known, the overall heat transfer coefficient (u) is calculated using energy balance for the reference:

$$uA = -\frac{\ln\left[\frac{\left(T(t)_n - T_\infty\right)}{\left(T_i - T_\infty\right)}\right]_{ref}}{t_n} m_{ref} C_{p,ref} \tag{8}$$

uA is calculated by the energy balance for the reference according to Equation (8), and as heat transfer area and conditions around reference and wood samples are identical, uA was calculated from the energy balance of the reference and used further to calculate C_p for the wood samples. After substitution Equation (8) in Equation (7), C_p of the samples is calculated as:

$$C_{p,samp} = \frac{\ln\left[\frac{\left(T(t)_n - T_\infty\right)}{\left(T_i - \infty\right)}\right]_{ref}}{\ln\left[\frac{\left(T(t)_n - T_\infty\right)}{\left(T_i - \infty\right)}\right]_{samp}} \frac{m_{ref}}{m_{samp}} C_{p,ref} \tag{9}$$

Enthalpy of the samples is obtained as[29]:

$$\Delta H = c_{p,samp}\left(T(t)_{n,samp} - T_{samp,i}\right) \tag{10}$$

where ΔH is enthalpy change from initial point to each time point n.

2.2.4 | Susceptibility of the materials to mold discoloration

The susceptibility of the TM wood/BPCM composites to mold growth and discoloration was tested according to the American Wood Protection Association Standard E24-06 (2015). Three mold fungi (*Aureobasidium pullulans* [d. By.] Arnaud, *Aspergillus niger* v. Tiegh and *Penicillium brevicompactum* Dierckx) were chosen and grown on 2.5% malt extract agar for 3 weeks. A mixed mold spore suspension was then prepared and inoculated on the sterilized soil in a plastic chamber. After inoculation, the chamber was incubated in a climate room at 20°C for 2 weeks. Afterwards, untreated, thermally modified and thermally modified impregnated samples with BPCM of Scots pine, spruce and beech were pit inside the chamber hanging approximately 5 cm above the soil. The climate in the chamber was maintained at 25°C and a relative humidity higher than 95%. After 2, 4, 6, and 8 weeks of exposure, the mold growth on the sample surfaces (90 × 90 mm) was classified by visual examination (Table 3) according to a scale from 0 (no visible growth) to 5 (very abundant growth, 100% coverage).

3 | RESULTS AND DISCUSSIONS

3.1 | Impregnation and leaching

Under the used impregnation schedules, WPG of 95% and 48% were targeted and achieved for the TMP samples, while a maximum of 47% WPG was possible for TMB (Table 1). This is due to the higher density of TMB than pine, which is in line with the findings in Nazari et al.[33] where the highest possible uptake for untreated beech was 43%. The effect of thermal modification on wood induces degradation of hemicelluloses, thus making the wood cell wall more porous and consequently easier to penetrate by liquids and gases. An example of the above effect is the improved permeability of TMS, where the refractory wood species spruce demonstrated 62% uptake of the BPCM.

Any BPCM is susceptible to leakage when integrated into buildings envelopes, which limits the application in buildings. Although suitable for encapsulation of BPCMs, the lignocellulose in any form can hardly prevent the leakage during exploitation.[36] The leaching test showed 4% and 3% loss of the BPCM for the TMP with 95% and

Wood species and treatments	2 weeks	4 weeks	6 weeks	8 weeks
Scots pine	2	3	4	4
TMP	0	0	1	1
TMP/BPCM 48%	1	1	2	2
TMP/BPCM 95%	1	2	3	4
Spruce	2	3	3	3
TMS	0	0	0	1
TMS/BPCM 62%	0	1	1	1
Beech	4	5	5	5
TMB	1	1	2	2
TMB/BPCM 47%	2	2	3	4

TABLE 3 Ratings of mold growth and discoloration on untreated, thermally modified and thermally modified samples impregnated with BPCM (0 - no visible growth; 1 - covering up to 10% of surface; 2 - covering between 10% and 30%; 3 - covering between 30% and 70%; 4 - more than 70% of surface; 5 - 100% coverage)

48% WPG respectively. The values for the TMS and TMB were 4% and 5%. The study confirmed the positive effect of thermal modification on the permeability and restrain of leaching from wood were compared to untreated woods reported in Nazari et al.[33] It can be concluded that the cell wall has increased ability to accommodate and retain BPCM after thermal modification.

3.2 | Thermal conductivity measurement with heat flow meter

Thermal conductivity measurements showed that TMB has higher thermal conductivity compared to TMP and TMS. Prior to the impregnation of the BPCM, the thermal conductivity of the TMB, TMS, and TMP were 0.11, 0.07, and 0.06 W/m K respectively. The thermal conductivity varies between wood species and depends upon density and moisture content.[37] The thermal conductivity of untreated spruce and pine was reported to be in the range of 0.11 to 0.12 W/m K at 12% moisture content, while the value of untreated beech were in the range 0.18 to 0.21 W/m K.[37,38] In addition, the study reported a reduction in thermal conductivity both in radially and tangentially directions after thermal modification as a results of lower density and moisture content. This corroborates our results, which are in line with the reported data.[38]

Once impregnated with BPCM, all composites experienced improvement in thermal conductivity due to the PCM thermal conductivity (0.2 W/m K[29]) which is higher than that of TMWs. The results showed that TMP/BPCM composites with 48% and 95% impregnation uptake (after leaching) had thermal conductivity of 0.1 and 0.14 W/m K, respectively. A value of 0.12 W/m K was measured for TMS/BPCM with 62% BPCM uptake and 0.13 W/m K for TMB/BPCM with 47% uptake. The results showed that the increase of the BPCM uptake in wood increases the conductivity of the composite.

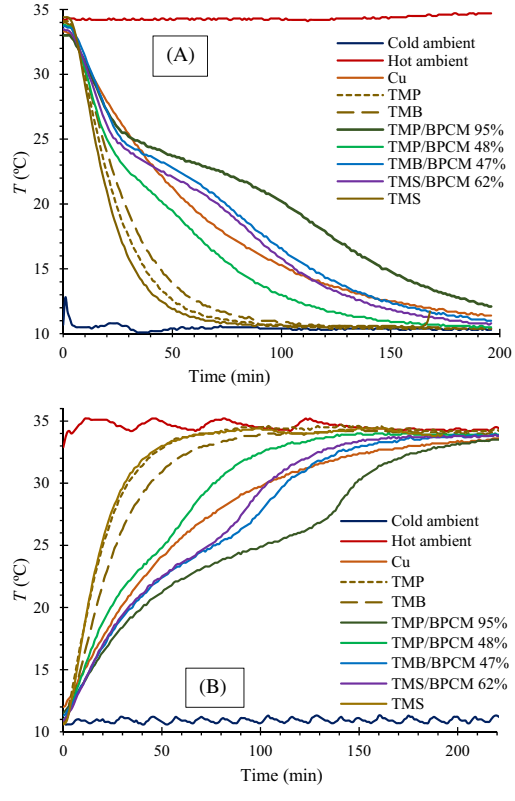

FIGURE 2 T-history curves over cooling/heating cycle for (A) cooling and (B) heating

3.3 | Thermal analysis by T-history

Figure 2 shows the T-history profile for the samples and the reference (Cu) during the cooling (2a) and heating

process (2b). The measured ambient temperatures were constant throughout the experiments with ±0.8°C maximum deviation. Once placed in the climate chamber at 10°C, the samples and the reference's temperatures decrease gradually from the starting temperature at 35°C and continues to decease with the time until it reaches the chamber's ambient temperature (10°C). During the course of cooling cycles, a phase change transition was observed for all the TMW/BPCM composites at temperature around 24°C, and the BPCM inside the composites fully solidified at temperature around 22°C. In addition, the BPCM inside TMW/BPCM composites solidifies congruently.

During the cooling and heating processes (Figure 2), thermally modified samples without BPCM reached the equilibrium faster than the samples impregnated with BPCM. This is due to the increment in thermal mass (heat capacity, mC_p) of the composites compared to non-impregnated samples. The temperature profile of the materials in transient conduction condition (Equation 7) is a function of thermal mass of the materials (mC_p). Increment in (mC_p) leads to absorption and storage of more energy by the material during heating and release more energy during cooling process, resulting in delay for reaching the ambient temperature.

The results shows that the amount of BPCM inside the composites defines the thermal mass of the composite when the TMW has comparable density, which is the case for TMS and TMP samples. It can be seen that TMP with 95% uptake has the highest thermal mass, TMP with 48% uptake has the lowest, while TMS with 62% is in the middle. TMB has higher density compared to TMP and TMS leading to comparable thermal mass to TMS with 62% uptake, although TMB has lower uptake (47%).

Figure 3 illustrates the specific heat capacity for the tested samples calculated using Equation (9) during cooling and heating processes. Specific heat capacity of wood is temperature and moisture content dependent, and the wood species and density has no effect on specific heat capacity.[37] The measured specific heat capacity of TMWs without BPCM is around 2 J/g K which is in line with the reported data in the literature.[37] After impregnated with BPCM, considerable improvements of specific heat capacity were observed, moreover the BPCM retention seems to have an effect of the specific heat capacity although it is not much clear.

Figure 4 shows the calculated enthalpy for TMWs and TMWs/BPCM composites during cooling and heating processes. The TMWs before impregnation followed a linear trend showing that they only store and release energy in terms of sensible heat during heating and cooling processes respectively. While, TMWs/BPCM composites can absorb energy in terms of latent heat during the phase transition from solid to liquid (heating process), and release it during cooling process. In addition,

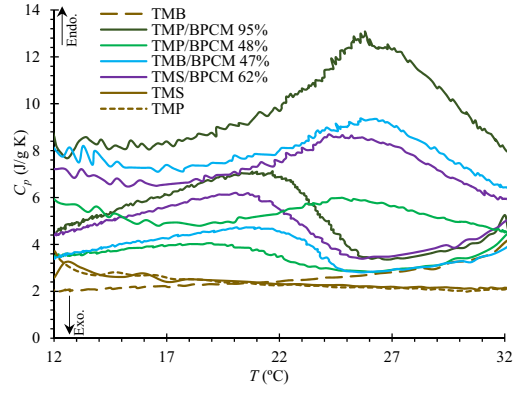

FIGURE 3 Melting and freezing specific heat capacity for TMWs and TMWs/BPCM composites. BPCM, bio-based phase change materials; TMWs, thermally modified woods

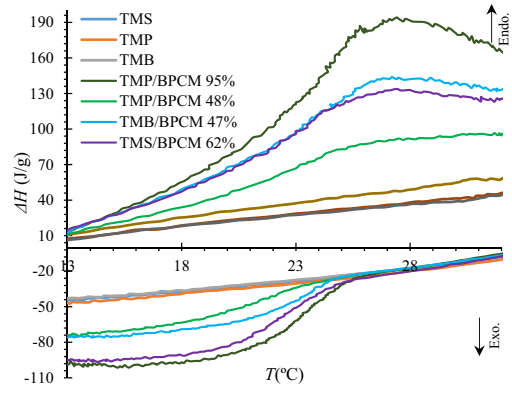

FIGURE 4 Melting and freezing enthalpy for the samples

before and after phase transition they can absorb/release energy in terms of sensible heat.

The latent heat of pure BPCM is around 100 J/g,[29] and it reduces to ca. 70 J/g for TMP/BPCM composites of 95% WPG, and 30 J/g at 48% WPG, while this value for TMB/BPCM and TMS/BPCM at 47% and 62% WPG were ca. 45 J/g. The trend of enthalpy during cooling and heating process was found to be similar.

3.4 | Susceptibility to mold discoloration of the TMW and TMW/BPCM composites

Health problems related to mold growth and release of mycotoxins affect the occupants in buildings,[28] which

emphasizes the importance of material selection and living climate. The above is particularly important when BPCM are going to be introduced as heat storage solutions in buildings. The intention of the mold test was to study and compare the susceptibility of untreated samples, TMW and TMW/BPCM composites. The selected mold fungi are very common and grow well on pine and spruce.[39] The laboratory test was performed at optimal temperature and relative humidity for growth of the selected fungi. Another intention was to evaluate the laboratory test as an accelerated predictor of the discoloration process in practice. The average growth of the test fungi is shown in Table 3.

There is a significant difference between the mold growth on the untreated and TMW samples of the three wood species. Untreated beech is very susceptible to growth reaching a rate of 5 after 4 weeks of exposure while pine and spruce samples are similarly discolored to rates of 4 and 3 after 8 weeks of exposure. Beech, Scots pine sapwood and spruce samples were very susceptible to mold growth, which is probably related to the amount of available low-molecular sugars on the wood surface, for example, glucose, fructose and sucrose.[40,41] A similar susceptibility to mold growth on pine has been observed recently by Lie et al.[42] Compared to pine, the mold susceptibility of spruce varies between the studies, for example, spruce was found relatively more resistant by Viitanen and Ritschkoff[43] or demonstrated similar susceptibility to discoloring fungi as Scots pine sapwood.[42,44] The present study classifies spruce as somewhat better than pine regarding mold susceptibility.

Thermal modification improves significantly the resistance of the material to mold growth, which does not cover more than 10% to 20% of the sample surface (rates 1 or 2, Table 3). The finding is in line with the literature data, for example, .[42,45,46] TMW has always significantly lower equilibrium moisture content than the untreated wood[47]; the decreased moisture adsorption is a main limiting factor for the growth of fungi. Although less distinct on the TMW surface, the barely mold growth was clearly visible.

The mold discoloration susceptibility of the wood/BPCM composites of the three species is rated as better than the untreated samples, but worse than TMW. The growth rates (Table 3) are 2 and 4 for TMP and 4 for the TMB samples impregnated with BPCM. TMS wood impregnated with BPCM does not show difference to only TMS and is ranked as 1. Apparently, the uptake of BPCM in the TMP wood has some influence the growth rates being higher in a sample with higher BPCM uptake. Although the BPCMs are normally encapsulated in various forms and materials, they are always used in indoor environments and thus, the susceptibility of the composites to biological deterioration and degradation should always be considered. According to our knowledge, no studies investigating the long-term resistance of the BPCM materials to mold discoloration have been performed. The compounds of the BPCM in the present study, that is, the fatty acids, are utilized by the mold fungi as nutrients in a similar manner as the available carbohydrates on the sample surface. After the impregnation of wood with the BPCM, the surface is enriched and available to the mold growth. The BPCM can play some role as water-repellent formulation in the wood and it can postpone but hardly prevent the moisture adsorption. It has been demonstrated that the most common airborne fungal genera *Cladosporium* spp., *Penicillium* spp, *Aspergillus* spp. and non-sporulating molds[48,49] found in indoor environment are restricted by availability of moisture. Thus, the mold discoloration on TMW and wood/BPCM composites is lower compared to the unimpregnated wood; the later one being widely used for building.

4 | CONCLUSIONS

TMW including TMP, TMS, and TMB were impregnated with a multicomponent BPCM resulting in an enhanced thermal mass composites with potential use for building applications. The main findings of the work are summarized as follow:

- TMW can serve as container for BPCM; the chemical and morphological changes in wood caused by the thermal degradation of the main structural polymers ensure better permeability and better "hold" of the BPCM in wood compared to the untreated wood. The above is valid regardless the wood species.
- Thermal assessments showed that TMW/BPCM composites had higher thermal mass, it can absorb and release energy in the human comfort temperature range in terms of latent heat. Specific heat capacity of the composites is also higher than TMW without BPCM. The specific heat capacity of the TMWs were around 2 J/g K, which was increased 4 to 8 J/g K after incorporation of BPCM, depending on the BPCM uptake.
- Thermal conductivity of the TMW is less than untreated wood. After impregnation with BPCM, it was found that thermal conductivity of TMW/BPCM composites were higher than TMW. Results also showed that by increasing BPCM uptake, the thermal conductivity increases. This parameter was 0.06 W/m K for TMP and increased to 0.1 and 0.14 W/m K for TMP/BPCM with 48% and 95% uptake respectively. Results showed also that TMB has higher thermal

conductivity than TMP and TMS, while incorporation of BPCM into these materials resulted in even improved thermal conductivity.

- The mold susceptibility test showed that the appearance and growth of molds is related to critical levels of moisture and temperature. BPCM encapsulated in TMW is less susceptible to mold discoloration than the untreated wood. Having in mind the intensive use of wood in buildings, it can be concluded that wood/BPCM composites can serve equivalently or better than comparable wood elements without BPCM.

ACKNOWLEDGMENTS

The study has been carried out within the framework of Smart Energy Systems Research and Innovation Program (ERA-Net E2B2) in the project "Bio-Based Phase Change Materials Integrated into Lignocellulose Matrix for Energy Store in Buildings (BIO-NRG-STORE)." The authors also thank the financial support by the Swedish Research Council for Sustainable Development (FORMAS), project number 2017-00686.

NOMENCLATURE

A	Heat transfer area [m^2]
c_p	Specific heat [J/g K]
H	Enthalpy [J/g]
L	Thickness of the samples [m]
m	Mass of the samples [kg]
Q	Heat [W]
q/a	Heat flux [W/m^2]
T	Temperature [°C]
t	Time [s]
u	Overall heat transfer coefficient [W/m^2 K]

Greek symbol

λ	Thermal conductivity [W/m K]
Δ	Difference
∞	Ambient

Subscripts

f	Final
i	Initial
n	Time point
ref	Reference
$samp$	Sample

DATA AVAILABILITY STATEMENT

Data sharing is not applicable to this article as no new data were created or analyzed in this study.

ORCID

Mohamed Jebrane https://orcid.org/0000-0003-0173-9467

REFERENCES

1. Bal BC. The effect of span-to-depth ratio on the impact bending strength of poplar LVL. *Construct Build Mater*. 2016;112:355-359.
2. Takano A, Hughes M, Winter S. A multidisciplinary approach to sustainable building material selection: a case study in a Finnish context. *Build Environ*. 2014;82:526-535.
3. Ramage MH, Burridge H, Busse-Wicher M, et al. The wood from the trees: the use of timber in construction. *Renew Sustain Energy Rev*. 2017;68:333-359.
4. Hepburn C, Adlen E, Beddington J, et al. The technological and economic prospects for CO_2 utilization and removal. *Nature*. 2019;575(7781):87-97.
5. Amiri A, Ottelin J, Sorvari J, Junnila S. Cities as carbon sinks—classification of wooden buildings. *Environ Res Lett*. 2020;15(9):094076.
6. Eaton RA, Hale MD. *Wood: Decay, Pests and Protection*. London: Chapman and Hall Ltd.; 1993.
7. Mathis D, Blanchet P, Landry V, Lagière P. Impregnation of wood with microencapsulated bio-based phase change materials for high thermal mass engineered wood flooring. *Appl Sci*. 2018;8(12):2696.
8. Esteves B, Pereira H. Wood modification by heat treatment: a review. *BioResources*. 2009;4(1):370-404.
9. Nazari M, Jebrane M, Terziev N. Bio-based phase change materials incorporated in lignocellulose matrix for energy storage in buildings—a review. *Energies*. 2020;13(12):3065.
10. Khudhair AM, Farid MM. A review on energy conservation in building applications with thermal storage by latent heat using phase change materials. *Energ Conver Manage*. 2004;45(2):263-275.
11. De Gracia A, Navarro L, Castell A, Ruiz-Pardo Á, Alvárez S, Cabeza LF. Experimental study of a ventilated facade with PCM during winter period. *Energ Buildings*. 2013;58:324-332.
12. Tyagi VV, Chopra K, Sharma RK, et al. A comprehensive review on phase change materials for heat storage applications: development, characterization, thermal and chemical stability. *Sol Energy Mater Sol Cells*. 2022;234:111392.
13. Singh P, Sharma RK, Ansu AK, Goyal R, Sarı A, Tyagi VV. A comprehensive review on development of eutectic organic phase change materials and their composites for low and medium range thermal energy storage applications. *Sol Energy Mater Sol Cells*. 2021;223:110955.
14. Al-Ahmed A, Mazumder MAJ, Salhi B, Sari A, Afzaal M, Al-Sulaiman FA. Effects of carbon-based fillers on thermal properties of fatty acids and their eutectics as phase change materials used for thermal energy storage: a review. *J Energy Storage*. 2021;35:102329.
15. Chen, F., Kessel, A. and Wolcott, M., 2012. A novel energy saving wood product with phase change materials. In Proceedings of the 55th International Convention of Society of Wood Science and Technology, Beijing, China (pp. 27-31).
16. Li J, Xue P, Ding W, Han J, Sun G. Micro-encapsulated paraffin/high-density polyethylene/wood flour composite as form-stable phase change material for thermal energy storage. *Sol Energy Mater Sol Cells*. 2009;93(10):1761-1767.
17. Sarı A, Hekimoğlu G, Tyagi VV. Low cost and eco-friendly wood fiber-based composite phase change material: development, characterization and lab-scale thermoregulation performance for thermal energy storage. *Energy*. 2020;195:116983.
18. Hu L, Lyu S, Fu F, Huang J, Wang S. Preparation and properties of multifunctional thermochromic energy-storage wood materials. *J Mater Sci*. 2016;51(5):2716-2726.

19. Hui B, Li Y, Huang Q, et al. Fabrication of smart coatings based on wood substrates with photoresponsive behavior and hydrophobic performance. *Mater Des*. 2015;84:277-284.
20. Zerriaa A, El Ganaoui M, Gerardin C, Tazibt A, Gabsi S. Physical incorporation of particles in a porous media: a path to a smart wood. *Eur Phys J Appl Phys*. 2016;74(2):24607.
21. Liang J, Zhimeng L, Ye Y, Yanjun W, Jingxin L, Changlin Z. Fabrication and characterization of fatty acid/wood-flour composites as novel form-stable phase change materials for thermal energy storage. *Energ Buildings*. 2018;171:88-99.
22. Ma L, Guo C, Ou R, Sun L, Wang Q, Li L. Preparation and characterization of modified porous wood flour/lauric-myristic acid eutectic mixture as a form-stable phase change material. *Energy Fuel*. 2018;32(4):5453-5461.
23. Guo X, Zhang L, Cao J, Peng Y. Paraffin/wood flour/high-density polyethylene composites for thermal energy storage material in buildings: a morphology, thermal performance, and mechanical property study. *Polym Compos*. 2018;39(S3):E1643-E1652.
24. Ma L, Wang Q, Li L. Delignified wood/capric acid-palmitic acid mixture stable-form phase change material for thermal storage. *Sol Energy Mater Sol Cells*. 2019;194:215-221.
25. Cheng L, Feng J. Form-stable phase change materials based on delignified wood flour for thermal management of buildings. *Compos A: Appl Sci Manuf*. 2020;129:105690.
26. Barreneche, C., Vecstaudza, J., Bajare, D. and Fernandez, A.I., 2017. PCM/wood composite to store thermal energy in passive building envelopes. In *IOP Conference Series: Materials Science and Engineering* (Vol. 251, No. 1, p. 012111). Riga, Latvia: IOP Publishing.
27. Temiz A, Hekimoğlu G, Köse Demirel G, Sarı A, Mohamad Amini MH. Phase change material impregnated wood for passive thermal management of timber buildings. *Int J Energy Res*. 2020;44(13):10495-10505.
28. Abbott SP. Mycotoxins and indoor molds. *Indoor Environ Connect*. 2002;3(4):14-24.
29. Nazari M, Jebrane M, Terziev N. Multicomponent bio-based fatty acids system as phase change material for low temperature energy storage. *J Energy Storage*. 2021;39:102645.
30. Meng X, Gao Y, Wang Y, Yan B, Zhang W, Long E. Feasibility experiment on the simple hot box-heat flow meter method and the optimization based on simulation reproduction. *Appl Therm Eng*. 2015;83:48-56.
31. Soares N, Martins C, Gonçalves M, Santos P, da Silva LS, Costa JJ. Laboratory and in-situ non-destructive methods to evaluate the thermal transmittance and behavior of walls, windows, and construction elements with innovative materials: a review. *Energ Buildings*. 2019;182:88-110.
32. Younsi, Z., Joulin, A., Zalewski, L., Lassue, S. and Rousse, D., 2008. Thermophysical characterization of phase change materials with heat flux sensors. *Proceedings of Eurotherm, The Nederlands*.
33. Nazari M, Jebrane M, Terziev N. Solid wood impregnated with a bio-based phase change material for low temperature energy storage in building application. *J Therm Anal Calorim*. 2022. doi:10.1007/s10973-022-11285-9
34. Badenhorst H, Cabeza LF. Critical analysis of the T-history method: a fundamental approach. *Thermochim Acta*. 2017;650:95-105.
35. Solé A, Miró L, Barreneche C, Martorell I, Cabeza LF. Review of the T-history method to determine thermophysical properties of phase change materials (PCM). *Renew Sustain Energy Rev*. 2013;26:425-436.
36. Prajapati DG, Kandasubramanian B. Biodegradable polymeric solid framework-based organic phase-change materials for thermal energy storage. *Ind Eng Chem Res*. 2019;58(25):10652-10677.
37. Simpson W, TenWolde A. *Physical properties and moisture relations of wood. Wood handbook: wood as an engineering material*. Madison, WI: USDA Forest Service, Forest Products Laboratory; 1999 General technical report FPL, pp. 3-1.
38. Łukasz C, Wiesław O, Jerzy W. Effects of heat treatment on thermal properties of European beech wood. *Eur J Wood Wood Prod*. 2020;78(3):425-431.
39. Bjurman J. Ergosterol as an indicator of mould growth on wood in relation to culture age, humidity stress and nutrient level. *Int Biodeter Biodegr*. 1994;33(4):355-368.
40. Saranpää P, Höll W. Soluble carbohydrates of Pinus sylvestris L. sapwood and heartwood. *Trees*. 1989;3(3):138-143.
41. Terziev N, Boutelje J, Larsson K. Seasonal fluctuations of low-molecular-weight sugars, starch and nitrogen in sapwood of Pinus sylvestris L. *Scand J For Res*. 1997;12(2):216-224.
42. Lie SK, Vestøl GI, Høibø O, Gobakken LR. Surface mould growth on wood: a comparison of laboratory screening tests and outdoor performance. *Eur J Wood Wood Prod*. 2019;77(6):1137-1150.
43. Viitanen H, Ritschkoff AC. *Mould growth in pine and spruce sapwood in relation to air humidity and temperature. Sveriges lantbruksuniversitet: Institutionen för virkeslära. Rapport*, Uppsala, Sweden: Swedish University of Agricultural Sciences; 1991.
44. Blom Å, Johansson J, Sivrikaya H. Some factors influencing susceptibility to discoloring fungi and water uptake of Scots pine (Pinus sylvestris), Norway spruce (Picea abies) and Oriental spruce (Picea orientalis). *Wood Mater Sci Eng*. 2013;8(2):139-144.
45. Frühwald E, Li Y, Wadsö L. Image analysis study of mould susceptibility of spruce and larch wood dried or heat-treated at different temperatures. *Wood Mater Sci Eng*. 2008;3(1–2):55-61.
46. Ahmed SA, Sehlstedt-Persson M, Morén T. Development of a new rapid method for mould testing in a climate chamber: preliminary tests. *Eur J Wood Wood Prod*. 2013;71(4):451-461.
47. Militz H, Altgen M. Processes and properties of thermally modified wood manufactured in Europe. *Deterioration and Protection of Sustainable Biomaterials*. United states: American Chemical Society; 2014:269-285.
48. Hunter CA, Grant C, Flannigan B, Bravery AF. Mould in buildings: the air spora of domestic dwellings. *Int Biodeterior*. 1988;24(2):81-101.
49. Shelton BG, Kirkland KH, Flanders WD, Morris GK. Profiles of airborne fungi in buildings and outdoor environments in the United States. *Appl Environ Microbiol*. 2002;68(4):1743-1753.

How to cite this article: Nazari M, Jebrane M, Gao J, Terziev N. Thermal performance and mold discoloration of thermally modified wood containing bio-based phase change material for heat storage. *Energy Storage*. 2022;e340. doi:10.1002/est2.340

Acta Universitatis Agriculturae Sueciae

Doctoral Thesis No. 2023:7

This study provides fundamental knowledge regarding the use of bio based phase change materials (BPCMs) incorporated in wood materials for production of energy smart bio-composites for building applications. The bio-composites of solid and thermally modified wood and wood particles with BPCMs confirmed improvement in the thermal properties of the composites enabling them to store the excess of energy in buildings and release the stored energy within human comfort temperature range leading to using energy more efficiently.

Meysam Nazari received his doctoral education at the Department of Forest Biomaterials and Technology/TRV, Swedish University of Agricultural Sciences in Uppsala. He holds a Master (MSc) degree in Energy Engineering from Sahand University of Technology in Iran, and a Bachelor (BSc) degree in Mechanical Engineering from Hormozgan University in Iran.

Acta Universitatis Agriculturae Sueciae presents doctoral theses from the Swedish University of Agricultural Sciences (SLU).

SLU generates knowledge for the sustainable use of biological natural resources. Research, education, extension, as well as environmental monitoring and assessment are used to achieve this goal.

ISSN 1652-6880
ISBN (print version) 978-91-8046-066-8
ISBN (electronic version) 978-91-8046-067-5